Max-Planck-Institut für Meteorologie
Max Planck Institute for Meteorology

Co_2 fluxes and concentration patterns over Eurosiberia: A study using terrestrial biosphere models and the regional atmosphere model REMO

Caroline R. L. Narayan

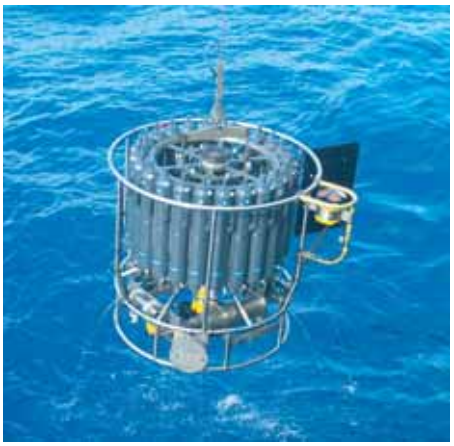

Berichte zur Erdsystemforschung 29/2006

Reports on Earth System Science

Hinweis

Die Berichte zur Erdsytemforschung werden vom Max-Planck-Institut für Meteorologie in Hamburg in unregelmäßiger Abfolge herausgegeben.

Sie enthalten wissenschaftliche und technische Beiträge, inklusive Dissertationen.

Die Beiträge geben nicht notwendigerweise die Auffassung des Instituts wieder.

Die "Berichte zur Erdsystemforschung" führen die vorherigen Reihen "Reports" und "Examensarbeiten" weiter.

Notice

The Reports on Earth System Science are published by the Max Planck Institute for Meteorology in Hamburg. They appear in irregular intervals.

They contain scientific and technical contributions, including Ph. D. theses.

The Reports do not necessarily reflect the opinion of the Institute.

The "Reports on Earth System Science" continue the former "Reports" and "Examensarbeiten" of the Max Planck Institute.

Anschrift / Address

Max-Planck-Institut für Meteorologie
Bundesstrasse 53
20146 Hamburg
Deutschland

Tel.: +49-(0)40-4 11 73-0
Fax: +49-(0)40-4 11 73-298
Web: www.mpimet.mpg.de

Layout:

Bettina Diallo, PR & Grafik

Titelfotos:
vorne:
Christian Klepp - Jochem Marotzke - Christian Klepp
hinten:
Clotilde Dubois - Christian Klepp - Katsumasa Tanaka

Berichte zur Erdsystemforschung 29/2006

CO_2 fluxes and concentration patterns over Eurosiberia: A study using terrestrial biosphere models and the regional atmosphere model REMO

Dissertation zur Erlangung des Doktorgrades der Naturwissenschaften
im Departement Geowissenschaften der Universität Hamburg
vorgelegt von

Caroline R. L. Narayan
aus Suva, Fidschi Inseln

Hamburg 2006

Reports on Earth System Science 29/2006

ISSN 1614-1199

Caroline R. L. Narayan
Max-Planck Institut für Meteorologie
Bundesstr. 53
20146 Hamburg
Germany

Als Dissertation angenommen
vom Departement Geowissenschaften der Universität Hamburg

auf Grund der Gutachten von
Herrn Professor Dr. Guy P. Brasseur
und
Herrn Dr. Christian Reick
Hamburg, den 31. Mai 2006
Professor Dr. Kay-Christian Emeis
Leiter des Departements für Geowissenschaften

ISSN 1614-1199

CO_2 fluxes and concentration patterns over Eurosiberia: A study using terrestrial biosphere models and the regional atmosphere model REMO

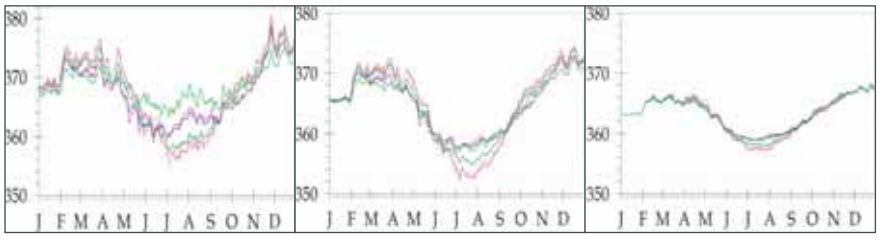

Caroline Narayan

Hamburg 2006

For Rutger

ABSTRACT

Regional scale studies on the carbon cycle have gained growing importance and play a crucial role in the understanding of biosphere-atmosphere interactions. Terrestrial biosphere modelling is an essential tool in the application of regional carbon budget estimates. However, the reliability of the estimates from the models is always questionable due to the uncertainties and limitations associated with the choice of the model, the input data, as well as the representation of the ecosystem processes. The current study investigated the contribution of the terrestrial biosphere to the intra-annual variability of atmospheric CO_2 concentrations over Eurosiberia. Because of the strong seasonal signal from the biosphere and the related seasonal variation of atmospheric CO_2 content, this study focuses on an annual time scale rather than synoptic variations. Two terrestrial biosphere models, BETHY and BIOME-BGC, were used in a number of experiments with various meteorology inputs to simulate the biosphere fluxes at single stands, and have been tested for their sensitivity to varying input parameters. Fluxes from the light-use efficiency model TURC, derived from a previous study, were included for comparison. The simulations were then extended to regional scale by applying the models to Eurosiberia. The uncertainties in the terrestrial biosphere fluxes were assessed by using an "ensemble" of the two models and different input vegetation maps that largely control the ecosystem processes included in the models. The range of flux estimates provides an indication of the

uncertainties related to flux simulations. The regional fluxes were subsequently used as input to the atmospheric transport model REMO to simulate the atmospheric concentrations. The propagation of the biosphere fluxes in the concentrations was investigated via the CO_2 concentration variations at different levels in the atmosphere.

The performance of BETHY and BIOME-BGC was tested against eddy covariance measurements at selected FLUXNET sites across Eurosiberia. The models adequately represented the seasonal cycles of the fluxes despite the limitations in the input data and the use of different input datasets. A sensitivity analysis of the models showed that model parameterisations and assumptions, the surface inputs and the different ways that the models handle these inputs play an important role in the estimation of the fluxes. While the use of modelled meteorology (instead of observations) leads to acceptable results, a proper representation of the site characteristics is equally important, and particularly parameters that relate to the availability of water (rooting depth and precipitation) sometimes leads to a breakdown in the simulated fluxes.

When extending local scale CO_2 flux exchange to regional scale, uncertainties are incorporated with the choice of the models and the input data provided to the models. Significant differences were seen in the simulated fluxes between BETHY and BIOME-BGC in the different experiments. As it is a basic assumption in the models that on an annual basis the net ecosystem fluxes balance out, it is not clear whether the biosphere in Eurosiberia act as a source or a sink on an annual scale. However, in winter both models, as well as TURC suggested that the biosphere behaves as a source. The net carbon release ranged from ~500 TgC in TURC to over 1000 TgC in BETHY and BIOME-BGC. In summer

the models agree that the biosphere acts as a sink but with a wide range in the amounts of carbon uptake, the values ranging from ~800 TgC from BIOME-BGC, to almost 2500 TgC from BETHY. The large differences in the simulated fluxes may at least partly be attributed to the vegetation map used in the models that is very important in determining the regional patterns and the seasonality of the simulated biosphere fluxes. The variability in the fluxes is in turn propagated in the atmospheric CO_2 when transported over the region using the transport model REMO.

The simulated CO_2 concentrations in the lowest atmosphere level, that is at ground level up to approximately 34m, showed a relatively high variability mainly due to the contribution of the biosphere. The variability was also visible at the planetary boundary layer height (~300m above ground) although the amplitude of the fluctuations was less than at the ground level. Above the planetary boundary layer, at approximately 3000m, as the air gets mixed the concentration variability decreases reflecting the reduced signal of the local terrestrial fluxes in atmospheric CO_2 concentrations. However, depending on the strength of the flux contributions the influence of the biosphere can still be seen in the planetary boundary layer. This was especially the case for the concentrations derived from BETHY-simulated fluxes. The concentrations derived from TURC and BIOME-BGC fluxes showed similar patterns but with lower values.

The present study demonstrates the influence of fluxes from the terrestrial biosphere on the seasonal variation in the CO_2 concentrations in the lower atmosphere over Eurosiberia. Above the planetary boundary layer, however, the signal of the biospheric fluxes virtually disappears. Higher in the atmosphere also the differences between the model experiments

became less prominent. Future studies of regional CO_2 fluxes and concentrations should take other sources of uncertainties, apart from the input vegetation maps, into account in a similar manner as was done here, in other words by adopting a larger ensemble of model experiments. For long-term studies of regional carbon budgets multi year runs should be performed.

TABLE OF CONTENTS

LIST OF FIGURES

LIST OF TABLES

LIST OF ABBREVIATIONS

BETHY	Biosphere-Energy-Transfer-Hydrology
BIOME-BGC	Biome-BioGeochemicalCycles
CO_2	carbon dioxide
c	fraction of incoming solar radiation
DEHM	Danish Eulerian Hemisphere Model
ECMWF	European Centre for Medium Range Weather Forecasts
ε	photosynthesis efficiency parameter
f	fraction of photosynthetically active radiation absorbed by the vegetation
FC	fractional cover
g	freezing factor
gC/m^2	grams carbon per square metre
GPP	gross primary product
LAI	leaf area index
MATCH	Multiple-Scale Atmosphere Transport Chemistry
NAO	North Atlantic Oscillations
NDVI	Normalised Difference Vegetation Index
NEE	net ecosystem exchange
NPP	net primary production
PAR	photosynthetically active radiation
PBL	planetary boundary layer

ppm	parts per million
PgC	Petagram carbon (x 10^{15} gC)
R_A	autotrophic or total plant respiration
R_M	maintenance respiration
R_G	growth respiration
R_h	heterotrophic or soil respiration
R_{total}	total respiration (sum of R_A and R_h)
REMO	Regional Model
SOM	soil organic matter
TBMs	Terrestrial Biosphere Models
TgC	Teragram carbon (x 10^{12} gC)
TM3	Tracer Model 3
TURC	Terrestrial Uptake and Release of Carbon

CHAPTER 1
INTRODUCTION

1.1 BACKGROUND

The terrestrial biosphere contributes significantly to the concentration of greenhouse gases, particularly carbon dioxide (CO_2), in the atmosphere. The exchange of carbon between the biosphere and the atmosphere, and whether the first acts as a source or as a sink, has been the subject of many studies. In recent years, regional scale studies on the carbon cycle have gained growing importance. Today they play a pivotal role in the refinement of our knowledge on biosphere-atmosphere interactions, thereby helping to understand how different areas of the globe will respond to perturbations in land cover or climate.

The evolution of the terrestrial carbon sink can be largely attributed to the changes in the land cover over time, such as re-growth on abandoned agricultural land and fire prevention in addition to the responses to environmental changes, such as longer growing seasons and fertilisation of CO_2 and nitrogen (Schimel *et al.*, 2001). At the same time, the biosphere can act as a source of carbon due to forest fires, accelerated decay or changes in land use. Fan and colleagues (1998) indicated that the partitioning of the Northern Hemisphere terrestrial sources and sinks could be estimated by using the West-to-East gradient of atmospheric CO_2

across the continents. However, the west-east signal is much smaller and more difficult to detect than the north-south signal due to the fact that the CO_2 distribution is smoothed out more by the relatively rapid zonal atmospheric transport than by the slower meridional transport (Fan *et al.*, 1998). Additionally, due to the traditional location of the atmospheric sampling stations, which are primarily offshore, away from the largest terrestrial signal to avoid the complexities associated with the continental atmospheric boundary layers, diurnal characteristics of photosynthesis, local fossil fuel emissions and topography, the retrieval of surface CO_2 fluxes between different continents and regions is still poorly constrained (Fan *et al.*, 1998; Lafont *et al.*, 2002). With the recent extensive aircraft sampling during the EUROSIBERIAN CARBONFLUX project (1998) this shortcoming has been overcome to some extent. The framework of the project provided the possibility of inferring the regional carbon balance over Eurosiberia (Europe and Western Siberia) from a combination of CO_2 measurements and modelling efforts on different scales.

Terrestrial biosphere modelling is an essential tool in the estimation of regional carbon budgets. However, the reliability of the estimates from the models is always questionable because of the uncertainty in the model parameters, the model's limitations in the representation of the biospheric processes and uncertainties in the input data to the models. When taken as "black boxes" in terms of their processes, can the biosphere models explain particular features in the observations? Are these models helpful in understanding measured CO_2 fluxes and atmospheric CO_2 concentrations?

A number of regional studies of CO_2 fluxes and concentrations have been conducted over the Northern Hemisphere using both, different regional

scale models and continuous measurements. Kjellström *et al.* (2002) studied the propagation of the flux signals into the atmosphere from regional sources in a limited area transport and diffusion model MATCH (Multiple-scale Atmosphere Transport Chemistry). Based on the simulated atmospheric concentrations they investigated how representative the station measurements and sparse vertical profiles of atmospheric CO_2 are for the estimation of the regional carbon budget. They used the model in an offline mode with terrestrial CO_2 fluxes from a light-use efficiency model TURC (Terrestrial Uptake and Release of Carbon), lateral boundary concentrations from the global tracer transport model TM3 and the driving meteorological fields from the ECMWF, the European Centre for Medium Range Weather Forecasts. For details on MATCH, TURC and TM3 models see Kjellström *et al.* (2002); Lafont, *et al.* (2002); Ruimy *et al.* 1996); Chevillard *et al.* (2002a) and Heimann and Körner (2003).

While the MATCH model represented the meteorological parameters (temperature, humidity and planetary boundary layer height) consistently with observations, and the simulated surface fluxes captured a large part of the observed variability on a diurnal time-scale, the synoptic time-scale agreements (over a few days) between observations and simulation were poor, leading to a disagreement between the time-series of observed and simulated CO_2 concentrations (Kjellström *et al.*, 2002). Analysis of the regional variability of CO_2 in the model domain showed that there was no ideal vertical level for detecting the terrestrial signal of CO_2 in the free troposphere, in contrast to the atmosphere layer within a few hundred meters above the ground where the terrestrial signal was found to be the strongest. This indicated that the modelled CO_2 variability in the lowest model layers is due to internal processes, namely the surface fluxes, with little influence from the boundaries of the model region (Kjellström *et al.*,

2002). The study concluded that single ground stations or a few vertical profiles are insufficient to determine regional fluxes mainly due to the synoptic scale variability in both the transport and the CO_2 surface fluxes. Regional studies of carbon budgets and atmospheric CO_2 concentrations therefore have to rely on biosphere models to estimate the fluxes of CO_2 and transport models to simulate the propagation of the biosphere fluxes into the atmosphere. The local measurements can, however, still be useful when fine-tuning and validating the performance of the models.

For the same region Chevillard *et al.* (2002a) conducted a companion study with the online regional atmospheric model REMO (Regional Model) with the boundary conditions from TM3, as in Kjellström *et al.* (2002) and the surface fluxes from TURC, which were computed on REMO grid using REMO meteorology. The transport of CO_2 over Eurosiberia was simulated to investigate the spatial distribution and temporal variability of atmospheric CO_2 in the region. The results of their study showed that REMO represented the diurnal variation of CO_2 near the ground, as well as the vertical profiles between the ground and 3000m, relatively well. REMO also simulated quite well the short-term variability of the fluxes and atmospheric CO_2. However, the study revealed that the mean observed CO_2 gradients from Western Europe to Western Siberia were absent in the REMO results. This model failure was attributed to the incorrect geographic and mean seasonal patterns of the biospheric fluxes estimated by TURC, and to the prescribed boundary conditions from the global coarse-grid TM3 model. These indicated the key role of the boundary conditions in a limited area model, as well as the need for realistic surface fluxes. This was a different finding than the one by Kjellström *et al.* (2002), who showed that the lateral boundary conditions

had very little influence on the CO_2 variability but significantly affected the large-scale patterns of regional atmospheric CO_2.

Other regional scale studies in the Northern Hemisphere include the development of a detailed tracer transport model (DEHM, Danish Eulerian Hemispheric Model) with the implementation of the main anthropogenic and natural emissions and exchange parameters, as well as inclusion of a nesting procedure to obtain a European sub-domain with a higher resolution (Geels, 2003). Another study by Geels *et al.* (2004) focussed on investigation of the mechanisms determining synoptic variability patterns of atmospheric CO_2 measurements (such as pronounced summer maxima and different seasonality with high variability observed at certain European sites) over the Northern Hemisphere. The biosphere fluxes in these studies were obtained from TURC and process-based land surface models. However, in order to reduce the synoptic variability it is necessary to investigate CO_2 fluxes over longer time scales of seasons to years.

Further studies include regional modelling of carbon sources and sinks via the use of various tracer transport models like DEHM, TM3, LMDZT3.3 and HANK, as well as inversion techniques, also referred to as "top-down" approach, such as Bayesian Synthesis Inversion, are used to calculate the fluxes required to match the atmospheric concentration. Other studies (Turner *et al.*, 2004; Cohen & Goward, 2004; Ustin, *et al.*, 2004; Wulder *et al.*, 2004) look at the suitability of remote sensing techniques in, for example, regional forest productivity assessment, spatial and temporal variability of CO_2 flux estimation, or determination of the parameters controlling biospheric CO_2 fluxes over Europe.

The studies mentioned above have mainly focussed on short-term variations from a few days to a month. These studies have identified the driving mechanisms of the regional fluxes and atmospheric variations at smaller time scales, or have addressed the uncertainties in the sources and sinks of carbon in Eurosiberia at short time scales. It is still unclear how the variability in the atmospheric CO_2 transport and how other sources (for example, anthropogenic emissions (fossil fuel) and ocean uptake) contribute to the overall concentration patterns in the region. In the above-mentioned studies fossil fuel emissions and ocean fluxes were constant. The importance of the terrestrial biosphere in the global carbon cycle is underlined by the possible existence of a substantial land carbon sink in the northern hemisphere. That sink may account for the absorption of one third of the CO_2 emitted from energy production (Schimel *et al.*, 1996). Additionally, the terrestrial vegetation seems to be the prime source of much of the fluctuations in atmospheric CO_2, both within a year (Heimann and Keeling, 1989) and over time spans of about a decade (Francey *et al.*, 1995; Kaduk and Heimann, 1994; Friedlingstein *et al.*, 1995).

1.2 RESEARCH QUESTION / AIMS

The current study aims at addressing the following research question:

What is the contribution of the terrestrial biosphere to the intra-annual variability of atmospheric CO_2 concentrations over Eurosiberia?

The terrestrial biosphere (hereafter referred to as biosphere) is one of the most critical and complex components of the Earth system, regulating fluxes of energy, water, aerosols and trace gases between the Earth's

surface and the atmosphere (Overpack *et al.*, 2002), thereby influencing atmospheric composition and climate. An important aspect of the climate-biosphere system is the response of the biosphere to increasing atmospheric CO_2, or changes in, for example, solar radiation reaching the ground, which in turn alters the surface climate (for example, temperature and specific humidity). As the biosphere affects the CO_2 uptake and evaporation rates, these changes to the terrestrial vegetation have the potential to feed back on climate (Steiner *et al.*, 2005). Therefore, the need arises for investigating the contributions of the biosphere to the variability in the atmospheric CO_2 concentrations. Other sources of variability include anthropogenic emissions, mainly fossil fuel, changes in ocean uptake due to climatic or NAO related factors, and the seasonal variation in solar radiation, the latter influencing the biosphere and the climate. However, the variability due to these factors is comparatively lower than that of the biosphere.

In contrast to previous research, this study concentrates on the annual time scale because of the strong seasonal signal from the biosphere and the related seasonal variation of atmospheric CO_2 content. To achieve this aim, two terrestrial biosphere models (TBMs) in combination with an atmospheric transport model were used. Observations of atmospheric CO_2 concentrations and fluxes were used for comparison and validation of the models. Uncertainties related to the choice of the model, the model parameters and input data have been quantified.

The present study specifically addressed the following objectives:

- To estimate CO_2 fluxes from the biosphere to the atmosphere over Eurosiberia and the related uncertainties;

- To quantify the contribution of the biosphere to the variability in annual atmospheric CO_2 concentrations;

- To compare the variability originating from the biosphere to other sources, and

- To assess whether the biosphere in Eurosiberia, on an annual scale, acts as a source or a sink

1.3 GENERAL APPROACH

To address these objectives the current study performed a number of simulations using two terrestrial biosphere models, BETHY (Biosphere-Energy-Transfer-Hydrology) and BIOME-BGC (Biome-BioGeochemicalCycles), and an atmospheric transport model, REMO (REgional MOdel). For comparison, the CO_2 flux results of the light-use efficiency model TURC (Terrestrial Uptake and Release of Carbon), derived from a previous study (Chevillard *et al.*, 2002a), have also been used. Details of these models and the corresponding input data are presented in the next chapter.

As a first step the behaviour of the TBMs was tested by performing CO_2 flux simulations at single sites in the study region. Three experiments were

performed with varying sources of meteorology inputs to investigate the influence of input data on the models. The simulated fluxes were compared with observations on carbon fluxes. Some sensitivity tests were also performed in order to test the model response by altering some key input parameters, such as temperature, precipitation and rooting depth.

From the single-stand investigations and comparisons, the TBM simulations were extended to the spatial scale over the entire study region. Five experiments have been conducted with the two TBMs using three different vegetation input maps in order to assess the model sensitivity and the CO_2 flux patterns over Eurosiberia, arising due to (a) the use of different types of models, and (b) the use of different input data in the models.

Both TBMs, despite being process-based, meaning that ecosystem processes, such as photosynthesis, respiration, transpiration and other canopy level processes are modelled explicitly (as explained in the next chapter), exhibit differences in the way the models handle these processes. It may therefore be expected that the differences between the model results are due to the use of different model types, as well as different input data. This hypothesis was tested via the use of statistical analysis.

In order to identify the sources of variability in the biospheric fluxes, the contributions of individual flux components, uptake due to photosynthesis and soil respiration were investigated. The differences and similarities of the fluxes and flux components from the TBMs were compared with those from the TURC model, which uses satellite-derived NDVI (Normalised Difference Vegetation Index) data instead of vegetation maps. Other sources of variability include changes in the

climate across the region, from coastal to continental. A few key meteorological parameters (precipitation, temperature) were investigated to establish their contributions to the flux variability. Humans also play an important role in bringing about ecological changes around them. Activities such as land clearing for construction or agriculture, forest burning and forest mining add to the variability in the fluxes. However, the models used for the present study do not include human dimension. BIOME-BGC has a possibility to incorporate forest fires but since this is not an option in BETHY it was not included in the current experiments for the purpose of consistency in the use of the TBMs. The analysis presented in this thesis excludes human interventions and focuses mainly on natural variability.

The propagation of the biospheric fluxes to the atmospheric CO_2 in the planetary boundary layer (PBL) was investigated via the CO_2 concentration variations at different levels in the atmosphere (for example, the biospheric level or the lowest model level at ~34m above the ground, in the PBL at ~300m and above the PBL at ~3000m). The influence of the uncertainties in the biosphere fluxes on the estimation of the atmospheric CO_2 was assessed by using the fluxes from the different experiments with the TBMs using different vegetation maps. In this way the influence of the choice of models and the input data on the modelling of CO_2 concentrations could be assessed.

1.4 STUDY REGION

The study region comprises of Europe and Western Siberia (Eurosiberia), covering an area of 36 x 10^6 km^2. To help visualise the region being

investigated Figure 1-1 shows the projection of the model domain relative to the global scale, while Figure 1-2 shows the topography of the model domain at the half-degree grid scale in the geographic projection used by the REMO model.

The region under investigation originated from the EUROSIBERIAN CARBONFLUX project that was designed as a pilot study to demonstrate the feasibility of estimating regional- or continental-scale carbon fluxes by means of a combination of atmospheric measurements, surface flux measurements and a hierarchy of models (Heimann, 1999).

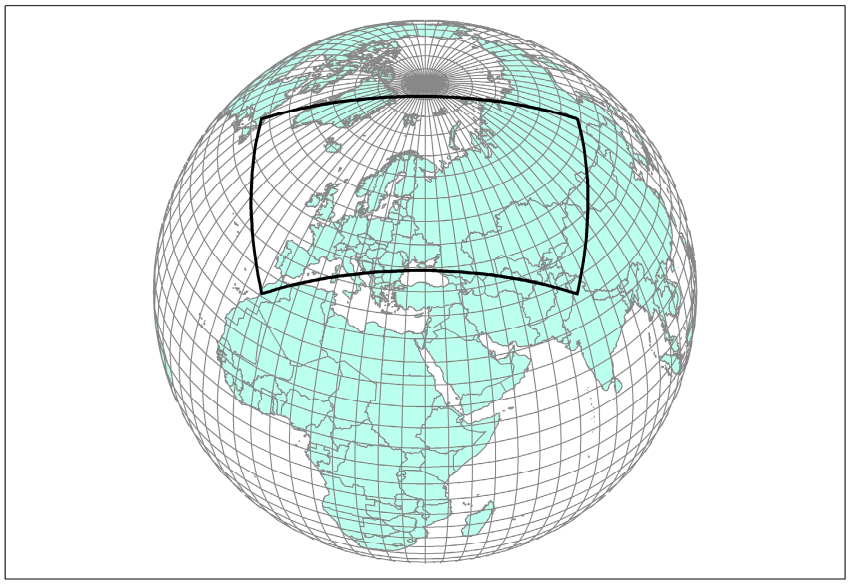

Figure 1-1 Model domain projection with respect to the global scale

The study region is covered by a range of natural vegetation types including coniferous, deciduous broadleaf and mixed beech forests in Europe, and mixed broadleaf/coniferous, spruce/boreal and dark coniferous/taiga forests in Western Siberia. In contrast to the maritime

and temperate European climate dominated by westerly winds in summer, the climate in West Siberia is dominated by southerly winds from the Arctic Ocean in summer and by northerly wind patterns in winter. This wind pattern continues across central and Eastern Siberia, enhancing the continental climate from West to East, as well as changing the length of the growing season (Schulze *et al.*, 2002). In Western Europe the average annual temperature ranges from 2 - 16°C and annual mean precipitation between 500 – 1200mm (Schulze *et al.*, 2002). In the taiga zone of European Russia, the average day temperatures above 0°C last for about 200 – 230 days, decreasing to about 170 days in central Siberia. The average rainfall decreases slightly from European Russia, 600mm, to West Siberia, 530mm (Schulze *et al.*, 2002).

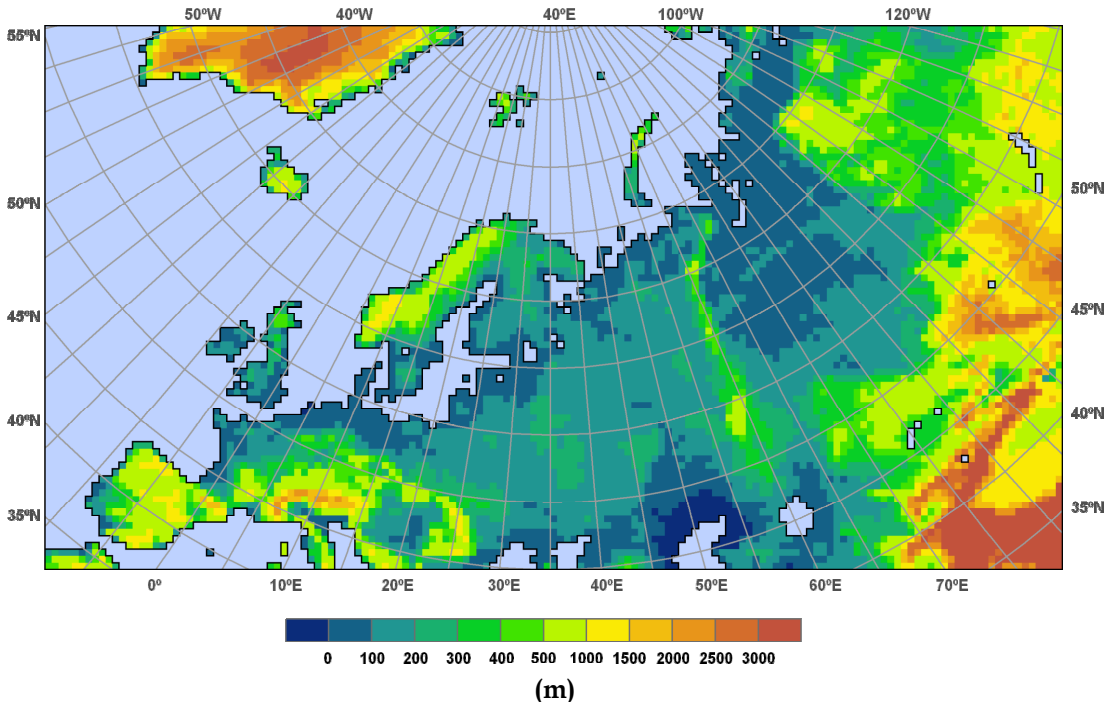

Figure 1-2 Topography of the model domain at the half-degree grid scale used by the REMO model

Western Siberia (defined here as the forested areas of Russia, east of the Ural mountains) is an important component of the global terrestrial carbon cycle, comprising about 90 PgC or ~4% of the global amount of carbon stored in vegetation and soils, and contributing about 2.4 PgC per annum to the global annual net primary production (Heimann, 2002). The Siberian environment also offers advantages for observations due to the interior climate of the Eurasian continent, which is dominated by large interannual variability thereby providing a natural laboratory for the investigation of longer-term climate impacts on terrestrial ecosystems (Heimann, 2002). The flat and homogeneous ecosystem mosaic of forests and wetlands in Western Siberia is beneficial for scaling studies by integrating observations and models. In comparison to Europe the Siberian environment is only modestly affected by anthropogenic impacts, implying that most of the vast boreal forest ecosystem is dominated by natural processes.

1.5 THESIS OUTLINE

Following this introductory chapter the remaining parts of the thesis describes in detail the different steps taken towards addressing the research question and the outlined aims. The next chapter, **Chapter 2** provides information on the tools and the corresponding input data used, firstly in the simulation of CO_2 fluxes using the TBMs and then in the simulation of atmospheric CO_2 concentrations using the tracer transport model. **Chapter 3** describes how the TBMs have been used in simulating CO_2 fluxes at selected measurement sites in the study region. Results of the flux comparisons with observations, as well as sensitivity tests and

analyses are presented. Following this, **Chapter 4** explains the spatial CO_2 flux simulations and patterns obtained from the two TBMs over the entire study region. **Chapter 5** describes how the spatial fluxes obtained in Chapter 4 have been used in the tracer transport model to simulate atmospheric CO_2 concentrations. Regional patterns over two contrasting seasons, winter and summer of 1998, are presented. **Chapter 6** revisits the research question and the aims of the study, providing a general discussion with a summary, recommendations and conclusions of the current study.

CHAPTER 2
MODELS AND INPUTS

2.1 INTRODUCTION

The tools used in the current study are two process-based TBMs (terrestrial biosphere models), BETHY (Biosphere-Energy-Transfer-Hydrology) and BIOME-BGC (Biome-BioGeochemicalCycles) and a regional atmospheric transport model REMO (REgional MOdel). The two TBMs have been widely used, particularly for global studies in the case of BETHY, and additionally, for regional scale studies in the case of BIOME-BGC. For comparison purpose, CO_2 fluxes from a light-use efficiency model TURC (Terrestrial Uptake and Release of Carbon) have been included in the present study. This chapter describes the models and discusses their characteristics. Prior to the descriptions of the models a few terms and abbreviations that appear frequently in the current chapter, as well as in later parts of the thesis are explained in Table 2-1.

2.2 DESCRIPTION OF THE TERRESTRIAL BIOSPHERE MODELS

This section describes and discusses the general characteristics and some of the key model processes of BETHY, BIOME-BGC and TURC, and

provides a comparison of the three models. Both process-based TBMs simulate the exchange of carbon with some assumptions.

Table 2-1 Commonly used carbon exchange terms

ACRONYMS	NAMES	DESCRIPTIONS
GPP	Gross primary productivity	Gross carbon uptake due to photosynthesis
NPP	Net primary productivity	Net production after autotrophic respiration $NPP = GPP - R_A$
R_A	Autotrophic or total plant respiration	Comprises of two components: R_g → growth respiration R_m → maintenance respiration $R_A = R_g + R_m$
R_h	Heterotrophic or soil respiration	Microbial respiration of plant litter and organic soil components
R_{total}	Total respiration	Comprises of the sum of R_A and R_h
NEE	Net ecosystem exchange	$NEE = NPP - R_h$ This is equivalent to NEP, net ecosystem productivity. Zero NEE indicates that the ecosystem is in balance, while positive NEE indicates uptake of CO_2 by the vegetation, and negative NEE indicates release by the vegetation

Assumptions:

1. Trees are not defined individually, as in a typical forest stand growth model. Only fluxes of carbon, water and nitrogen are expressed in mass units;

2. Vegetation species are not identified explicitly, but species-specific physiological characterisation are represented;
3. The geometric complexities of different tree canopies are reduced to a simple quantification of the sum of all leaf layers as LAI;
4. All biogeochemical processes are simulated within the vertical extent of a vegetation canopy and its rooting system;
5. An arbitrary unit of horizontally projected area is defined over which all fluxes and storage are quantified. Complete horizontal homogeneity is assumed within that unit area, and
6. The defined horizontal area and the vertical extent of the canopy and its rooting system define the maximum physical boundaries of the simulation system and includes: all living and dead plant materials, leaf or shoot boundary layer, litter and soil surfaces, all mineral and organic matters making up the soil and litter down to a depth at which root penetration is negligible, all water held in the soil down to that same depth and any snow cover.

The following sub-sections describe the general model structure of the TBMs, followed by a discussion of how the important ecosystem processes are handled by the individual models.

2.2.1 BETHY

The vegetation model BETHY, developed by Knorr (1997) is a global process-oriented TBM that simulates CO_2 uptake by vegetation as a process that is simultaneously limited by light, heat, soil water and nitrogen (Knorr and Heimann, 2001). Contained within the full energy and water balance of the Earth's surface, the model structure comprises of

four modules: energy and water balance, photosynthesis, carbon balance and phenology. A complete detail of each module is described in Knorr (1997). An overview of the model structure is provided in figure 2-1.

1. Energy and water balance:

Using temperature, precipitation, solar radiation, soil texture, soil albedo and roughness length as input, together with LAI (leaf area index) and FC (fractional cover) from the phenology part, the energy and water balance module computes on a daily basis surface albedo, net radiation, latent and sensible heat fluxes, air humidity, soil water and snow balance.

2. Photosynthesis:

As input this module uses PAR (photosynthetically active radiation), solar angle, soil albedo, atmospheric CO_2 content and vegetation-type dependent parameters, with LAI and FC from the phenology part and air humidity and transpiration rate from the energy balance part. It computes PAR absorption and GPP on hourly time step.

3. Carbon balance:

The carbon balance module computes the surface-atmosphere CO_2 fluxes, using GPP from the photosynthesis part, and soil water content and leaf temperature from the energy balance part to compute R_A and R_h. Using these components, one part of the calculation computes NPP each time the photosynthesis part is executed. The other part concerns heterotrophic respiration, drawing from a short-lived litter pool of time-varying size, and a long-lived soil organic matter pool that is assumed constant in size at the time-scale of the simulation. R_h is adjusted to zero for the annual fluxes.

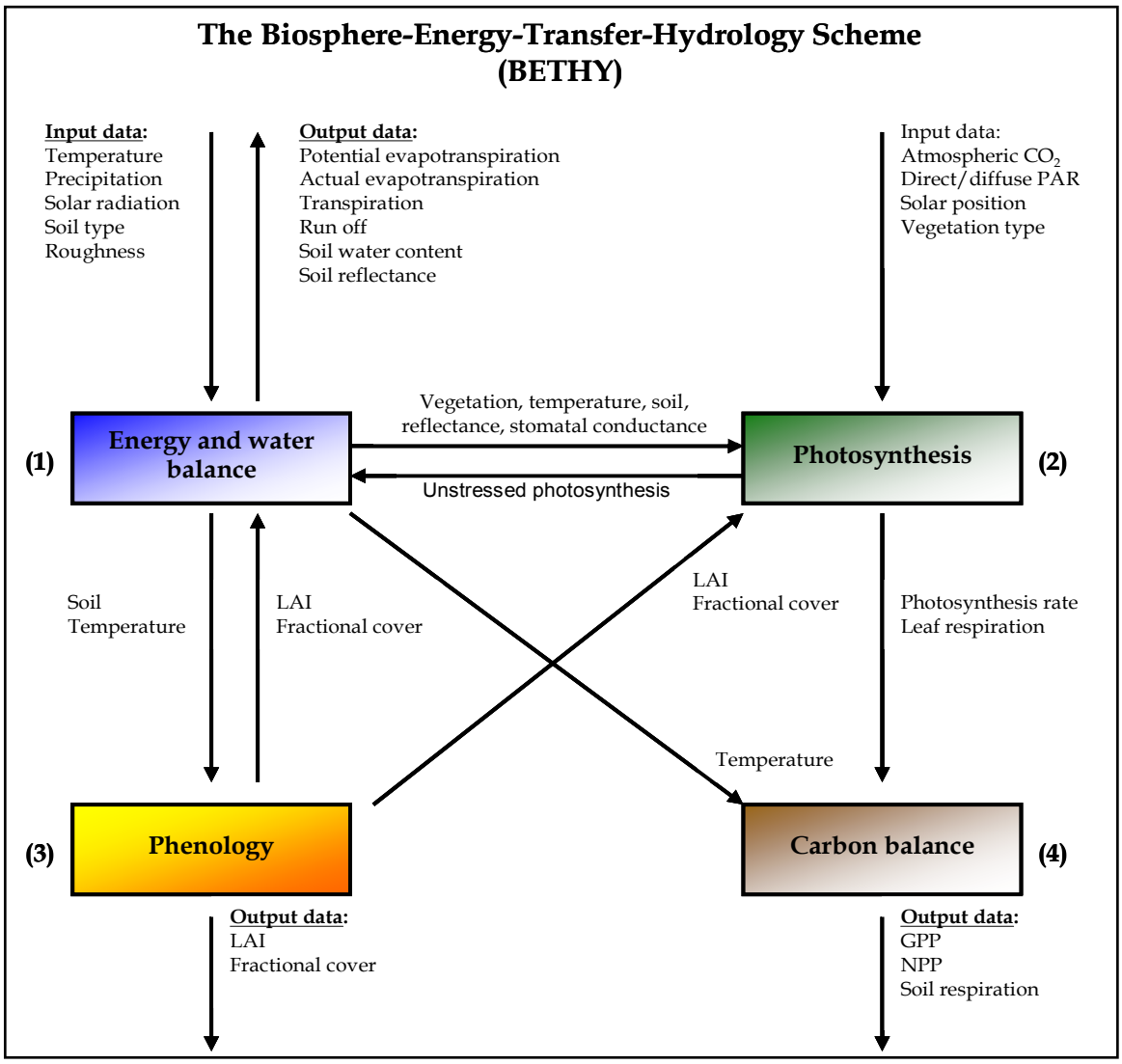

Figure 2-1 Schematic diagram of BETHY model illustrating data input, output and exchange between the modules *(Source: Knorr, 2000)*

4. Phenology:

This module uses soil temperature and vegetation-specific phenological parameters, for example, evergreen/deciduous, as input and computes the time course of LAI and the vegetation fractional cover, which is assumed to be constant over time.

2.2.2 BIOME-BGC

BIOME-BGC is a mechanistic model that simulates water, carbon and nitrogen dynamics in plants, litter and soil in the terrestrial ecosystems. The structure of the model used in the current study (Version 4.1.1) is based on some key simplifying assumptions, proven to be particularly valuable in extending ecosystem analysis to regional levels. Details of the model can be found in Thornton (1998).

The basic structural components of BIOME-BGC are compartments or pools, capable of accepting, releasing and storing the state quantities (namely, water, carbon and nitrogen), while the basic functional components of the model are fluxes linking these pools to each other and to the external environment, and which are driven and controlled simultaneously by a range of external and internal factors (Thornton, 1998).

Figure 2-2 shows a summary of the fluxes and state variables for carbon and nitrogen in BIOME-BGC. The figure is reproduced from Thornton (2002).

2.2.3 TURC

The biospheric fluxes resulting from TURC model are used here for the purpose of comparing with the results of the presently used process-based TBMs. For completeness a brief description of the model is included here.

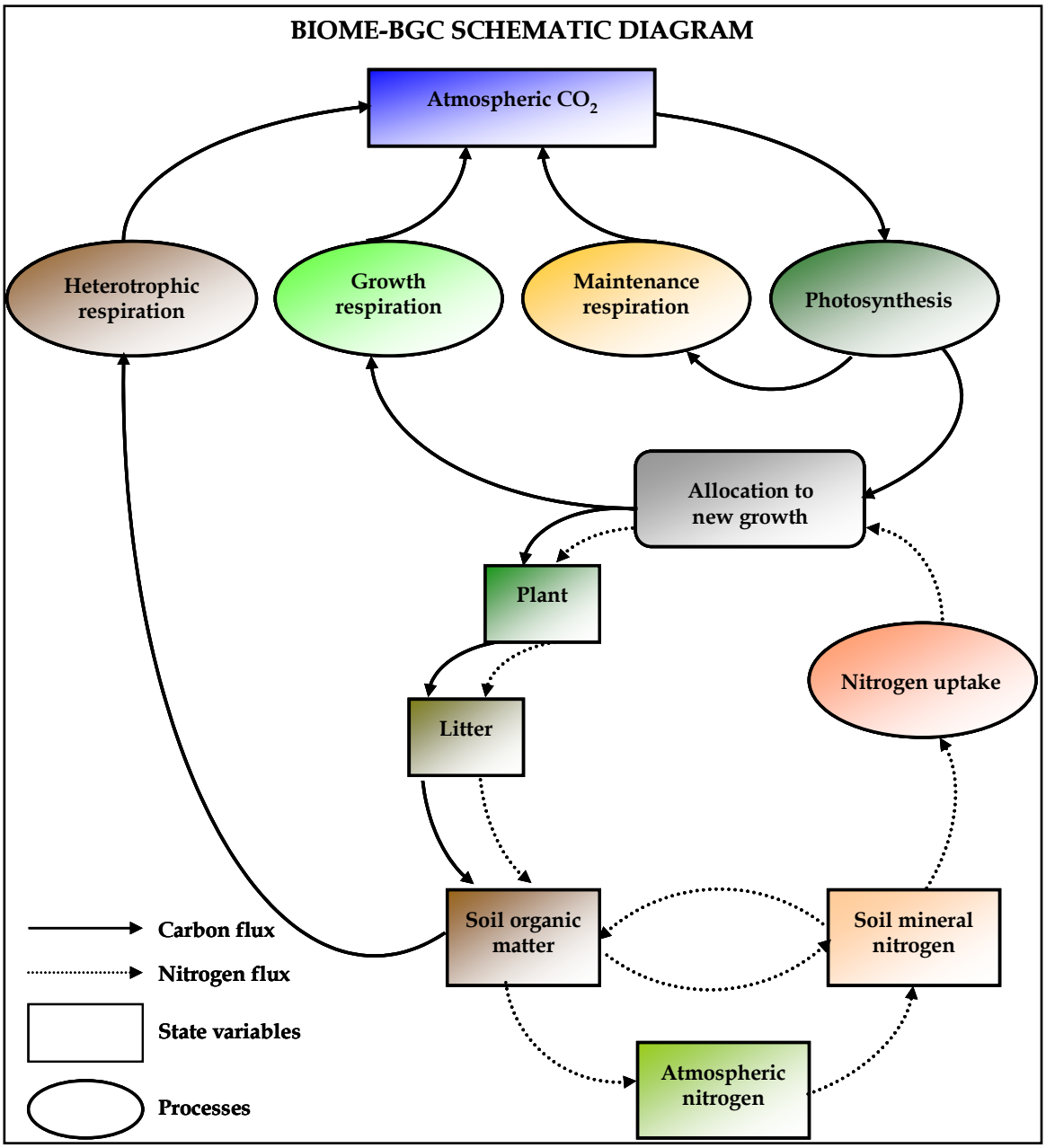

Figure 2-2 A simplified schematic diagram of fluxes and state variables for carbon and nitrogen components of the BIOME-BGC model. (*Source: Thornton, 2002)*

TURC is a light-use efficiency model that estimates NPP as for process-based TBMs on a daily basis on a 1° x 1° grid. However, unlike BETHY and BIOME-BGC, ecosystem processes, such as photosynthesis,

respiration and nutrient cycle, and other processes at ground and canopy levels are not modelled explicitly. Such models are termed diagnostic and use simple equations and assumptions to calculate the biospheric fluxes. TURC uses meteorological forcing of air temperature, humidity and incoming solar radiation, together with satellite observations of NDVI (normalised difference vegetation index) and a global map of ecosystem biomass to compute photosynthesis and respiration. The model works on the assumption that for every grid cell GPP is in balance with the sum of plant respiration for growth and maintenance, and soil respiration over one year. This means that the net CO_2 flux is null on an annual basis. This assumption restricts the use of the simulated fluxes to seasonal or shorter time scales, as in the case of BETHY.

2.2.4 Representation of key processes in the biosphere models

Common ecosystem processes:

A variety of ecosystem processes are included in BETHY and BIOME-BGC, such as new leaf growth and litter fall, snow accumulation and melting, drainage and runoff of soil water and transpiration of water through the leaf stomata. However, two key processes are handled in a similar manner by both TBMs: photosynthesis and total plant respiration. These are described below.

Photosynthesis

GPP in BETHY and BIOME-BGC is computed using the Farquhar formulation that uses two key parameters derived from the so-called, "A – C_i curve"[1]. These are:

1. V_{cmax}, the maximum carboxylation rate of ribulose-1,5-biphosphate carboxylase/oxygenase (Rubisco), and
2. $J_{max,}$ the maximum electron transport rate (Ethier *et al.,* 2004)

In their model, Farquhar *et al.* (1980) link equations describing Rubisco kinetics with others on the stoicheometry of the photosynthesis carbon reduction cycle and the photorespiratory carbon oxidation cycle, particularly on their energetic (electron transfer and ATP synthesis) requirements (Farquhar *et al.,* 2001).

In BETHY the Farquhar model computes GPP as the minimum of a carboxylation limited and an electron transport limited rate. Enzyme kinetic rates depend on vegetation temperature, the CO_2 compensation point and the two parameters describing the photosynthetic capacity, V_m and J_m (mentioned above), which are assumed to be vegetation type dependent (Knorr, 1997).

In BIOME-BGC this is computed with kinetic constants from Woodrow and Berry (1988) and DePurry and Farquhar (1997). The maximum rate of carboxylation is calculated separately by sunlit and shaded canopy fractions as a function of the canopy layer SLA, the leaf C:N ratio and the fraction of leaf nitrogen assumed to be deployed in the Rubisco enzyme.

[1] "A – C_i curve" describes net CO_2 assimilation rate (A_n) of a leaf as a function of leaf intercellular CO2 concentration (C_i) [For details see Farquhar *et al.,* 1980].

Autotrophic or total plant respiration

In BETHY, BIOME-BGC, as well as in TURC, the total plant respiration is computed as a composite of growth, R_g and maintenance respiration, R_m. In the two process-based TBMs, R_m is calculated as a function of tissue mass and tissue temperature, additionally with tissue nitrogen concentration in BIOME-BGC. In TURC, R_m depends linearly on air temperature (T_{air}) and organ biomass, B (of which three are distinguished: leaves, fine roots and wood (Lanfont *et al.,* 2002)). However, R_g in all is a simple proportion of total new carbon allocated to growth.

Differing ecosystem processes:

Apart from photosynthesis and total plant respiration, there are other important ecosystem processes that are modelled differently in the biosphere models. A few of these uniquely modelled processes are described here. The details can be found in Knorr (1997), Knorr (2000), and Knorr and Heimann (2001) for BETHY; Thornton (1998); Thornton *et al.* (2002) and Kimball *et al.* (1997) for BIOME-BGC; and Ruimy *et al.* (1996) and Lafont *et al.* (2002) for TURC.

1. Photosythesis in TURC

In TURC, the incoming solar radiation at the surface drives the day-to-day variability of the biosphere acting as CO_2 source or sink, as well as determines the amount of photosynthesis taking place. A linear relation between GPP and absorbed PAR is assumed as follows:

$$GPP = g\varepsilon fcRAD$$

where

c is the fraction of incoming solar radiation, *RAD*

f is the fraction of PAR actually absorbed by the vegetation derived from NDVI

ε is the photosynthesis efficiency parameter, and

g is a "freezing factor" that divides GPP by two when daily average air temperature is lower than -2°C during more than three consecutive days

2. *Stomatal conductance:*

The parameterisation of stomatal conductance in BETHY combines a reduced form of the Jarvis model with a dependance on the photosynthetic rate and a root-dependent supply rate (Knorr, 1997). In this scheme light is the primary regulating factor caused by the demand for CO_2 by photosynthesis. As a consequence of this, leaf internal CO_2 content stays near constant over a wide range of conditions. Additionally, a root signal is responsible for the closing of stomata so that a vapour pressure deficit of the surrounding air will not result in a reduction of stomatal conductance, as long as the root supply is sufficient. As modelling of root and leaf water potential is not feasible in the bucket model like BETHY, a simple empirical dependence on water vapour deficit is chosen, with a variable form depending on daily soil water content.

In BIOME-BGC, stomatal conductance varies in response to the radiant flux incident on the leaf, the leaf temperature, the difference in water vapour pressure between the atmosphere and the interior of the leaf, the soil water potential in the rooting zone and the atmospheric CO_2 concentration. This variation on the stomatal conductance has a strong influence on the rate of transpiration. The environmental parameters that

are assumed to influence stomatal conductance are: radiant flux density, air temperature, soil water potential, daily minimum temperatures below freezing and VPD (vapour pressure deficit). Of these, only radiant flux density is assumed to vary between the shaded and sunlit canopy fractions.

3. Heterotrophic respiration, R_h

For R_h a number of empirical descriptions exist (see, for example, Meentemeyer, 1978; Raich and Schlesinger, 1992; Lloyd and Taylor, 1994; Raich and Potter, 1995) that agree on an approximately exponential dependence of R_h on temperature, and on the fact that soil moisture is required for the heterotrophic organisms to produce CO_2 (Knorr, 1997). Such studies have also found clear temperature dependence with a Q_{10} of 1.58 related to air temperature for natural vegetation and of 1.49 for all types of vegetation. Q_{10} is a multiplicative factor describing the rise in respiration for a temperature increase of 10°C (Knorr, 1997) and is used in BETHY to simulate R_h. BETHY assumes that the annual soil respiration at each grid point of the model equals the annual NPP.

Unlike in BETHY model, in BIOME-BGC litter and SOM (soil organic matter) decomposition produces a heterotrophic respiration flux, which depends on the size of the litter and SOM pools and their decomposition rate constants. These rate constants depend on soil temperature and moisture. Decomposition also depends on the availability of soil mineral nitrogen, N, for those steps that are immobilising N.

The contribution of microbial respiration, which varies slowly as compared with, for example GPP, is not calculated in TURC. Instead, it is estimated as a function of soil temperature through a Q_{10} relationship:

$$R_h = V_0 \times Q_{10}^{(T_{soil}(t)-T_0)/10}$$

where

$Q_{10} = 2$

T_0 is the reference temperature of 0°C

V_0 is a factor through which a simple soil moisture impact is included in order to force a decrease in decomposition rate during periods with high soil moisture content

4. Phenology:

The phenology of vegetation describes the timing of the leaf onset, as well as the shedding of leaves for deciduous plants and grasses. The main purpose of such a periodical build-up and loss of leaves is the avoidance of frost and drought damage (Knorr, 1997). In BETHY, phenology is defined by the determination of the time dependence of the LAI as a function of air temperature, drought and carbon balance (Knorr, 1997).

In BIOME-BGC the phenology module consists of two independently formulated components, one for the predictions of the dates of onset and offset of leaves in forest systems and the other for such predictions in grasslands. For all vegetation types, some energy for growth of leaves and shoots can be stored for display during the following growing season. For this stored growth, the model developed by White *et al.* (1997) is used to estimate the leaf expansion and litter fall periods for deciduous broadleaf trees and for grasses. For all vegetation types the user can specify the proportion of the total growing season during which the stored growth is displayed. The growth that is not stored is displayed immediately. Thus the overall seasonal growth signal consists of one component due to

stored growth and a second due to current growth, the latter having a strong dependency on stored growth since it is the stored growth that augments the canopy leaf area and changes the growth potential independent of the current growing season conditions.

5. Processes not included in BETHY:

Compared to BETHY, BIOME-BGC additionally includes uptake of nitrogen from the soil, decomposition of fresh plant litter and old soil organic plant matter, plant mortality and fire (Coops *et al.*, 2001). Other N-related processes incorporated in BIOME-BGC but absent in BETHY include:

- allocation of carbon and nitrogen
- plant mineral nitrogen uptake, and
- litter and SOM pools

Details of each of these processes can be found in Thornton (1998) and Thornton *et al.* (2002).

2.2.5 Model setup of BETHY and BIOME-BGC

In the present study the spatial resolution used by the TBMs was 0.5°, latitude by longitude. This was chosen in order to be consistent with the atmosphere model REMO, which has a horizontal resolution of 0.5° and which used the simulated fluxes as input to estimate atmospheric CO_2 concentrations (see Chapter 5). Using the REMO resolution in the biosphere models enabled the simulated fluxes to be used directly in the

transport model without undergoing interpolation. The temporal resolution of the TBMs was daily.

BETHY

In the current study the output parameters GPP, NPP, R_h, LAI, surface reflectance, plant available soil water, actual and potential evapotranspiration, soil evaporation and rainwater runoff were computed after two years of spin-up. The spin-up simulation uses monthly mean climate at each grid point and gridded maps of vegetation and soil type as input data. The model has no long-term pools. The only memory comes from LAI and soil water. Therefore a spin-up is needed whereby equilibrium is assumed on a short time scale. There is no distinction in the model between the spin-up and normal runs. For the model runs, BETHY uses a control file containing information on the simulation and spin-up years, flags for selecting different processes (for example, photosynthesis scheme and type of vegetation map to use), and paths and names of input and output files. An illustration of BETHY control file is presented in Appendix A1.

BIOME-BGC

While in BETHY a single run accounts for both the spin-up and normal runs, regardless of point or grid simulations, BIOME-BGC requires two separate runs, one to take account of the model spin-up, and the actual model run to simulate the required state variables. For single-stand simulations the model requires a static description of the ecophysiological characteristics to establish the physiology, biochemistry, structure and allocation patterns of vegetation functional types. It is possible at single sites to measure such data, but as spatial resolution increases so does data unavailability (White *et al.*, 2000).

In BIOME-BGC carbon and nitrogen state variables represent the amounts of carbon or nitrogen stored in the simulated plant and soil pools. As a first step the model needs to be initialised for these state variables. This is done in the spin-up run, where the model is allowed to run to a steady state to obtain the size of the pools, assuming that the ecosystem is in equilibrium with the long-term climate. For this run, an initialisation file is used where general information about the simulation is defined, such as descriptions of the physical characteristics of the site (for example, elevation, latitude, root depth, sand/clay/silt percentages), the timeframe of the simulation, names of other input files (such as meteorology), names of output files that are generated at the end of the simulation, and a list of variables to be stored in the output files (Thornton, 2000). An example of the initialisation file is provided in Appendix A2. Following the spin-up a normal model run is required to simulate the ecosystem fluxes. A similar file as the initialisation file is used for the normal run with appropriate flags for the type of run (that is, spin-up or normal).

2.3 THE ATMOSPHERIC TRANSPORT MODEL REMO

The regional atmosphere-chemistry model REMO is based in the dynamical part on the Europamodell (EM version 2.1.1), the former numerical weather prediction model of the German Weather Service (Majewski, 1991). It includes physical parameterisations from the global climate model ECHAM-4 (Roeckner *et al.*, 1996). A detailed model description of the meteorological part and a number of sensitivity studies with REMO are presented in Jacob and Podzun (1997). Langmann (2000) implemented the tracer transport and chemistry part in the model. A brief

description of REMO is presented below, as well as the model setup in the current study.

REMO calculates the transport of atmospheric tracers online, together with the meteorology. The tracer transport is represented as horizontal and vertical advection according to the algorithms of Smolarkiewitz (1983). Detailed descriptions of the schemes used in REMO for the tracer transport can be found in the following references: Louis (1979), Mellor and Yamada (1974), (Langmann, 2000) and Tiedtke (1989).

Several studies have been done to evaluate the performance of REMO in simulating the atmospheric circulation on a regional scale (for example, Karstens *et al.,* 1996; Rockel and Karstens, 2001; Jacob *et al.,* 2001; Jürrens, 1999; van Meijgaard *et al.,* 2001). A number of studies have also investigated the transport properties of REMO through a detailed comparison of simulations of, for example the passive tracer ^{222}Rn with continuous measurements in Europe (Chevillard *et al.,* 2002b), showing the ability of REMO to represent fairly well the transport features on a synoptic and sub-synoptic scale.

In a companion study Chevillard *et al.* (2002a) investigated the spatial distribution and temporal variability of atmospheric CO_2 over Europe and Western Siberia using REMO, together with TURC. Comparisons with continuous measurements at ground stations and vertical profiles from aircraft measurements showed for their study period of July 1998 that REMO is able to simulate reasonably well the short-term variability of CO_2 concentrations.

In the present study, REMO (version 5.0) with ECHAM-4 physics parameterisation package (Roeckner *et al.,* 1996; Jacob, 2001; Jacob *et al.,* 2001) and a new vegetation cycle (Rechid, Pers. Comm., 2004) has been used. The land surface processes, controlled by the physiological vegetation properties, are represented in REMO by LAI (here, the ratio of one-sided leaf area to ground area), fractional vegetation cover (here, the fraction of photosynthetically active vegetation), background surface albedo, surface roughness length, forest ratio and water holding capacity (Rechid and Jacob, 2006). The vegetation cycle in REMO is independent of what is used in the TBMs to simulate the biosphere fluxes. REMO uses 20 vertical layers of unequal thickness between the ground and the 10hPa pressure level in a hybrid coordinate system with six layers below 1500m and an average thickness of the lowest layer of 60m.

Model setup

In the present study, REMO model was run on a horizontal resolution of 0.5^{o} on a rotated spherical grid system where the equator lies almost in the centre of the computational domain. Interpreted physically, this results in a horizontal grid size of approximately 55km x 55km. For the meteorological part of the model, analyses of the ECMWF, the European Centre for Medium-Range Forecasts, were used as initial and boundary conditions. These data have a time resolution of six hours. REMO uses time discretisation according to the leapfrog scheme with a time step of five minutes (Jacob and Podzun, 1996; Hagemann *et al.*, 2002). For the transport of chemical tracer species, a forward-in-time scheme (Langmann, 2000) with the storage of only one time level is used. This means that the transportation of the tracer specie is calculated at every time step of the meteorology computation in the model.

REMO can be operated in two different modes, "climate mode" or "forecast mode". In the climate mode (Jacob and Podzun, 1997) the model is initialised once and is then continuously forced at the lateral boundaries using either the results obtained from a global climate model or from ECMWF analyses. In the forecast mode (Karstens *et al.*, 1996), the mode of simulation used in the present study, the results of consecutive short-range forecasts of 30-hours are used. REMO is started for each day at 00UTC from the ECMWF analyses and a 30-hour forecast is computed. This forces the model state to stay close to the weather situation of these analyses. To account for a spin-up time the first six hours of the forecast are neglected. This spin-up time, as used in the above-mentioned previous studies, has been shown to be sufficient for the EM (Rockel and Karstens, 2001). It was therefore assumed adequate also for the present study. The transport of tracer species in REMO was calculated continuously by simulating only the meteorology in the first six hours of each run and passing the tracer fields directly from the last time step of the previous 30-hour forecast.

During a model run of REMO, a limited area model, the influence of CO_2 sources and sinks outside of the model domain has to be taken into account (Karstens *et al.*, 2006). In addition, the CO_2 that has been emitted from a source inside the model area and then left the area to be transported back in also needs to be allowed for. In this study simulation results from the global transport model TM3 (Heimann and Körner, 2003) have been used.

2.4 DATA SETS USED IN THIS STUDY

The data sets that were used in the present study include measurements of CO_2 fluxes and concentrations at single sites that have been used to validate the model simulations. The sources of the default model inputs of the two TBMs and the atmosphere model are described below.

2.4.1 Station observations

1. Standard meteorology data

The standard meteorology parameters required by the biosphere models (maximum and minimum air temperature, precipitation, downward solar radiation and vapour pressure deficit), as well as information on the site characteristics were obtained from the FLUXNET database (http://www.fluxnet.ornl.gov), a global network of micrometeorological flux measurement sites (Baldocchi *et al.*, 2001). This database contains continuous measurements of terrestrial ecosystem, carbon and energy exchange, key meteorological variables and ancillary data describing the location, vegetation and climate of the sites (Falge *et al.*, 2002). Long time series of meteorological data for a number of individual sites were obtained from the Max Planck Institute for Biogeochemistry in Jena, Germany.

2. CO_2 flux measurements:

The flux measurements were also obtained from the EUROFLUX database. FLUXNET provides estimates of NEE (net ecosystem exchange, or net CO_2 fluxes) at five temporal resolutions – half-hourly, daily, weekly, monthly and yearly – for both day and night. In the current study,

daytime data were used. One should be aware that the components of the net fluxes, such as GPP and respiration, are not measured directly. They are derived or estimated using algorithms and nocturnal fluxes (Falge *et al.,* 2002).

It is also important to note that, on average, the NEE measurements of the eddy covariance systems in the EUROFLUX project cover only 65% of the year due to system failures or data rejections (Falge *et al.,* 2001). This has led to the use of standardised gap-filling procedures to provide complete data sets. The EUROFLUX database reports gap-filled flux data, based on mean diurnal variation, look-up tables and non-linear regressions (Falge *et al.,* 2001). Detailed descriptions of these methods can be found in Falge *et al.* (2001). In the present study, NEE data were used that has been gap-filled by the mean diurnal variation method, as this was reported to be the most robust for most sites.

In addition to the EUROFLUX database, flux data for two Russian stations were included in the current study, which were obtained from the EUROSIBERIA CARBONFLUX project. Data for only July 1998 were available.

3. *CO_2 concentration measurements:*

For concentration data, measurements were obtained from the WDCGG, World Data Centre for Greenhouse Gases
(URL: http://gaw.kishou.go.jp/wdcgg.htm). These data were believed to be more reliable than the EUROFLUX database, as they are well calibrated.

Very limited aircraft profile measurements from West Siberia were made available from EUROSIBERIA CARBONFLUX project.

2.4.2 Model inputs

1. Meteorology input parameters:

The TBMs were driven by NCEP Reanalysis data, originally obtained from the NOAA-CIRES Climate Diagnostic Centre, Boulder Colorado, USA (http://www.cdc.noaa.gov). For the current study, the data were provided by the Max Planck Institute for Biogeochemistry, Jena, Germany, where they had previously been used in BIOME-BGC and were already in the format used by the model. These data cover the period 1948-2002 with a daily time step, on a spatial resolution of 1^{o} x 1^{o}, interpolated from the original 2.5^{o}, latitude by longitude. For consistency with other input data used in the current study, the required meteorology parameters were further interpolated to 0.5^{o} x 0.5^{o}, keeping the daily time step. The NCEP Reanalysis was used for both, the single-stand runs, as well as for spatial runs. In the latter, the spatial data was further interpolated to REMO grid, for the purpose of consistency with other spatial input data.

Specific to BETHY, the CRU (Climate Research Unit) climate data (http://www.cru.uea.ac.uk/cru/data) was used only for the spin-up. As there are no carbon pools in BETHY, a long time series of daily input, such as from NCEP Reanalysis, were not necessary. Instead, long-term climatology data from CRU was used, as in the previous studies with BETHY (for example, Knorr, 1997; Knorr and Heimann, 2001a, 2001b).

The atmosphere model used information from the ECMWF Reanalysis at the boundary and computes meteorology online during the model run.

2. *Surface input parameters:*

BETHY uses one input file containing all the required surface input information on a global scale at 0.5° x 0.5° spatial resolution. It uses the latitude and longitude positions, orographic information, soil type dataset by Dunne and Willmott (1996), based on the maps of the FAO (Food and Agriculture Organisation) and land cover type descriptions from DeFries and Townshend (1994). It should be noted that BETHY can be used with different vegetation maps but it has been developed using the DeFries and Townshend map (Knorr, 1997). Other information in the surface input file contains volumetric maximum plant available soil water fraction and maximum plant available soil water content. Other surface inputs, such as surface albedo, LAI, phenology, root depth and Q_{10} value are provided as constants. For station runs, the input data were selected for the nearest latitude and longitude positions of the stations, while for spatial runs the data were interpolated to REMO grid.

BIOME-BGC, when used for single-stand investigations, uses site-specific information (meaning measured or derived information for the particular site being investigated), such as the location of the site, effective soil depth, percentages of sand, silt and clay, pre-defined ecophysiological (EPC) information (see Appendix A3) on the vegetation types at the sites and information on atmospheric CO_2 and nitrogen deposition, as well as surface albedo, as described in the initialisation file. When extended to spatial investigations, the surface information is provided to the model by means of 0.5° regridded spatial maps of industrial and pre-industrial nitrogen concentration (NONH), clay and sand cover, and a land cover map based on the Global Land Cover Characterisation Data Base (http://www.edcsns17.cr.usgs.gov/glcc/), containing the EPC indices.

Each index in the map corresponds to one input EPC file, as shown in Appendix 3. As for all other spatial inputs, BIOME-BGC maps were also interpolated to REMO grid.

In REMO, the land surface processes are simulated using LAI, fractional vegetation cover, background surface albedo, surface roughness length due to vegetation, forest ratio and water holding capacity. Within the model domain CO_2 fluxes were prescribed from three main sources: the terrestrial biosphere (provided by the outputs of BETHY and BIOME-BGC after being resolved for their diurnal cycles); fossil fuel burning (derived from the global emissions data set EDGAR – Emissions Database for Global Atmospheric Research (http://gcmd.nasa.gov/records/GCMD_EDGAR_RIVM.html); and ocean fluxes (taken from Takahashi). At the boundary the CO_2 concentrations due to fossil fuel burning, ocean and terrestrial biosphere were prescribed from the global atmosphere model TM3, which was obtained as part of an earlier study during the EUROSIBERIA CARBONFLUX project (1998). The biosphere fluxes were provided from TURC.

CHAPTER 3
CO_2 FLUX SIMULATIONS AT SELECTED SITES

3.1 INTRODUCTION

Terrestrial biosphere models have widely been used to simulate carbon fluxes at a regional or continental scale, but their performance can only be evaluated on a local scale. Continuous measurements of biosphere fluxes are only available at single sites where measurement towers have been constructed. Comparison of the simulated fluxes with observations is important in order to gain confidence in the model results, as well as to identify weaknesses and to explain the differences that may arise due to the choice of the model and the input data that are being used.

The aim of the present chapter is to compare the simulated CO_2 fluxes of the two process-based TBMs BETHY and BIOME-BGC with observations at selected FLUXNET sites located in the study domain. For this purpose the TBMs were run for a single year (1998), with site-specific input parameters and meteorology. It should be noted here that TURC is not included in this chapter, as the fluxes simulated by TURC serve only as comparison material on regional scale (see Chapter 4).

Due to their structural differences and the complexities of the processes involved the model performance of the two TBMs will be different. As

discussed in the preceding chapter, BETHY simulates the carbon and water cycles, while BIOME-BGC additionally includes a complete nitrogen cycle. The fact that BIOME-BGC has carbon and nitrogen pools means that it requires a long time series of meteorological inputs for spin-up of the model. However, for most FLUXNET stations this long-term information is not available. Three experiments were therefore designed to test the response of the two models to different choices of meteorological input. First, the models were forced with the observed meteorology at the measurement sites; in the second experiment, the models were driven by NCEP Reanalysis data of historical climate conditions (see Chapter 2); and finally, a combination of the two data sets was used to compensate for the lack of long time series of meteorological observations. As the NCEP Reanalysis data have also been used in the next step of this study (i.e. the regional simulations, see Chapter 4), a comparison with the observations may also provide an indication of some shortcomings of this dataset.

Most of the input parameters of the two TBMs cannot be measured with great accuracy, even at single sites. To gain insight as to how uncertainties in the different input data sets contribute to the uncertainties in the estimation of the biosphere fluxes, some sensitivity tests were conducted. This was done by means of altering the values of a few important process-driving input parameters, such as the amount of precipitation and the rooting depth, and investigating the response of the models.

The following sections provide some details of the FLUXNET sites that have been investigated, as well as the experimental approach that was adopted. The results section is divided in two parts: the first presents the outcomes of the three model experiments using different choices of input

meteorology, the second part discusses the sensitivity tests that were conducted.

3.2 STATIONS INVESTIGATED

Within the study domain of Eurosiberia, which stretches from Europe to Western Siberia, a total of nine stations were investigated for the study period of 1998. This particular year was selected due to the availability of the necessary observed data for this year. The selection of the stations was mainly based on the availability of observation data, both for the standard meteorology and for CO_2 fluxes from eddy covariance measurements at the sites.

Figure 3-1 shows the study domain with the sites that were investigated. In Western Siberia there have been very few flux measurement towers until recently, whereby several measurement campaigns and continuous measurement projects, such as FLUXNET, ASIAFLUX, and AMERIFLUX are currently underway, with the aim of establishing a global network of flux information. One such measurement campaign was the EUROSIBERIA CARBONFLUX project that was conducted in 1998 as part of a feasibility study for the development of an observing system to quantify the regional and continental scale fluxes of CO_2 and other trace gases (Heimann, 1998).

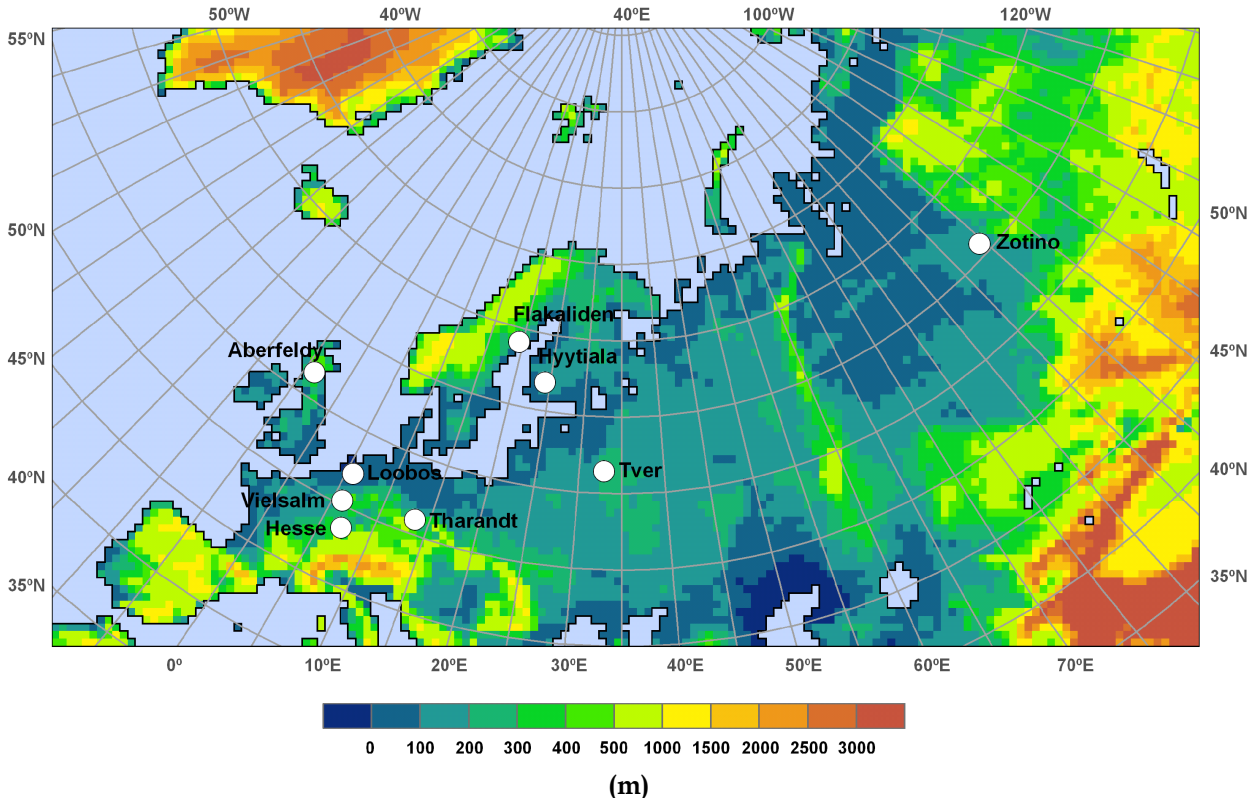

Figure 3-1 Topography of the study region with the FLUXNET sites investigated in this chapter

Table 3-1 provides a summary of the station characteristics for the sites investigated in the present study. Details of the European sites are on the FLUXNET World Wide Web database site (http://fluxnet.ornl.gov), while information on the Russian sites, Tver and Zotino, was obtained from the EUROSIBERIAN CARBONFLUX project.

The soil types at individual sites are of particular importance, as they play a major role in the carbon cycling process. They contribute to the water availability for plants depending on their water holding capacity. For single-stand simulations BIOME-BGC uses the site-specific soil type while BETHY uses the dataset by Dunne and Willmott (1996), based on the maps

of the FAO (Food and Agricultural Organisation), on 0.5° grid scale. In both TBMs the bucket size is 1m.

Table 3-1 Summary of site characteristics

Stations	Lat/Lon	Elev (m)	Climate	Annual mean T_{air} (°C)	Annual mean precip (mm)	Vegetation type	Avg forest age	Soil type	Soil depth (m)	Tower meas height (m)
Aberfeldy (UK)	53°37″N 03°47″W	340	Atlantic	8°C	1200	Coniferous forest	14	Stony podsolised	0.7	15.5
Flakaliden (Sweden)	64°07″N 19°27″E	225	Boreal	1.9°C	587	Evergreen coniferous	31	Till	0.45	14
Hesse (France)	48°40″N 07°05″E	300	Temperate-continental	9.2°C	885	Deciduous broadleaf	30	Greyic luvisol	1.6	18
Hyytiälä (Finland)	61°51″N 24°17″E	170	Boreal	3.5°C	640	Evergreen coniferous	30	Till	0.4	23.3
Loobos (The Netherlands)	52°10″N 05°44″E	25	Temperate	9.8°C	786	Evergreen coniferous, spruce	80	Sandy	0.5	27
Tharandt (Germany)	50°58″N 13°34″E	380	Temperate-continental	7.5°C	820	Evergreen coniferous	140	Brown earth (rhyolith)	1.5	42
Vielsalm (Belgium)	50°18″N 06°00″E	450	Temperate	7.5°C	1000	Deciduous broadleaf, mixed beech	60-90	Dystric cambisol	1	40
Tver(*) (Russia)	56°27″N 32°55″E	220-280	Continental	Not available	Not available	Spruce, boreal	150	Non-calcareous loam and loamy sand	1	48
Zotino(*) (West Siberia)	60°45″N 89°23″E	505	Continental	Not available	Not available	Coniferous forest	203	Not available	1	Not available

(Derived from FLUXNET site, http://www-eosdis.ornl.gov/FLUXNET/)
(*) Derived from the EUROSIBERIAN CARBONFLUX project

The specifications of the vegetation types in the TBMs for single-stand simulations are also crucial. As for the soil types, BIOME-BGC uses site-specific vegetation type information that are described in terms of the ecophysiological constants while BETHY uses the land cover dataset by DeFries and Townshend (1994).

3.3 APPROACH TO SINGLE-STAND SIMULATIONS

3.3.1 Experimental design

For the single-stand investigations the two TBMs BETHY and BIOME-BGC were forced with different sources of standard meteorology inputs, keeping all other input parameters specific to the models constant. Although the TBMs use a daily time-step, the length of the time series of meteorological data required by each model is different. The limited availability of long-term observations is the prime motivation for designing and conducting three different model experiments using (1) the observed meteorology, (2) model-derived re-analysis data and (3) a combination of station observations and re-analysis data. The influence of these different input data sets and their effects on the estimation of biosphere fluxes, as well as their possible contribution towards the uncertainties in the flux estimation were investigated. Figure 3-2 shows a schematic flow diagram of the experimental design for single-stand experiments.

The use of the three different types of datasets in the models, keeping all other variables constant, allowed for the responses of the TBMs to be monitored and evaluated in terms of the influence that the input data has

on the model estimations of the fluxes. In this way an insight is also gained in the way the models handle the input data.

3.3.2 Model experiments

In Experiment 1 the TBMs were run with the available observational meteorology data, which for most stations were up to three years. BIOME-BGC requires longer time series (at least 10 years or more) in order to bring the carbon and nitrogen state variables to equilibrium before the simulation of CO_2 fluxes. However, in this experiment, during the spin-up simulation the limited meteorology was used repeatedly until the model reached the assumed equilibrium. This poses a danger that, due to the incorrect dynamics in the climate data, the initial state of the variables is either over- or under-estimated, hence affecting the estimation of the simulated flux variables. In BETHY there are no litter, soil or carbon pools. Long spin-up time is therefore not needed for the state variables to come to equilibrium.

In Experiment 2 the NCEP Reanalysis data was used for spin-up, as well as the actual simulation. A total of 55 years of the data was used for BIOME-BGC run, while in the case of BETHY four years of data was sufficient. A major disadvantage of this method is that climate data at a half-degree grid scale is combined with site-specific information of a single location within the grid. This is particularly the case for BIOME-BGC that used site-specific surface inputs; for BETHY the surface data for each station were originally also on a half-degree grid and have been extracted from corresponding grid boxes. Here, the assumption is that the

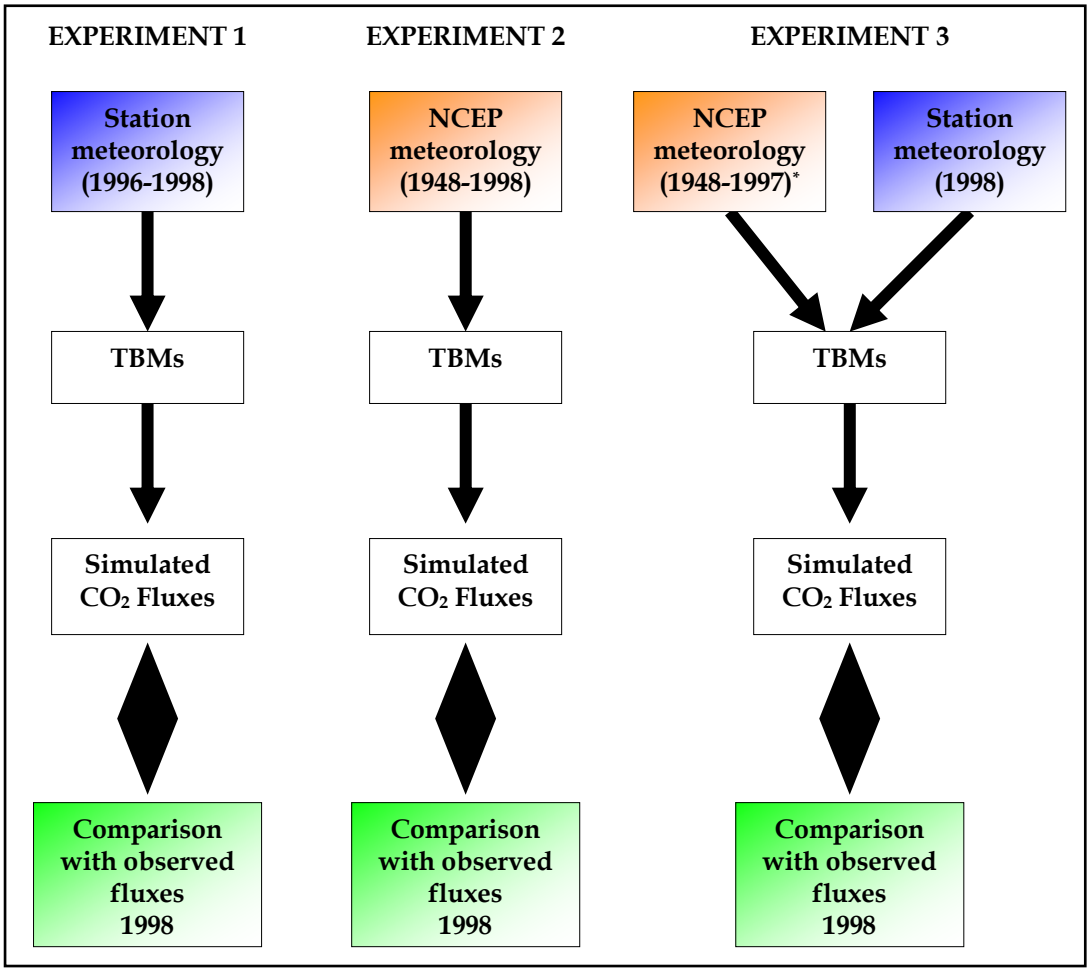

Figure 3-2 Schematic flowchart of single-stand model experiments. * indicates the length of NCEP data used in BIOME-BGC for Experiment 3. In BETHY a shorter time period was used, 1995-1997. Experiment 2 was used further for sensitivity tests.

large-scale data provide the best-available estimate of the local climatological conditions.

In Experiment 3 the NCEP Reanalysis data was used for spin-up, followed by the use of observed meteorology for the actual simulation period of 1998. It was believed that in this way the re-analyses data could compensate for the limited observations needed for the spin-up of BIOME-

BGC, meanwhile maintaining the local weather conditions for the actual flux simulations.

3.3.3 Sensitivity tests

In a second series of experiments the sensitivity of the TBMs to uncertainties in the model input was tested by changing a few process-driving input parameters and other important but uncertain input, like the rooting depth. The selection of the parameters to test was based mainly on the uncertainty in their measurement. Presented here are the results for rooting depth, precipitation levels and air temperature.

Rooting depth is the depth at which plants are able to grow roots and which, to some extent, determines the water availability. This has important implications for the whole ecosystem, specifically the hydrological balance, as well as the carbon and nutrient cycling (Canadell *et. al*, 1996). Rooting depths play an important role in determining the net primary production and transpiration in the terrestrial ecosystems, particularly in water stress situations, but information on the rooting depth is hardly ever available, certainly at large spatial scales. It is therefore important to test the behaviour of the models when subjected to varying root depths.

The water availability for plant functions is important in growth and reproduction, nutrient cycling and net ecosystem productivity. It depends not only on the rooting depth but also on the amount of precipitation. Large-scale precipitation estimates are however subject to errors. The sensitivity of the TBMs to this was investigated and explained in terms of

productivity by altering the precipitation levels that were provided as input to the models.

Temperature is a fundamental factor that affects the rates of most biological and chemical reactions in the ecosystems and thus plays an important role in regulating the flow of energy, water and nutrients within and through ecosystems (Rustad & Norby, 2002). The responses of BETHY and BIOME-BGC to changing temperature inputs were therefore included in the sensitivity analysis.

In each of the sensitivity runs the TBMs were forced with the NCEP Reanalysis data, as used in Experiment 2. In this way the outcomes are comparable with the regional flux simulations on a spatial scale that also used reanalysis data (see Chapter 4). Here, the outputs of each of the tested parameters have been analysed and compared with the control run of Experiment 2.

3.4 RESULTS AND ANALYSES

This section is divided into two parts. The first part describes the results of model-model and model-observation comparisons and analyses of the three experiments performed at single-stands in the study region using the two TBMs. The second part discusses the results of the sensitivity tests.

3.4.1 Flux comparisons at single stands

Nine FLUXNET stations were investigated. For detailed discussions and explanations the results of two stations are presented here as examples. The stations were chosen from two different climatic zones. Aberfeldy, located at 56° 37′ N and 3° 48′ W in the United Kingdom, is situated in the temperate/oceanic climate zone at an elevation of 340m above sea level. The dominant vegetation type at this site is coniferous forest. The second station shown as example is Hyytiälä in Finland, located at 61° 51′ N and 24° 17′ E, and situated in the boreal climate zone at an elevation of 170m above sea level, also with coniferous forests as the dominant vegetation type. The results of the two stations are presented in figure 3-3, while those of the other stations can be found in Appendix A4.

The analyses work focussed mainly on the net carbon exchange of the ecosystem, NEE, computed as the difference between GPP and R_{total}:

$$NEE = GPP - R_{total}$$
$$R_{total} = \left(R_g + R_m + R_h\right)$$

It should be noted that the flux components GPP and R_{total} are not measured directly at the FLUXNET stations. Instead they are estimated or model-derived, which should be kept in mind when comparing the station data of GPP and R_{total} with the TBM simulated components, particularly where large differences occur. NEE, however, is not model-derived but measured directly by the use of eddy covariance technique (Dennis *et al.*, 2001). Comparison plots of simulated and station fluxes at two FLUXNET stations, Aberfeldy and Hyytiälä, are presented.

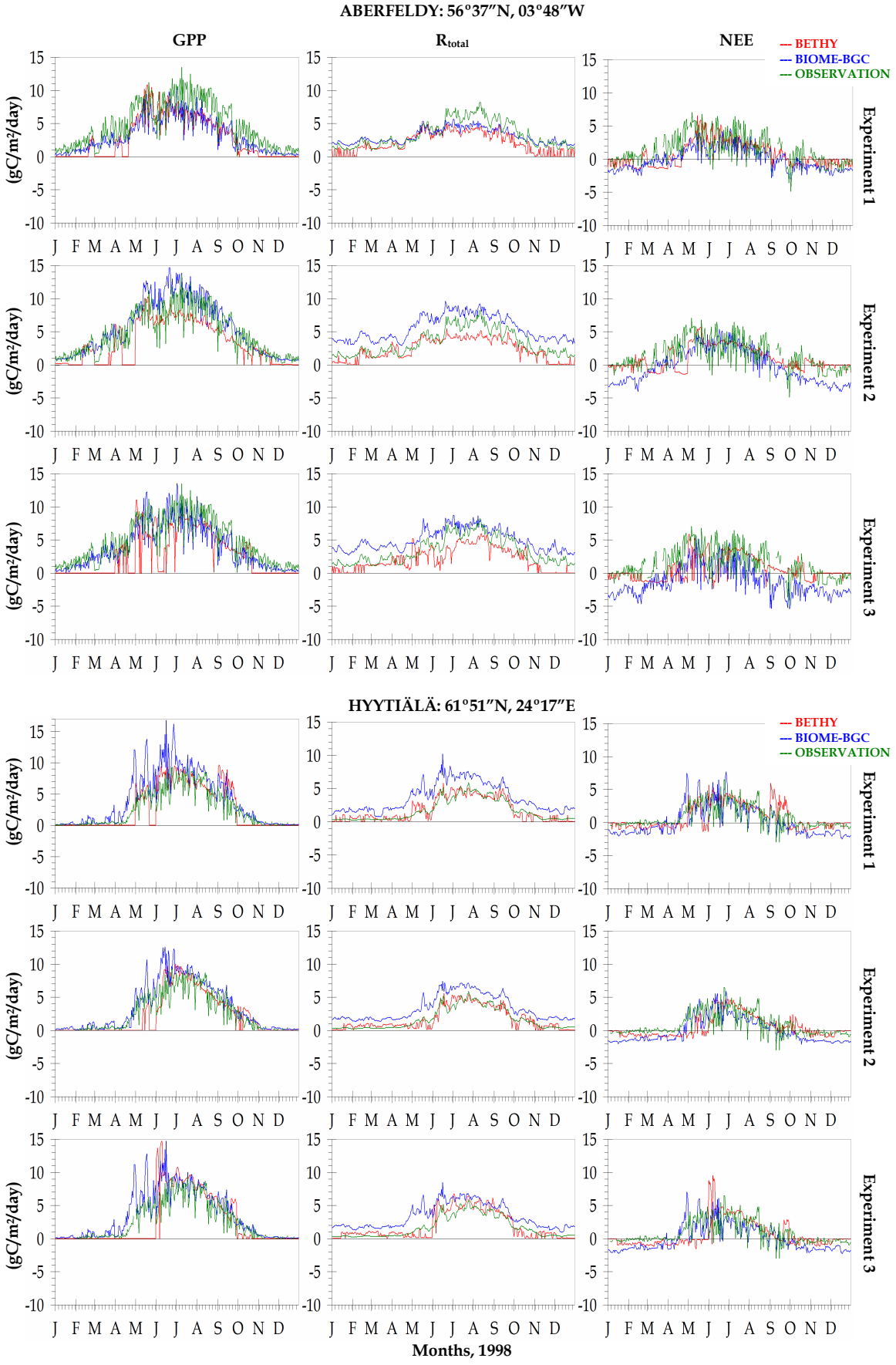

Figure 3-3 Simulated versus observed CO_2 fluxes for 1998 at Aberfeldy and Hyytiälä for three experiments

Gross Primary Production, GPP:

Figure 3.3 shows in general that both TBMs are able to simulate the seasonal cycles of net CO_2 fluxes and flux components over 1998. Features, such as low productivity at the beginning and at the end of the year during the colder seasons, and peak production during summer correspond with what is expected. However, a closer look at the plots shows differences, both between the two models and between the models and observations.

An interesting behaviour of BETHY, particularly obvious in the plots of production and net fluxes, is related to the sudden dips that occur before summer, whereby both the GPP and the corresponding NEE suddenly drop to zero. A possible explanation for this behaviour lies in the availability of the plant soil water in the model. If the water available to plants goes below a certain threshold, the so-called "wilting point" is reached, causing production to cease (Reick, Pers. Comm., 2005). The amount of water available to the plants in the model depends directly on the precipitation, which is one of the most important input parameters to both TBMs and is directly related to the productivity processes. Figure 3-4 shows the observed daily precipitation for Aberfeldy and Hyytiälä, as compared with the NCEP precipitation, for 1998.

In the BETHY experiments the days when GPP go to zero correspond to those periods when the observed precipitation is low, as shown in figures 3-3 and 3-4, respectively. For example, early spring at Aberfeldy show no production, which corresponds to low precipitation from NCEP and observation. During winter, production is zero at both stations from BETHY experiments, while BIOME-BGC shows some productivity, which is consistent with the observations. Comparing particularly Experiments 1

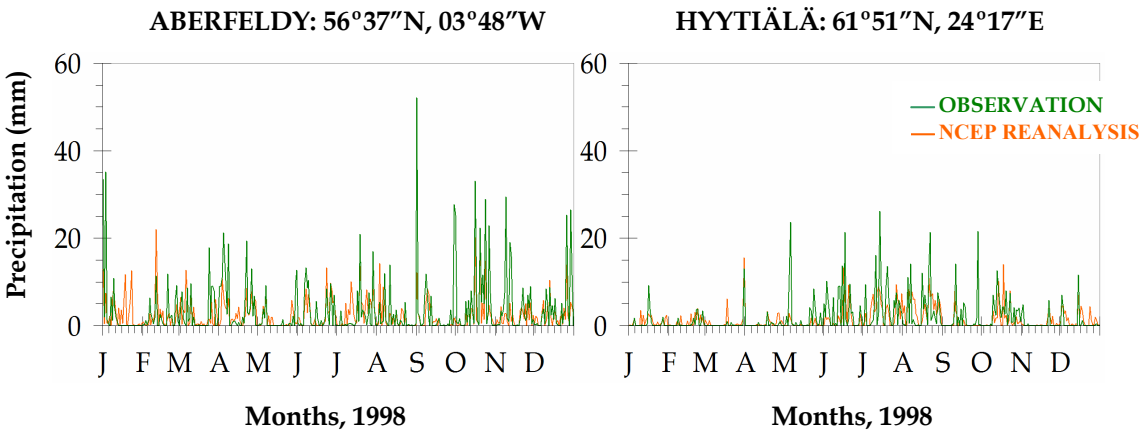

Figure 3-4 NCEP Reanalysis and observed daily precipitation comparison at Aberfeldy and Hyytiälä

and 3 shows that BETHY seems to have a memory from the previous year, indicated by the prolonged period of zero productivity at both stations. The temperature plots for the two stations in figure 3-5 also show dips occurring in minimum and maximum temperatures on the respective days when GPP in BETHY is at its minimum. Looking at the three experiments at both stations in figure 3-3 we see that BIOME-BGC simulated GPP is closer to observations than BETHY where frequent wilting point thresholds are encountered.

To summarise the comparison of GPP for all stations investigated, the annual sums were calculated and plotted as xy-plots (figure 3-6). The data points lying above the x=y line indicate an over-estimation of the simulated GPP, while those lying below indicate underestimation.

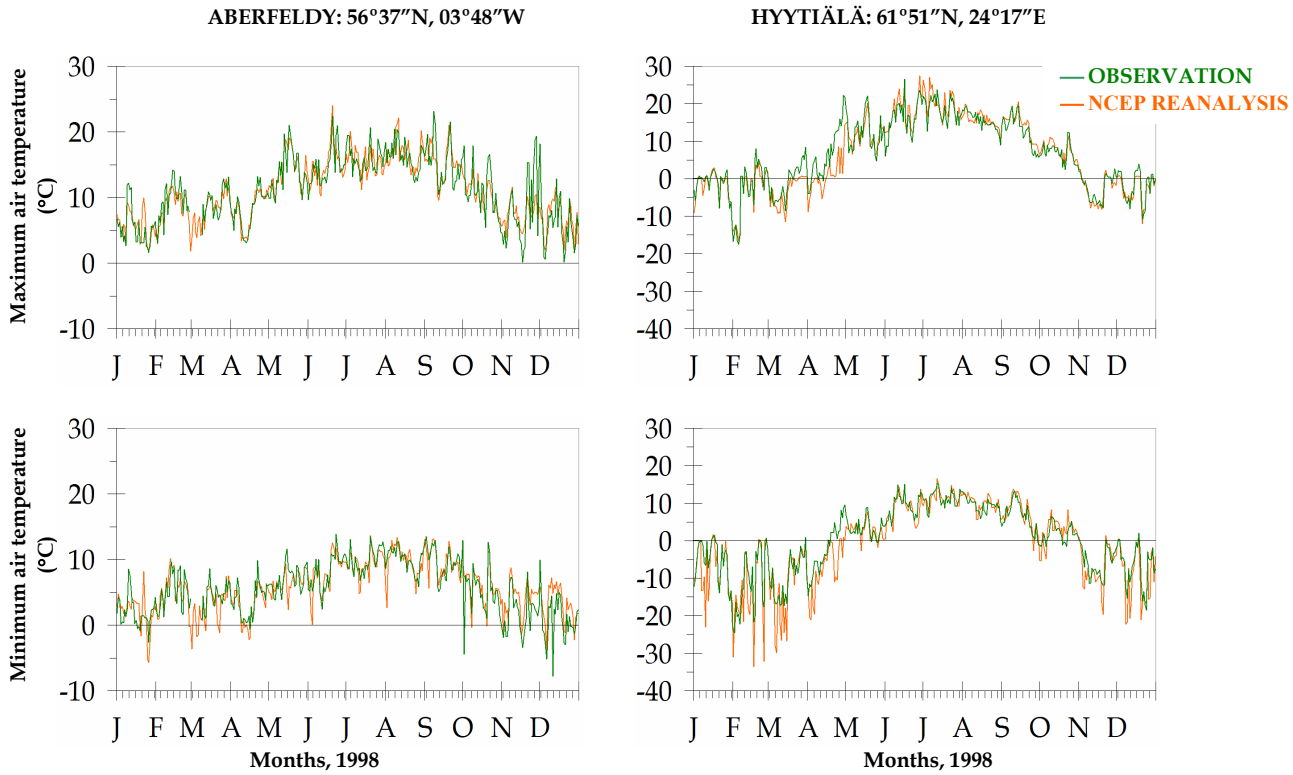

Figure 3-5 NCEP Reanalysis and observed daily maximum and minimum temperature comparisons

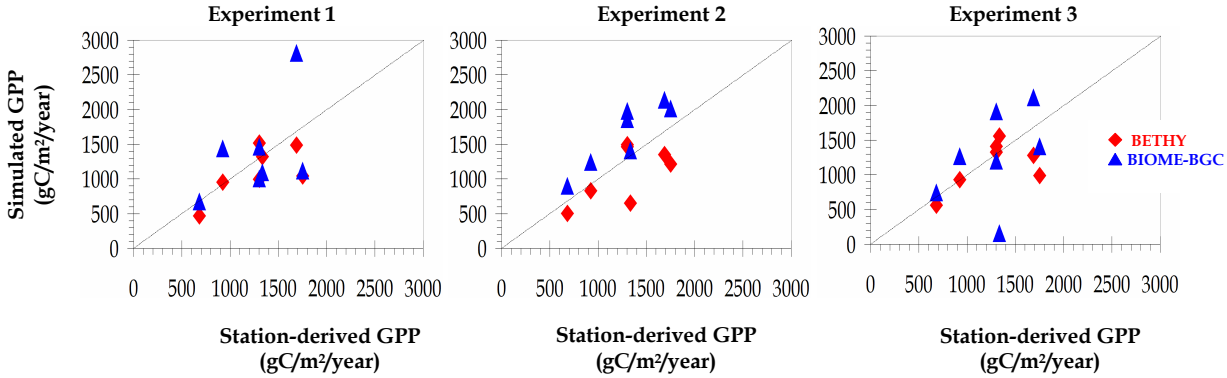

Figure 3-6 Summary XY-plots of GPP to show model-model and model-observation comparisons at all stations

Overall the xy-plot of Experiment 1 shows a better correspondence of the simulated GPP with each other, as well as with the observations despite the limitation on the meteorology input. However, at one station (Tharandt) BIOME-BGC shows a strong over-estimation of the annual sum of GPP. Likewise it shows a strong under-estimation at Hesse in Experiment 3. In Experiment 2 BIOME-BGC tends to over-estimate GPP at all stations except Hesse, where both models show good comparison with each other, as well as with the observation.

The high productivity at Tharandt from Experiment 1 can in part be explained by the LAI projected by BIOME-BGC. LAI is a measure of lateral leaf density in the canopy, and is defined as the projected area of leaves over a unit of land, which can serve as a possible measure of carbon accumulation (Churkina *et al.*, 2003). The high LAI, and consequently a high total carbon in the model, lead to high production. According to Churkina *et al.* (2003), the over-estimation of LAI and hence GPP in BIOME-BGC also illustrates the problem with modelled respiration, which in the present study is also over-estimated at Tharandt (see for example the summary plot for Experiment 1 in figure 3-8).

Another possible reason for the high GPP at Tharandt lies in the way the simulations were performed. BIOME-BGC is a model that simulates mature forest stands (Vetta, Pers. Comm., 2005), and the history of each simulating stand becomes important in order to have the right carbon and nitrogen pools at the initialisation stage of the model. In reality, natural and anthropogenic disturbances, such as cultivating and grazing, not only affect the ecosystems but also change the sizes of their carbon and nitrogen pools, thereby shifting most of the world's ecosystems away from the assumed equilibrium. Ignoring disturbance impacts in the model can

lead to under-estimation of the state variables (Churkina *et al.,* 2003). Therefore the knowledge of the site history becomes important in order to correctly initialise the model state variables representing disturbed ecosystems. Churkina *et al.* (2003) performed a study where such a correction for re-initialising the carbon and nitrogen pools was exercised, using the same model at the same site as in the present study. The outcome of this re-initialisation exercise was shown to have greatly improved the simulated fluxes. In the present study this was not performed. However, it is important to note that stand history may play a role in ecosystem productivity.

Total respiration, R_{total}:

The two main components of terrestrial ecosystem respiration that contribute to R_{total} are autotrophic, R_A, and soil or heterotrophic respiration, R_h. R_A comprises of growth and maintenance respirations, R_g and R_m, respectively, while R_h includes microbial and litter respirations. In both TBMs used in the current study, R_{total} is estimated on a daily basis as the sum of R_g, R_m and R_h. See table 2-1.

Figure 3-3 (shown earlier) indicates a good comparison of simulated and observed R_{total} in terms of the seasonality and amplitude, for Experiments 1 (at Aberfeldy) and 3 (at Hyytiälä). Generally, R_{total} simulated by BIOME-BGC tends to be higher in amplitude for most experiments at the two stations. One possible explanation for this may lie in the initial state variables of carbon and litter pools. In both TBMs, R_h represents the loss of carbon from the system resulting from soil microbial respiration, estimated as a proportion of prescribed soil and litter carbon pools. The amount of carbon being respired on a daily basis is regulated by soil water potential and soil temperature. If the initial pools are high it leads to a

high total ecosystem respiration. BETHY has a simple soil model that estimates R_h as a function of soil temperature and Q_{10} value (see Knorr, 1997).

Figure 3-7 shows the contribution of the components of respiration common to the two TBMs, R_A and R_h, towards R_{total}. These components are not available from station observations, as they are not easily measured. Therefore only the two model estimates are presented. The plots show that while R_h of the two models are closer together, BIOME-BGC always shows higher R_A and R_h then BETHY, which leads to high total respiration in BIOME-BGC, seen in figure 3-3. The high R_A can be attributed to the high LAI estimation that leads to high production, hence high plant respiration.

As for GPP, summary xy-plots for the three experiments are presented in figure 3-8. The plots show the model-model and model-observation comparison of total ecosystem respiration for all stations. As can be seen, the BIOME-BGC estimates are generally higher than those of BETHY, and in Experiments 2 and 3 mostly higher than observations as well.

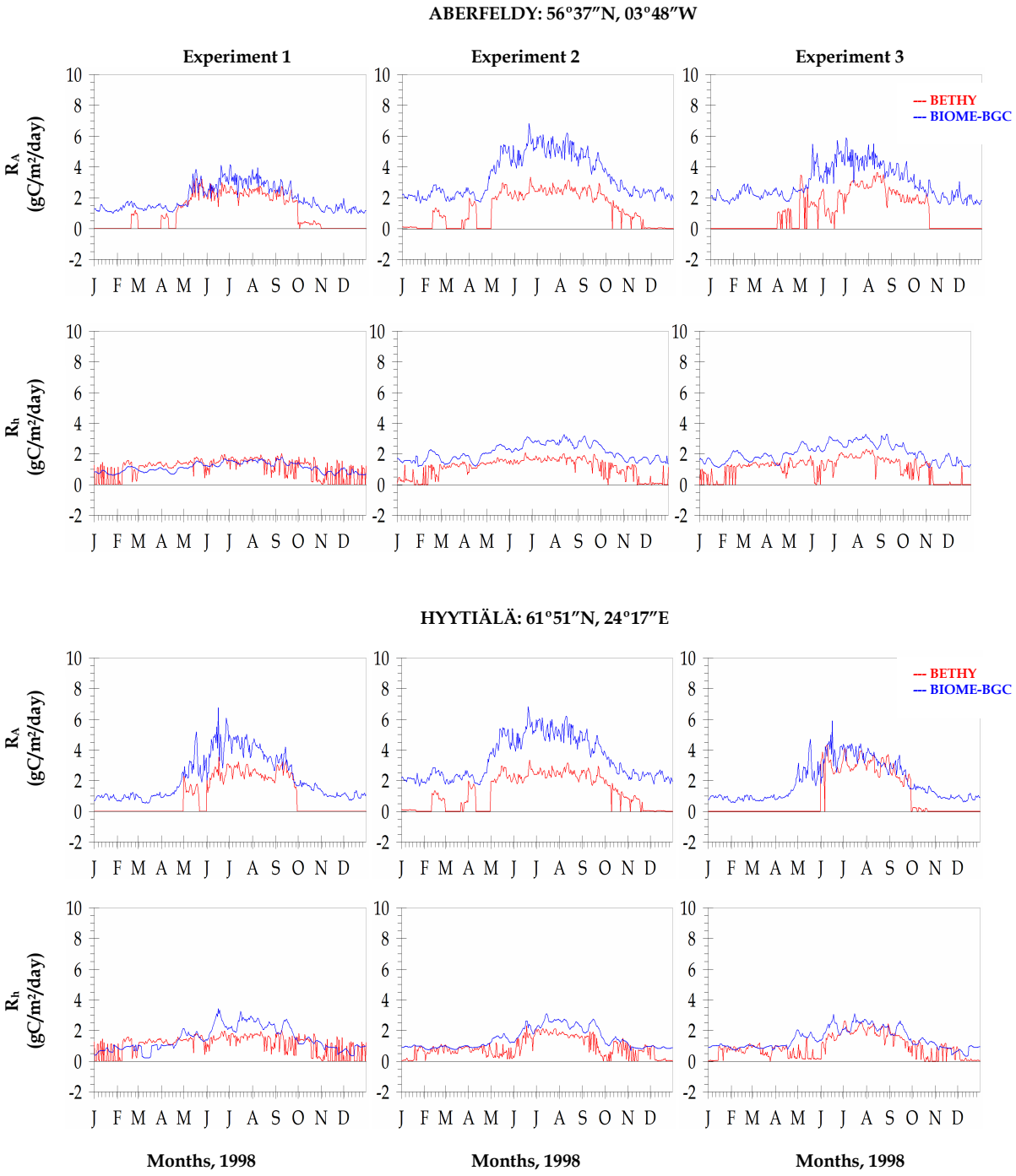

Figure 3-7 Total respiration components, R_A and R_h, comparisons from BETHY and BIOME-BGC at Aberfeldy and Hyytiälä

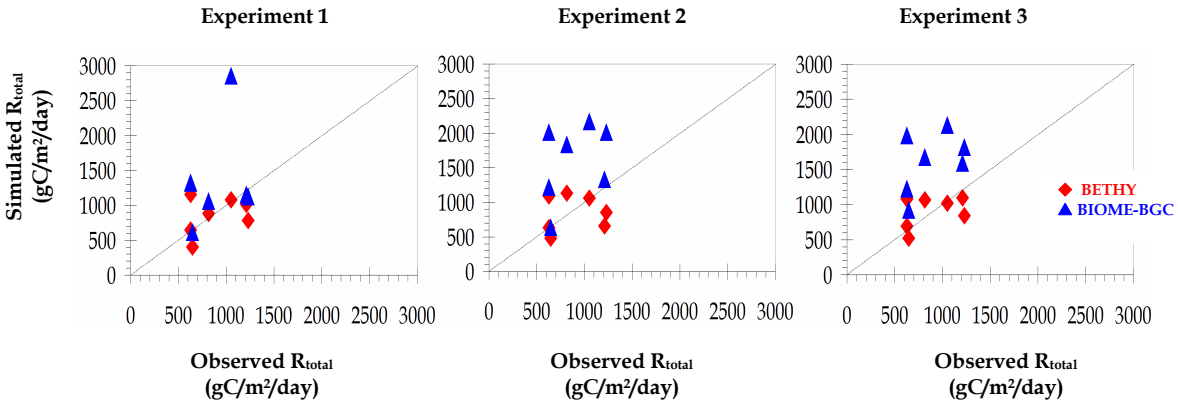

Figure 3-8 Summary XY-plots of total respiration to show model-model and model-observation comparisons at all stations

Net ecosystem exchange, NEE:

The plots of NEE in figure 3-3 show that in all experiments the simulated and observed net fluxes are in better agreement than the individual components. Although differences in NEE can be seen between the observations and simulations, as well as between the two model simulations, they are not as large as, for example, seen in GPP or R_{total}. This is due to the fact that the errors in the components compensate to bring the simulated fluxes closer to the observations.

Fluxes at all stations:

Figure 3-9 shows an overview of the simulated and observed fluxes for all stations. In both TBMs, GPP is balanced with R_{total} annually, assuming an equilibrium state of the system where NEE on an annual basis is zero. For this reason it doesn't make much sense to calculate annual sums of the fluxes. Instead the seasonal sums of two contrasting seasons i.e. the winter and summer of 1998 have been calculated (see Figure 3-9).

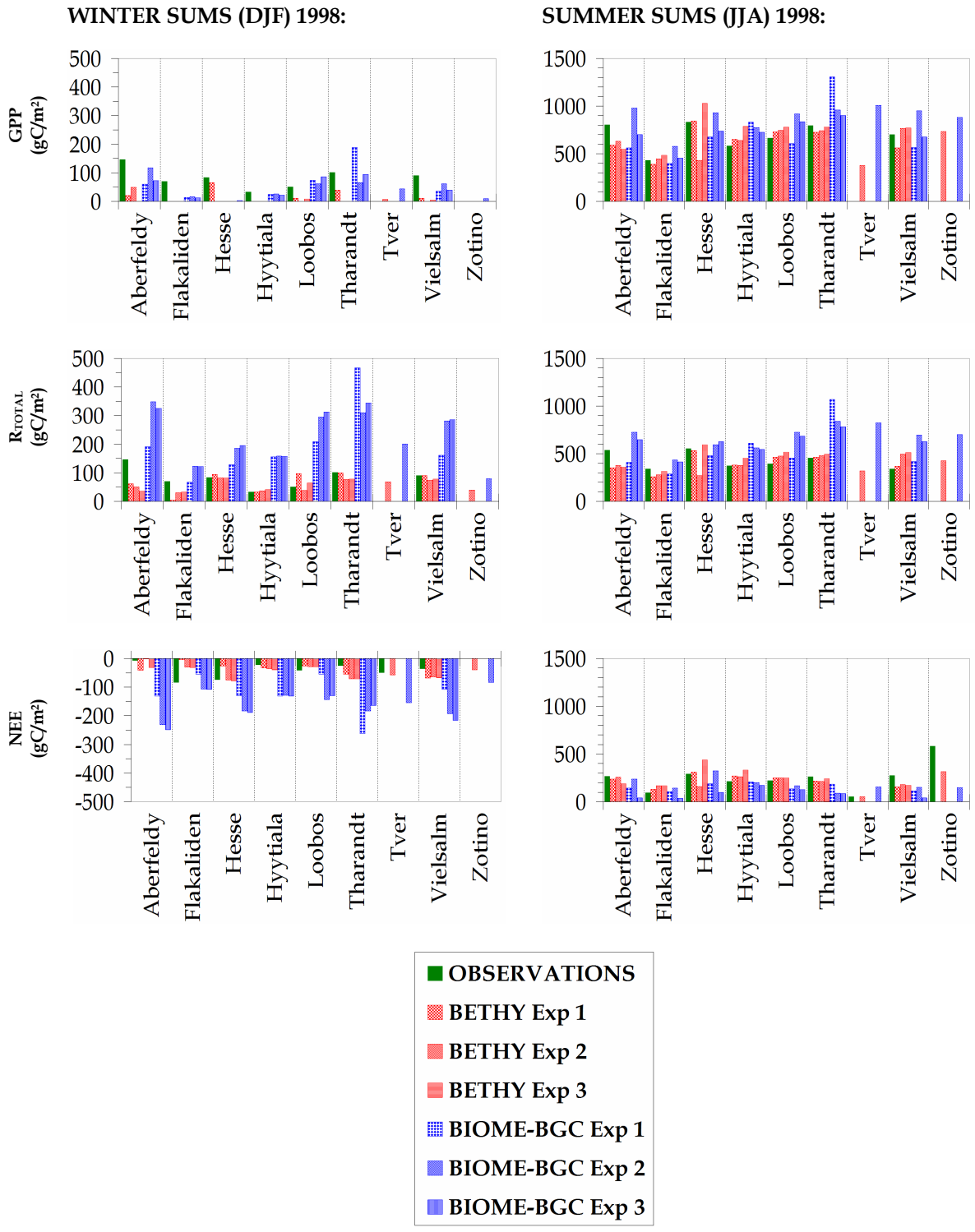

Figure 3-9 **Summary plots of flux comparisons with observations at nine FLUXNET stations. Negative NEE implies a release of CO_2 by the vegetation, while positive values indicate an uptake.**

Over all stations, BIOME-BGC simulates a higher total respiration than BETHY during winter and summer. Both models, however, show increased GPP and total respiration over summer, with amplitudes closer to each other than to observations, indicating that the ecosystem processes in both models are handled in a similar way, as indicated in the previous chapter. The simulated and observed net fluxes at most stations correspond better than the flux components, as the errors in the components are compensated, bringing the simulated NEE closer to observations. It should be noted that due to unavailability of observed meteorology for Tver and Zotino stations, Experiments 1 and 3 could not be performed and the comparison had to be limited to Experiment 2, simulations with NCEP meteorology.

Tables 3-2 and 3-3 provide a summary of winter and summer sums, respectively, of the fluxes for all nine stations investigated. Standard deviations of the simulated and observed fluxes were computed over 90-day values to obtain an estimate of the variability.

3.4.2 TBM sensitivity analysis

Sensitivity analysis, as defined by Saltelli (2000), studies the relationship between information flowing in and out of a model, thereby enabling characterisation and understanding of model behaviour. The current study is a "traditional" sensitivity analysis, whereby the effects of some key input data and parameter uncertainty on model output were investigated. It is expected that in drier areas, GPP would be improved with increasing root depths, as the plants would be able to extract ground water. Respiration is expected to decrease as the plants conserve moisture

loss through transpiration and evaporation. However, in less dry areas the plants try to minimise excess moisture entering the leaves thus causing low productivity. Likewise, changes in precipitation and temperature will affect productivity and respiration. Increasing precipitation is expected to lead to an increase in GPP, particularly in water-prone areas

The sensitivity results in this sub-section are presented, as in the previous section, for only two stations. For the results at other stations the reader is referred to the appendix. In the context of this study the control simulation refers to the models runs with their input parameters unaltered and the meteorology derived from NCEP Reanalysis data (i.e. Experiment 2).

Root depths:

In the control simulations BETHY used a constant root depth of 1m at all stations. For the sensitivity tests the root depth was first decreased by 0.5m and then increased by 1.5m, 2.0m and 3.0m, respectively. The same increment and reduction values were applied to the root depths of the individual stations used in BIOME-BGC. Figure 3-10 shows the influence on the productivity due to changing root depths.

Table 3-2 Seasonal sums of GPP, R_{total} and NEE for all stations for winter 1998

Stations	Exp #	WINTER SUMS 1998 (gC/m²)								
		GPP			R_{total}			NEE		
		BETHY	BIOME-BGC	STATION	BETHY	BIOME-BGC	STATION	BETHY	BIOME-BGC	STATION
ABERFELDY	1	21 ± 0.73	60 ± 0.52	134 ± 0.93	61 ± 0.69	191 ± 0.38	146 ± 0.49	-40 ± 0.69	-151 ± 0.46	-6 ± 0.85
	2	49 ± 0.97	117 ± 0.75		50 ± 0.74	349 ± 0.52		-1.0 ± 0.50	-232 ± 0.68	
	3	0	72 ± 0.67		36 ± 0.53	325 ± 0.67		-36 ± 0.52	-253 ± 0.68	
FLAKALIDEN	1	0	14 ± 0.27	8 ± 0.27	3 ± 0.11	66 ± 0.27	69 ± 0.72	-3 ± 0.11	-52 ± 0.34	-83 ±0.92
	2	0	17 ± 0.33		30 ± 0.35	123 ± 0.13		-30 ± 0.35	-106 ± 0.24	
	3	0	12 ± 0.29		32 ± 0.35	122 ± 0.15		-32 ± 0.35	-110± 0.23	
HESSE	1	66 ± 1.35	0	11 ± 0.18	94 ± 0.94	128 ± 0.41	84 ± 0.19	-28 ± 1.07	-128 ± 0.39	-74 ± 0.32
	2	0	0		81 ± 0.27	186 ± 0.29		-81 ± 0.27	-186 ± 0.26	
	3	0	3 ± 0.17		83 ± 0.28	196 ± 0.65		-83 ± 0.28	-193 ± 0.59	
HYYTIÄLÄ	1	0	25 ± 0.36	12 ± 0.19	33 ± 0.41	156 ± 0.31	33 ± 0.09	-33 ± 0.42	-131 ± 0.38	-22 ± 0.28
	2	0	25 ± 0.30		37 ± 0.39	158 ± 0.19		-37 ± 0.39	-133 ± 0.26	
	3	0	21 ± 0.33		40 ± 0.39	157 ± 0.29		-40 ± 0.39	-136 ± 0.36	
LOOBOS	1	11 ± 0.47	74 ± 0.39	57 ± 0.66	97 ± 0.74	209 ± 0.38	51 ± 0.37	-86 ± 0.76	-135 ± 0.85	-41 ± 0.66
	2	0	62 ± 0.39		39 ± 0.43	295 ± 0.28		-39 ± 0.57	-233 ± 1.39	
	3	8 ± 0.29	86 ± 0.45		64 ± 0.50	313 ± 0.59		-56 ± 0.61	-227 ± 1.13	
THARANDT	1	189 ± 1.09	189 ± 1.39	75 ± 0.84	99 ± 0.59	467 ± 0.69	101 ± 0.35	-90 ± 0.75	-278 ± 1.01	-25 ± 0.66
	2	0	66 ± 1.05		77 ± 0.38	310 ± 0.43		-77 ± 0.40	-244 ± 0.75	
	3	0	94 ± 1.29		78 ± 0.32	344 ± 0.54		-78 ± 0.33	-250 ± 0.93	
TVER	1	X	X	Not available	X	X	Not available	X	X	-49 ± 1.55
	2	44 ± 0.35	44 ± 0.54		69 ± 0.28	201 ± 0.27		-25 ± 0.21	-157 ± 1.55	
	3	X	X		X	X		X	X	
VIELSALM	1	36 ± 0.47	36 ± 0.37	53 ± 0.54	91 ± 0.47	161 ± 0.15	90 ± 0.25	-55 ± 0.39	-125 ± 0.36	-36 ± 0.49
	2	0	62 ± 0.49		74 ± 0.44	281 ± 0.36		-74 ± 0.44	-219 ± 0.58	
	3	39 ± 0.17	95 ± 0.41		78 ± 0.45	286 ± 0.23		-39 ± 0.42	-181 ± 0.43	
ZOTINO	1	X	X	Not available	X	X	Not available	X	X	Not available
	2	0	9 ± 0.87		39 ± 0.18	80 ±0.16		-39 ± 0.18	-71 ± 0.11	
	3	X	X		X	X		X	X	

Table 3-3 Seasonal sums of GPP, R_{total} and NEE for all stations for summer 1998

Stations	Exp #	SUMMER SUMS 1998 (gC/m²)								
		GPP			R_{total}			NEE		
		BETHY	BIOME-BGC	STATION	BETHY	BIOME-BGC	STATION	BETHY	BIOME-BGC	STATION
ABERFELDY	1	590 ± 1.29	563 ± 1.65	804 ± 2.04	352 ± 0.51	412 ± 0.56	536 ± 1.25	238 ± 1.10	151 ± 1.24	-6 ± 1.9
	2	632 ± 0.86	980 ± 1.86		375 ± 0.46	725 ± 0.77		257 ± 0.70	295 ± 1.43	
	3	551 ± 2.71	701 ± 2.29		362 ± 1.37	647 ± 0.82		189 ± 1.62	96 ± 1.81	
FLAKALIDEN	1	389 ± 2.18	397 ± 1.73	431 ± 2.34	257 ± 0.99	289 ± 0.66	341 ± 1.73	132 ± 1.43	108 ± 1.18	-83 ± 2.1
	2	448 ± 2.37	580 ± 1.18		279 ± 0.96	436 ± 0.59		169 ± 1.56	144 ± 0.88	
	3	482 ± 2.39	454 ± 1.89		314 ± 1.23	415 ± 0.86		168 ± 1.53	39 ± 1.28	
HESSE	1	844 ± 3.90	676 ± 1.60	834 ± 2.86	534 ± 1.79	478 ± 0.76	552 ± 1.65	310 ± 2.47	189 ± 1.20	-74 ± 3.0
	2	430 ± 5.80	930 ± 2.31		271 ± 2.92	594 ± 1.31		151 ± 3.01	325 ± 1.27	
	3	1030 ± 1.10	736 ± 1.82		592 ± 0.97	627 ± 0.97		438 ± 0.94	98 ± 1.38	
HYYTIÄLÄ	1	651 ± 1.49	832 ± 2.57	581 ± 1.93	382 ± 0.64	610 ± 0.99	371 ± 0.86	269 ± 1.13	210 ± 1.85	-22 ± 1.8
	2	640 ± 1.87	775 ± 1.75		377 ± 0.99	562 ± 0.75		263 ± 1.18	202 ± 1.41	
	3	789 ± 2.17	726 ± 1.94		456 ± 0.88	544 ± 0.79		333 ± 2.00	171 ± 1.41	
LOOBOS	1	730 ± 1.05	608 ± 1.14	663 ± 2.20	463 ± 0.65	456 ± 0.54	394 ± 0.74	252 ± 0.71	136 ± 0.81	-41 ± 2.1
	2	744 ± 1.03	920 ± 2.29		476 ± 0.72	724 ± 1.04		252 ± 0.74	167 ± 1.64	
	3	780 ± 0.83	836 ± 3.04		516 ± 0.84	683 ± 1.08		249 ± 0.98	126 ± 2.53	
THARANDT	1	727 ± 1.09	1306 ± 3.75	794 ± 1.83	462 ± 0.93	1072 ± 2.02	453 ± 0.83	215 ± 0.82	185 ± 2.42	-25 ± 1.6
	2	743 ± 1.08	961 ± 1.36		479 ± 0.88	840 ± 1.39		213 ± 0.74	90 ± 0.73	
	3	782 ± 1.53	900 ± 1.76		494 ± 0.66	781 ± 1.41		242 ± 1.60	88 ± 0.89	
TVER	1	X	X	Not available	X	X	Not available	X	X	-49 ± 10
	2	377 ± 0.74	1010 ± 2.30		319 ± 0.56	823 ± 1.41		52 ± 0.41	157 ± 10.0	
	3	X	X		X	X		X	X	
VIELSALM	1	562 ± 1.94	567 ± 2.17	699 ± 2.00	370 ± 0.98	418 ± 0.88	338 ± 0.70	155 ± 1.23	116 ± 1.43	-36 ± 1.8
	2	766 ± 1.11	951 ± 2.38		497 ± 0.93	698 ± 1.41		180 ± 0.75	154 ± 1.38	
	3	771 ± 0.85	674 ± 2.63		513 ± 0.91	626 ± 1.19		170 ± 0.88	42 ± 1.74	
ZOTINO	1	X	X	Not available	X	X	Not available	X	X	Not available
	2	734 ± 3.62	883 ± 2.26		428 ± 1.45	702 ± 1.96		317 ± 2.55	148 ± 1.01	
	3	X	X		X	X		X	X	

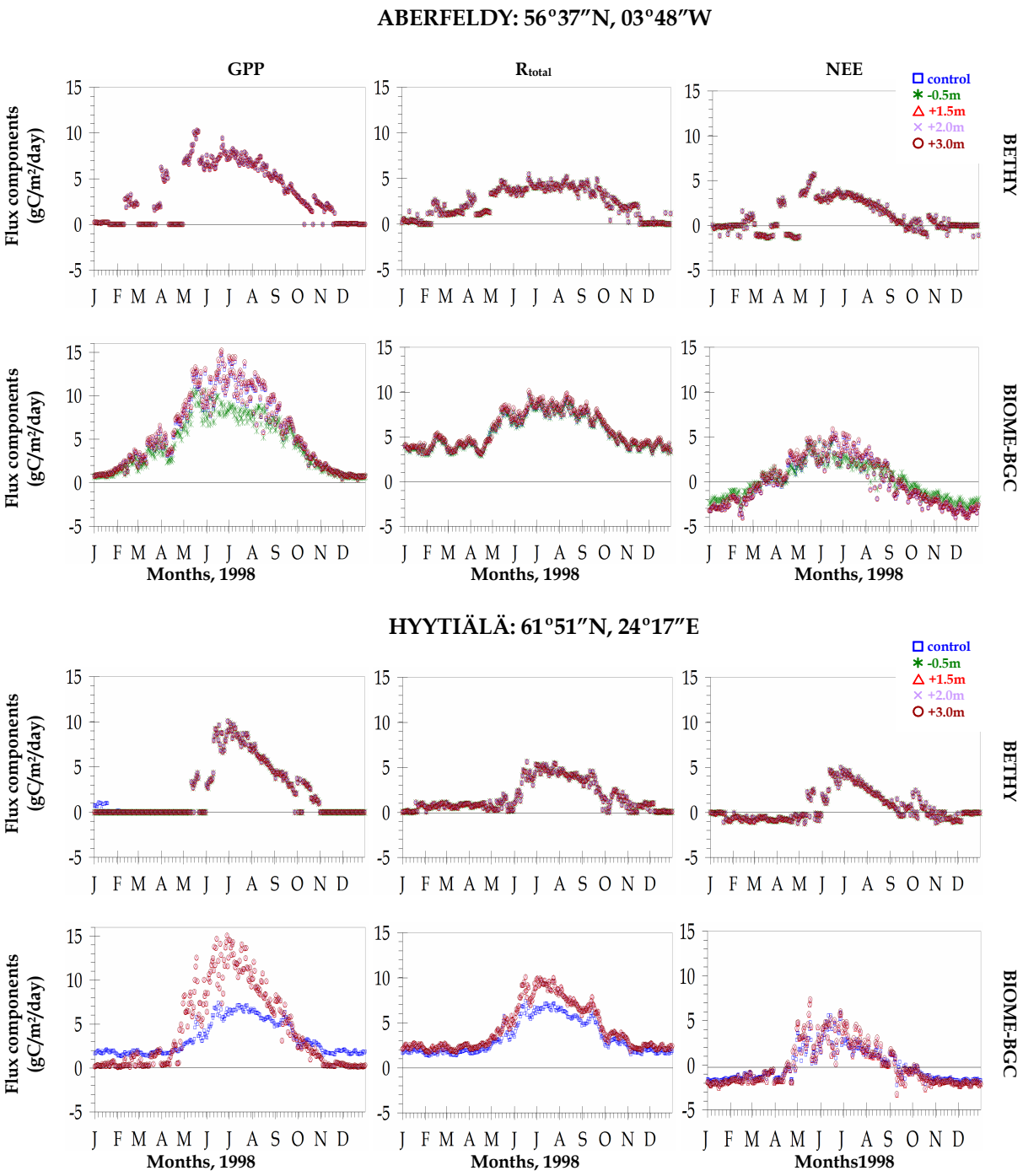

Figure 3-10 Sensitivity Test I: Plots of simulated fluxes from varying root depth inputs. Results for Aberfeldy and Hyytiälä

Figure 3-10 shows that the response of BETHY to changing root depths is not very strong at Aberfeldy and Hyytiälä. BIOME-BGC shows some sensitivity, particularly at lower root depths, whereby production is reduced at Aberfeldy. It should be noted that Hyytiälä already has a shallow root depth (see Table 3-1). Reducing it further will result in negative root depth, which has no physical meaning. The reduced GPP at the onset of summer at Hyytiälä, seen in the control run of BIOME-BGC (denoted by blue squares), tends to disappear when maximum root depth is applied. This behaviour of the model relates to the soil water availability for the plants. The extent and depths of a root system determines how much water can be extracted by the vegetation from the soil. With deeper roots more soil volume is explored and hence more soil water is accessible for evapotranspiration during dry periods (Hagemann and Kleidon, 1999). This is also evident from BETHY at, for example, Hesse (see Appendix A5), where an improvement in GPP is seen at maximum root depth. At Vielsalm, on the other hand, while no improvement in productivity is visible, BETHY simulation shows a prolongation of production process at higher root depths.

To get an overview of the sensitivity of the models due to varying root depths, annual sums of GPP for 1998 were plotted against the changing root depths. At most stations, figure 3-11 shows that BIOME-BGC is more sensitive to the changing root depths then BETHY, albeit not very strong.

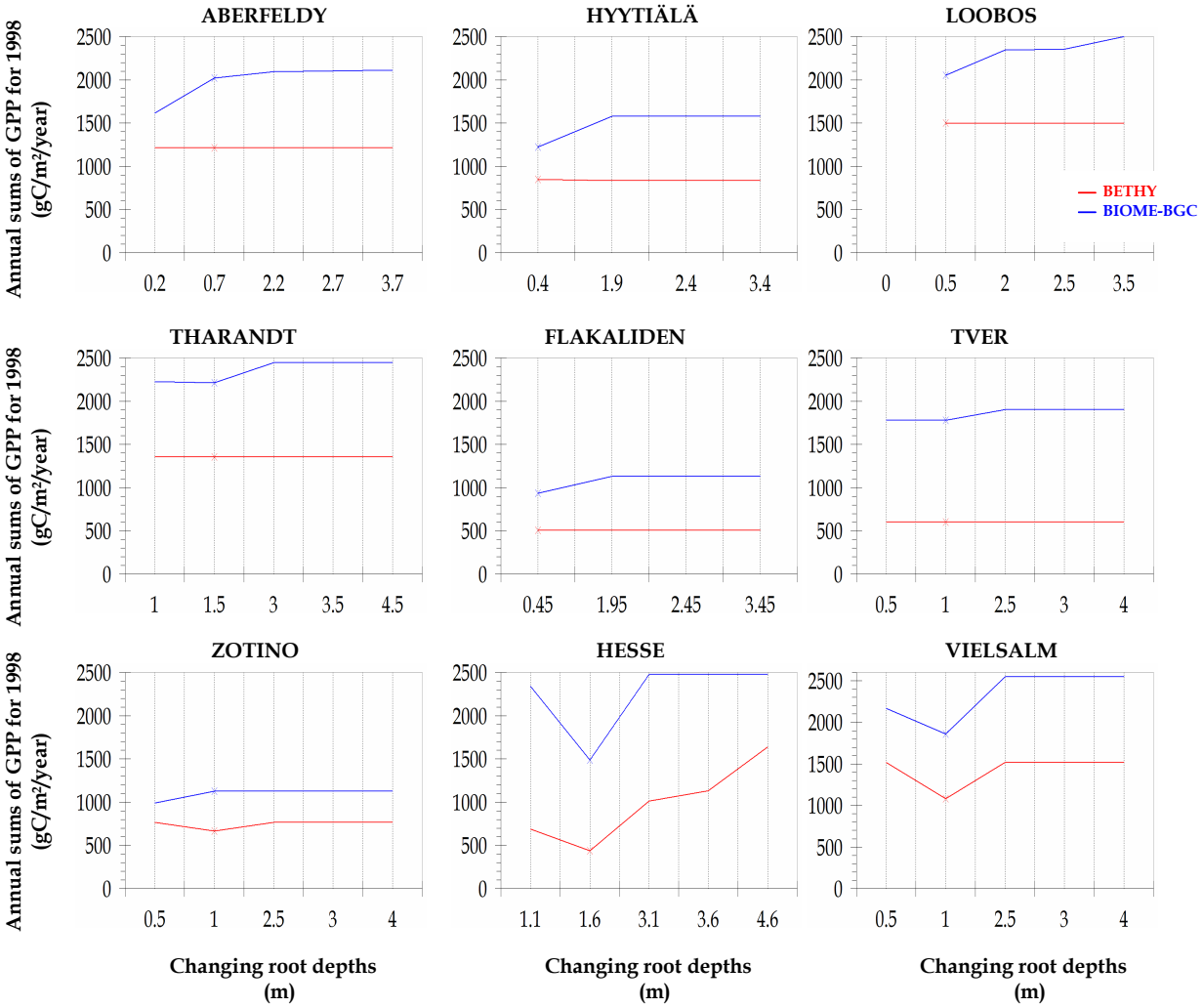

Figure 3-11 Summary plots to show overall response of productivity in the TBMs due to changing root depths. The crosses on the plots indicate the measured root depth at the sites

At Hesse and Vielsalm both models show a similar behaviour in that production increased when the root depths were reduced. BETHY continued to show improved productivity at Hesse with the root depth increment, while at Vielsalm the two models behaved in the same manner. This response in productivity due to changing root depth at these stations could be attributed to the similarities in the site characteristics, particularly the vegetation type, which is deciduous broadleaf at both locations. At other station locations, evergreen needle leaf forests are dominant.

Precipitation amounts:

The second sensitivity test was conducted by changing the precipitation amounts provided to the TBMs as daily input. The changes were incorporated by first decreasing the amount by a half of that used in the control run, and then increasing the amount by 1.5 times that of the control input, doubling the control input and finally increasing the control amount by three times. Figure 3-12 shows the model behaviour to the changing precipitation amounts at Aberfeldy and Hyytiälä. Results for all other stations are presented in Appendix A6.

Reducing the precipitation by a factor of two limits productivity in BETHY at Aberfeldy, while BIOME-BGC at the same station does not show a very strong sensitivity. However, at Hyytiälä, BIOME-BGC simulated GPP is slightly lower than the control, indicating the model's sensitivity to the changing precipitation amount at this site. This shows that the sensitivity of the TBMs to the changing precipitation is site-specific. For example, the response of both models at Hesse, shown in figure 3-13, is much greater than that seen at other stations presented in Appendix A6.

While both models show slight improvement and prolongation of productivity at, for example, Loobos, Vielsalm and in case of BETHY, at Zotino, with increasing precipitation (Appendix A6), reduced precipitation at the same stations limits productivity, particularly in BETHY.

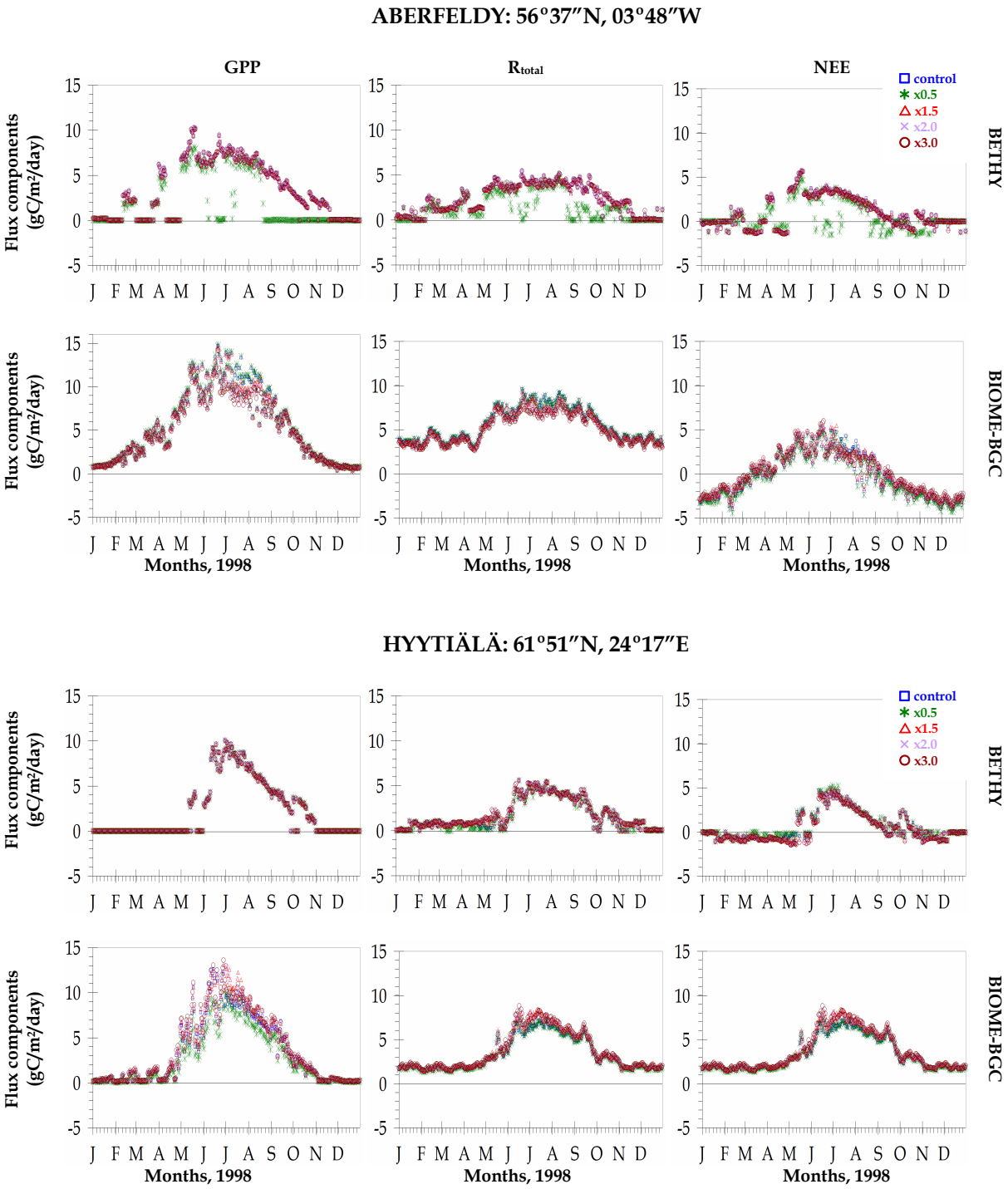

Figure 3-12 Sensitivity Test II: Plots of simulated fluxes using varying precipitation amounts. Results for Aberfeldy and Hyytiälä

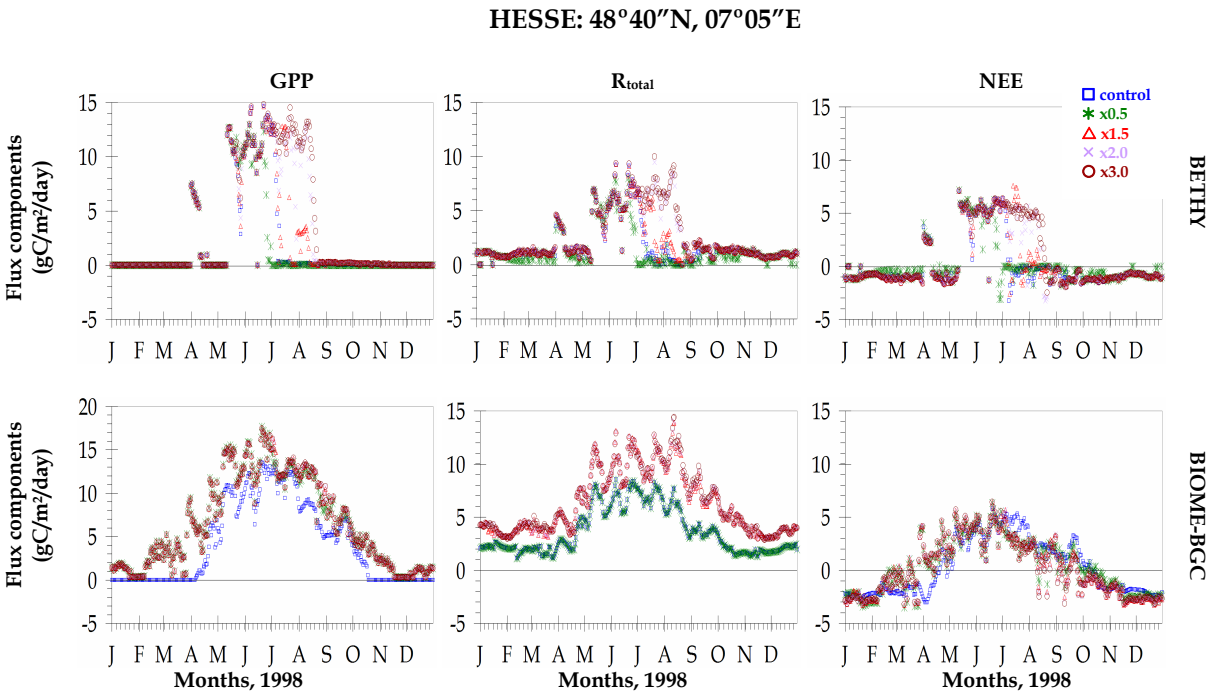

Figure 3-13 Sensitivity Test II: Plots of simulated fluxes using varying precipitation amounts at Hesse to show that the models are more sensitive to the changing precipitation at this site than at some of the other sites presented in Figure 3-12 and Appendix A6.

To get an overall picture of the response of the two TBMs at all stations, summary plots of annual sums of GPP versus changing precipitation are presented in figure 3-14. The site-specific responses of the TBMs suggest that other parameters, such as soil and vegetation types, in addition to precipitation, also play an important role in the model processes. In general, BETHY is less sensitive to the changing precipitation amounts than BIOME-BGC.

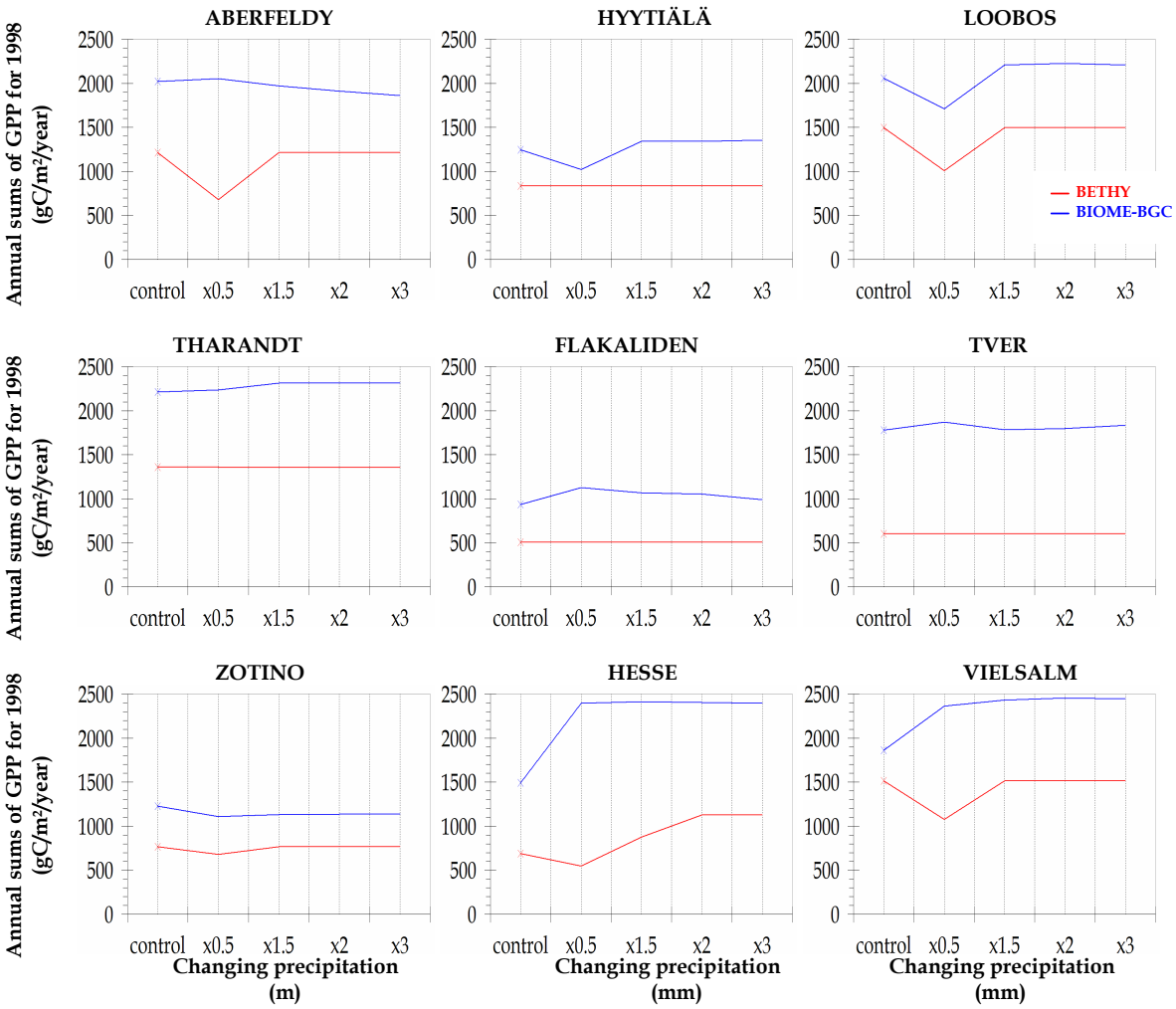

Figure 3-14 **Summary plots to show overall response of productivity in the TBMs due to changing precipitation inputs. The crosses on the plots indicate the daily precipitation data used at the sites without any alterations.**

Temperature:

The sensitivity of the TBMs to changes in temperature was tested by first reducing the temperature input used in the control simulation by 2.5°C, and then incrementing it by 2.5°C, 5.0°C and 5.5°C, respectively. These incremental temperature values were chosen after initial tests of a range of temperatures to see at which point the models responded most. Figure 3-15 shows the results for the same two stations, Aberfeldy and Hyytiälä, as shown for the previous two tests. The results for other stations are presented in Appendix A7.

Both TBMs show a relatively high sensitivity to temperature changes, as shown in figure 3-15. At both stations productivity is enhanced with increasing temperature. However, BETHY simulates a higher GPP at Aberfeldy in the middle of summer for a few days when the simulation is performed with lower temperature. A similar behaviour in BETHY is seen at Flakaliden (shown in figure 3-16) towards the end of summer. Such response of the model indicates the effect of local conditions on ecosystem production and flux exchange. For example, the decrease in temperature input at both Aberfeldy and Flakaliden causes lower evaporation. BIOME-BGC shows a consistent increase in GPP with increasing temperature. Both TBMs also show an increase in the total ecosystem respiration with increasing temperatures.

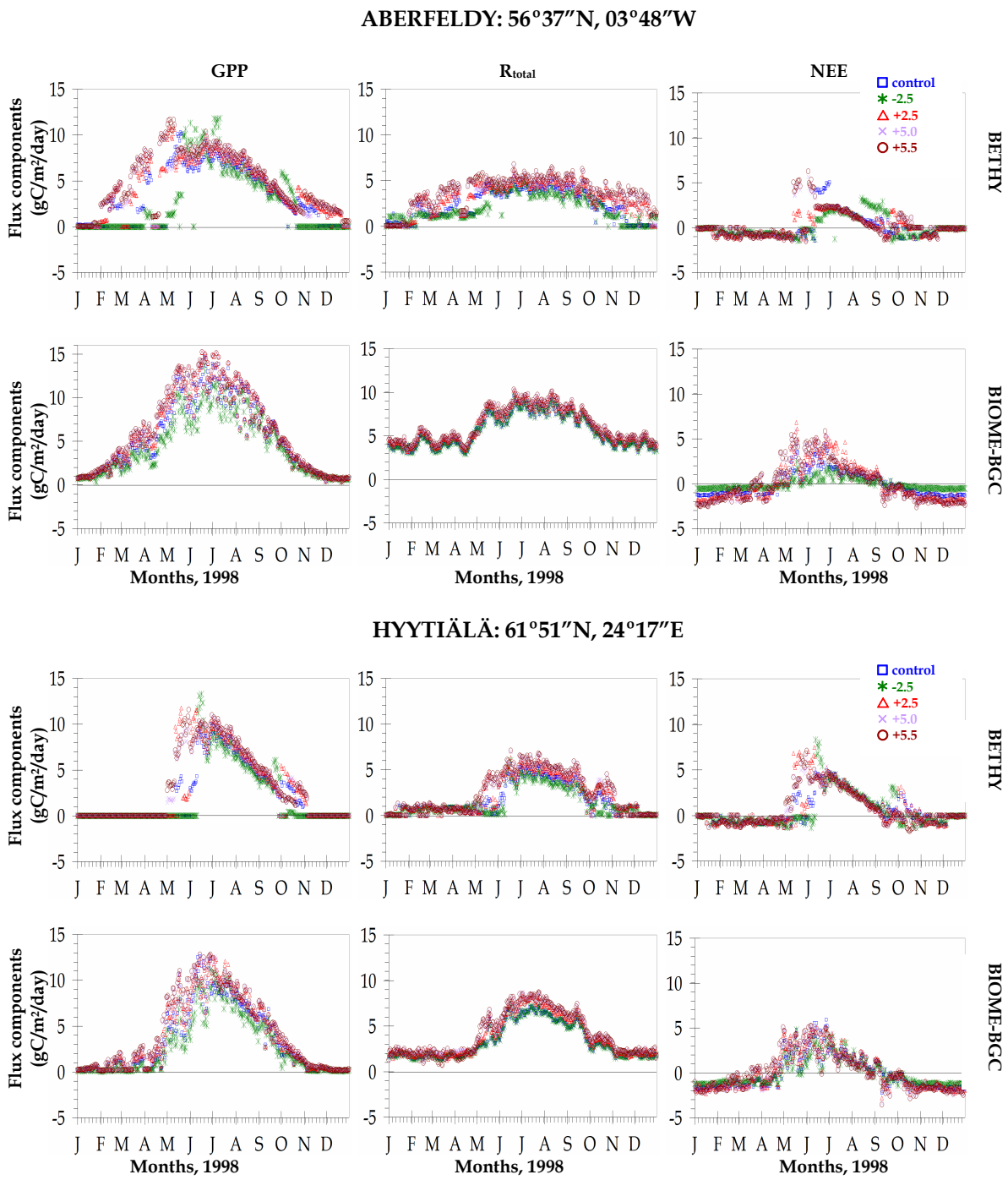

Figure 3-15 Flux plots of varying temperature simulations at Aberfeldy and Hyytiälä

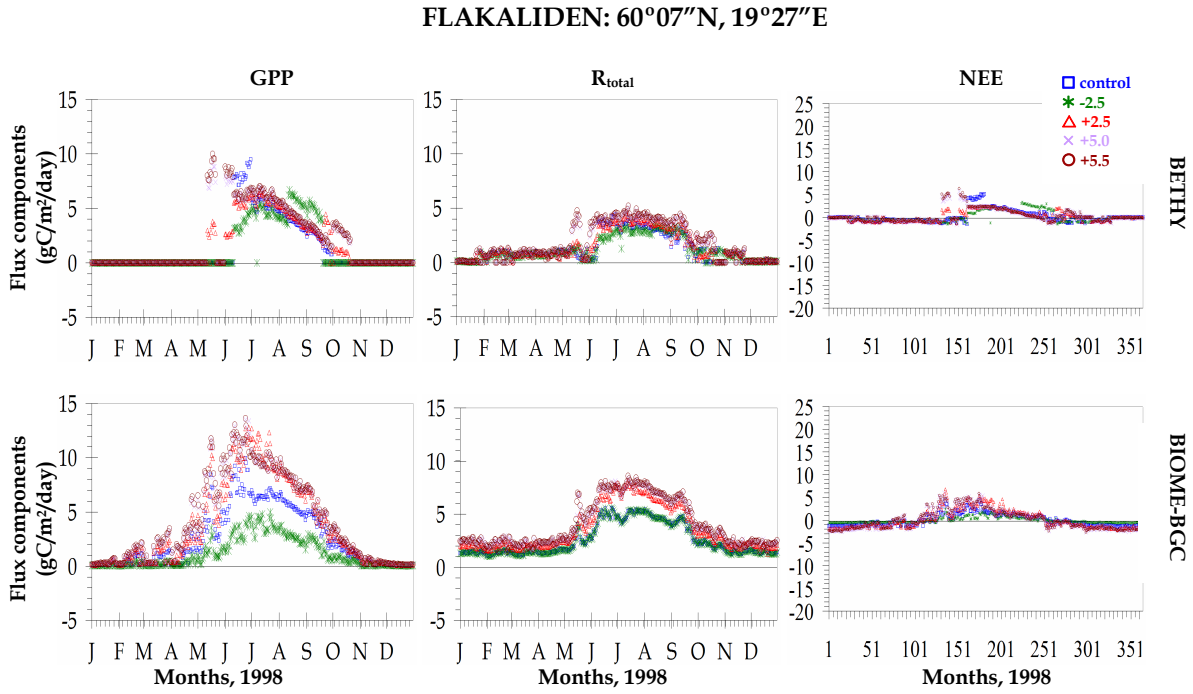

Figure 3-16 Flux plots of varying temperature simulations at Flakaliden to compare with the patterns from Aberfeldy and Hyytiälä

To summarise the effect of changing temperatures, the annual productivity is plotted for all stations in figure 3-17.

Over all, figure 3-17 shows that BETHY and BIOME-BGC respond in a similar manner to the changing temperature inputs. At low temperature both show reduced annual productivity, except at Tharandt where BETHY shows a maximum GPP. At all stations there appears to be an optimum temperature for maximum productivity in BIOME-BGC. A further increase in temperature has little effect or even causes a slight decrease in production. A similar pattern can also be seen in BETHY.

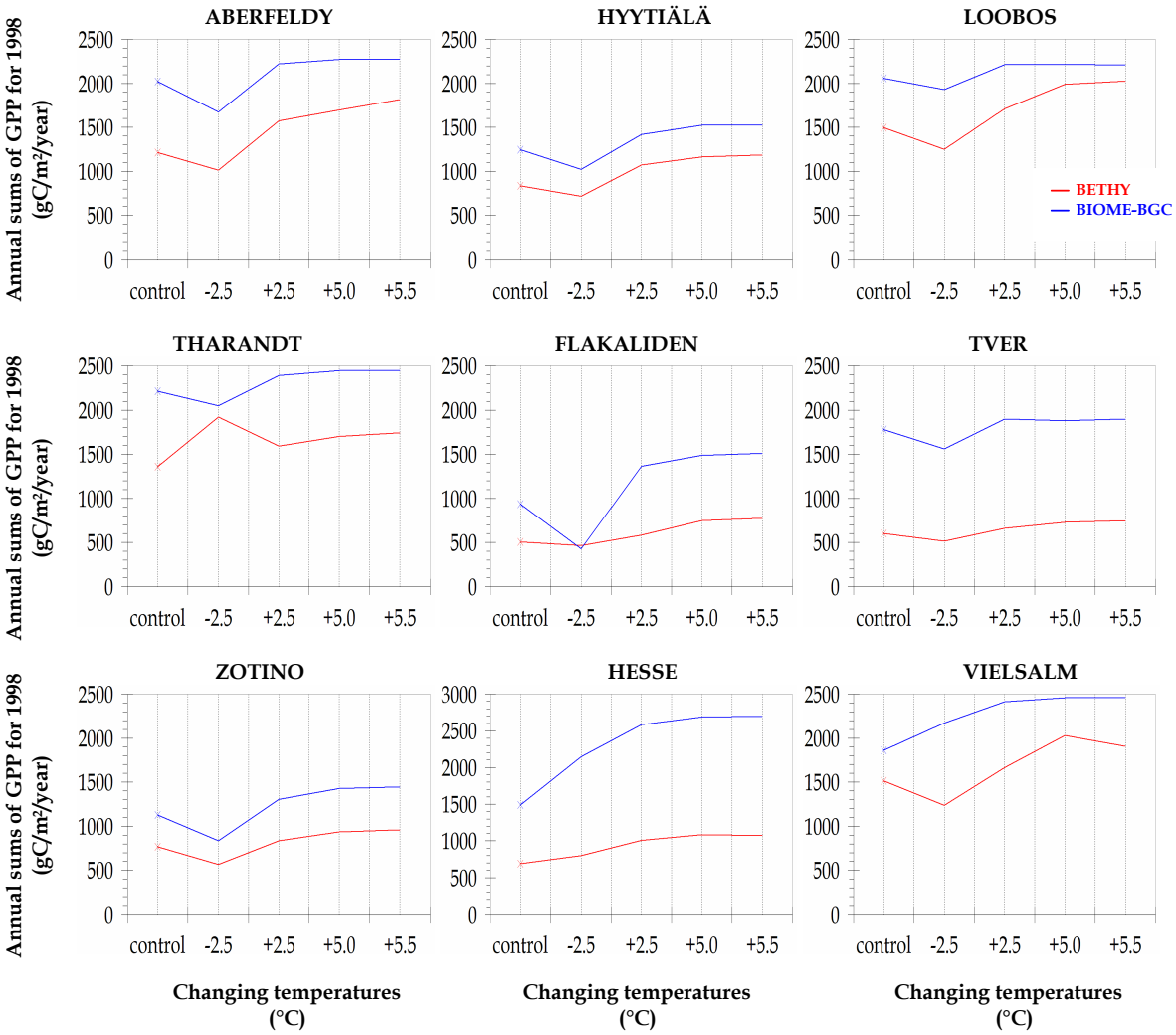

Figure 3-17 Summary plots to show overall response of productivity in the TBMs due to changing temperature inputs. The crosses on the plots, as before, indicate the daily temperature data used at the sites without any alterations. Note the change in vertical scale for Hesse station.

3.5 DISCUSSION

I. Flux validation:

The three experiments of the validation study showed that the simulated net fluxes from the two TMBs capture the observed flux seasonality. At most stations Experiment 1 (simulations with observed meteorology)

shows a better agreement of simulated GPP with the observations than the other two experiments, as was expected. However, the disadvantage of the limited meteorology, particularly in BIOME-BGC, can be seen at some stations (e.g. Hesse and Vielsalm (Appendix A3)). Comparison of R_{total} shows that the simulations generally compare better with each other than with observations, which can be explained by the similarities in the way respiration is modelled in BETHY and BIOME-BGC.

The use of modelled meteorology (Experiment 2) as input for the single-stand simulations produced comparatively good results despite the scale problems associated with the large grid size and the actual measurements taken at single sites. While at some stations the simulated and observed fluxes correspond well, there are other stations where one or the other TBM shows differences. One such example can be seen at Hesse where BETHY simulated GPP, and correspondingly R_{total}, gradually cease around mid-summer. The behaviour of BETHY at this particular station can be explained by the use of model-derived surface inputs, such as soil and vegetation types. The input meteorology is important, and here it is reasonably well reproduced by NCEP; equally important are the site characteristics, as well as the model differences and how these inputs are handled in simulating the ecosystem processes. The current investigations and results provide a foundation for the spatial simulations of CO_2 fluxes, which are discussed in the next chapter and also used NCEP Reanalysis data as input meteorology.

II. Sensitivity analysis

The different levels of complexities of the two TBMs and the way in which they utilise the meteorology input and other surface forcing lead to some differences in the behaviour of the models. The sensitivity tests showed

that the response of BIOME-BGC to the changing input parameters is stronger than that of BETHY. Generally, over all stations investigated the responses of the TBMs are site-specific, indicating the influence of local conditions and other input forcing other than the changing parameter being tested. The production process in both models is the most affected with the changing inputs, which in turn affects the ecosystem respiration.

Over all stations both models showed a stronger sensitivity to a lower root depth than when provided with increasing root depths. The TBMs use a so-called bucket model for the soil part where the models assume a uniform soil layer with a minimum bucket depth of 1m. This is a limiting assumption in the models, as the root depths for temperate forests go beyond 1m in the soil. In their study on maximum root depth of vegetation types, Canadell and colleagues (1996) reported a maximum rooting depth of (2.0 ± 0.3)m for boreal forest, (3.9 ± 0.4)m for temperate coniferous forest, and (2.9 ± 0.2)m for temperate deciduous forest, the most common forest types in the northern hemisphere. Figure 3-18a and 3-18b, reproduced from Canadell *et al.* (1996), show their findings of maximum rooting depth in meters grouped by terrestrial biome.

Furthermore, they reported that although a small fraction of root biomass might be found at depths below 1m, the functional significance of those roots may nevertheless be most important for ecosystem water and carbon fluxes, and nutrient cycling and hence should be appropriately taken into account in the ecosystem models.

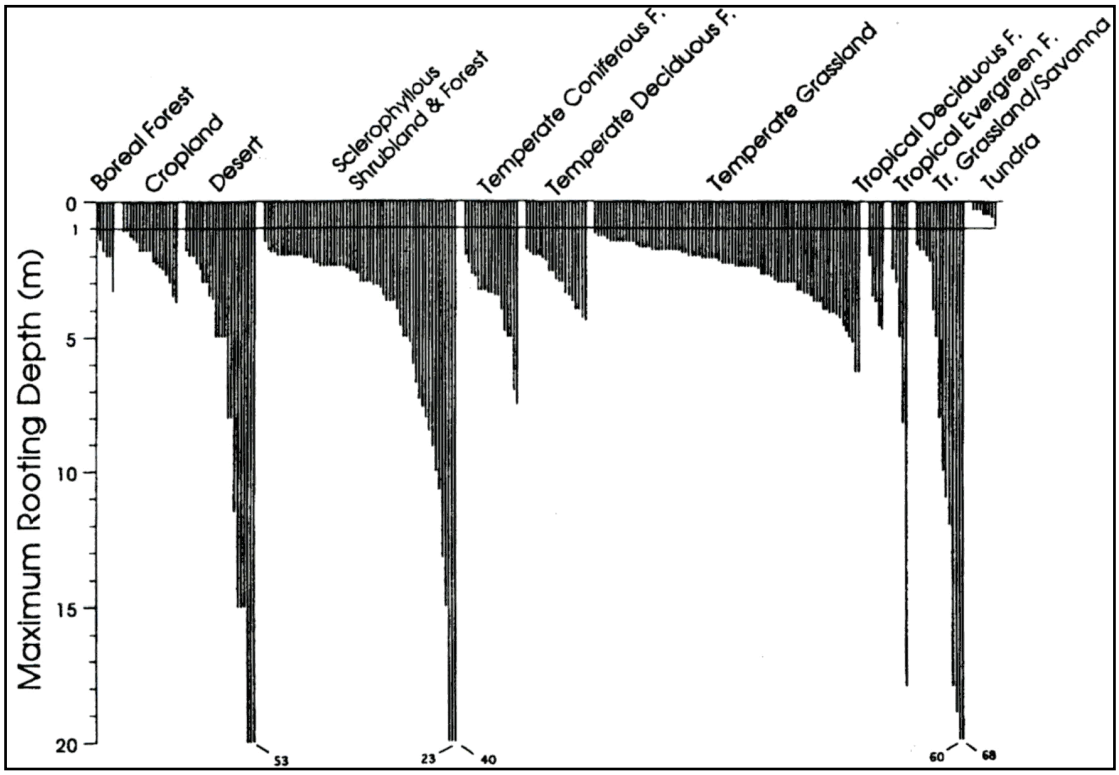

Figure 3-18a Reported species maximum rooting depth (m) grouped by terrestrial biome. *[Source: Canadell et al. (1996)]*

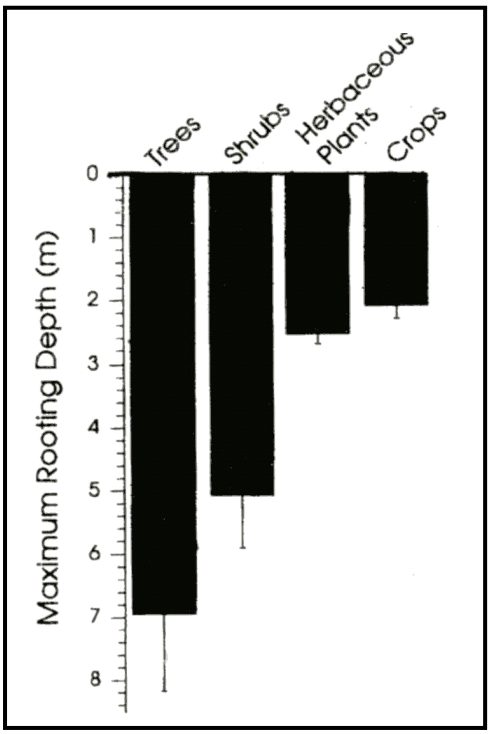

Figure 3-18b Mean of reported maximum rooting depth (m) by three major functional groups (trees, shrubs and herbaceous plants) and crops. *[Source: Canadell et al. (1996)]*

Providing the TBMs with different amounts of precipitation input resulted in a stronger response to lower precipitation than when the amounts were increased. Precipitation influences the dynamics of natural ecosystems through soil moisture, a direct link between precipitation and ecological systems (Weltzin *et al.,* 2003). According to McAuliffe (2003), the basic phenomena associated with precipitation events, such as interception, infiltration and runoff, are well understood; the main difficulty lies in describing the rates of soil moisture change between precipitation events. These rates are mainly driven by evaporation from soils, transpiration by plants, horizontal and vertical soil water transport and hydraulic redistribution of soil water, all of which depend in complex ways on vegetation and soil characteristics and on the timing and size of precipitation inputs (Weltzin *et al.,* 2003). Models used to investigate the role of precipitation and water in ecosystems range from mechanistic models, such as the TBMs used in the current study, that link hydrology and vegetation thereby exposing the fundamental relationships between patterns of precipitation, characteristics of soil and vegetation properties, to rule-based models that have a variety of ecohydrologic assumptions related to the parameterisation of precipitation inputs and modelling of the soil water budgets. The differences seen in the sensitivity test of changing precipitation inputs can therefore be explained by such process-level differences in the two models.

Changing the input temperature showed the strongest sensitivity in the photosynthesis process in both TBMs. The temperature sensitivity in photosynthesis is primarily through the membrane-bound photochemical reactions, as well as the carboxylation efficiency of the primary photosynthetic enzyme, which is also sensitive to temperature (Rustad and Norby, 2002). The TBMs used in the current investigations model this

process in a similar manner. Typically, ecosystem respiration increases exponentially with increasing temperature. However, this is not obvious at all stations for each of the two models, depending on the local site-specific conditions.

3.6 CONCLUSIONS

Terrestrial ecosystem fluxes are influenced by a combination of meteorological and environmental factors, such as incident radiation, precipitation and temperature, site-specific factors like soil type, nutrient availability and site history, and interspecific differences in tree physiology. Terrestrial biosphere models are suitable tools for studying the influences of these factors on the ecosystem fluxes.

The main aim of this chapter was to identify how well the TBMs are able to simulate some of the important processes in a terrestrial ecosystem. This was achieved by comparing the simulated fluxes with eddy covariance measurements at individual FLUXNET sites. The results showed that despite the limitations, mainly in the input data, the two TBMs are able to adequately reproduce the observed fluxes. The seasonal cycle is reproduced in a realistic manner, and the simulated NEE is within the variation of the observations. The flux components GPP and R_{total} generally showed larger differences, but tend to compensate for each other. The sensitivity analysis showed that model parameterisations and assumptions, the surface inputs and the different ways that the models handle these inputs play an important role in the estimation of the fluxes. It seems that the use of simulated meteorology leads to acceptable results, also at single stand sites. However, a proper representation of the site

characteristics seems to be equally important, and particularly parameters that relate to the availability of water (rooting depth and precipitation) sometimes lead to a breakdown in the simulated fluxes. The differences in the input data and the model structure can explain the differences seen in the simulation results between the two models and how the uncertainties due to these factors can get incorporated in the estimated fluxes from the TBMs.

CHAPTER 4
CO_2 FLUX SIMULATIONS OVER EUROSIBERIA

4.1 INTRODUCTION

While single-stand investigations, coupled with field studies on the terrestrial ecosystem CO_2 and water vapour exchange, help in the understanding of the biogeochemical processes in the ecosystem, they do not provide information on the biosphere-atmosphere interactions on a regional scale or how the different areas of the globe will respond to changes in land cover or climate. To better understand the spatial patterns of terrestrial CO_2 fluxes and its propagation into the atmosphere, an extension from local scale investigations to regional scale is needed where terrestrial biosphere models become indispensable.

The uptake and release of carbon by the biosphere over space and time is affected by natural and anthropogenic factors. The present study focuses on the natural variability of CO_2 fluxes in Eurosiberia. Compared to Europe, the Siberian environment – consisting of vast boreal forests – is largely dominated by natural processes and is hardly affected by anthropogenic impacts. The continental climatic variations over the region, vegetation types, changes due to natural forest fires and ecological parameters, such as the length of the growing season that changes from

west to east, are some of the natural factors that influence the biospheric carbon fluxes.

In the previous chapter it was shown that terrestrial biosphere models are capable of reproducing the seasonal variations in the net carbon exchange at a variety of measurement sites in different ecosystems across Eurosiberia. However, it was also found that the models are sensitive to some of their input parameters, some of which are not well known particularly at larger spatial scales, and also that this sensitivity is not the same for each model. When simulating carbon fluxes at a regional scale the uncertainties arising from the model inputs, especially the surface parameters, as well as the representation of ecosystem processes in the models need to be taken into account. This can be achieved by not relying on a single model and a single set of input parameters, but to use an ensemble of different models and parameter sets instead.

The main aim of this chapter is to assess the regional patterns of, and natural variability in the CO_2 fluxes from the terrestrial biosphere in Eurosiberia using the two process-based terrestrial biosphere models BETHY and BIOME-BGC. To investigate the influence of the choice of model and the input vegetation map that largely controls the surface parameters, five experiments were designed using different combinations of the maps used by the individual TBMs.

The two TBMs, BETHY and BIOME-BGC, used in the current study are unique in their structural composition, and handle not only some of the important input parameters but also some ecosystem processes in different ways. One of the features of BETHY is its ability to use a vegetation class map that comprises 13 plant functional types, with the

possibility of each grid cell either having 100% cover of one type or having fractions of up to six types. BIOME-BGC does not have this feature. Instead, it is designed to using seven common classes of the world's biomes, each grid representing 100% coverage of one vegetation type.

This chapter starts with explanations on the approach taken towards the CO_2 flux simulations over Eurosiberia and presents the details of the experimental design. As a first step, the seasonal cycles of the simulated fluxes will be compared with those obtained from the single-stand simulations in Chapter 3 to determine the differences occurring, if any, when going from local to spatial scale simulations. This may already indicate a first source of uncertainty in the estimation of the biospheric fluxes at a regional scale. Comparison is also made with the FLUXNET observations. Seasonal analyses over winter and summer across the study region are presented to illustrate the spatial patterns of CO_2 fluxes from different experiments, and how similar or dissimilar the model estimates are from each other.

4.2 APPROACH TO FLUX SIMULATIONS

4.2.1 Experimental design

To investigate the regional scale flux patterns, a number of model experiments were designed with the two TBMs used in the present study, such that a common driving input variable could be changed in the TBMs while keeping all other input parameters identical. As mentioned in the model descriptions (Chapter 2), BETHY and BIOME-BGC are two process-based ecosystem models that use similar principles in modelling

ecosystem processes. However, the representation of some of these processes, as well as some input data and the way these data are handled by the models are different. While both the TBMs were forced with NCEP Reanalysis meteorology for the year 1998, with 0.5° x 0.5° lateral and daily temporal resolution, the standard surface input parameters of the individual models, also 0.5° x 0.5° latitude by longitude, differed. In order to investigate to what extent the differences between the model estimates can be attributed to the different input vegetation maps and hence contribute to the modelling uncertainties, it was decided to do several model experiments in which the two input vegetation maps (from BETHY and BIOME-BGC) were applied interchangeably to the TBMs.

In total five experiments were designed, out of which two involved running the TBMs with their own standard input maps, while in the other three experiments the vegetation maps were adapted and modified in order to be used interchangeably in the two models, i.e. BIOME-BGC was run with a vegetation map derived from BETHY, and BETHY was run with the BIOME-BGC vegetation map (see Table 4-1). By analysing the range of the simulated fluxes from these experiments, the uncertainties in the carbon flux estimations, arising from uncertainties in the vegetation input maps, as well as the representation of ecosystem processes in the two models, could be assessed.

As an additional sixth experiment, the fluxes from the widely used light-use efficiency model TURC were included in order to compare the performance of the two process-based TBMs and the variations in their estimates of CO_2 fluxes with those of TURC (Chevillard *et al*, 2002a).

Table 4-1 provides detailed explanations of the experiments. Figure 4-1 shows a simplified flow diagram of the experimental set-up. Figure 4-2 shows the vegetation maps that were used in the different experiments. Note that for practical reasons the vegetation map of Experiment 3 (BETHY run with its own fractionated vegetation map) is not shown here, as each grid cell contains a fractional cover of up to six vegetation types.

Table 4.1 Summary of regional CO_2 flux experiment description

Experiment Number	Model used	Simulation description
1	BIOME-BGC	Simulation with own vegetation map, with seven vegetation classes, one vegetation type per grid cell
2	BIOME-BGC	Simulation with BETHY-derived vegetation map
3	BETHY	Simulation with own vegetation map with 13 vegetation classes, each grid containing fractions of up to six vegetation types
4	BETHY	Simulation with 13 classes of vegetation type but each grid having majority class of vegetation type
5	BETHY	Simulation with BIOME-BGC derived vegetation classes, seven types, single vegetation class per grid
6	TURC results	No model runs performed. Flux results from (Chevillard *et al.*, 2002a) were used for comparison purpose

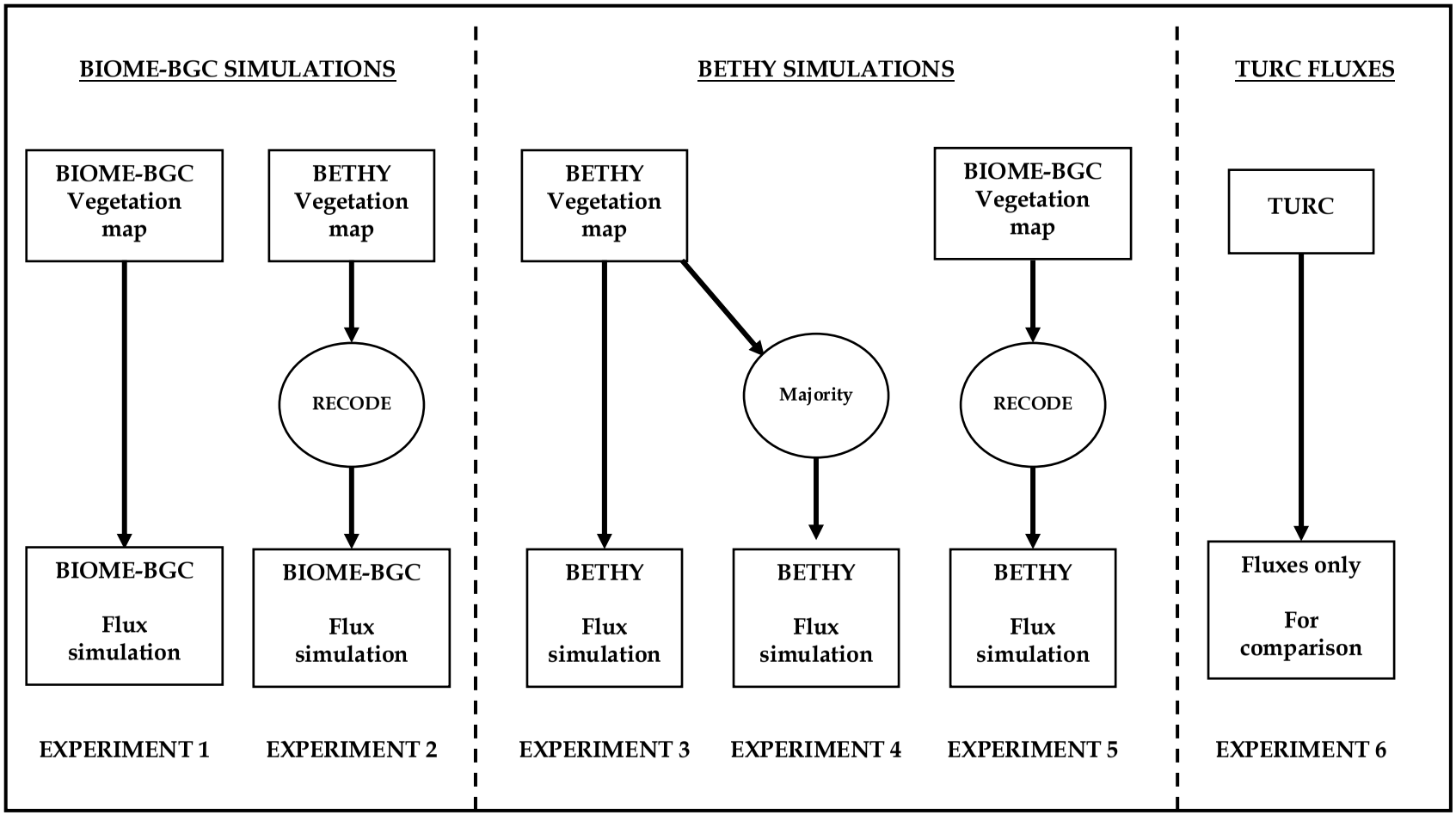

Figure 4-1 Experimental design of regional CO_2 flux simulations with BETHY and BIOME-BGC, including the fluxes from TURC.

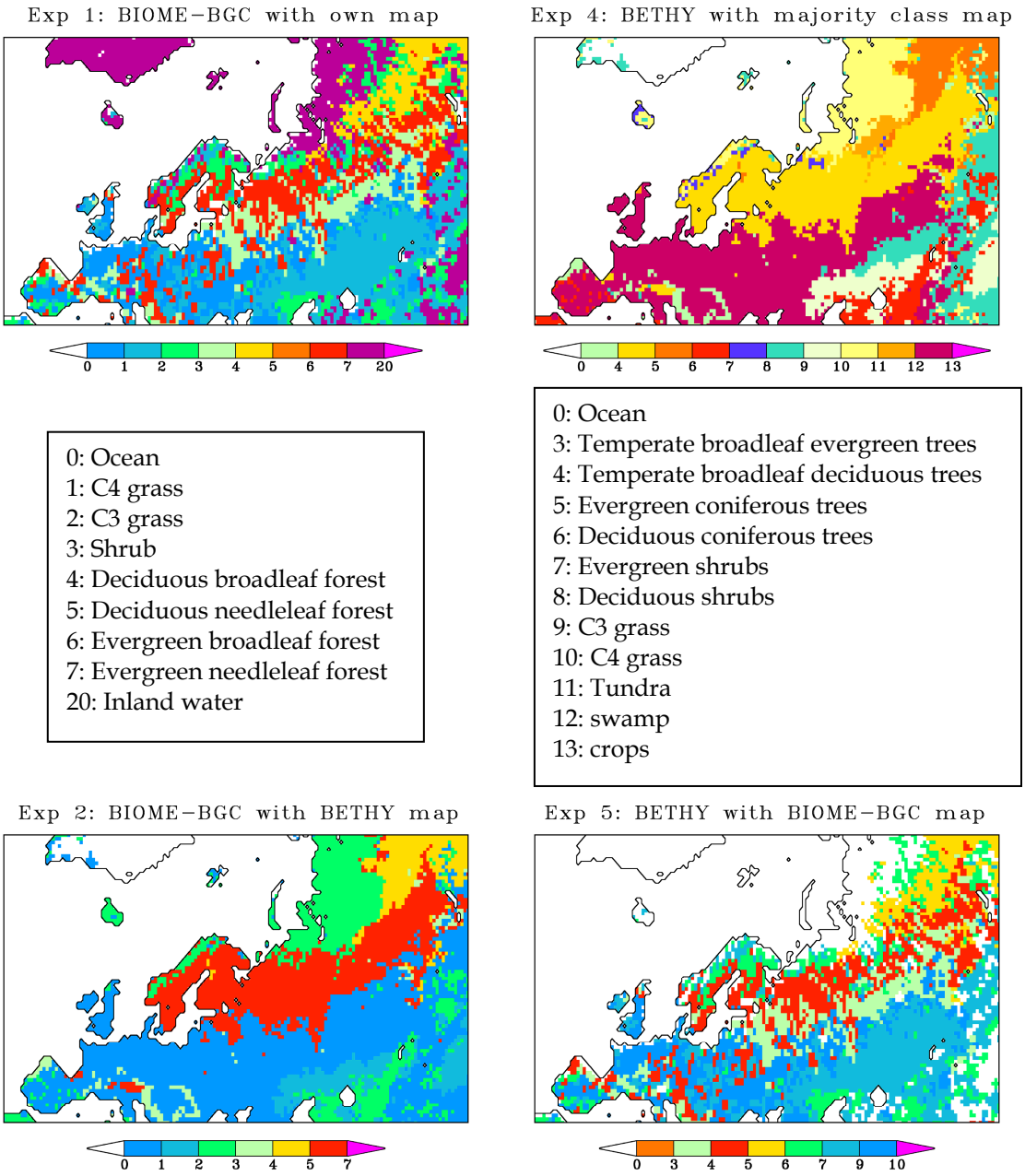

Figure 4-2 **Vegetation maps used for different experiments. Note that the map for Experiment 3 is not shown, as it includes fractions of vegetation type per grid cell**

4.2.2 Analysis method

As a first step in the analysis procedure the regionally simulated fluxes from each experiment were extracted for selected FLUXNET stations and compared with the observations and single-stand simulations at those sites. For consistency reasons the stations presented as examples are the same as those in Chapter 3. The intention of the comparison is not to validate the simulated fluxes with the observations but rather to determine whether or not the seasonal cycle is still being realistically represented by the TBMs when extended from point runs to regional runs, and secondly, when they are supplied with different vegetation inputs. Due to the scale difference – a point location where the measurements are made and a grid size spanning approximately 55km x 55km – a perfect match of the simulated fluxes with the observations should not be expected.

In addition to a visual inspection of the seasonal cycles, correlation coefficients were computed between the extracted fluxes and station observations, as well as between the different simulation experiments. The computation was conducted using the PINGO - ***P****rocedural* ***In****terface for* ***G****rib formatted* ***O****bjects* – package developed by the DKRZ (Deutsches Klimarechenzentrum) in Hamburg, Germany. This package provides many functions for standard post-processing of climate data sets on workstations, as well as a range of computations from basic arithmetic, to statistics to spectral analysis and empirical orthogonal functions (http://www.mad.zmaw.de/PINGO/downloads.html). The correlation coefficients computed from the regional data were compared with those computed from single-stand simulations to show quantitatively the model performances when going from point to regional scale. This provides

some indication on the introduction of uncertainties in the simulations at regional scale.

Correlation coefficients were also calculated on a regional scale between the different sets of experiments to deduce quantitatively the differences and similarities between them. Furthermore, the total fluxes over the entire Eurosiberian region were computed, not only from the biosphere but also from other contributing sources, such as fossil fuel and ocean. To analyse the activity of the biosphere in the study region, the amplitudes of the regional net fluxes were calculated from 10-daily running averages of the daily fluxes in order to remove the noise.

4.3 RESULTS AND ANALYSIS

This section is divided into three parts. The first part comprises of an examination of the regional fluxes, looking at the seasonal cycles represented in each experiment by extracting station fluxes and comparing with observations, as well as with the results of the station simulations (Chapter 3). The second part includes spatial flux patterns over the region for the summer and winter seasons. In these seasons the behaviour of the biosphere in terms of CO_2 flux exchange via the release and uptake can be seen. Results of the behaviour of the models when provided with different vegetation input maps are also presented. The third part provides a summary of the flux results over the entire region and looks at the sources of uncertainties in modelling terrestrial biosphere fluxes.

4.3.1 Flux comparison at single sites

Simulated CO_2 fluxes change when going from single stand investigations to spatial scale, thereby introducing uncertainties in the model estimates of the biosphere fluxes on regional scale. To understand how these changes occur and the possible sources contributing to the uncertainties, this section looks at the seasonal cycles of station fluxes extracted from the spatial data and compares this with the observations and with the results of the single site simulations presented in the previous chapter. As the focus is on understanding the variability of the net carbon exchange of the biosphere, the results presented are for NEE, and where appropriate, for two driving parameters of NEE, namely GPP and R_{total}.

As in the preceding chapter, results of two out of the nine stations investigated are presented and discussed in detail. The analyses of all other stations were carried out in a similar manner and are presented in Appendix A8. The stations discussed here are Aberfeldy and Hyytiälä. Figure 4-3 shows the seasonal cycles of the fluxes of three model experiments, 1, 3 and 6 in which each of the TBMs used their standard vegetation input maps.

When simulated on regional scale with their specific input data, the models are able to produce the seasonal cycle at single stands despite the differences seen in their amplitudes and the start and end of, for example summer NEE. BIOME-BGC shows better correspondence of the fluxes at Aberfeldy, while at Hyytiälä NEE from mid-summer onwards becomes very low. The fluxes from TURC show a lot of fluctuations in the components while BETHY, particularly at Hyytiälä, show production occurring only for a short period in summer. The differences are mainly

due to the fact that the extracted data represents a larger area than a specific single point obtained from the observations. The responses of the models also differ at individual stations, as seen from the results of other stations in Appendix A8.

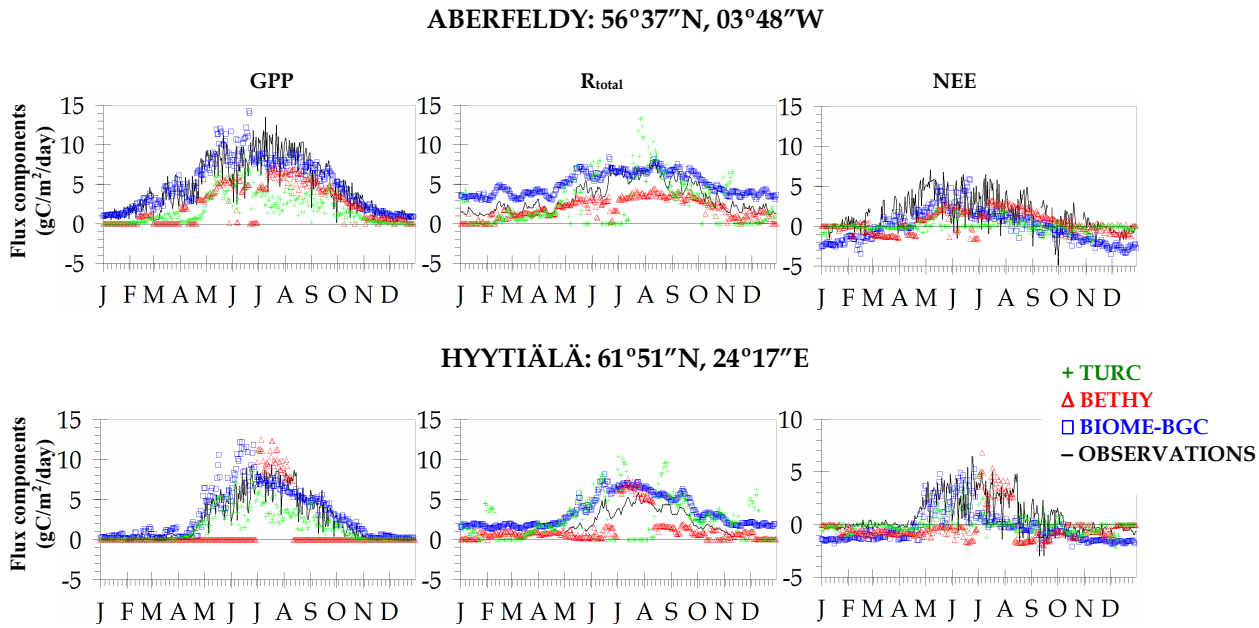

Figure 4-3 **Comparison and illustration of the seasonal cycles of the biosphere fluxes from different models extracted from the regional simulations. The models represent the experiments as follows: BIOME-BGC: Experiment 1, BETHY: Experiment 3 and TURC: Experiment 6. Note the change in scale for the Hyytiälä plots**

The results of the simulated NEE in the other experiments are shown in figure 4-4, indicating the responses of the models in terms of their representation of NEE. The presentation of the components is omitted here but is included in Appendix A8.

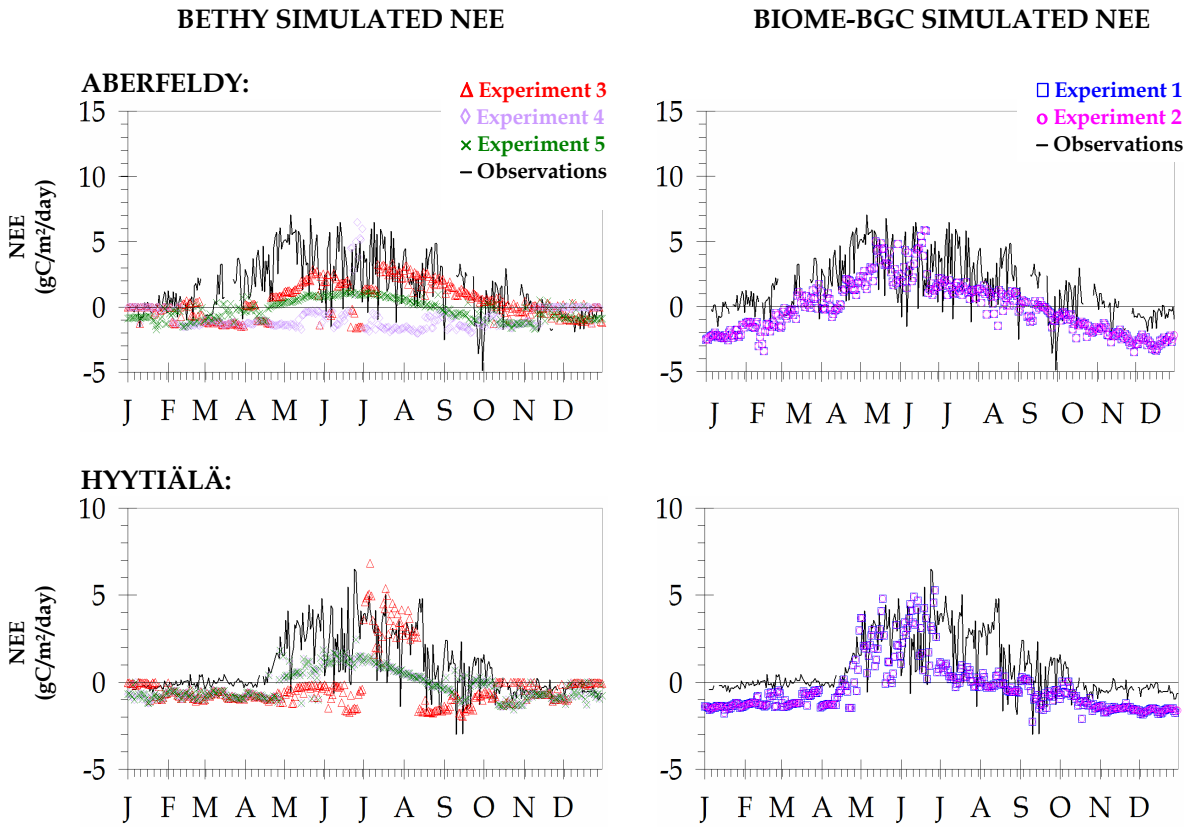

Figure 4-4 Seasonal cycles of NEE from BETHY and BIOME-BGC experiments at Aberfeldy and Hyytiälä. Note the different vertical scales.

BETHY shows greater sensitivity to changing input vegetation maps than BIOME-BGC. At Aberfeldy, Experiment 4 (BETHY simulation with its majority class vegetation map) shows a very poor NEE representation by BETHY, while Experiment 3 (simulation using its own vegetation map) shows a lot of fluctuations but still comparable with Experiment 5 for the first half of the year and with observations for the second half after summer. Experiment 5 shows a clearer seasonal pattern although the amplitude is lower in comparison with the observations. BIOME-BGC does not show a large sensitivity towards the change in its input map. While at Aberfeldy the seasonal cycle is reproduced fairly well in both experiments in comparison with the observations, at Hyytiälä the summer

maximum is not well represented. The difference, as mentioned above, arises due to the difference in the spatial and single point data.

In order to assess the differences between the model experiments and observations, and between different experiments, the correlation coefficients are presented in tables 4-2a and 4-2b, respectively. Comparisons are also made with the correlations obtained from the single-stand simulations (see Chapter 3).

As seen in table 4-2a the simulated fluxes show a moderately strong correlation with the observations, except for Tver station. BIOME-BGC generally performs better in the station runs using site-specific input data, but for BETHY this is not always the case. The behaviour of the models becomes difficult to assess where large amounts of observations are missing (for example, stations like Loobos (The Netherlands), Tver (Russia) and Zotino (West Siberia)).

Differences in the flux simulations occur when going from local scale to regional scale, as seen from the lower correlations at the stations for the regionally simulated fluxes. The correlation coefficients act as indicators for the uncertainties that arise in the model estimates of the biosphere fluxes. One of the major sources of errors in biosphere flux modelling from local to regional scale is scarcity of accurate spatial data. While simulations at single stands have the advantage of using site-specific data, most of which can be obtained from direct measurements, regional simulations are disadvantaged and rely on other modelled data representative of the area under investigation.

Table 4-2a Comparison of correlation coefficients of NEE between observations and model experiments

Stations	Exp 1		Exp 2	Exp 3	Exp 4		Exp 5	Exp 6	% missing observation data
	Regional Simulation	Station Simulation			Regional Simulation	Station Simulation			
Aberfeldy	0.68	0.71	0.68	0.43	-0.12	0.52	0.54	0.63	11
Flakaliden	0.58	0.62	0.57	0.45	0.45	0.23	0.45	0.81	1
Hesse	0.39	0.65	0.39	0.64	0.61	0.67	0.64	0.72	0
Hyytiälä	0.68	0.76	0.68	0.38	0.69	0.59	0.69	0.81	3
Loobos	0.53	0.57	0.53	0.58	0.33	0.54	0.56	0.66	33
Tharandt	0.75	0.75	0.75	0.69	0.54	0.70	0.69	0.59	7
Tver	0.29	0.29	0.29	0.23	0.24	0.22	0.22	0.46	27
Vielsalm	0.64	0.81	0.64	0.63	0.41	0.61	0.69	0.59	19
Zotino	0.38	0.61	0.38	0.76	0.68	0.63	0.68	0.40	55
MEAN	**0.55**	**0.64**	**0.55**	**0.53**	**0.43**	**0.52**	**0.57**	**0.63**	
VARIANCE	**0.02**	**0.02**	**0.02**	**0.03**	**0.06**	**0.03**	**0.02**	**0.02**	

Table 4-2b Comparison of correlation coefficients of NEE between different model experiments

Stations	Exp 1, 3	Exp 1, 6	Exp 3, 6	Exp 2, 4	Exp 1, 5
Aberfeldy	0.51	0.76	0.44	-0.07	0.77
Flakaliden	0.78	0.63	0.58	0.78	0.78
Hesse	0.67	0.47	0.51	0.37	0.67
Hyytiälä	0.10	0.65	0.24	0.76	0.76
Loobos	0.75	0.61	0.71	0.39	0.78
Tharandt	0.74	0.49	0.60	0.53	0.74
Tver	0.87	0.49	0.47	0.82	0.83
Vielsalm	0.60	0.54	0.64	0.33	0.71
Zotino	0.54	0.29	0.55	0.63	0.63
MEAN	**0.62**	**0.55**	**0.33**	**0.50**	**0.71**
VARIANCE	**0.05**	**0.02**	**0.02**	**0.07**	**0.003**

Not only the driving input data but also the models as tools play a crucial role in estimating CO_2 fluxes. Table 4-2b shows the correlation coefficients of NEE between different model experiments performed over the study region. The correlations are computed from the daily extracted data for individual stations, the experiments being grouped according to the input vegetation maps used in the models. BETHY and BIOME-BGC, when simulated with their own vegetation maps, show correlation coefficients of 0.7 or higher at only a few stations (red shades in column 1 of Table 4-2b), indicating the model similarities at those stations. The lowest correlation coefficient of 0.1 between the two TBMs was found at Hyytiälä. The daily time series of NEE, shown in figure 4-3, explains how this is so. The NEE plot in figure 4-3 shows a timely start of summertime uptake by BIOME-BGC but decreases gradually in mid-summer. BETHY, on the other hand, does not show summertime uptake until mid-July, which lasts only for a very short period, until mid-August. When a comparison is made with the single stand simulations at the same station, initially shown in figure 3-3 but reproduced here in figure 4-5 for quick comparison, we see that in those model runs the seasonal cycles from the two TBMs are not only corresponding well with each other but also with the observations.

The differences in the results when going from local to regional scale investigations can be attributed to site-specific characteristics that need to be compromised in regional simulations, as well as the common problem faced also by other models of the spatial resolution of the fluxes being compared (grid data to a point location). The limitations of the tools and the input data used add to the modelling uncertainties of regional carbon fluxes.

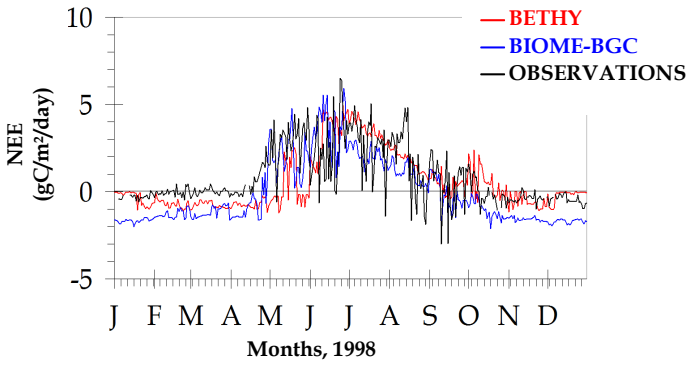

Figure 4-5 **Time series of single stand simulated NEE at Hyytiälä to show the seasonal cycle from BETHY and BIOME-BGC. In comparison with the regionally simulated NEE in figure 3-3 at the same station, a better correspondence between the models can be seen here.**

In comparison to TURC, BETHY and BIOME-BGC show varied correlations at individual stations (columns 2 and 3 of Table 4-2b), sometimes with improved correlations (e.g at Aberfeldy and Hyytiälä, Exp 1, 6), and sometimes with not so good correlations (e.g. at Hesse, Loobos and Tharandt) where both TBMs in comparison to TURC show low correlations. Additionally, BIOME-BGC at these stations is not able to capture the seasonality. The reasons for such behaviour are explained above.

To summarise the outcome of the comparison of regional flux data with observations and with different experiments, average of the daily differences between observations and model results and between experimental pairs were computed. These are shown in figure 4-6.

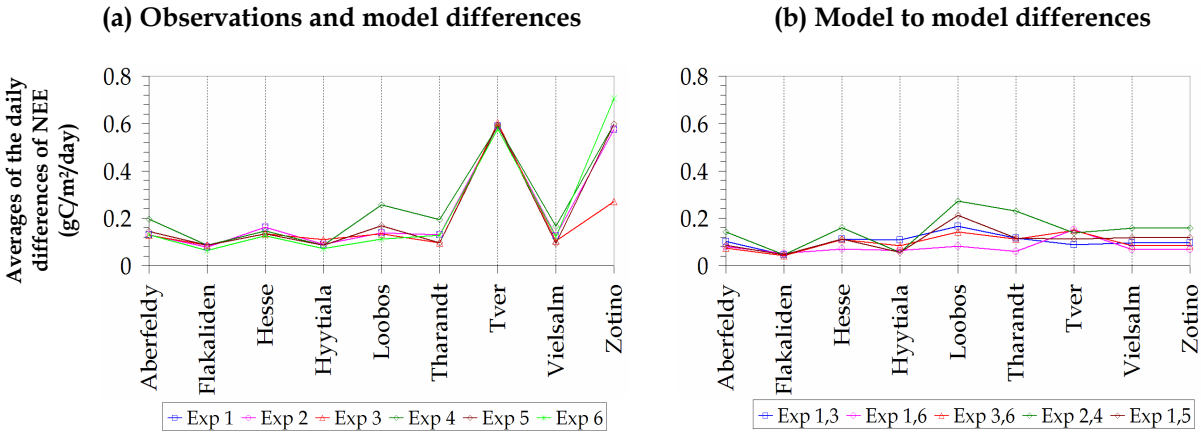

Figure 4-6 Average of the daily differences of NEE between observations and simulations (a), and between model experiments (b)

The figure shows that the different model simulations using different vegetation input maps do not deviate by a huge amount from the observations (Figure 4-6 (a)). At most stations the average differences of both TBMs and TURC are fairly low, between 0.08 and 0.3 gC/m²/day. In Figure 4-6 (b), the average differences between the model experiments at the stations are shown. The largest average difference can be seen between Experiments 2 and 4, in which both the TBMs used the BETHY model's vegetation map. In comparison, the curve for Experiments 1 and 5 that used the BIOME-BGC map (maroon line), shows a lower average difference but with a pattern that is consistent with the simulations using the BETHY map. This indicates that the input vegetation maps provided to the models are important and contribute to the differences seen in the station fluxes.

4.3.2 Regional flux patterns

The regional CO_2 flux patterns are presented here. The analyses focus on the winter and the summer of 1998, as these two seasons provide the largest contrast and the TBMs used in the current study assume that annual NEE is zero. In the last section we have seen how differences in the simulated fluxes arise when local scale investigations are extended to regional scale. This section shows how these differences, and hence the uncertainties, at each stage of terrestrial biosphere modelling are brought forward and get incorporated in the estimation of regional fluxes. In the previous section the main reasons for the experimental differences were the input data, in particular the vegetation maps, used by the different models and the model processes representing the dynamics of ecosystem. These are investigated further in the present section on regional scale.

Figures 4-7a and 4-7b show winter and summer sums, respectively, of the net fluxes and the two components, GPP and R_{total} from Experiments 1, 3 and 6 - the simulated fluxes from BIOME-BGC and BETHY, and the fluxes from TURC, respectively. Note the different scales for each season. The white regions in the maps represent extremely low values.

Figure 4-7a shows the flux patterns from three different model runs during the winter season. As expected for the season, all experiments largely show a release of CO_2 by the biosphere, denoted by the negative NEE, with increasing magnitude from southwest of the region to northeast, as seen from the NEE panels. However, all experiments show a net uptake in Southern Spain, where the wintertime climatic conditions are warmer than the rest of the region.

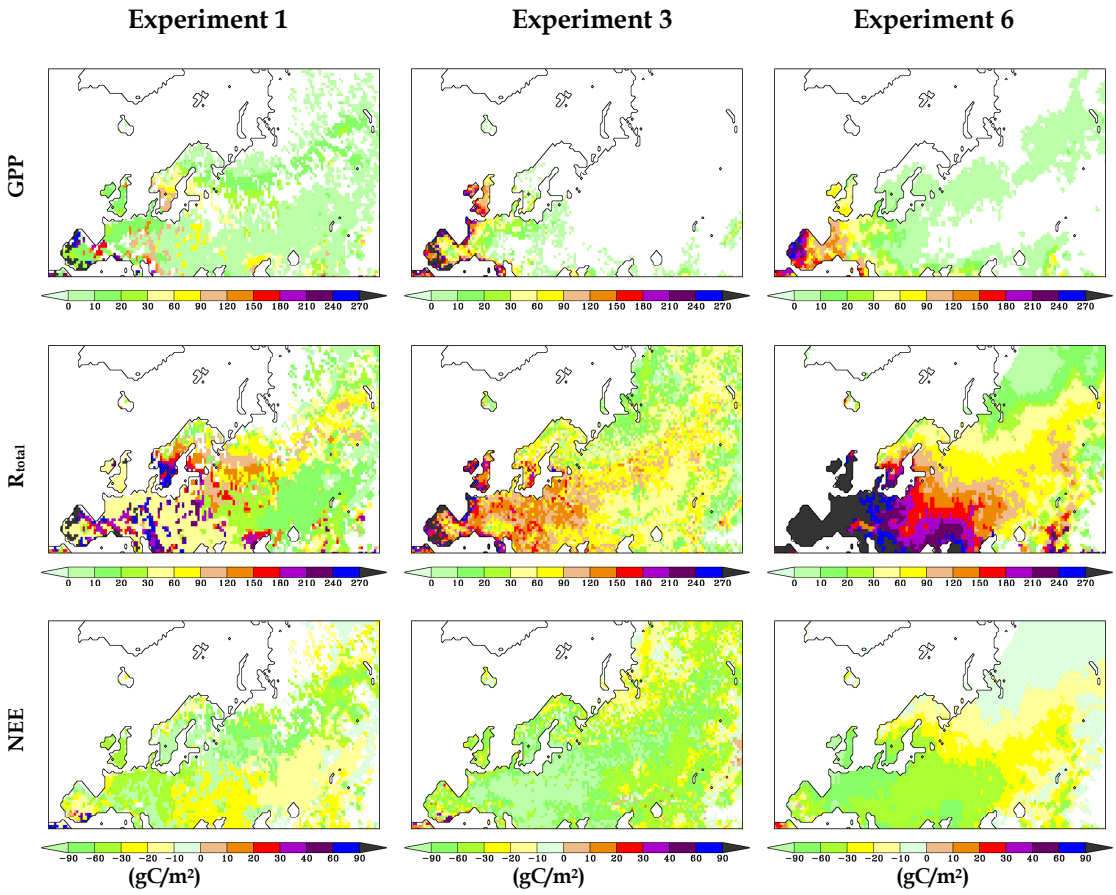

Figure 4-7a Winter (DJF 1998) sums of regional flux components for Experiments 1, 3, 6. Positive NEE indicates uptake by the biosphere (sink), while negative means release by the biosphere (source). NEE is computed as the difference between GPP and R_{total}.

During summer biosphere activities dominate the region, as seen in the different experiments in figure 4-7b. All experiments show a net uptake by the biosphere, denoted by positive NEE, with varying magnitudes. BETHY shows the highest uptake, ranging from 0 to 350 gC/m², with net releases mainly in the southern part of the region, which is a continental area at high altitudes without much vegetation. This pattern of NEE corresponds with the low GPP and R_{total} simulated by BETHY. BIOME-BGC shows a lower net uptake than BETHY, with magnitude ranging from 0 to 25 gC/m² in the southern part of the region, with a small band in

Europe of 200-350 gC/m^2. Some features of the net release can also be seen as in BETHY experiment, but at different locations. For example, the southern part of Spain shows a net release larger than 100 gC/m^2, which could be due to water shortage during the summer.

The low summer uptake in the northernmost latitudes, particularly in Experiments 1 and 6 can be explained by the fact that the onset of summer is late in this part of the region. Siberia typically has only 120-150 days per year with average temperatures greater than 5°C, as compared with about 210 days in Western Europe (Schulze *et al.*, 1999). The TURC fluxes, in comparison with the process-based model experiments, generally show a stratified pattern of net exchange, with higher uptake occurring in the southern part of the region (25-200 gC/m^2). Net releases are comparatively sparser in TURC than in BETHY and BIOME-BGC, showing up only in a few high altitude areas.

The differences in the net flux patterns seen from the different experiments can further be attributed to the distribution and productivity of the vegetation in the region. In BETHY and BIOME-BGC photosynthesis is represented by the driving parameters, V_m and J_m. V_m represents the maximum 'carboxylation rate'[1] at 25°C, while J_m represents the maximum 'electron transport rate'[2] at the same temperature (Knorr, 1997). The values of V_m and J_m are vegetation specific. Further details of these parameters can be found in Knorr (1997). The reason for explaining these processes here is to emphasise that the differences in the regional flux patterns seen from the different experiments are not so much due to

[1] The carboxylation rate is the maximum turnover rate of the primary CO_2 fixating enzyme, Rubisco, which limits the rate of photosynthesis at sufficient light (Knorr, 1997)
[2] Electron transport rate is the rate of carbon assimilation, which becomes the limiting factor at low light levels (Knorr, 1997)

the amount of vegetation that is there but rather due to the efficiency of the photosynthetic rate of the vegetation that is present. The latter determines how active the biosphere is in terms of terrestrial carbon exchange.

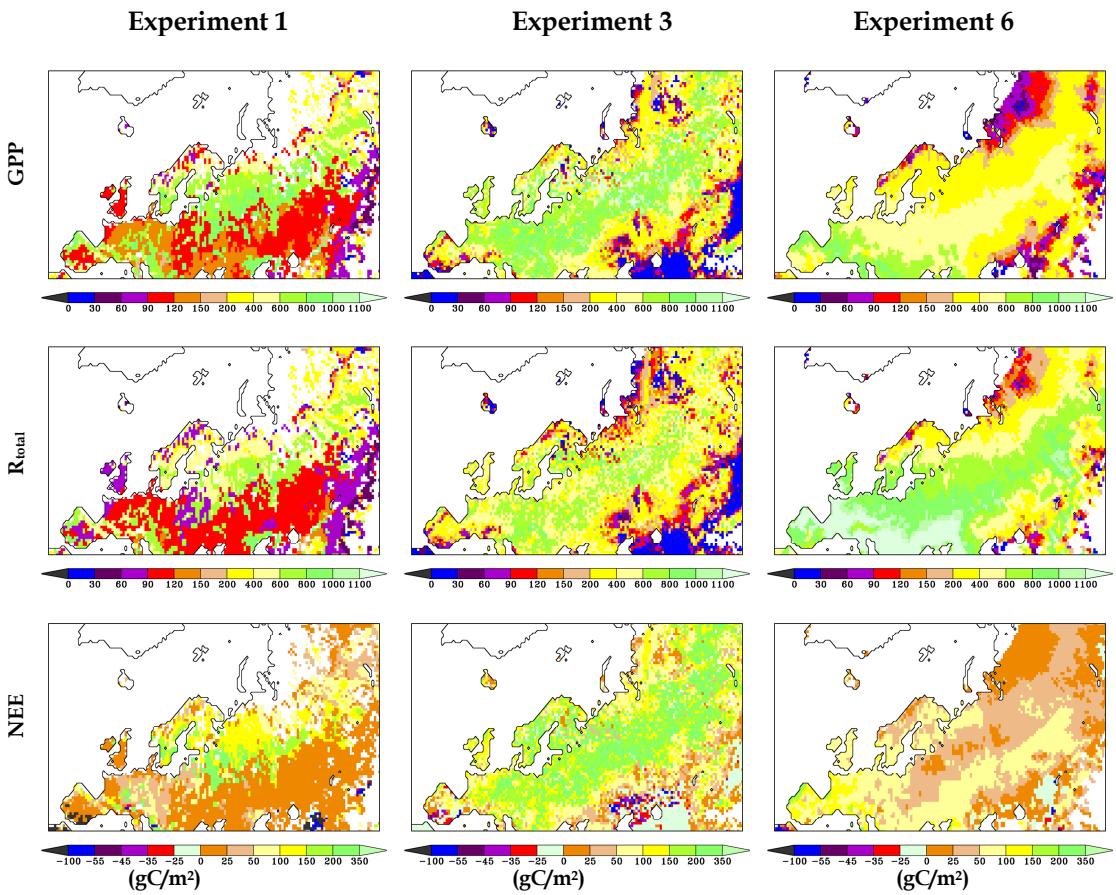

Figure 4-7b Summer (JJA 1998) sums of regional flux components for Experiments 1, 3, 6. Positive NEE indicates uptake by the biosphere (sink), while negative means release by the biosphere (source). NEE is computed as the difference between GPP and R_{total}.

To explain the differences between the results and the sources of uncertainties arising in the estimated fluxes, correlation coefficients of NEE were computed between the different experiments. Additionally, the

significance of the correlations was computed using Pearson's significance test. These are presented in figure 4-8.

The correlation maps generally show that the different experimental pairs are significantly correlated in most parts of the region. In some regions of Eastern Europe and Siberia BETHY and BIOME-BGC correlate well (correlation coefficients between 0.6 and 0.9 of Experiments 1, 3) when

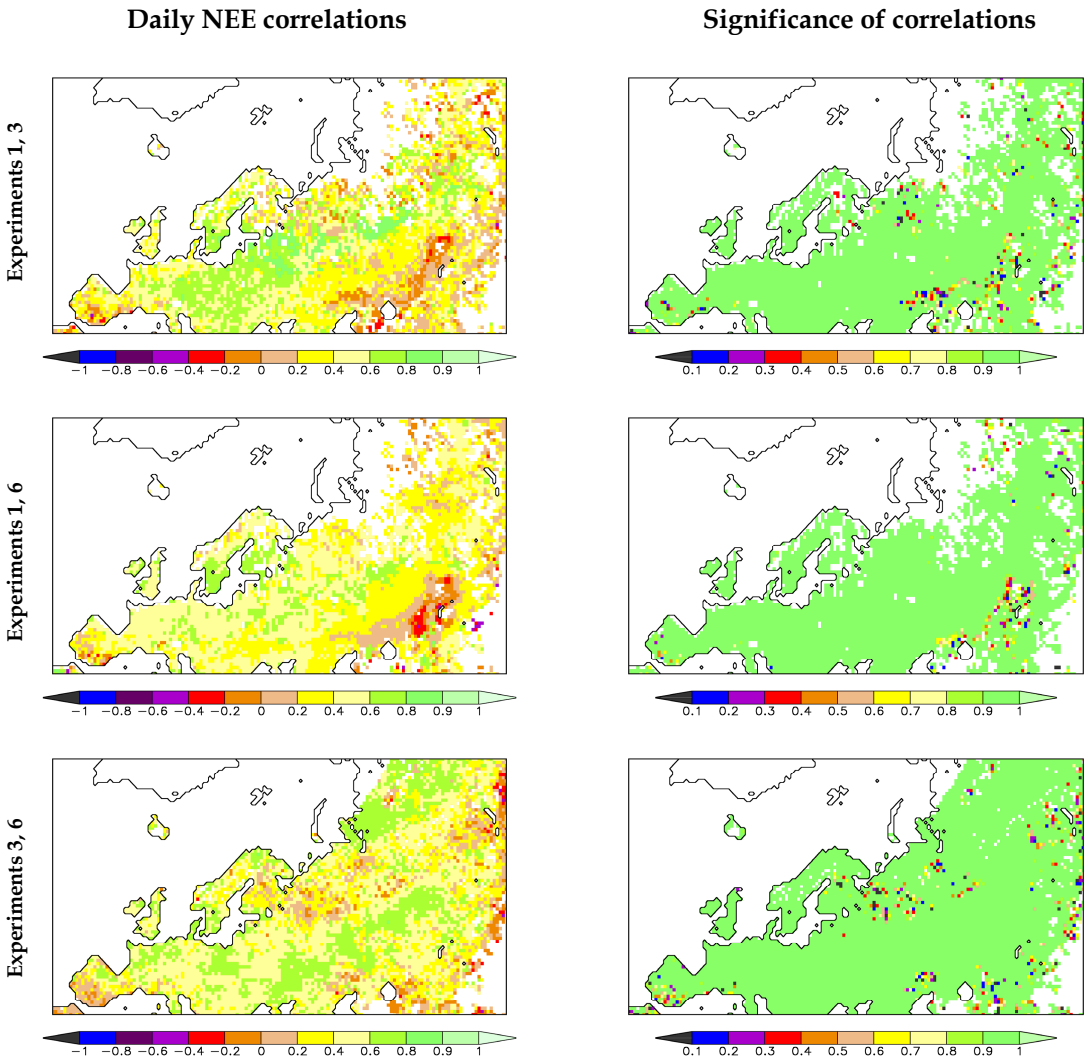

Figure 4-8 Daily NEE correlations between different experiments with corresponding significance of the correlations

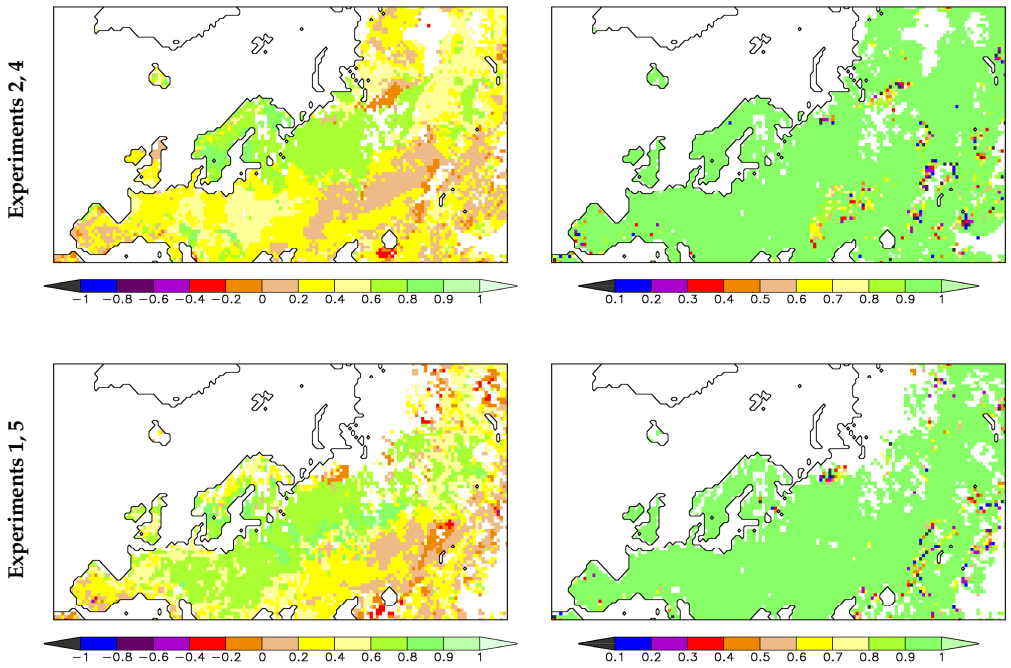

Figure 4-8 (continued)

simulated with their own vegetation maps, indicating similarity in their seasonal cycle. Low correlations between 0.4 and 0.6 can also be seen, indicating the differences between the two models. Relatively weak but significant correlations (between 0.4 and 0.6) between Experiments 1 and 6, and 3 and 6 can be seen together with sparsely distributed pixels of high (0.8) correlations. High correlations can also be seen between Experiments 1 and 5. The correlation between Experiments 2 and 4 varies – for Western Europe, significantly low correlations are seen while in Scandinavia and European Russia the experiments show high correlations. In all maps very low, as well as negative correlations can be seen (values between –0.2 to 0.2) but these are not significant.

To summarise, the simulated fluxes show relatively large differences between the different model experiments, not only in magnitude but also

in the spatial patterns, although the models do agree on some general patterns such as the net uptake of carbon in winter in Southern Spain. However, the differences seem to be larger in the individual flux components than in the net ecosystem exchange. Even when the two TBMs are using the same input vegetation map, the correlation coefficients are generally not very strong (figure 4-8, Exp 1, 5 and Exp 2, 4), indicating that at least part of the differences can be attributed to model structure and process representation.

4.3.3 Overall regional flux patterns

To summarise the net flux patterns in the region, the overall regional fluxes are presented in this section. Figure 4-9 illustrates the seasonal cycles of the regional sums of NEE resulting from the different experiments.

Although the models produce a strong seasonal cycle over the region, there are differences in timing and amplitude between the models due to the use of different vegetation maps that influence the phenological processes and relative distribution of NEE in the models. Such differences in the seasonal behaviour of the models were already seen in the station investigations (Chapter 3), where one model (BIOME-BGC) uses specific station information while the other (BETHY) uses model-derived information for the sites.

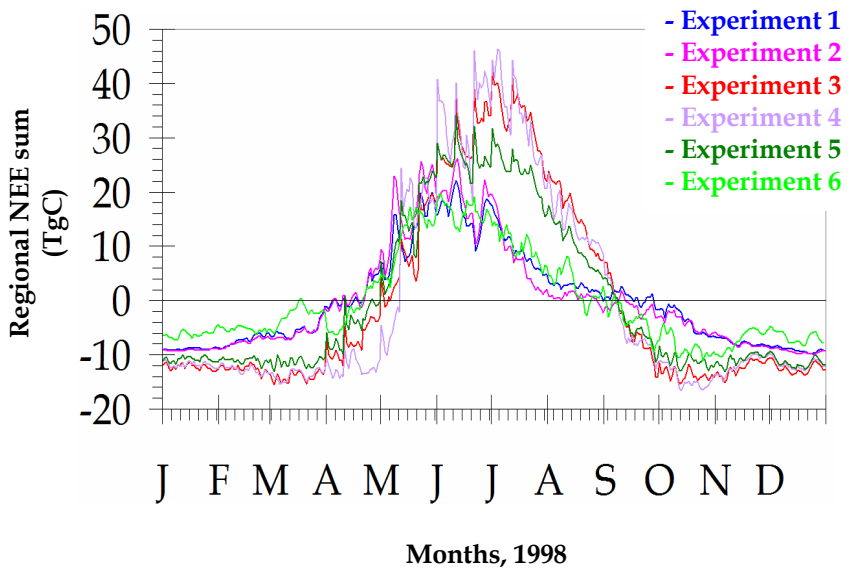

Figure 4-9 Seasonal cycle of the regional sums of NEE from the different biosphere model experiments

The time series of the overall regional sum of the fluxes shows that the onset of summer for the different experiments with the three models occurs within one month of each other. However, the summer peak in BIOME-BGC and TURC occur earlier than in the experiments with BETHY, which also shows overall optimal performance with its own vegetation maps (Experiments 3 and 4). When simulated with the map derived from BIOME-BGC the net uptake is reduced but still higher than either BIOME-BGC or TURC.

To further investigate the model differences, the amplitudes of the seasonal cycle were extracted to find out how active the biosphere in the region is during the year. The maps of the amplitudes from each experiment are shown in figure 4-10.

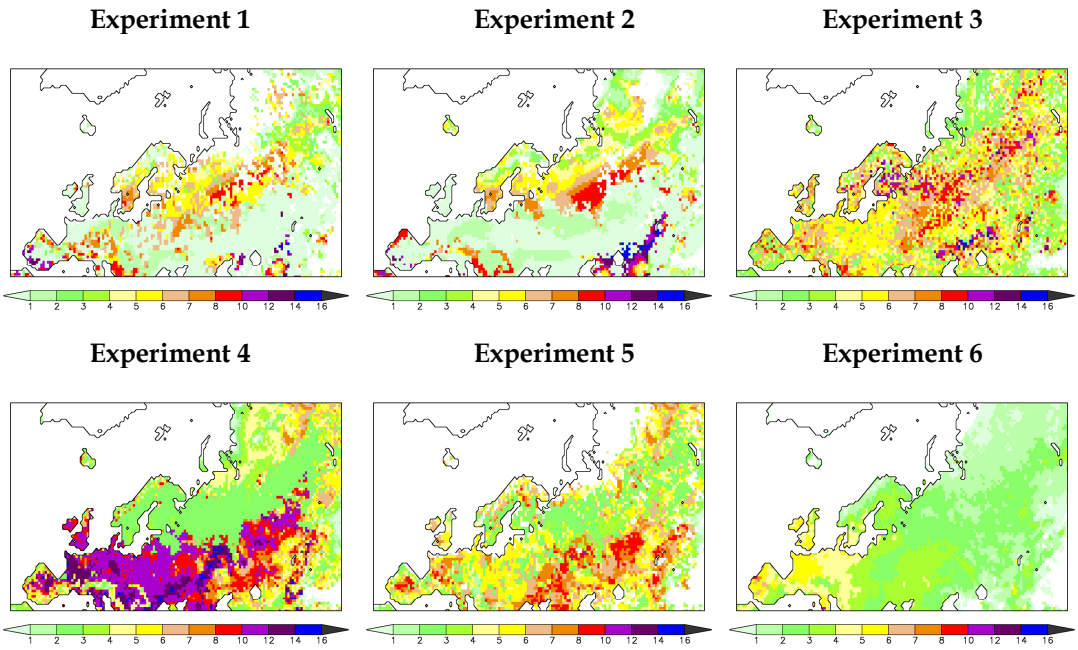

Figure 4-10 Amplitudes in gC/m² of NEE over the region for each experiment, to illustrate how active the biosphere is during the study period, 1998

The maps of the amplitudes of NEE, computed from 10-day running mean values to eliminate noise for each experiment, show that BETHY is highly active, with large amplitudes of NEE in all three (BETHY) experiments (3, 4 and 5), as compared with BIOME-BGC (1 and 2) and TURC (6). However, the patterns of the biosphere activities in each experiment are different, regardless of the fact that the same model was used. For example, Experiments 4 and 5 show patterns that are comparatively similar to each other but different from Experiment 3, as seen in the high values in Western Europe and lower values in European Russia, extending up to West Siberia. Experiment 3, on the other hand, shows stronger biosphere activities in Russia and West Siberia. BIOME-BGC shows sparsely distributed high amplitudes mainly in the southern part of the region and in Russia in both its experiments. The model does not show large sensitivity towards the change in its vegetation input. TURC shows

the lowest amplitudes throughout the region indicating low biosphere activity.

Figure 4-11 shows the contributions of the fluxes from the different vegetation types in the region.

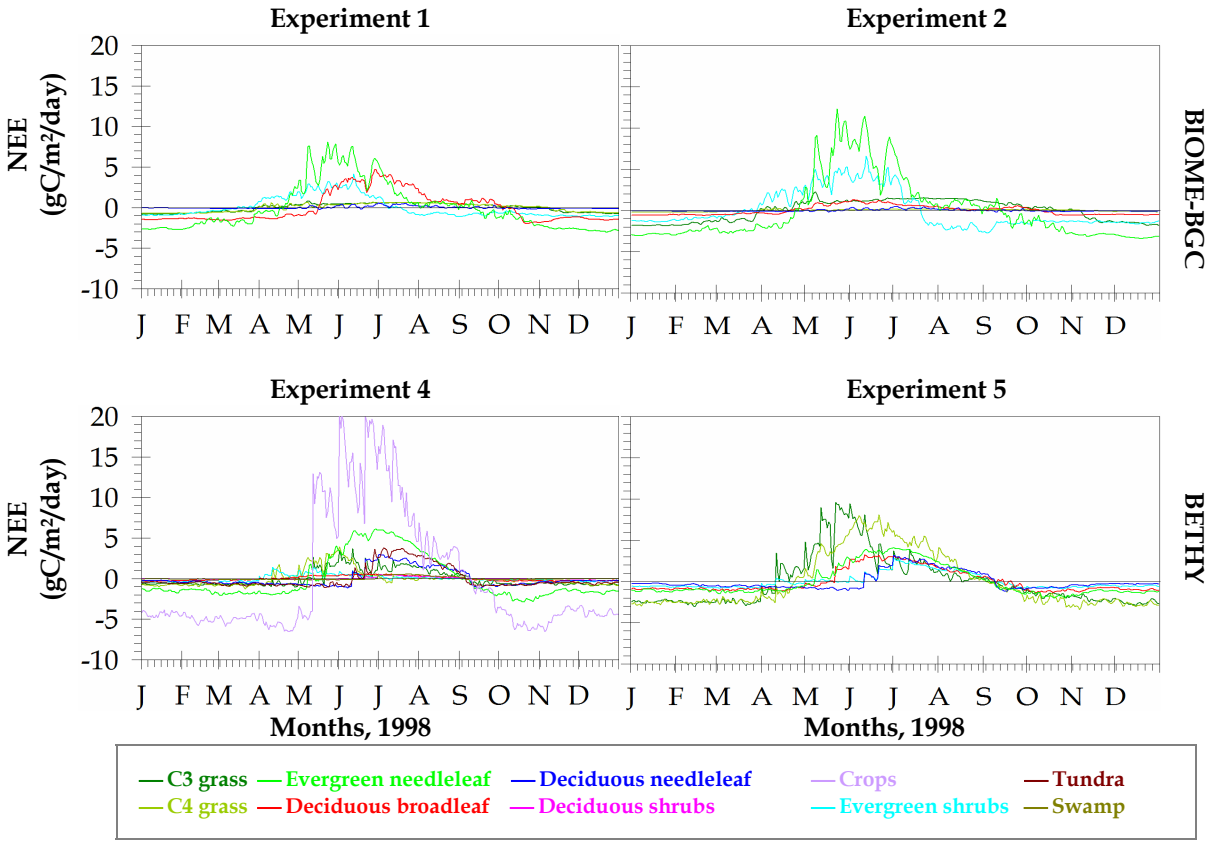

Figure 4-11 **Contributions of the biosphere fluxes from different vegetation types used in BETHY and BIOME-BGC. Note that the contributions from Experiment 3 are not included in the plots because the map used contained fractions of vegetation types per grid. Instead, the contributions from Experiment 4 are shown, that used the majority class of the fractionated map.**

In both models evergreen needle leaf, deciduous broad and deciduous needle leaf forests dominate the seasonal cycles of NEE, except Experiment 4 of BETHY, whereby crops dominate the biospheric

contributions showing large summer uptake, in the order of about 20 gC/m²/day. In contrast, the contributions of C3 and C4 grasses from BIOME-BGC are very low. Both C3 and C4 grass is more active at the onset of summer, showing approximately 4 gC/m²/day of net exchange. When BETHY is simulated with BIOME-BGC vegetation map (Experiment 5), net exchange of C4 grass is improved over summer. While the net uptake of C3 grass is enhanced the overall seasonality does not change much.

Other sources of flux contributions include fluxes from the ocean and from fossil fuel burning, the latter being kept constant for 1998. Figure 4-12 presents the summer and winter net CO_2 exchange from the individual components of the fluxes - biosphere, ocean and fossil fuel - over the whole region.

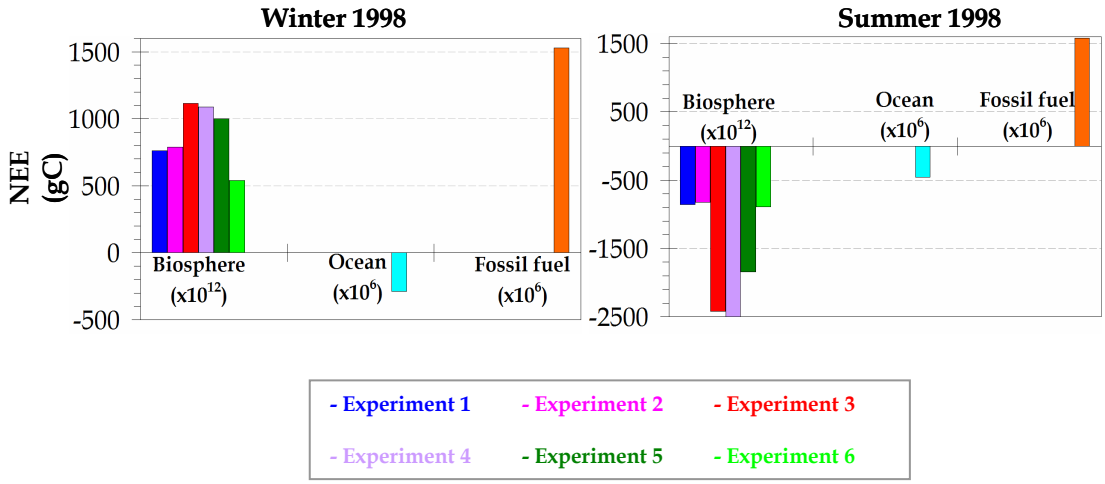

Figure 4-12 Regional sums of NEE from the flux components for winter and summer 1998: biosphere - from different flux experiments; ocean and fossil fuel – from Takahashi and EDGAR database, respectively. Positive NEE denotes release to the atmosphere, while negative indicates uptake

The bar plots show that the net exchange due to the biosphere is dominant, showing net release during winter (in the range of approximately -500 to –1000 TgC) and net uptake during summer (ranging from 800 to 2500 TgC). Contributions from fossil fuel and ocean are low over the region.

The regional seasonal fluxes from fossil fuel and ocean are shown in figure 4-13. Note that fossil fuel fluxes remain constant. Ocean uptake during summer is higher than during winter.

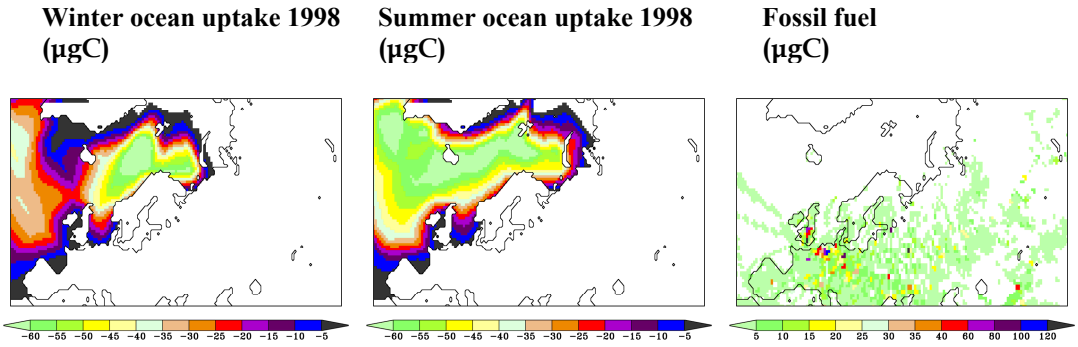

Figure 4-13 Regional patterns of CO_2 flux contributions from the components: ocean, for winter and summer 1998, and fossil fuel, which is assumed constant during the year

4.4 DISCUSSION

The use of different models and different input data to the models leads to significant differences in the estimation of terrestrial CO_2 fluxes. At single stations (where the fluxes were extracted from regional simulations) the models are able to produce the seasonal cycles, but differences are seen,

for example in the onset and at the end of summer period, as well as in the amplitudes of the net flux exchange. These differences arise first of all due to the fact that in the regional simulations, each grid represents a much larger area then a single point being compared. However, the differences in the amplitudes and the phasing of the seasons were already noted for the station simulations, and therefore they can at least partly be attributed to the representation of the ecosystem processes in the models. Overall, the performance of BIOME-BGC for station simulations (see Table 4-2a) is better in comparison with the experiments from BETHY, as well as other regional experiments.

When extending local scale investigations of flux exchange to regional scale, uncertainties are incorporated firstly with the choice of the model and secondly with the input data provided to the model. Even when the two TBMs are using the same input vegetation map, the regional patterns of the flux amplitudes (figure 4-10) and correlation coefficients (figure 4-8) show some significant differences, indicating that at least part of the differences in simulated fluxes can be explained by the model that is used. However, the use of a different vegetation map in the same model also introduces uncertainties in the results. BETHY showed greater sensitivity towards changing the vegetation maps than BIOME-BGC due to the assigned values of the photosynthesis parameters, V_m and J_m. The vegetation maps affect the phenology in the models, which affects the spatial patterns, as well as the seasonality of the simulated biosphere fluxes. All in all, it seems that the large uncertainties seen in the flux simulations are due to the choice of the model, as much as the type of input data that are being used. Regional and global studies on carbon fluxes from the biosphere should therefore try to take these uncertainties into account and not rely on the results of a single model.

4.5 CONCLUSIONS

In this chapter we found significant differences in the simulated fluxes between the two TBMs and the different input vegetation maps used in these models. Overall, the flux values over 1998 simulated in the different experiments in this study range from -600 to –1100 TgC for the winter season and ~820 to 2500 TgC for the summer, indicating large uncertainties due to the input data, as well as the choice of the model. The vegetation type classification is very important in terrestrial ecosystem modelling, as it directly influences the modelling of the phenology, and hence the overall seasonality. The limitations on the complexity with which the ecosystem processes are represented in the models also contribute to the uncertainty in the flux estimations, as seen from the different models. The uncertainties in the biosphere flux estimations, in turn, will be propagated in the estimation of the atmospheric CO_2 concentrations. This is discussed in the next chapter.

CHAPTER 5
CO_2 CONCENTRATION SIMULATIONS OVER EUROSIBERIA

5.1 INTRODUCTION

The surface fluxes from the terrestrial biosphere contribute to the variability of atmospheric CO_2. The land surface processes among the vegetation and soil types affect the biophysical land-atmosphere interactions, thereby providing the terrestrial CO_2 fluxes into the climate system and controlling the diurnal and annual cycles of atmospheric CO_2 concentrations.

In the previous chapter process-based terrestrial biosphere models were used to simulate the biosphere fluxes. It was shown that the flux estimations are influenced by the choice of the models, as well as the driving input data to the models. The current chapter investigates how the uncertainties in the flux estimations are translated into atmospheric CO_2 when transported across the region. The focus therefore is on the variability of CO_2 concentrations, arising due to the uncertainty of the fluxes from the biosphere models. Additionally, the current chapter explores how influential the biosphere fluxes are in the estimation of atmospheric CO_2 higher up in the atmosphere. To this end, the flux estimates of the different experiments with the terrestrial biosphere

models (see Chapter 4) were fed into the regional transport model REMO that simulated the atmospheric CO_2 concentrations over the study region. Investigations were carried out for three different model levels: ground level (level 20), which represents approximately 34m above ground; level 18, which is within the PBL at approximately 300m, and level 12, which is above the PBL at approximately 3000m. The heights represented by these levels are where most of the mixing of air takes place, hence are considered appropriate for the investigations of the biosphere fluxes and their influence in the atmosphere concentration estimations.

The next section in this chapter explains the approach towards simulating the atmospheric CO_2 using the regional transport model REMO, followed by an analysis of the concentration patterns in the region. Here, the focus will be on investigating the uncertainties arising from the use of different biosphere models and different input data.

5.2 APPROACH TO ATMOSPHERIC CONCENTRATIONS SIMULATION

The CO_2 fluxes obtained from the terrestrial biosphere simulations (Chapter 4) were used as input to the regional transport model REMO for simulating atmospheric CO_2 concentrations over Eurosiberia. The regional fluxes from the five different experiments were used in an offline mode, while the meteorology in REMO was online. Using ECMWF analysis information at the boundary of the study region, together with the tracers – that is, concentrations due to fossil fuel, ocean and biosphere at the boundary simulated by TM3, also using ECMWF analysis - REMO generates its own meteorology. The boundary CO_2 fluxes used in REMO

are ocean-atmosphere fluxes estimated by Takahashi *et al.* (1999) and fossil fuel from the emissions database EDGAR, as explained in Chapter 2. During the REMO run the contribution of fossil fuel emissions is kept constant in time. These boundary fluxes were the same as those used in the global TM3 model to generate the tracers used at the boundaries in REMO, except for the fact that they were interpolated to REMO grid before being used in REMO.

In the present study REMO was run in the "forecast mode" (Karstens *et al.,* 1996) whereby the results of consecutive short-range forecasts of 30 hours are used. For each day REMO was started at 00 UTC from the weather forecast analyses and a 30-hour forecast is computed. To account for a spin-up time the first 6 hours of the forecast are neglected. This spin-up time has been shown to be sufficient for EM of DWD and has also been used in previous study by Chevillard *et al.* (2002a). Therefore, it is also assumed adequate in the present study. By restarting the model everyday from the reanalyses, the model state was forced to stay close to the weather situation of these analyses.

Additional uncertainties, other than those from the TBM-generated fluxes, are introduced in the estimation of atmospheric concentrations due to the use of the coarse resolution global data (for boundary conditions), constant fossil fuel fluxes which in reality are not constant, and interpolation of the global data to REMO grid, where information could get lost depending on the reliability of the interpolating scheme.

The simulated CO_2 fluxes of the five experiments with the terrestrial biosphere models BETHY and BIOME-BGC obtained in Chapter 4 were, together with the flux estimates of the TURC model, fed into REMO in

order to calculate the atmospheric transport. To take account of the diurnal cycle, the daily flux estimates were interpolated to hourly values according to the variation of incoming solar radiation at each location. The REMO model subsequently calculated the atmospheric concentrations for each of the different biosphere flux inputs (Experiments 1 to 5 plus TURC). Figure 5-1 shows a flow diagram of the simulation of atmospheric CO_2 by REMO.

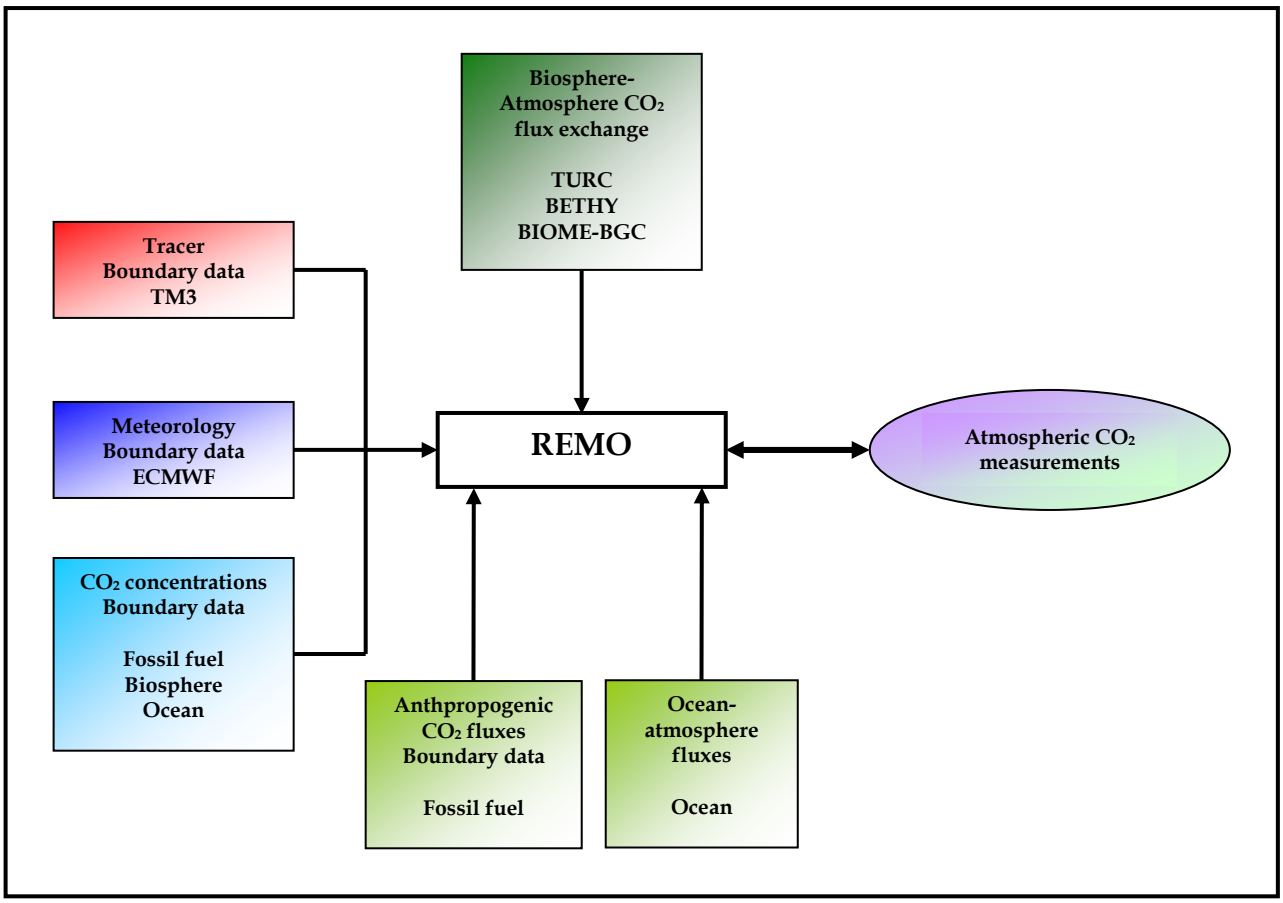

Figure 5-1 **Modelling framework to simulate atmospheric CO_2 concentrations with the regional transport model REMO, using the boundary meteorology from ECMWF analysis, tracers from TM3 and simulated biosphere fluxes from BETHY, BIOME-BGC and TURC. The simulated concentrations are compared with station observations.**

5.3 RESULTS AND ANALYSIS

The results are presented in three parts: the first part looks at comparison of the simulated concentrations with observations at single sites, with the aim of illustrating that the use of terrestrial fluxes from different biosphere models affects the simulated concentrations at different atmosphere levels. Seasonal cycles of the concentrations using the fluxes from three biosphere model experiments, namely Experiments 1, 3 and 6 (the same as in Chapter 4), are presented as examples. Out of the 16 stations investigated, two contrasting stations (one coastal and one continental) were selected for detailed analysis and will be presented in this section. The remaining station analyses are provided in Appendix 9, for the three parts of the results, respectively.

The second part presents the regional concentration patterns over the study region. Two contrasting seasons were investigated: summer and winter of 1998. The focus of the analysis is on the variability of CO_2 concentrations and the variability arising due to the fluxes from the TBMs.

The final part of the section summarises the main findings of the patterns and uncertainties propagated from the regional fluxes to the regional atmospheric concentrations.

5.3.1 Concentration comparisons at single sites

Results for two stations are presented here: the first is a coastal station that conducts fixed *in-situ* measurements in Germany on the island of Sylt in

the North Sea (site name Westerland). The station is situated directly at the coast at 54° 56′ N and 8° 19′ E, at 12m elevation. The second site is a continental station in Hungary (site name Hegyhatsal), situated at 46° 57′ N and 16° 38′ E, at a height of 344m. Figure 5-2 shows the seasonal cycles of the simulated concentrations using different flux inputs as compared with the observations at the two stations.

The figure shows that at ground level the fluctuations of the simulated concentrations sometimes exceed the observations but they show reduced variability higher up in the atmosphere (level 12). This indicates that the mixing of the tracers in REMO in the higher atmosphere is modelled as expected, meaning that the air at high altitudes is well mixed thereby leading to lower concentration amplitudes. Generally the simulated concentrations lie closer to each other than to the observations. A look to Appendix 9, where the seasonal cycles of all stations investigated are presented, shows that there are stations where the simulated and observed concentrations compare well in the sense that the simulations are closer to the observations (e.g. Hyytiälä and Schauinsland). Comparison of hourly concentration variation at synoptic scale, for example over one month, as seen in figure 5-3 for the Russian stations, Tver and Zotino, not only shows a relatively good agreement between simulations and observations but also a timely phasing of the diurnal cycle, a feature not clearly seen on larger time-scales like in figure 5-2. In figure 5-3 we see that while REMO simulates the synoptic scale variation well, differences can still be seen in the amplitudes. The low observed concentrations at Tver between days 6 and 10 appear strange with respect to the rest of the days in the month where the diurnal cycle between the models and the observations correspond well. A possible reason for these low observations could be due to instrument failure.

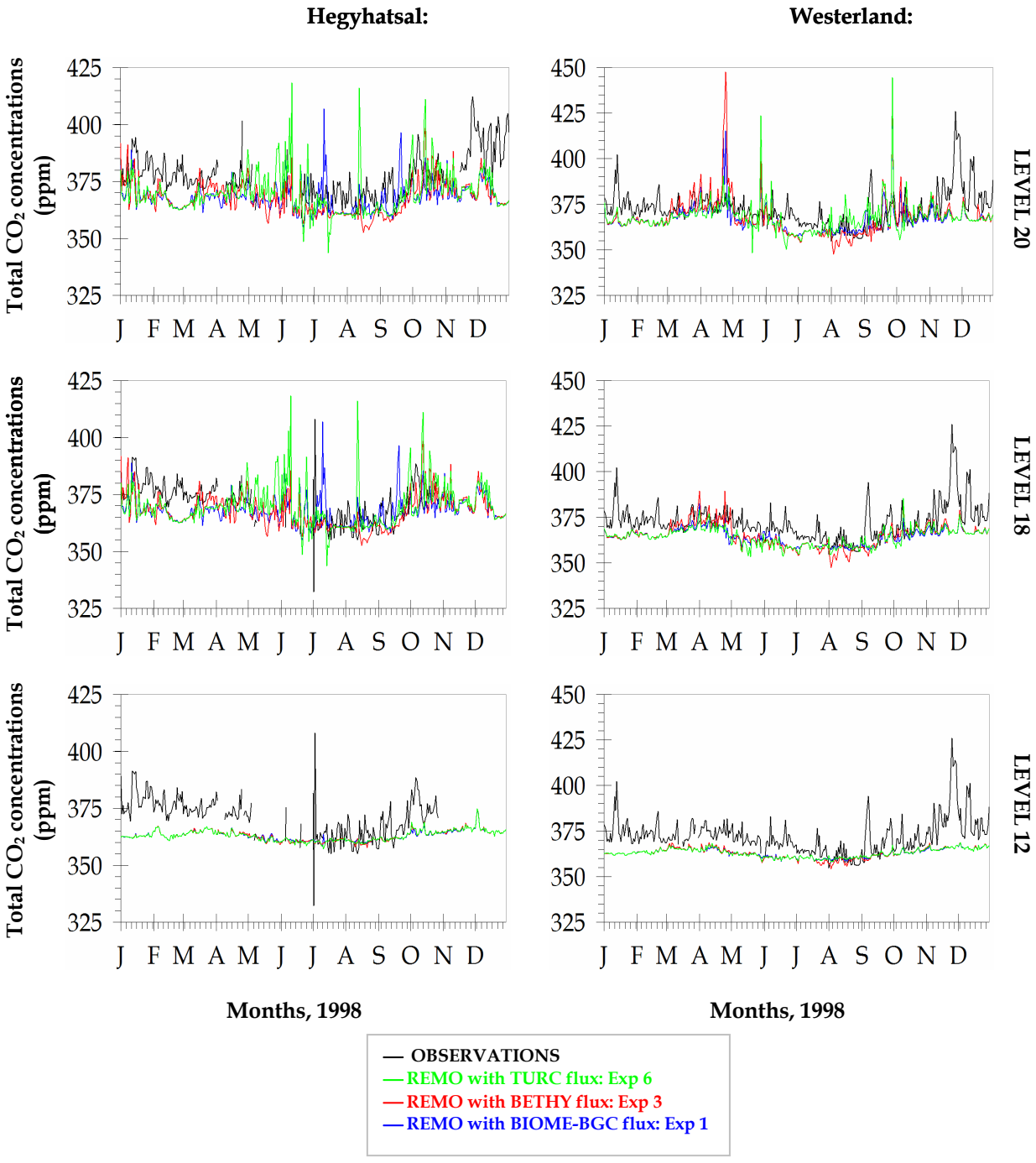

Figure 5-2 **Seasonal cycles of simulated and observed atmospheric concentrations (ppm) at Hegyhatsal and Westerland stations. Flux inputs are from BIOME-BGC, BETHY and TURC models (Experiments 1, 3 and 6, respectively). The observed total concentrations are from the WDCGG database. Note the different atmospheric levels for which the concentrations are shown. The results for other stations are presented in Appendix 9.**

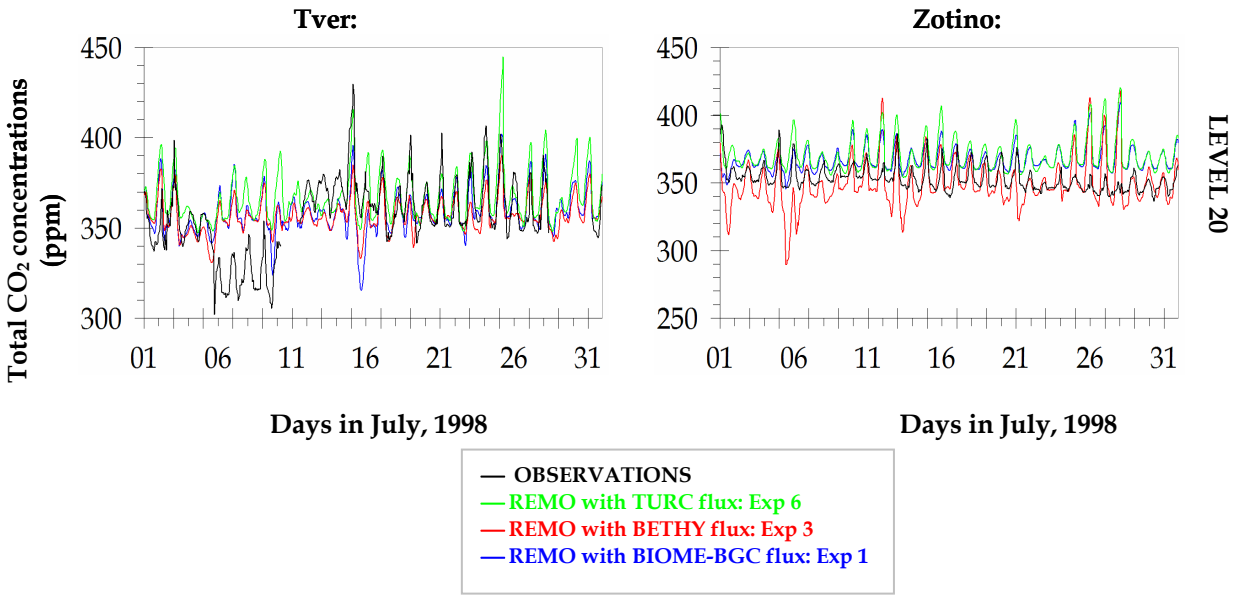

Figure 5-3 **Diurnal cycles of simulated and observed concentrations for July 1998 for the lowest model level at Tver and Zotino.**

The differences between the observed and simulated concentrations (Figure 5-2) can be explained by the contribution of the concentration components from the model. Figure 5-4 shows the contributions of biosphere and fossil fuel emissions and oceanic uptake for the two stations Hegyhatsal and Westerland at different atmospheric levels. At ground level the contribution of the fossil fuel emissions at Westerland show a spike at the end of September/beginning of October, while the biosphere contributions are low. The corresponding total concentration plot in figure 5-2 also shows a sharp peak around the same time in the simulated concentrations using TURC fluxes. Similarly, the peaks occurring from the component concentrations at other times during the year show corresponding peaks in the total concentrations. This type of seasonal patterns is not only seen at Westerland but also at Hegyhatsal, as well as at other stations investigated (see Appendix 9).

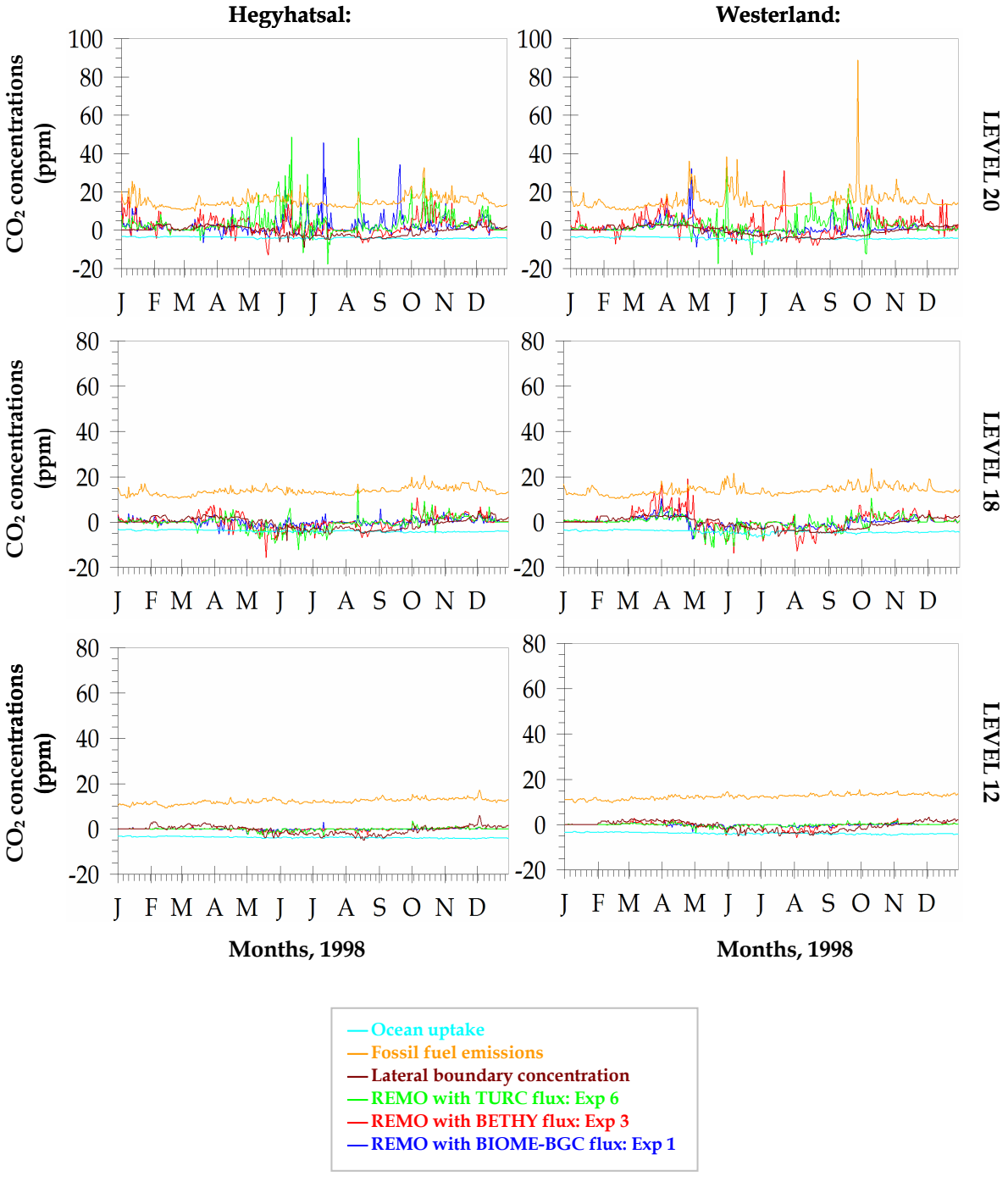

Figure 5-4 **Seasonal cycles of concentration components from the model. Shown are emission contributions from the biosphere, fossil fuel, lateral boundary and uptake by ocean.**

With increasing atmosphere height, the peaks from the component plots, as well as the total concentration plots gradually diminish, indicating the increased mixing layer. The high variability of the total concentrations, particularly at ground level, shows the strong contributions from the biospheric components, which are important in determining the patterns seen in the overall total concentrations. The contribution of the lateral boundary in all cases is small.

In addition to the individual components, a background atmospheric concentration of 355ppm was added to get the total concentration. It can be seen from figure 5-4 that the biosphere contribution to the total atmospheric CO_2 variability is the largest in comparison with emissions from fossil fuel and ocean uptake. The largest variability of all emissions can be seen mainly at the ground level, indicated by varying amplitudes. This is reduced higher up in the atmosphere where the air is well mixed. At 300m, within the PBL, significant fluctuations can still be seen in the biosphere emissions. Above the PBL, the mixing of the air further reduces the fluctuations, making the emissions from the different sources approximately constant. However, the biospheric emissions still show some minor variations.

As a summary for all stations, daily correlation coefficients between observations and simulations, and between simulations using different biosphere fluxes were calculated. These are presented in Tables 5-1a and 5-1b, respectively. Due to the short-term fluctuations the correlations between measurements and simulations are sometimes rather low (Table 5-1a), suggesting poor agreement. Appendix 9, however, shows that at several stations the observations and simulations lie in fact close to each other.

On a synoptic scale, as in the case of Tver and Zotino, the phasing of the diurnal cycles corresponds well with the observations, although the correlations for July 1998 are not very high. In contrast, Table 5-1b shows good correlations between the simulated concentrations using the biosphere fluxes from different experiments. Overall, the modelled concentrations correspond better with each other than with the observations.

Table 5-1a Correlation coefficients of CO_2 concentrations between observations and simulations – 1998

Stations	Tracer simulation using Exp 1 flux	Tracer simulation using Exp 2 flux	Tracer simulation using Exp 3 flux	Tracer simulation using Exp 4 flux	Tracer simulation using Exp 5 flux	Tracer simulation using Exp 6 flux
Aberfeldy	0.28	0.26	0.24	0.16	0.26	0.09
Hesse	0.22	0.33	0.18	0.20	0.15	0
Hyytiälä	0.48	0.35	0.40	0.45	0.42	0.41
Loobos	0.16	0.16	0.22	0.21	0.18	0.13
Tharandt	0.30	0.33	0.32	0.28	0.34	0.07
Tver (Only July data)	0.45	0.48	0.44	0.21	0.47	0.54
Zotino (Only July data)	0.36	0.46	0.30	0.27	0.33	0.47
Mace Head	0.40	0.36	0.45	0.27	0.46	0.01
Plateau Rosa	0.10	0.28	0.46	0.50	0.45	0.2
K-Pustza	0	0.09	0.13	0.12	0.15	0.1
Hegyhatsal	0.19	0.07	0.39	0.35	0.36	0.21
Monte Cimone	0.22	0.12	0.41	0.46	0.42	0.19
Schauinsland	0.37	0.14	0.47	0.46	0.51	0.17
Westerland	0.25	0.25	0.25	0.26	0.24	0.14
Ny-Alesumd	0.41	0.40	0.55	0.51	0.58	0.32
Pallas	0.62	0.70	0.73	0.73	0.76	0.5

Table 5-1b Correlation coefficients of CO_2 concentrations between the tracers simulated using different biosphere model fluxes

Stations	Tracer simulation using fluxes from Exp 1, 3	Tracer simulation using fluxes from Exp 1, 6	Tracer simulation using fluxes from Exp 3, 6	Tracer simulation using fluxes from Exp 2, 4	Tracer simulation using fluxes from Exp 1, 5
Aberfeldy	0.80	0.72	0.69	0.62	0.83
Hesse	0.69	0.45	0.56	0.49	0.71
Hyytiälä	0.84	0.77	0.71	0.75	0.86
Loobos	0.95	0.94	0.88	0.89	0.97
Tharandt	0.71	0.63	0.59	0.69	0.67
Tver (Only July data)	0.89	0.82	0.83	0.36	0.89
Zotino (Only July data)	0.87	0.89	0.78	0.72	0.79
Mace Head	0.89	0.64	0.59	0.59	0.86
Plateau Rosa	0.68	0.63	0.71	0.71	0.63
K-Pustza	0.44	0.48	0.57	0.36	0.36
Hegyhatsal	0.58	0.63	0.72	0.35	0.54
Monte Cimone	0.63	0.64	0.69	0.48	0.61
Schauinsland	0.55	0.54	0.53	0.27	0.59
Westerland	0.92	0.79	0.69	0.85	0.91
Ny-Alesumd	0.83	0.96	0.75	0.87	0.89
Pallas	0.77	0.86	0.65	0.83	0.78

The low correlations between the measurements and the concentrations derived from the different experiments suggest that the REMO model is not well able to capture the short-term fluctuations in atmospheric concentrations. This could partly be due to an incorrect representation of the flux variability by the biosphere models, but may also be attributed to other (for example, local) factors not taken into account here.

To illustrate further how the atmospheric CO_2 concentration changes with the atmosphere heights, profiles of concentration data were plotted using the available aircraft measurements taken during the summer of 1998, within the framework of the EUROSIBERIA CARBONFLUX project. For the corresponding days and time of the availability of measurements, simulated concentrations were also plotted. The aircraft profile measurements for Zotino station in Russia is presented in figure 5-5, together with the corresponding simulated profiles, plotted according to the days for which measurements were available – two days in July and two days in August of 1998.

It should be noted here that the aircraft profiles are taken only for a couple of hours per flight at very short time intervals, several seconds up to a minute interval. However, the simulated concentrations are for every hour. Instead of interpolating and plotting the simulated profiles together with the measurements, they are plotted separately here to show the variations in the profile results from experiment to experiment and how they compare with the measured profile in a general way.

The measurement profile plots show significant fluctuations in the concentration patterns for different days. The profile of 9 July (blue line) shows higher concentrations than those later in July and August and at the end of summer (01-September) for low atmospheric heights. The simulated profiles show a smoother pattern higher up in the atmosphere than at lower heights, where the differences are much larger. As shown previously, the tracers from different biosphere fluxes show greater variability near to the ground. The simulated range of the concentration magnitude is mostly within the range of the measurements.

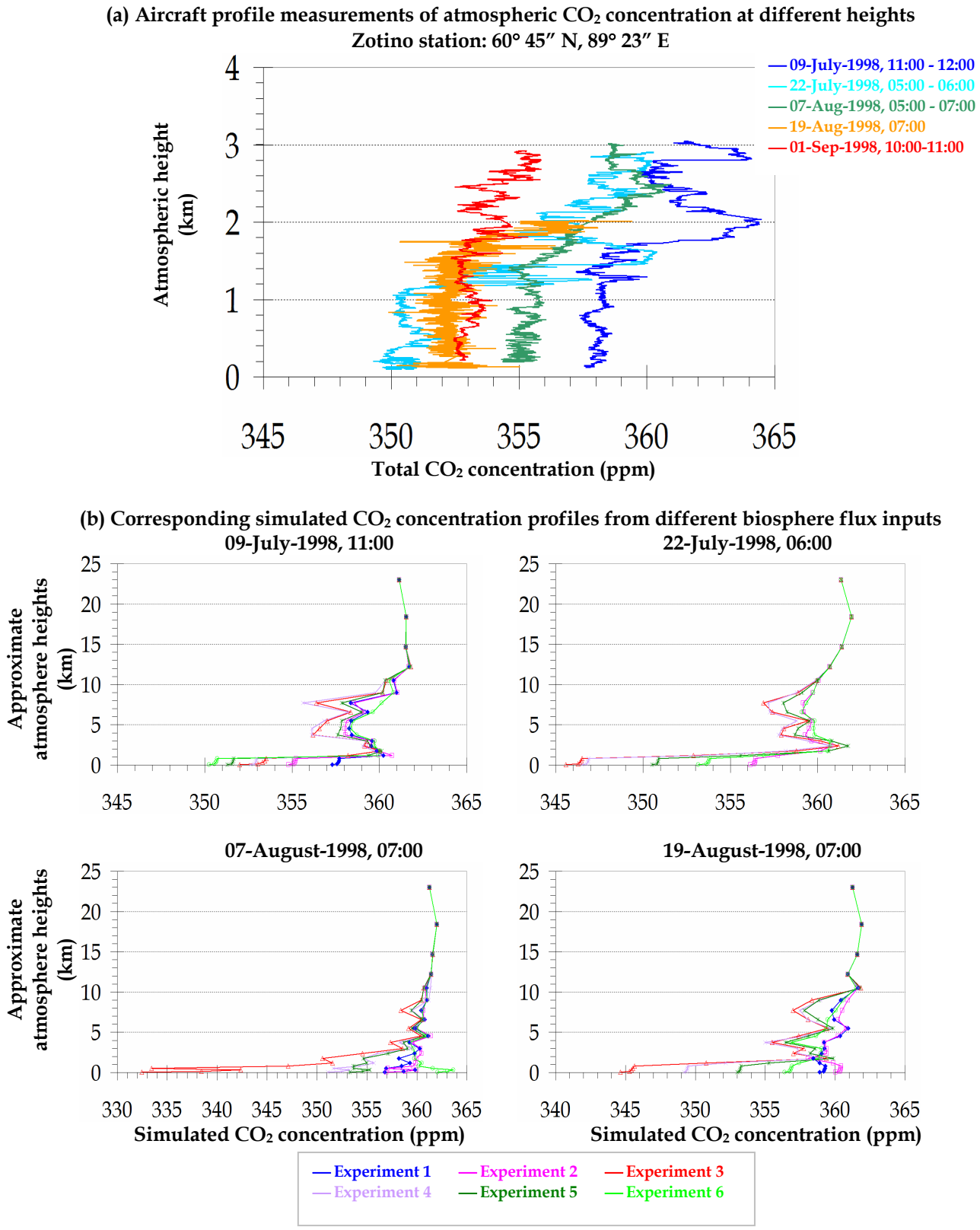

Figure 5-5 Atmospheric CO_2 profiles from aircraft measurements for selected days (a), and corresponding simulated concentration profiles from different biosphere flux inputs (b)

To summarise the outcomes of the comparison of spatial concentrations with observations, the average differences between observations and model results and between model runs of the tracers using different flux experiment pairs were computed. These are shown in figure 5-6.

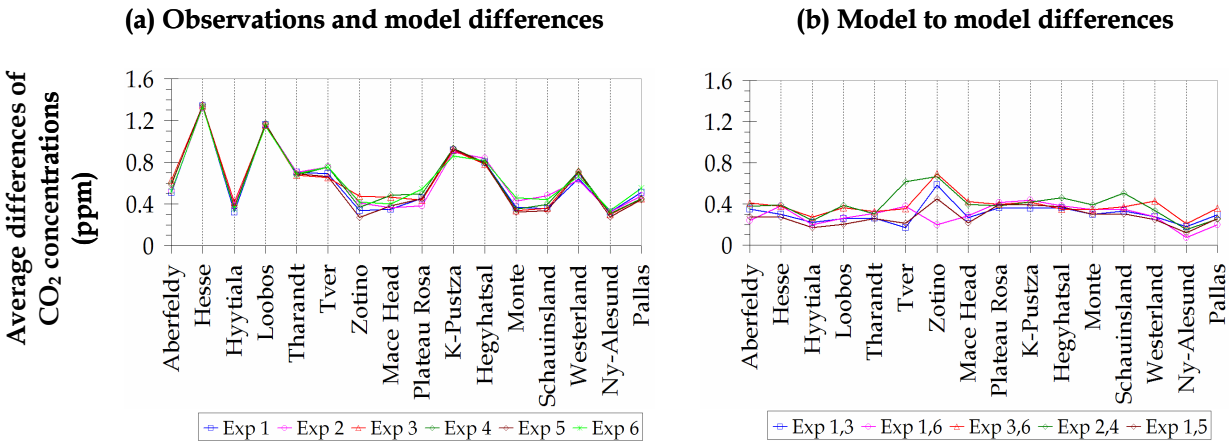

Figure 5-6 Average differences of CO_2 concentrations (ppm) between observations and simulations (a), and between simulated concentrations (b). Both are at ground level, (model level 20, ~34m).

On average, the differences between the simulated concentrations and observations are small (Figure 5-6 (a)), lying in the range of 0.3 to approximately 1.5. Figure 5-6 (b) shows slightly greater fluctuations between the simulated tracers from the different biosphere fluxes. Although the magnitudes of the average differences between the simulated tracers are not large, the use of different biosphere models and model input data results in different fluxes and flux variability, as was shown in Chapter 4. The errors arising from these differences are carried forth in the atmosphere concentrations. The next section will show how these errors are propagated on regional scale.

5.3.2 Regional concentration patterns

This section presents the regional concentration patterns. The focus is on the variability in the concentrations arising from the use of biosphere fluxes from different models to transport the tracers using REMO. As for the spatial flux investigations, seasonal patterns for summer and winter at three atmospheric levels are analysed (level 20, 18 and 12). Results are presented for the tracers from three flux experiments (Experiment 1, 3 and 6).

Figure 5-7 shows wintertime contributions of CO_2 emissions from the fossil fuel and the biosphere, and ocean uptake. Included in the figure are also the emissions that are entering the study domain from the boundary. The contributions from the ocean are the least important, as it is largely responsible for an uptake of atmospheric CO_2, as opposed to the emissions from fossil fuel and biosphere, which are large contributors during wintertime. In comparison, the emissions coming from the lateral boundary is small. At the lowest model level, large variability can be seen mainly in the patterns of fossil fuel and biosphere emissions, the former contributing the most during the winter season. Higher up in the atmosphere the westerly winds are well mixed, hence a reduction in the atmosphere concentrations can be seen as CO_2 gets transported from the west of the region to the east.

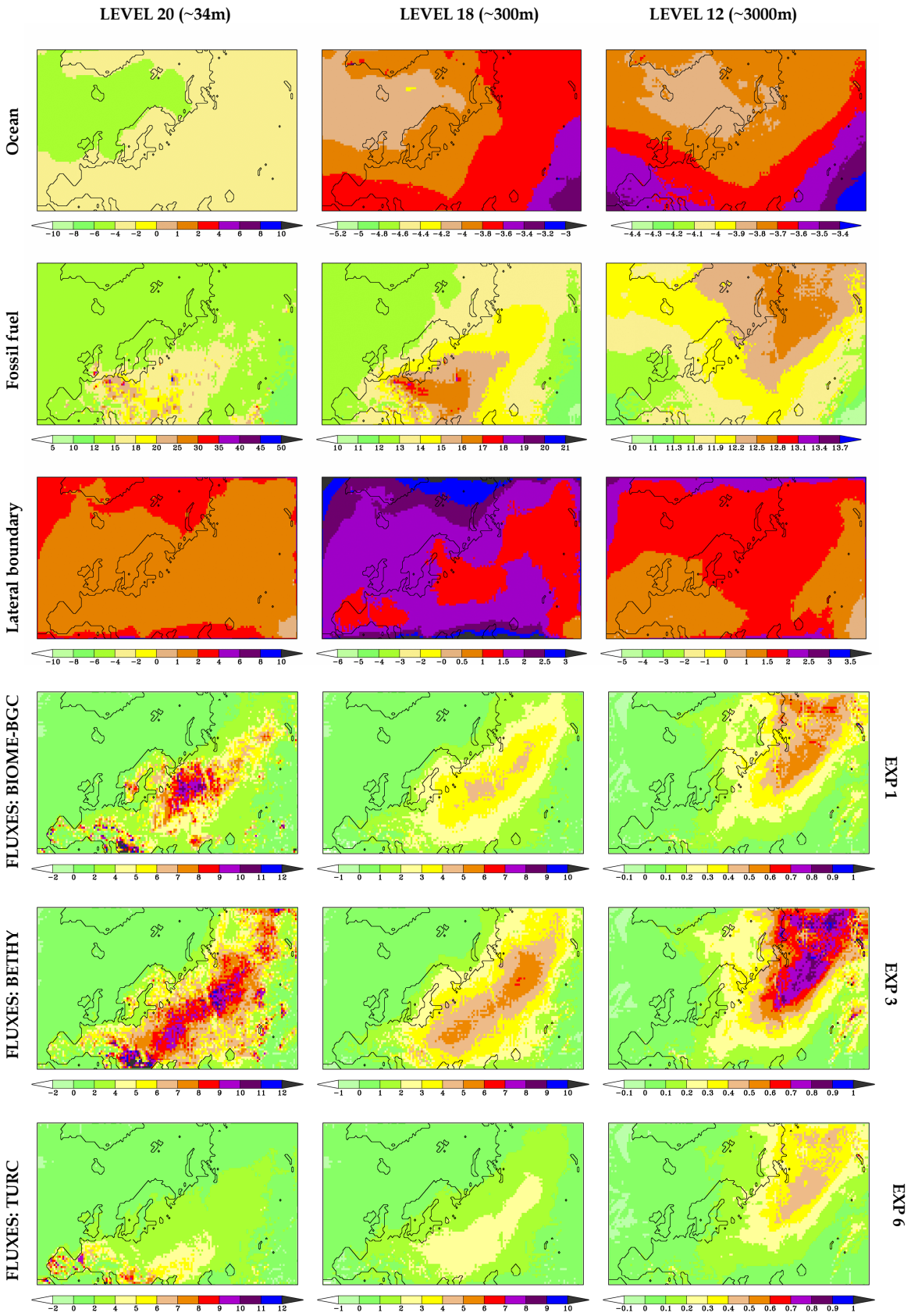

Figure 5-7 Wintertime (DJF 1998) average emission contributions (ppm) from the different atmospheric concentration components

During the winter season the biosphere uptake is not prominent, as the ecosystem activities are reduced. However, as for fossil fuel emissions, the simulated concentrations from the different biosphere model fluxes do show a decrease in the concentrations from the west of the region to the east, particularly at ground level. The main emissions during the winter season come from a combination of plant (evergreens) and soil respiration. The patterns and the order of magnitude of the emissions are comparatively similar. Figure 5-8 shows wintertime total concentrations, computed as the sum of all the components with the added background value of 355ppm.

The total concentrations for the different tracers show consistent patterns at the different atmosphere levels in that they decrease higher up in the atmosphere and when being transported from west to east. The simulated concentrations using BETHY model fluxes are higher at 300m compared to the concentrations from TURC and BIOME-BGC fluxes. This is consistent with the regional flux patterns seen from BETHY in the previous chapter, where the productivity and hence the net ecosystem exchange is high. The reason for the high productivity, high NEE and hence high CO_2 concentration lies in the vegetation types assigned to BETHY during the simulation. The area is assigned dominantly as crops, where productivity is enhanced by artificial means, leading to higher emissions during winter. Additionally, the influence from fossil fuel, particularly during winter, is not insignificant.

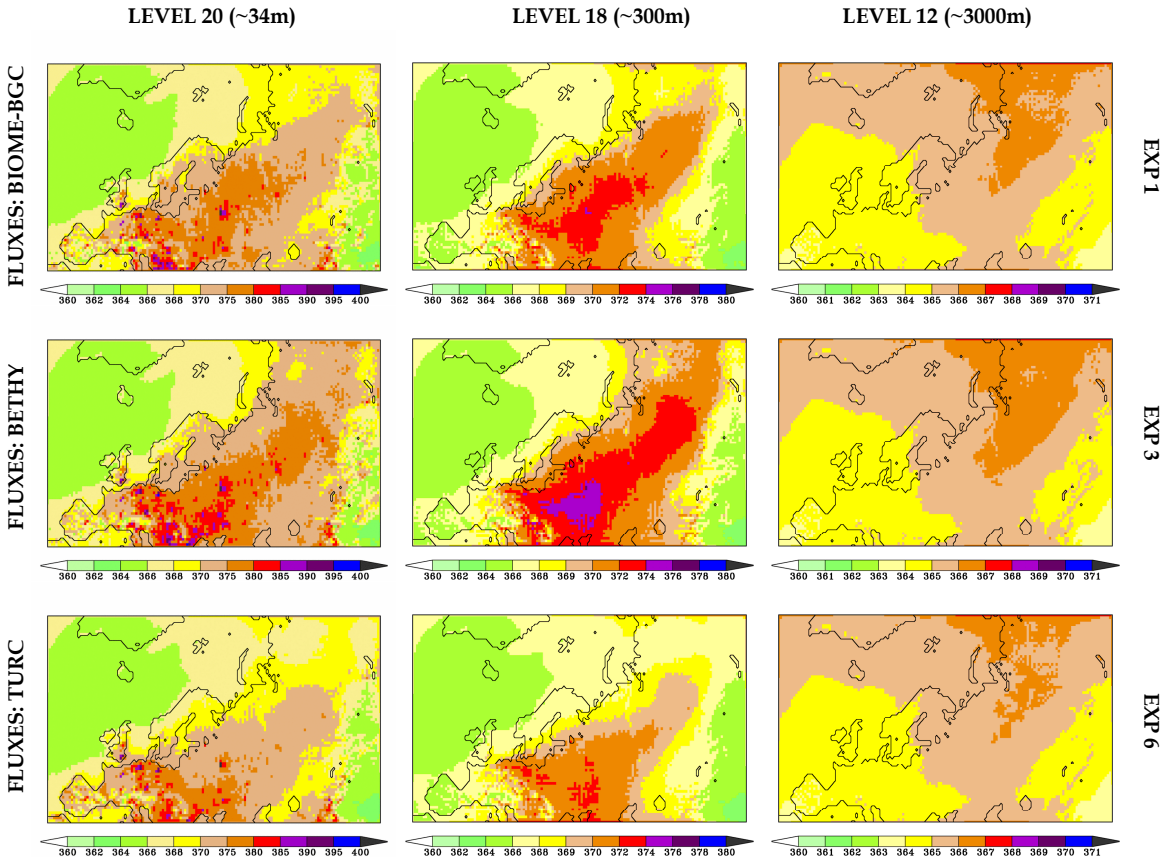

Figure 5-8 Wintertime (DJF 1998) total concentrations (ppm) simulated using biosphere fluxes from BIOME-BGC, BETHY and TURC.

Figure 5-9 shows the summertime concentrations contributed from the different components. As in winter, ocean continues to act as a sink during summer. Fossil fuel emissions are higher than during winter at ground level and at 300m. At level 12, 3000m above the ground, the pattern of CO_2 is similar to that during winter, but the magnitude of the concentrations is slightly lower, indicating good mixing during summer. The ground level concentrations from the lateral boundary, in comparison to the winter season, act as a sink, denoted by the negative magnitudes of the concentrations coming in from the boundary, which is mainly ocean in the west and north, and continents in the south and east. The biosphere activities during summer are enhanced, leading to an increase in the

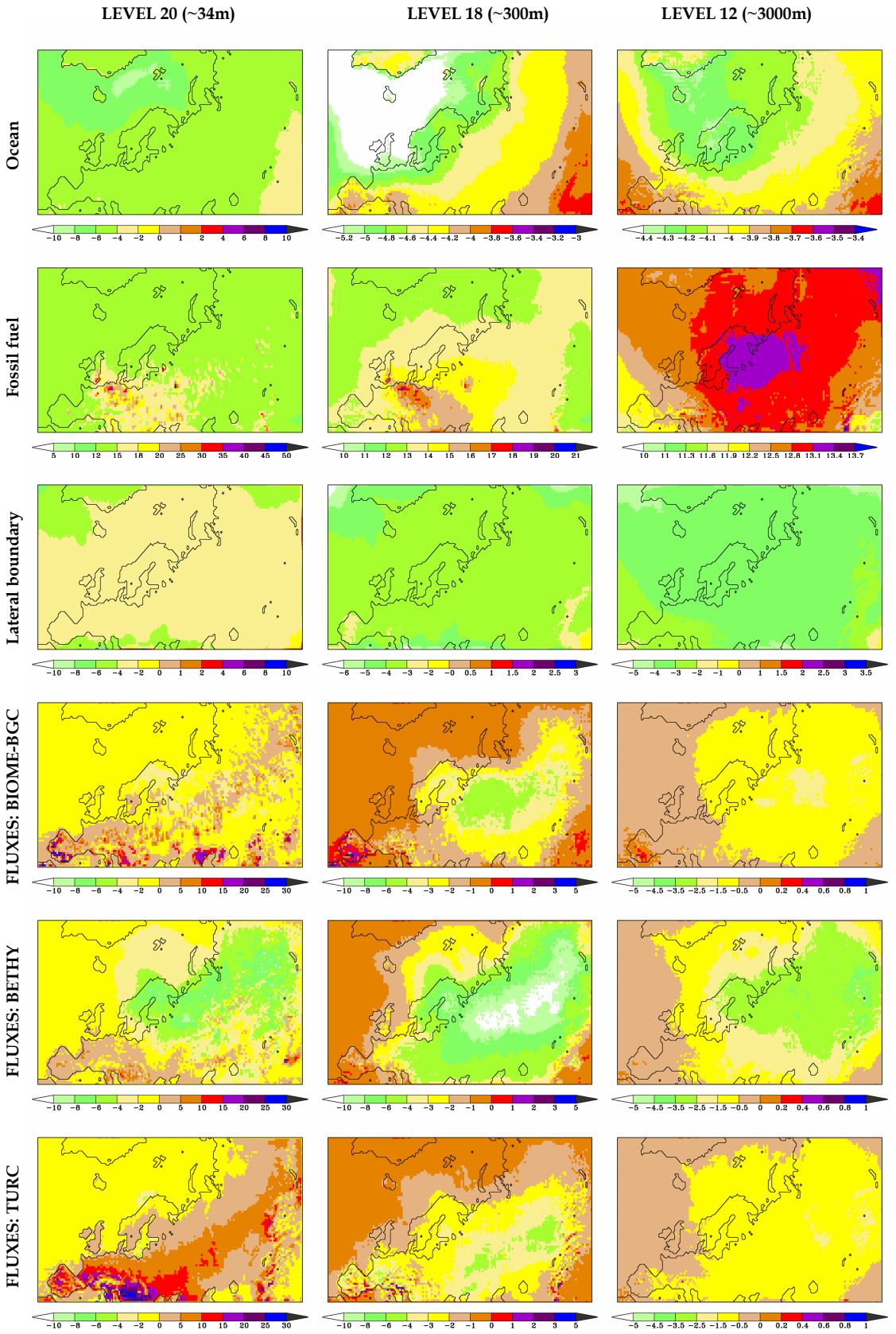

Figure 5-9 Contribution of summer (JJA 1998) CO_2 emissions (ppm) from the different components

uptake of CO_2 from the atmosphere rather than emitting to the atmosphere. This is indicated by the negative values.

Figure 5-10 shows the total concentrations for summer.

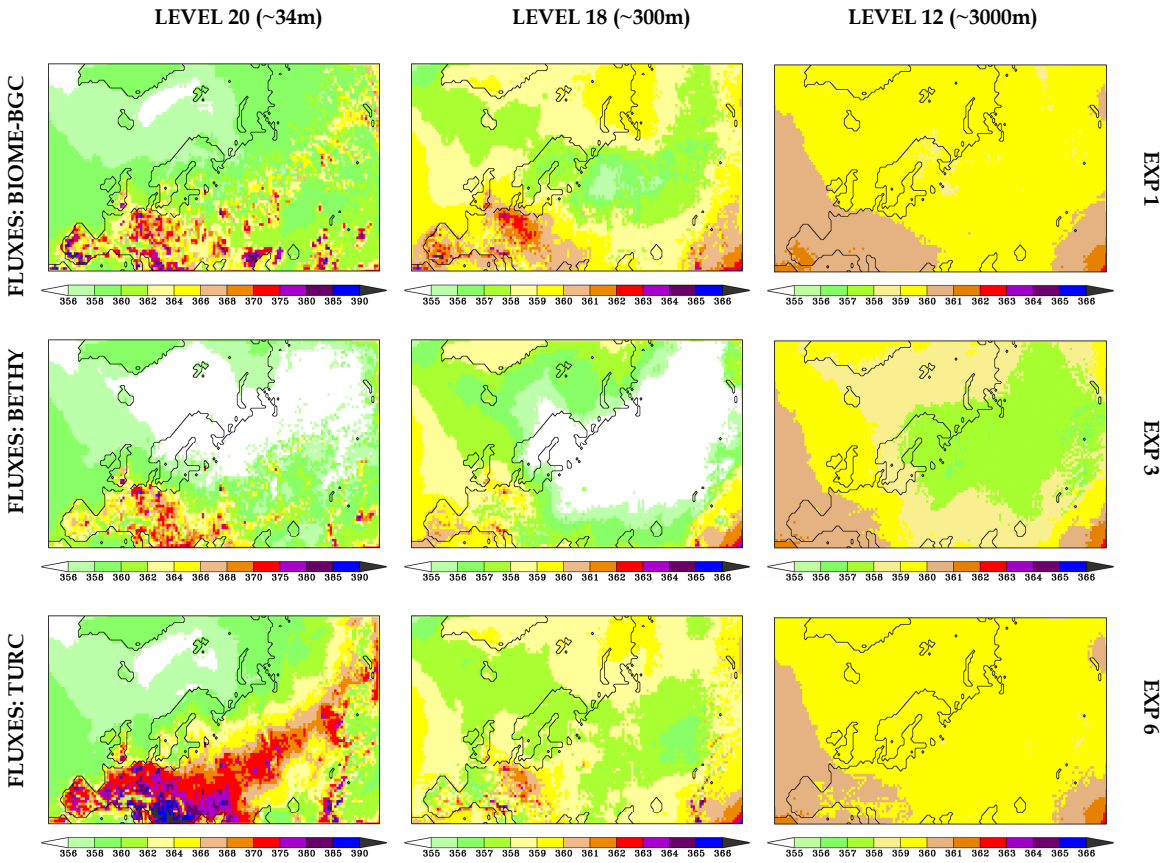

Figure 5-10 Summertime (JJA 1998) total concentrations (ppm) simulated using biosphere fluxes from BIOME-BGC, BETHY and TURC.

At ground level summertime total concentrations are generally lower than during winter, largely due to the drawdown of atmospheric CO_2 by the biosphere. Differences can be seen in the simulated concentrations using different biosphere fluxes. Such differences were already noted for station analysis presented earlier (figure 5-2, and Appendix 5A).

To quantitatively explain the differences between the simulated concentrations using different biosphere fluxes, correlation coefficients between the different tracers were computed for two model levels: level 20 and level 18, as these are the atmosphere heights where the variations are prominent (at least approximately up to the PBL height). Above this, the air is assumed to have well mixed, as shown in the third column of the panel of maps in figure 5-10. The results of the correlations are presented in figure 5-11, where we see that the concentrations higher in the atmosphere are strongly correlated, despite the differences in the absolute values seen in figure 5-10. Also at ground level the correlations are generally high, except for a few areas, such as Southern Spain, where the models show a different behaviour. These differences become more important as the biosphere is more active. It should be noted though that

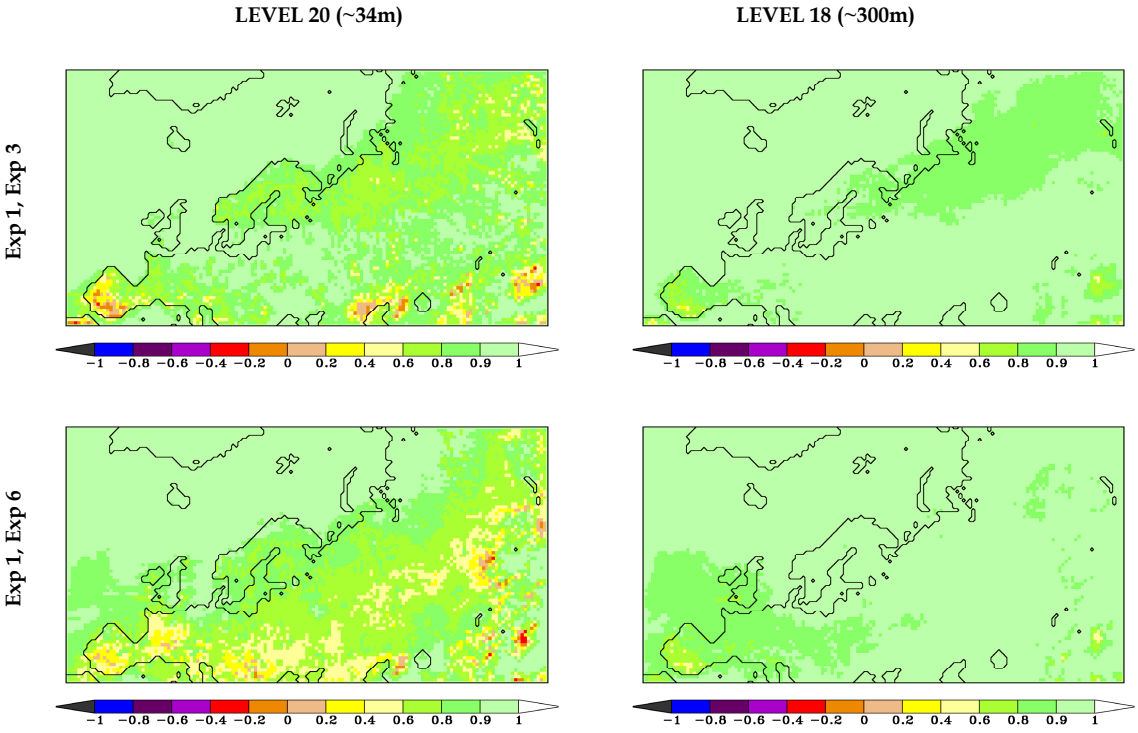

Figure 5-11 Daily CO_2 concentration correlations between different experiments at the lowest model level and within the PBL

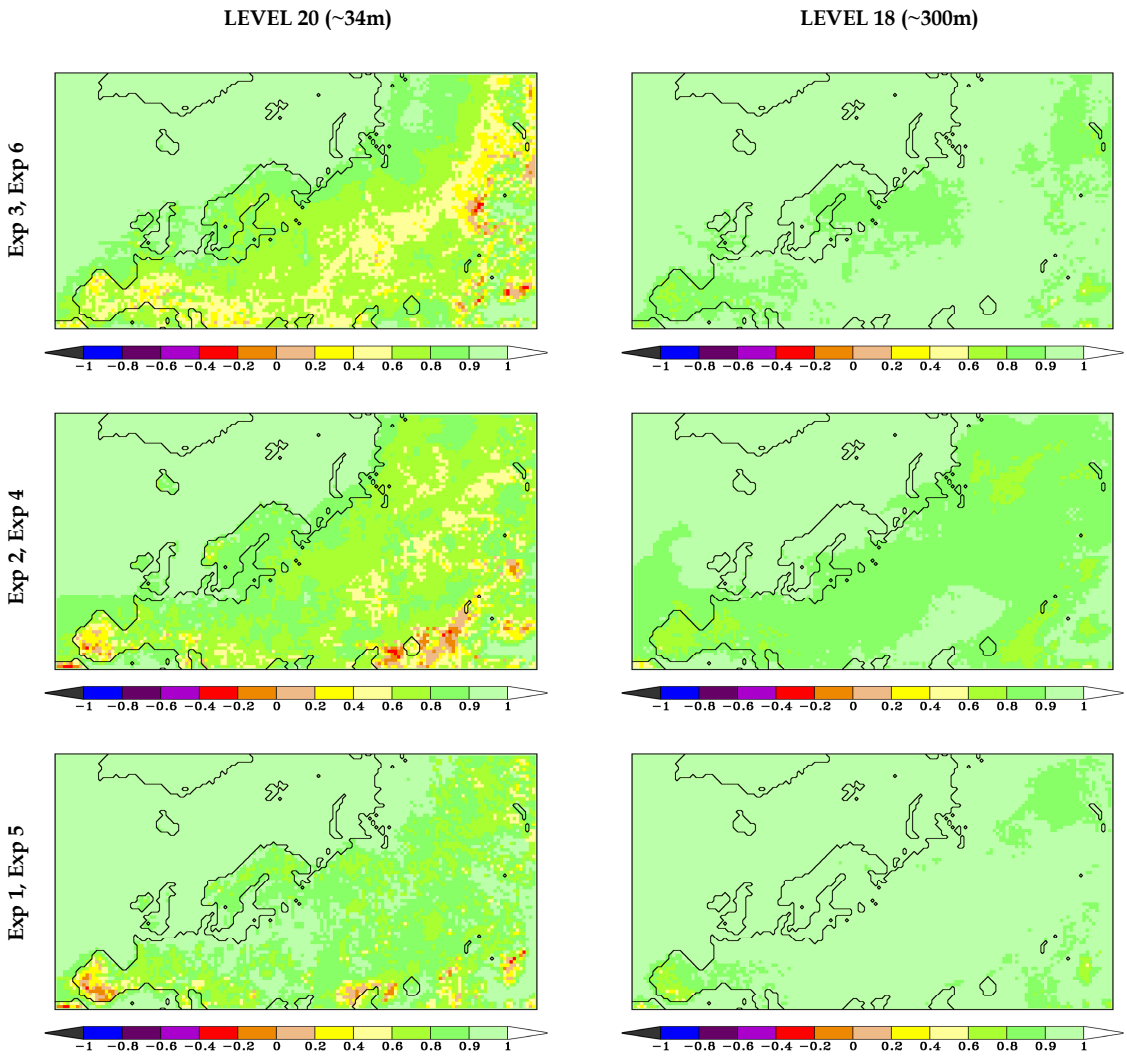

Figure 5-11 (continued)

the correlations are much stronger than between the fluxes of the different model experiments presented in Chapter 4.

5.3.3 Concentrations over the region

This section presents a summary of the CO_2 concentration patterns over the entire region. Figure 5-12 summarises the seasonal cycle of total CO_2 concentrations over Eurosiberia at three different model levels. The

seasonal cycle is consistent from model to model, which correspond well with the

regional seasonal cycle of NEE (Figure 4-9). The positive summertime NEE in figure 4-9 indicates CO_2 uptake by the vegetation. Correspondingly, there is summertime dip for the concentration, as CO_2 is lost from the atmosphere.

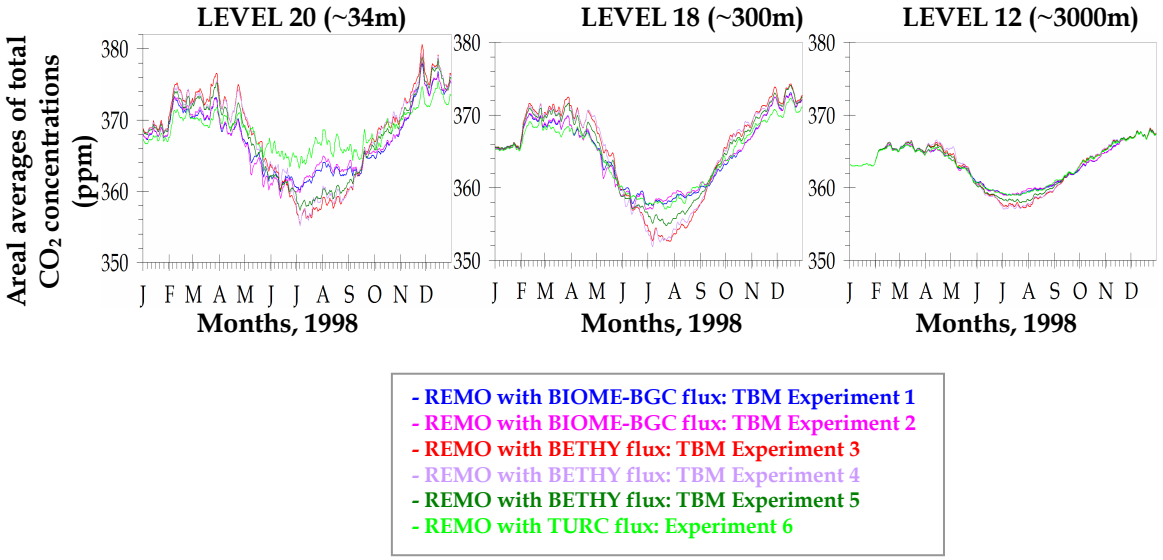

Figure 5-12 Areal averages of total CO_2 concentrations (ppm) over the region at three different model levels

At ground level all models show a relatively high variability as a result of other contributions of CO_2 in addition to the biosphere (for example, fossil fuel emissions, ocean uptake, and influence from the lateral boundary, though small). The variability is visible also at the PBL height although the intensity of the fluctuations is less then at the ground level. Similarly, the summertime dip reduces with increasing atmosphere levels, indicating well-mixed air in the vertical and horizontal scales of the

model. Above the PBL the simulated CO_2 with various biosphere fluxes lie closer to each. However, small differences in the simulated concentrations are still there but not as large as at the interface of the biosphere and atmosphere. Here the use of different models and different input vegetation maps leads to significantly different regional CO_2 concentrations, particularly during summer.

The regional flux plots in figure 4-8 shows similar patterns within the biosphere flux experiments, whereby the peaks indicating summertime uptake are not the same for all experiments. They are out of phase by approximately one month. The uncertainties arising due to the different flux sources are brought further in the concentrations when used for transporting the tracers across the region. However, the atmospheric CO_2 is also controlled by other sources, and hence the differences in total concentration between the 6 experiments are not as prominent as in the fluxes. The decrease in the concentration variability higher up in the atmosphere reflects the reduced effect of local terrestrial fluxes in estimating atmospheric CO_2 concentrations.

The results presented so far have been on total concentrations. In order to see the influence of individual components of concentrations over the region and their role in contributing to the overall atmospheric concentrations, seasonal cycles of the components were plotted. This is shown in figure 5-13.

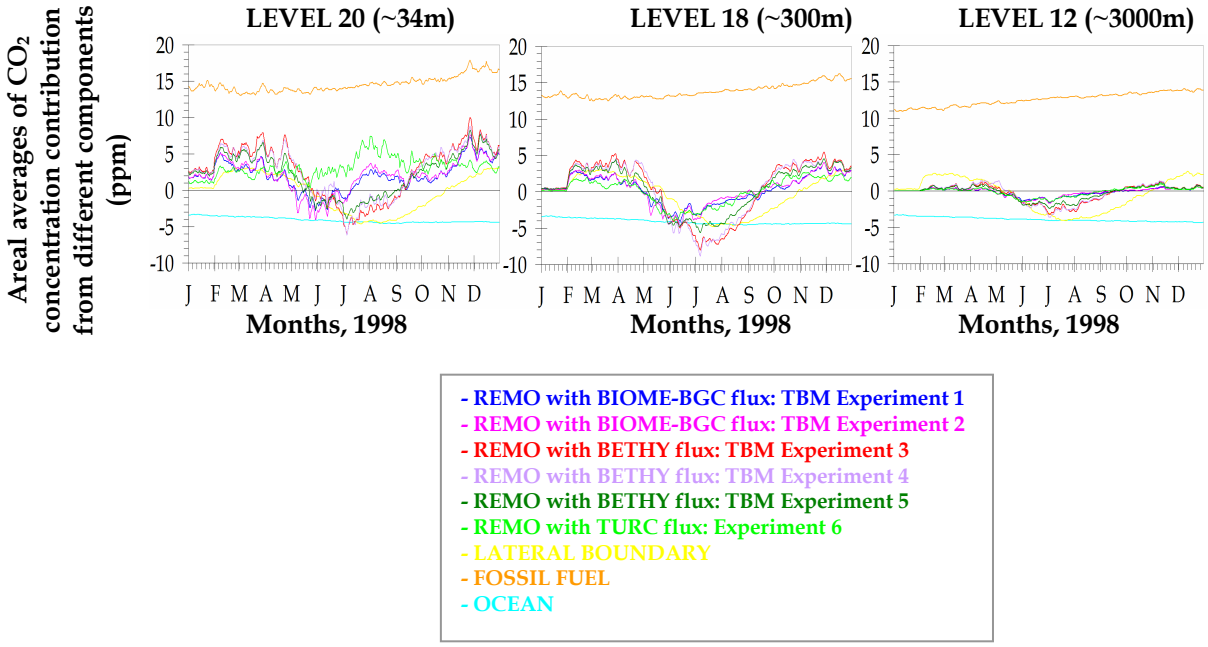

Figure 5-13 Areal averages of CO_2 concentration (ppm) contribution from the different components over the region at three different model levels

Among the components of concentrations, emissions from fossil fuel, which are fairly constant throughout the year, contribute largely to the total concentrations. The ocean acts as a sink. The emissions coming from the lateral boundary of the region show a seasonal cycle similar to that of the biosphere fluxes. The biosphere contributions are highly variable at ground level, but bring about the seasonal cycle seen over the year. The high variability in the biosphere fluxes is propagated higher up in the atmosphere.

At ground level the draw down of atmospheric CO_2 is prominent mainly due to the biosphere. In and above the PBL the role of mixing of the air and transportation of the tracers become more influential in reducing both the fluctuations and the seasonal cycle. During wintertime the boundary

layer height is lower leading to lower mixing in the atmosphere hence high concentrations during winter. The opposite happens in summer.

To further investigate the biosphere activity in the region and its influence higher up in the atmosphere, the amplitudes of the concentrations due to the biosphere component were computed at different model levels. This is illustrated in figure 5-14.

The amplitudes maps show the biosphere activity of uptake and release of CO_2 with magnitudes ranging from 25 to 50ppm. The patterns correspond to NEE amplitudes shown in the previous chapter (figure 4-9), where the simulated net exchange is shown for each biosphere model experiment. When these different fluxes are used in the transport model, the concentrations also show a high variability at ground level due to the contribution of the biosphere, as well as other natural (ocean uptake) and anthropogenic activities (fossil fuel emissions). As for NEE, the simulated concentrations using BETHY fluxes show a higher variability than BIOME-BGC or TURC fluxes.

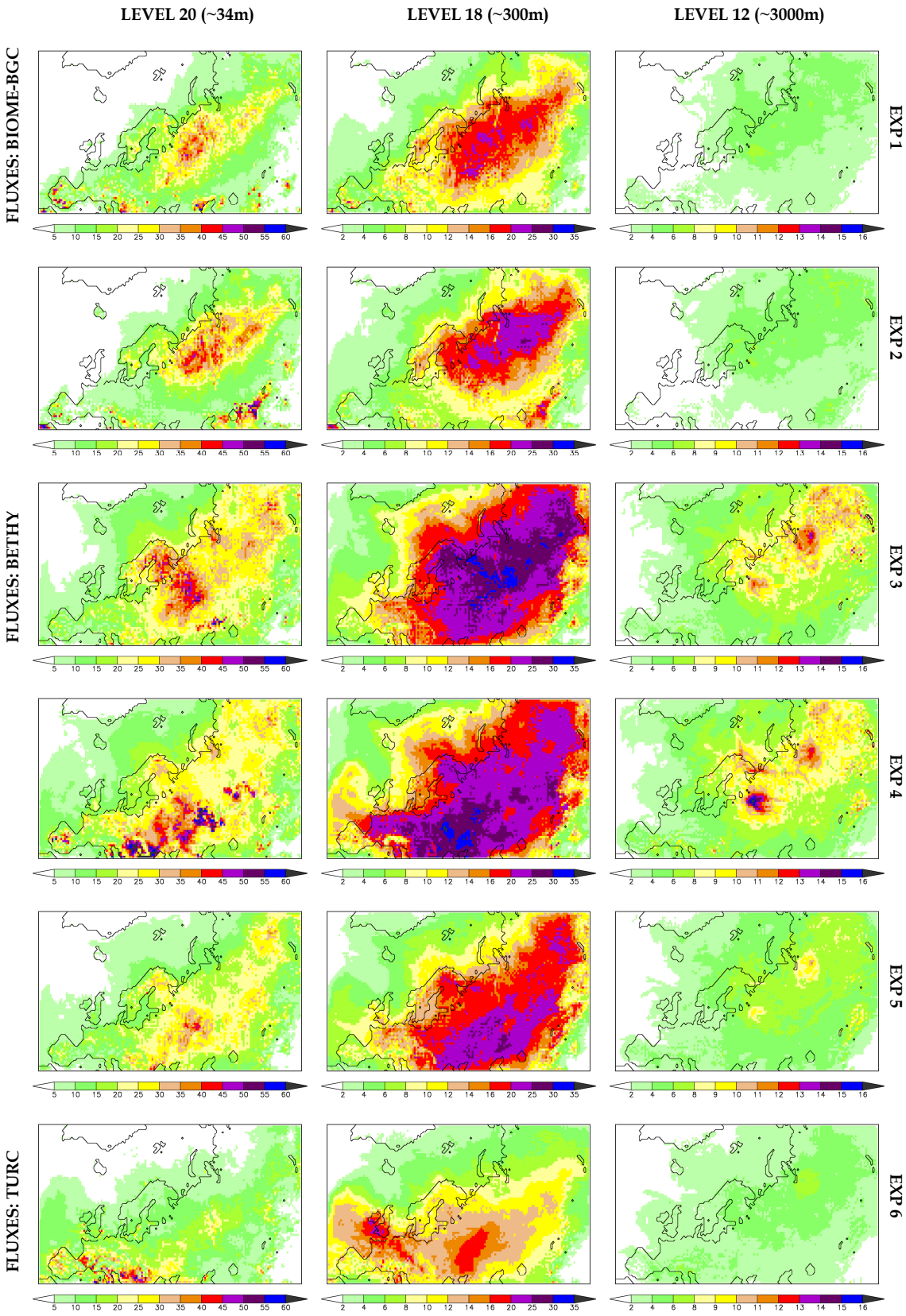

Figure 5-14 Amplitudes of 10-day running averages of CO_2 concentration due to the biosphere activity at different model levels. Note the different scales at each level.

Unlike the net ecosystem exchange of CO_2, which is restricted to the biosphere-atmosphere interface, the concentrations are constantly transported in the vertical and horizontal directions. In figure 5-14 this can be easily seen when going from level 20 to level 12. In the PBL (level 18), although the amplitudes are not as high as at ground level, high variability can still be seen in the patterns from the different flux inputs. Above the PBL, not only the amplitude decreases but also a shift in the patterns occurs from west to east. This is particularly visible where BETHY fluxes are used. The patterns of the amplitudes from BIOME-BGC and TURC flux inputs are similar.

5.4 DISCUSSIONS

The atmospheric CO_2 concentration simulation using the fluxes from various terrestrial biosphere models shows varying results. The station comparisons show the seasonal cycle in the simulated CO_2 concentrations but the phasing and amplitudes of the fluctuations are not always consistent with the observations. Generally, the concentrations simulated using the different fluxes lie closer to each other than to the observations. The differences with the measurements may partly be explained by the difference in the measurement heights at which observations are gathered and the lowest height above the ground represented in the transport model. On average, the tower height at measurement sites range between 40 and 60m above ground, whereas the lowest height in the model is approximately 34m, the next height being 140m. Another reason for the large differences lies in the contribution of the components, such as fossil fuel, which is kept constant during the model simulation.

The regional patterns show that during winter the contribution of fossil fuel emissions, in comparison with the contribution of other components, is large. The ocean acts as a sink throughout the year, while the biosphere is mostly inactive during winter in terms of uptake. The total concentration simulated using BETHY fluxes is always high while the results using TURC and BIOME-BGC fluxes show similar patterns, but lower than BETHY. Likewise, during summer the uptake by the biosphere is high particularly when BETHY fluxes are used. The different tracers from the various flux experiments were highly correlated for some experiments, which may at least partly be explained by the influence of other sources of atmospheric CO_2 that were kept the same.

The implication of such patterns in the atmospheric concentrations is the importance of the biosphere fluxes being input to the transport model. If large variations are present at the onset of the flux simulations, as in the case of BETHY, they get propagated at different modelling steps and appear in the atmospheric concentrations. This indicates the propagation of uncertainties from the biosphere flux simulations to the estimation of the concentrations. The variable tested in this study was the vegetation type input maps to the biosphere models. However, other factors, such as fossil fuel emissions and other natural and anthropogenic activities that are not fully taken into account, would add further uncertainty. Over the study region the contribution from fossil fuel emissions is larger than of the other components. Nevertheless, a clear seasonal cycle can be seen particularly at ground level, which is primarily due to the terrestrial ecosystem activities.

In the lowest model level the largest variability arises due to the biosphere components. This relates to the simulation of biosphere fluxes in the different TBMs. The main uncertainty in these simulations arises as a result of using different vegetation type maps in the models, as well as the differences in handling of the ecosystem processes in the models. The variability at ground level reduces with increasing atmosphere heights as a result of atmospheric mixing and transportation of the tracers. This is also depicted in the vertical profiles (figure 5-13). Generally speaking, the influence of biosphere fluxes decreases with increasing height in the atmosphere both in and above the PBL.

5.5 CONCLUSIONS

The terrestrial biosphere fluxes play an important role in the estimation of atmospheric CO_2 concentrations. Although fossil fuel emissions contribute more than the other components, the biosphere fluxes contribute significantly to the variability of atmospheric CO_2, particularly in the lower levels. The variability in the simulated concentration is the highest at ground level where not only ecosystem activities but also other natural and anthropogenic processes take place. In the planetary boundary layer, as the air gets mixed, the variability in the concentration decreases. However, depending on how strong the flux contributions are the influence of the biosphere can still be seen in the PBL. This was especially the case for the concentrations derived from BETHY-simulated CO_2 fluxes. The concentrations from TURC and BIOME-BGC fluxes showed similar patterns, but with lower concentrations. In all cases the variability was reduced further with increasing atmosphere heights, although the tracers from the BETHY flux experiments continued to show some seasonal variation, albeit not as large as at ground level or within the PBL.

The use of the fluxes from three different biosphere models enables to assess how the differences and the variability in the fluxes propagate to atmospheric CO_2. The use of different models driven by different input vegetation maps leads to different concentrations at ground level, particularly during summer, but these differences virtually disappear with increasing atmosphere heights and with mixing of the air and transportation of the tracers. Generally speaking the experiments of BIOME-BGC and TURC show better agreement while the results from BETHY show greater uncertainty, both in the flux simulations (presented in the preceding chapter), as well as in the corresponding concentrations. This was seen in the three BETHY experiments, which gave quite different results due to the use of different vegetation maps that were tested. In case of BIOME-BGC, the two experiments gave consistent results.

CHAPTER 6
SYNTHESIS, CONCLUSIONS AND RECOMMENDATIONS

This chapter summarises and discusses the principal findings of the study according to the objectives outlined in Chapter 1. Conclusions and recommendations are presented at the end.

6.1 SYNTHESIS

The current study assessed the contribution of the terrestrial biosphere to the intra-annual variability of atmospheric CO_2 concentrations over Eurosiberia. Previous studies (e.g. Chevillard *et al.* 2002a; Kjellström *et al.*, 2002; Lafont *et al.*, 2002) mainly looked at variations at synoptic scales (up to a few weeks). To improve our understanding of the role the biospheric carbon fluxes at longer time scales, the current study investigated the variability over the course of a whole year (1998) because of the strong seasonal signal from the biosphere and the related seasonal variation in atmospheric CO_2.

CO_2 fluxes from the biosphere and its contribution to atmospheric CO_2 variability:

The CO_2 fluxes from the biosphere to the atmosphere were estimated firstly at single-stand locations over the study region. The performance of the terrestrial biosphere models, BETHY and BIOME-BGC was tested against the flux measurements at selected FLUXNET sites across Eurosiberia. To this end, the two models were driven by site-specific input parameters and three different meteorology datasets. The results showed that despite the limitations in the input data and the use of different input datasets, the biosphere models adequately represented the seasonal cycles of the fluxes. While the simulated NEE was mostly within the range of variations in the observations, the flux components GPP and R_{total} generally showed larger deviations.

At a regional scale the CO_2 fluxes from the biosphere were estimated by applying the same biosphere models to Eurosiberia on a half-degree grid in five different model experiments. The contribution of the biosphere to the variability in annual atmospheric CO_2 was in the order of 10^2 TgC with a strong seasonal signal of net release of CO_2 during winter and net uptake during summer. Despite this general feature, the simulated fluxes showed relatively large differences between the different model experiments, not only in magnitude but also in the regional patterns. The differences, however, seemed larger in the individual flux components than in the net ecosystem exchange, a pattern already noted in the single-stand investigations. The correlation coefficients were generally not very strong but were significant (for example Experiments 1 and 5 in Figure 4-8, with values ranging from 0.2 to 0.4 in the lower left part of the region). Even when the two TBMs used the same input vegetation map, the correlation coefficients were generally not very strong, indicating that at

least part of the differences was attributed to the model structure and process representation. The influence of the biosphere in the variability of atmospheric CO_2 concentrations was strongest in the ground level up to the planetary boundary layer, but virtually disappeared at higher levels (Figures 5-2 and 5-9). This is attributed to the enhanced vertical mixing, as well as lateral transport.

Uncertainties in the terrestrial biosphere flux estimations:

In assessing the role of the biosphere fluxes in the atmospheric concentration variability, uncertainties get incorporated at different stages. When simulating the carbon fluxes from the terrestrial biosphere, uncertainties are introduced by (1) the input data that are unknown or cannot be measured, especially at a regional scale, and (2) the representation and parameterisation of ecosystem processes in the two models. A sensitivity analysis of the models at the FLUXNET sites showed that at most stations the biosphere models responded in a similar manner to changes in the input parameter values (rooting depth, precipitation and temperature). However, there were stations where either BETHY or BIOME-BGC showed greater sensitivity, indicating the differences in the models in the way they handle the input parameters.

The uncertainties arising from the model structure and parameterisation get incorporated when extending the simulations from local to regional scale, and are further propagated when used in atmospheric transport modelling. This study found significant differences in the simulations of the fluxes over Eurosiberia between the process-based models BETHY and BIOME-BGC, but when being used to simulate the atmospheric concentration levels of CO_2 these differences become less dominant, particularly higher in the atmosphere. Although both TBMs produced a

strong seasonal cycle over Eurosiberia, differences were seen in the timing and amplitude between the five experiments. This was due to the use of different input vegetation maps that influenced the phenological processes and relative distribution of NEE in the models. In both models evergreen needle leaf, deciduous broadleaf and deciduous needle leaf forests dominated the seasonal cycles of the biospheric fluxes. However, in Experiment 4 (BETHY using its own vegetation class type) crops dominated the biospheric contributions showing a large summer uptake, in the order of about 20 $gC/m^2/day$, in contrast to approximately 5 $gC/m^2/day$ on average when other vegetation maps were used. This illustrates the importance of the vegetation classification in estimating biosphere fluxes.

In the present study the uncertainties in the terrestrial biosphere fluxes were assessed by using an "ensemble" of different models and different input vegetation maps that largely control the ecosystem processes included in the models. The range of flux estimates provides an indication of the uncertainties related to flux simulations. To quantify these, other sources of uncertainty, such as the input meteorology and soil parameterisation, need to be taken into account. Moreover, it is difficult to assess flux estimates based on disparate model experiments. Although the input data were kept as consistent as possible, differences are inevitable because of the unique process representation and accordingly the specific input requirements by each of the models.

Other sources of variability in atmospheric CO_2

The propagation of the terrestrial fluxes into the atmosphere was simulated with the atmospheric transport model REMO. The findings suggest that during the year the biosphere largely controls the seasonality

of CO_2 concentrations in the lower levels, but higher in the atmosphere the biospheric signal tends to disappear. Part of the variability seen in the total concentration is due to inflow from the lateral boundaries. The contribution of these boundary conditions is supposed to be highly uncertain, because they are derived from a coarse-resolution global model (TM3) and were interpolated to the 0.5 x 0.5 degree grid of REMO. Other sources of carbon included in this study were ocean uptake and fossil fuel emissions. Of these components, fossil fuel emissions contributed the most (Figure 5-13), but the variability in this was ignored as the focus was on the influence of the biosphere.

The terrestrial biosphere: a source or a sink?

The current model experiments do not give a decisive answer whether the biosphere in Eurosiberia behaves as a source or a sink. The values of net ecosystem exchange on an annual basis are very small, ranging from –0.7 to (8×10^{-5}) TgC (with negative sign indicating a release of CO_2 by the biosphere). However, one should be aware that a basic assumption in the models is that on annual scale the net fluxes balances out. In winter the biosphere acts as a source with values ranging from (-6×10^2) to (-11×10^2) TgC. In summer the models agree that the biosphere act as a sink but have a wide range in the amounts of carbon uptake, ranging from (8×10^2) to almost (25×10^2) TgC (Figure 4-12). Year-to-year variations have not been looked at in the present study, but are likely to occur in response to variations in the amount of precipitation and temperature.

6.2 CONCLUSIONS

Regional carbon fluxes from the terrestrial biosphere determine, to a large extent, the seasonal variation in the CO_2 concentrations in the lower atmosphere over Eurosiberia. Above the planetary boundary layer the signal of the biospheric fluxes tends to diminish or even disappear due to the enhanced vertical mixing, as well as lateral transport. However, the simulations of terrestrial biosphere fluxes are uncertain. These uncertainties, arising from the model structure and parameterisation, get incorporated when extending the simulations from local to regional scale, and are further propagated when used in atmospheric transport modelling. This study found significant differences in the simulations of the fluxes over Eurosiberia between the different process-based models BETHY and BIOME-BGC, but when being used to simulate the atmospheric concentration levels of CO_2 these differences become less dominant, particularly higher in the atmosphere.

6.3 RECOMMENDATIONS

In view of the growing importance of regional carbon budget estimates, it is essential to use reliable tools and to be aware of the limitations and uncertainties. The present study provided a first estimate of the role of the terrestrial carbon fluxes and their natural variability at longer time scales in the regional atmospheric CO_2 concentrations. Three main recommendations can be made:

(1) The methodological approach could be further improved by the use of consistent input and boundary data in both the biosphere models

as well as the atmospheric transport model. The recommendation therefore is to force the biosphere models with meteorology and surface parameters from REMO.

(2) To gain a better understanding of the uncertainties related to the estimation of biosphere fluxes, other sources of uncertainties should be taken into account in a similar manner as was done in the present study. In other words, a larger ensemble of model experiments should be used. Apart from the input vegetation maps, other uncertain inputs, such as the rooting depth, should be included.

(3) In studies of climate and land use change, it is important to take potential feedbacks into account. This can be achieved by an online coupling of the process-based terrestrial biosphere models used in the present study with the regional atmosphere model. Furthermore, for long-term studies of regional carbon balance multi-year model runs should be performed.

BIBLIOGRAPHY

Canadell, J.; Jackson, R. B.; Ehleringer, J. R.; Mooney, H. A.; Sala, O. E. and Schulze, E. D. (1996). Maximum rooting depth of vegetation types at the global scale. Oecologia, 108(4): 583-595

Chevillard, A. Karstens, U. Ciais, P.; Lafont, S. and Heimann, M. (2002a). Simulation of atmospheric CO_2 over Europe and Western Siberia using the regional scale model REMO. Tellus, 54B: 872-894

Chevillard, A.; Ciais, P.; Karstens, U.; Heimann, M.; Schmidt, M.; Levin, I.; Jacob, D.; Podzun, R.; Kazan, V.; Sartorius, H. and Weingartner, E. (2002b). Transport of ^{222}Rn using the regional model REMO: A detailed comparison with measurements over Europe. Tellus, 54B(5): 850-871

Churkina, G.; Tenhunen, J.; Thornton, P.; Falge, E. M.; Elbers, J. A.; Erhard, M.; Grünwald, T.; Kowalsi, A. S.; Rannik, Ü. and Sprinz, D. (2003). Analysing the ecosystem carbon dynamics of four European forests using a biogeochemistry model. Ecosystems, 6: 168-184

Cohen, W. B. and Goward, S. N. (2004). Landsat's role in ecological applications of remote sensing. BioScience, 54(6): 535-545

Coops, N. C.; Waring, R. H. and Running, S. (2001). Comparisons of predictions of net primary production and seasonal patterns in water use derived with two forest growth models in Southwestern Oregon. Ecological Modelling, 142: 61-81

de Pury, D. G. G. and Farquhar, G. D. (1997). Simple scaling of photosynthesis from leaves to canopies without the errors of big-leaf models. Plant Cell Environment, 20(5): 537-557

DeFries, R. S. and Townshend, J. R. G. (1994). NDVI-derived land-cover classifications at a global scale. International Journal of Remote Sensing, 15: 3567-3586

Dunne, K. A. and Willmott, C. J. (1996). Global distribution of plant-extractable water capacity of soil. International Journal of Climate, 16: 841-859

Ethier, G. J. and Livingston, N. J. (2004). On the need to incorporate sensitivity to CO_2 transfer conductance into Farquhar-von-Crammerer-Berry leaf photosynthesis model. Plant, Cell and Environment, 27: 137-153

Falge, E.; Baldocchi, D.; Olson, R.; Anthoni, P.; Aubinet, M.; Bernhofer, C.; Burba, G.; Ceulemans, R.; Clement, R.; Dolman, H.; Granier, A.; Gross, P.; Grünwald, T.; Hollinger, D.; Jensen, N-O.; Katul, G.; Keronen, P.; Kowalski, A.; Lai, C. T.; Law, B. E.; Meyers, T.; Moncrieff, J.; Moors, E.; Munger, J. W.; Pilegaard, K.; Rannik, Ü.; Rebmann, C.; Suyker, A.; Tenhunen, J.; Tu, K.; Verma, S.; Vesala, T.; Wilson, K. and Wofsy, S. (2001). Gap-filling strategies for defensible annual sums of net ecosystem exchange. Agricultural and Forest Meteorology, 107: 43-69

Falge, E.; Baldocchi, D.; Tenhunen, J.; Aubinet, M.; Bakwin, P.; Berbigier, P.; Bernhofer, C.; Burba, G.; Clement, R.; Davis, K. J.; Elbers, J. A.; Goldstein, A. H.; Grelle, A.; Granier, A.; Guðmundsson, J.; Hollinger, D.; Kowalski, A. S.; Katul, G.; Law, B. E.; Malhi, Y.; Meyers, T.; Manson, R. K.; Munger, J. W.; Oechel, W.; Kyaw Tha Paw, U.; Pilegarrd, K.; Rannik, Ü.; Rebmann, C.; Suyker, A.; Valentini, R.; Wilson, K. and Wofsy, S. (2002a). Seasonality of ecosystem respiration and gross primary production as derived from FLUXNET measurements. Agricultural and Forest Meteorology, 113: 53-74

Falge, E.; Baldocchi, D.; Tenhunen, J.; Aubinet, M.; Bakwin, P.; Berbigier, P.; Bernhofer, C.; Bonnefond, J. –M.; Burba, G.; Clement, R.; Davis, K. J.; Elbers, J. A.; Goldstein, A. H.; Grelle, A.; Granier, A.; Grünwald, T.; Guðmundsson, J.; Hollinger, D.; Janssens, I. A.; Keronen, P.; Kowalski, A. S.; Katul, G.; Law, B. E.; Malhi, Y.; Meyers, T.; Manson, R. K.; Moors, E.; Munger, J. W.; Oechel, W.; Kyaw Tha Paw, U.; Pilegarrd, K.; Rannik, Ü.; Rebmann, C.; Suyker, A.; Thorgeirsson, H.; Tirone, G.; Turnipseed, A.; Wilson, K. and Wofsy, S. (2002b). Phase and amplitude of ecosystem carbon release and uptake potentials as

derived from FLUXNET measurements. Agricultural and Forest Meteorology, 113: 75-95

Fan, S.; Gloor, M.; Mahlman, J.; Pacala, S.; Sarmiento, J.; Takahashi, T. and Tans, P. (1998). A large terrestrial carbon sink in North America implied by atmospheric and oceanic carbon dioxide data and models. Science, 282: 442-446

Farquhar, G. D.; von Crammerer, S. and Berry, J. A. (1980). A biogeochemical model of photosynthetic CO_2 assimilation in leaves of C3 species. Planta, 149: 78-90

Farquhar, G. D.; von Crammerer, S. and Berry, J. A. (2001). Models of photosynthesis. Plant Physiology, 125: 42-45

Francis, R. J.; Tans, P. P.; Allison, C. E.; Enting, I. G.; White, J. W. C. and Trolier, M. (1995). Changes in oceanic and terrestrial carbon uptake since 1982. Nature, 373: 326-330

Friedlingstein, P.; Fung, I.; Holland, E.; John, J.; Brasseur, G.; Erickson, D. and Schimel, D. (1995). On the contribution of CO2 fertilisation to the missing sink. Global Biogeochemical Cycles, 9: 541-556

Geels, C. (2003). Simulating the current CO_2 content of the atmosphere: Including surface fluxes and transport across the Northern hemisphere. PhD Thesis. Niels Bohr Institute for Astronomy, Physics and Geophysics and National Environmental Research Institute, Department of Atmospheric Environment, The University of Copenhagen. 238pp

Geels, C.; Doney, S. C.; Dargaville, R.; Brandt, J. and Christensen, J. H. (2004). Investigating the sources of synoptic variability in atmospheric CO_2 measurements over the Northern Hemisphere continents: a regional model study. Tellus, 56B(1): 35-50

Haefner, J. W. (1996). Modelling Biological Systems: Principles and Applications. Chapman and Hall. 473pp

Hagemann, S. and Kleidon, A. (1999). The influence of rooting depth on the simulated hydrological cycle of a GCM. PhyPhys. Chem. Earth (B), 24(7): 775-779

Hagemann, S.; Machenhauer, B.; Christensen, O. B.; Déqué, M.; Jacob, D.; Jones, R. and Vidale, P. L. (2002). Intercomparison of water and energy budgets simulated by regional climate models applied over Europe. Max Planck Institute for Meteorology Report No. 338. 52pp

Heimann, M. (1999). EUROSIBERIAN CARBONFLUX: ANNUAL REPORT 1999. Max Planck Institute for Biogeochemistry, Jena Germany. 74pp

Heimann, M. and Keeling, C. D. (1989). A three-dimensional model of atmospheric CO_2 transport based on observed winds: 2. Model descriptions and simulated tracer experiments. AGU Monograph 55, Washington, American Geophysical Union. 237-275pp

Heimann, M. and Körner, S. (2003). The Global Atmospheric Tracer Model TM3: Model description and User's Manual. Technical Report, Release 3.8a. Max Planck Institute for Biogeochemistry, Jena. 131pp

Jacob, D. (2001). A note to the simulation of the annual and inter-annual variability of the water budget over the Baltic Sea drainage basin. Meteorology and Atmospheric Physics, 77: 61-73

Jacob, D. and Podzun, R. (1997). Sensitivity studies with the regional climate model REMO. Meteorology and Atmospheric Physics, 63: 119-129

Jacob, D.; van den Hurk, B. J. J. M.; Andræ, U.; Elgered, G.; Fortelius, C.; Graham, L. P.; Jackson, S. D.; Karstens, U.; Köpken, Chr.; Lindau, R.; Podzun, R.; Rockel, B.; Rubel, F.; Sass, B. H.; Smith, R. N. B. and Yang, X. (2001). A comprehensive model inter-comparison study investigations to water budget during the BALTEX-PIDCAP period. Meteorology and Atmospheric Physics, 77: 19-43

Jürrens, R. (1999). Validation of surface fluxes in climate simulations of the Arctic with the regional model REMO. Tellus, 51A(5): 698-709

Kaduk, J. and Heimann, M. (1994). The climate sensitivity of the Osnabrück Biosphere Model on the ENSO timescale. Ecological Modelling, 75/76: 239-256

Karstens, U.; Gloor, M.; Heimann, M. and Rödenbeck, C. (2006). Insights from simulations with high resolution transport and process models on sampling of the atmosphere for constraining mid-latitude and

land carbon sinks. Journal of Geophysical Research, 111(D12301), doi: 10.1029/2005JD006278

Karstens, U.; Holube, R., N-. and Rockel, B. (1996). Calculation of the water budget over the Baltic Sea catchment area using the regional forecast model REMO for June 1993. Tellus, 48A(5): 684-692

Kimball, J. S.; White, M. A. and Running, S. W. (1997). BIOME-BGC simulations of stand hydrologic processes for BOREAS. Journal of Geophysical Research, 102(D24): 29043-29051

Kjellström, E.; Holmén, K.; Eneroth, K. and Engardt, M. (2002). Summertime Siberian CO_2 simulations with the regional transport model MATCH: A feasibility study of carbon uptake calculations from EUROSIB data. Tellus, 54B: 834-849

Knorr, W. (1997). Satellite remote sensing and modelling of the global CO_2 exchange of land vegetation: A synthesis study. PhD Thesis. Faculty of the Earth Sciences of the University of Hamburg. 189pp

Knorr, W. (2000). Annual and interannual CO_2 exchanges of the terrestrial biosphere: process-based simulations and uncertainties. Global Ecology & Biogeography, 9:225-252

Knorr, W. and Heimann, M. (2001a). Uncertainties in global terrestrial biosphere modelling, Part I: A comprehensive sensitivity analysis with a new photosynthesis and energy balance scheme. Global Biogeochemical Cycles, 15(1): 207-225

Knorr, W. and Heimann, M. (2001b). Uncertainties in global terrestrial biosphere modelling, Part II: Global constraints for a process-based vegetation model. Global Biogeochemical Cycles, 15(1): 227-246

Kucharik, C. J.; Foley, J. A.; Delire, C.; Fisher, V. A.; Coe, M. T.; Lenters, J. D.; Young-Molling, C.; Ramankutty, N.; Norman, J. M. and Gower, S. T. (2000). Testing the performance of a dynamic global ecosystem model: water balance, carbon balance and vegetation structure. Global Biogeochemical Cycles, 14(3): 795-825

Lafont, S.; Kergoat, L.; Dedieu, G.; Chevillard, A.; Karstens, U. and Kolle, U. (2002). Spatial and temporal variability of land CO_2 fluxes estimated with remote sensing and analysis data over Western Eurasia. Tellus, 54B(5): 820-833

Langmann, B. (2000). Numerical modelling of regional scale transport and photochemistry directly together with meteorological processes. Atmospheric Environment, 34: 3585-3598

Louise, J. –F. (1979). A parametric model of vertical eddy fluxes in the atmosphere. Boundary Layer Meteorology, 17: 187-202

Majewski, D. (1991). The Europa Modell of the Deutscher Wetterdienst. Seminar Proceedings ECMWF, 2: 147-191

McAuliffe, J. R. (2003). The atmosphere-biosphere interface: the importance of soils in arid and semi-arid environments. In: Changing Precipitation Regimes and Terrestrial Ecosystems: A North American Perspective. Weltzin, J. F. and McPherson, G. R. (Eds.). The University of Arizona Press. 9-27pp

McGuire, A. D.; Melillo, J. M.; Joyce, L. A.; Kicklighter, D. W.; Grace, A. L.; Moore III, B. and Vorosmarty, C. J. (1992). Interactions between carbon and nitrogen dynamics in estimating net primary productivity for potential vegetation in North America. Global Biogeochemical Cycles, 6(2): 101-124

McGuire, A.D.; Sitch, S.; Clein, J. S.; Dargaville, R.; Esser, G.; Foley, J.; Heimann, M.; Joos, F.; Kaplan, J.; Kicklighter, D. W.; Meier, R. A.; Melillo, J. M.; Moore III, B.; Prentice, I. C.; Ramankutty, N.; Reichenau, T.; Schloss, A.; Tian, H.; Williams, L. J. and Wittenberg, U. (2001). Carbon balance of the terrestrial biosphere in the twentieth century: analysis of CO_2, climate and land use effects with four process-based ecosystem models. Global Biogeochemical Cycles, 15(1): 183-206

Monteith, J. L. (1965). Light distribution and photosynthesis in field crops. Annals of Botany, 29: 17-37

Myachkova, N. A. (1983). Climate of the UDSSR. Moscow State University Publishers, Moscow, 119pp (In Russian)

Olson, J. S.; Watts, J. A. and Allison, L. J. (1985). Major world ecosystem complexes ranked by carbon in live vegetation. NDPO17, Carbon dioxide Information Centre, Oak Ridge National Laboratory, Oak Ridge, Tennessee, USA.

Overpack, J.; Whitlock, C. and Huntley, B. (2002). Terrestrial biosphere dynamics in the climate system: Past and future. American Geophysical Union. Fall Meeting 2002, abstract #PP62B-06. 81-103

Plummer, S.; Rayner, P.; Raupach, M.; Ciais, P. and Dargaville, R. (2005). Monotoring carbon from space. EOS, 86(41): 384-385

Rechid, D. and Jacob, D. (2006). Influence of monthly varying vegetation on the simulated climate in Europe. Meteorologische Zeitschrift, 15(1): 99-116

Rockel, B. and Karstens, U. (2001). Development of the water budget for three extra-tropical cyclones with intense rainfall over Europe. Meteorology and Atmospheric Physics, 77: 75-83

Roeckner, E.; Arpe, K.; Bengtsson, L.; Christoph, M.; Claussen, M.; Dümenil, L.; Esch, M.; Giorgetta, M.; Schlese, U. and Schulzweider, U. (1996). The atmospheric general circulation model ECHAM-4: Model description and simulation of the present day climate. Max Planck Institute for Meteorology, Scientific Report No. 218. 90pp

Ruimy, A.; Dedieu, G. and Saugier, B. (1996). TURC: A diagnostic model of continental gross primary productivity and net primary productivity. Global Biogeochemical Cycles, 10(2): 269-285

Rustad, L. E. and Norby, R. J. (2002). Volume 2, The Earth System: biological and ecological dimensions of global environmental change. In: Encyclopedia of Global Environmental Change. Mooney, H. H. and Canadell, J. G. (Eds.). John Wiley & Sons, Ltd., Chichester. 575-581pp

Ryan, M. G. (1991a). Effects of climate change on plant respiration. Ecol. Appl. 1: 157-167

Ryan, M. G. (1991b). A simple method for estimating gross carbon budgets of vegetation in forest ecosystems. Tree Physiology, 9: 255-266

Saltelli, A. (2000). What is Sensitivity Analysis? In: Sensitivity Analysis. Saltelli, A.; Chan, K. and Scott, E. M. (Eds.), Wiley Series in Probability and Statistics, John Wiley & Sons, Ltd., England. 3-13pp

Schimel, D. S.; Alves, D.; Enting, I.; Heimann, M.; Joos, M.; Raynaud, D. and Wigley, T. (1996). The Global Carbon Cycle. In: Climate Change

1995. Houghton, J. T.; Meira Filho, L. G.; Callander, B. A.; Harris, N.; Kattenberg, A. and Markell, K. (Eds.). Intergovernmental Panel on Climate Change, Cambridge University Press, Cambridge. 76-86pp

Schimel, D. S.; House, J. I.; Hibbard, K. A.; Bouquet, P.; Ciais, P.; Peylin, P.; Braswell, B. H.; Apps, M. J.; Baker, D.; Bondeau, A.; Canadell, J.; Churkina, G.; Cramer, W.; Denning, A. S.; Field, C. P.; Friedlingstein, P.; Goodale, C.; Heimann, M.; Houghton, R. A.; Melillo, J. M.; Moore III, B.; Murdiyarso, D.; Noble, I.; Pacala, S. W.; Prentice, I. C.; Raupach, M. R.; Rayner, P. J.; Scholes, R. J.; Steffen, W. L. and Wirth, C. (2001). Recent patterns and mechanisms of carbon exchange by terrestrial ecosystems. Nature, 414: 169-172

Schimel, D. S.; Melillo, D. J.; Tian, H.; McGuiure, A. D.; Kicklighter, D.; Kittel, T.; Rosenbloom, N.; Running, S.; Thornton, P.; Ojima, D.; Parton, W.; Kelly, R.; Sykes, M.; Neilson, R. and Rizzo, B. (2000). Contribution of increasing CO_2 and climate to carbon storage by ecosystems in the United States. Science, 287: 2004-2006

Schulze, E.-D.; Vygodskaya, N. N.; Tchebakova, N. M.; Czimczik, C. I.; Kozlov, D. N.; Lloyd, J.; Mollicone, D.; Perfenova, E.; Sidorov, K. N.; Varlagin, A. V. and With, C. (2002). The Eurosiberian Transect: An introduction to the experimental region. Tellus 54B(5): 421-428

Smolarkiewitz, P. K. (1983). A simple positive definite advection scheme with small implicit diffusion. Monthly Weather Review, 111: 479-486

Steiner, A. L. and Chameides, W. L. (2005). Aerosol-induced thermal effects increase modelled terrestrial photosynthesis and transpiration. Tellus 57B(5): 401-411

Takahashi, T.; Wanninkhof, R. H.; Feely, R. A.; Weiss, R. F.; Chipman, D. W.; Bates, N.; Olafsson, J.; Sabine, C.; Sutherland, S. C. (1999). Net sea-air CO_2 flux over the global oceans: An improved estimation based on the sea-air pCO_2 difference. Proceedings of the 2nd CO_2 in Oceans Symposium, Tsukuba, Japan, 18-23 January

Thornton, P. E. (1998). Regional ecosystem simulation: combining surface- and satellite-based observations to study linkages between terrestrial energy and mass budgets. PhD Thesis, The University of Montana, Missoula, 231pp

Thornton, P. E. (2000). User's Guide for BIOME-BGC Version 4.1.1. Numerical Terradynamic Simulation Group, School of Forestry, The University of Montana, Missoula, 21pp

Thornton, P. E.; Law, B. E.; Gholz, H. L.; Clark, K. L.; Falge, E.; Ellsworth, D. S.; Goldstein, A. H.; Monson, R. K.; Hollinger, D.; Falk, M.; Chen, J. and Sparks, J. P. (2002). Modelling and measuring the effects of disturbance history and climate on carbon and water budgets in evergreen needleleaf forests. Agricultural and Forest Meteorology, 113: 185-222

Tiedtke, M. (1989). A comprehensive mass flux scheme for cumulus parameterisation in large-scale models. Monthly Weather Review, 117: 1779-1800

Turner, D. P.; Ollinger, S. V. and Kimball, J. S. (2004). Integrating remote sensing and ecosystem process models for landscape- to regional-scale analysis of the carbon cycle. BioScience, 54(6): 573-583

Ustin, S. L.; Roberts, D. A.; Gamon, J. A.; Asner, G. P. and Green, R. O. (2004). Using image spectroscopy to study ecosystem processes and properties. BioScience, 54(6): 523-534

van, Meijgaard, E.; Andræ, U. and Rockel, B. (2001). Comparison of model predicted cloud parameters and surface radiative fluxes with observations on the 100km scale. Meteorology and Atmospheric Physics, 77: 109-130

Weltzin, J. F.; Loik, M. E.; Scwinning, S.; Williams, D. G.; Fay, P. A.; Haddad, B. M.; Harte, J.; Huxman, T. E.; Knapp, A. K.; Lin, G.; Pockman, W. T.; Shaw, M. R.; Small, E. E.; Smith, M. D.; Smith, S. D.; Tissue, D. T. and Zak, J. C. (2003). Assessing the response of terrestrial ecosystems to potential changes in precipitation. BioScience, 53(10): 941-952

White, M. A.; Thornton, P. A.; Running, S. W. and Nemani, R. R. (2000). Parameterisation and sensitivity analysis of the BIOME-BGC terrestrial ecosystem model: Net Primary Production Controls. Earth Interactions, 4(3): 1-85

Woodrow, I. E. and Berry, J. A. (1988). Enzymatic regulation of photosynthetic CO_2 fixation in C3 plants. Ann Rev. Plant Physiol. Plant Mol. Biol. 39: 533-594

Wulder, M. A.; Hall, R. J.; Coops, N. C. and Franklin, S. E. (2004). High spatial resolution remotely sensed data for ecosystem characterisation. BioScience, 54(6): 511-521

APPENDICES

APPENDIX A1

Illustration of BETHY control file

```
# Options for 4 years daily forced run
# - 0.5 deg
# - daily meteo data, 1995-1998
# - for full forward runs
### Simulation years ########################
     1     4    1995    ; minyear, maxyear, year0
### Grid and Region  ########################
    0.5  -180.00  180.00      ; grdwid, lonw, lone
  90.00  -90.00                ; latn, lats
### landcover, vegetation type and interannual mode
     -1     -2     -1     ; lcmode, selflg, iaflgs   # daily
### Optimisation / pheno time steps per month ?? / C fractionation flag
#forward
     1      3      00     ; pmode, nmopt, frctflgs   # T1/T5
### mode of rainfall, weather gen. and snow
# - stochastical rainfall / no weather generator / update snow
     0      0      1     ; rflg, wflg, snflg
### photosynth. method and soil data ##############################
     0      2      1     ; fflg, stflg, sflg # - Monteith /supply/demand/Jarvis / read in Theta (surface6, c10) soil
### number of canopy layers and of sunlit layers and mode of N scaling
     3      0      2     ; nsh, sunflg, nsclflg # - 3 canopy layers/ no additional sunlit layer / nitrogen scaling
### diffuse/direct radiation
     0      0            ; radin, dirpfrac
### I/O pathes and files ############################
## file extension
.dat
# - forced with CRU data
_CRU
## Input path:
#./input/eurosib_site_input_duplicate/
./input/eurosib_site_input_rounded/
## Output path:
./output_rounded.vegbgc/
#
## Periodically (daily) output
#HEW-DEL ./output_perd/
#
1  SeaWifs
## max number of years / first year /last year (for FAPAR assimilation)
  50    1995    1998  ; nxitmax, payear0, payear1
```

APPENDIX A2

Illustration of BIOME-BGC initialisation file

Biome-BGC v4.1.1 example : (spinup simulation, Hyytiala, evergreen needleleaf)

```
MET_INPUT     (keyword) start of meteorology file control block
/scratch/local1/m218/m218057/biomebgc_point/unixbgc/ncep_data/bgc.Hyytiala.nce
p.48-98.asc meteorology input filename
4         (int)     header lines in met file

RESTART       (keyword) start of restart control block
0         (flag)    1 = read restart file    0 = don't read restart file
1         (flag)    1 = write restart file   0 = don't write restart file
0         (flag)    1 = use restart metyear  0 = reset metyear
/scratch/local1/m218/m218057/biomebgc_point/unixbgc/sensitivity_rdepth_output/r
estart/HY+2.0m
input restart filename
/scratch/local1/m218/m218057/biomebgc_point/unixbgc/sensitivity_rdepth_output/r
estart/HY+2.0m output restart filename

TIME_DEFINE  (keyword - do not remove)
51        (int)     number of meteorological data years
51        (int)     number of simulation years
0         (int)     first simulation year
1         (flag)    1 = spinup simulation   0 = normal simulation
10000     (int)     maximum number of spinup years (if spinup simulation)

CLIM_CHANGE          (keyword - do not remove)
0.0       (deg C)   offset for Tmax
0.0       (deg C)   offset for Tmin
1.0       (DIM)     multiplier for Prcp
1.0       (DIM)     multiplier for VPD
1.0       (DIM)     multiplier for shortwave radiation

CO2_CONTROL          (keyword - do not remove)
0         (flag)    0=constant 1=vary with file 2=constant, file for Ndep
311.00    (ppm)     constant atmospheric CO2 concentration
/scratch/local1/m218/m218057/biomebgc_point/unixbgc/co2_data/eur_co2_1744-
2001.txt
annual variable CO2 filename

SITE      (keyword) start of site physical constants block
2.4       (m)               effective soil depth (corrected for rock fraction)
70.0      (%)               sand percentage by volume in rock-free soil
20.0      (%)               silt percentage by volume in rock-free soil
10.0      (%)               clay percentage by volume in rock-free soil
170       (m)               site elevation
61.85     (degrees)         site latitude (- for S.Hem.)
0.2       (DIM)             site shortwave albedo
```

```
0.0006   (kgN/m2/yr)    wet+dry atmospheric deposition of N
0.0002   (kgN/m2/yr)    symbiotic+asymbiotic fixation of N

RAMP_NDEP    (keyword - do not remove)
1        (flag) do a ramped N-deposition run? 0=no, 1=yes
1998     (int)  reference year for industrial N deposition
0.0004   (kgN/m2/yr) industrial N deposition value
/scratch/local1/m218/m218057/biomebgc_point/unixbgc/nitrogen_data/HA_N1906_2
001.txt
annual variable Ndep filename

EPC_FILE         (keyword - do not remove)
/scratch/local1/m218/m218057/biomebgc_point/unixbgc/epc/enf.epc
evergreen needleleaf forest ecophysiological constants

W_STATE          (keyword) start of water state variable initialization block
0.0      (kg/m2)          water stored in snowpack
0.5      (DIM)   initial soil water as a proportion of saturation

C_STATE          (keyword) start of carbon state variable initialization block
0.0001   (kgC/m2)        first-year maximum leaf carbon
0.0      (kgC/m2)        first-year maximum stem carbon
0.0      (kgC/m2)        coarse woody debris carbon
0.0      (kgC/m2)        litter carbon, labile pool
0.0      (kgC/m2)        litter carbon, unshielded cellulose pool
0.0      (kgC/m2)        litter carbon, shielded cellulose pool
0.0      (kgC/m2)        litter carbon, lignin pool
0.0      (kgC/m2)        soil carbon, fast microbial recycling pool
0.0      (kgC/m2)        soil carbon, medium microbial recycling pool
0.0      (kgC/m2)        soil carbon, slow microbial recycling pool
0.0      (kgC/m2)        soil carbon, recalcitrant SOM (slowest)

N_STATE          (keyword) start of nitrogen state variable initialization block
0.0      (kgN/m2)        litter nitrogen, labile pool
0.0      (kgN/m2)        soil nitrogen, mineral pool

OUTPUT_CONTROL    (keyword - do not remove)
/scratch/local1/m218/m218057/biomebgc_point/unixbgc/sensitivity_rdepth_output/h
y+2.0m
prefix for output files
1        (flag)    1 = write daily output   0 = no daily output
0        (flag)    1 = monthly avg of daily variables  0 = no monthly avg
0        (flag)    1 = annual avg of daily variables   0 = no annual avg
1        (flag)    1 = write annual output  0 = no annual output
1        (flag)    for on-screen progress indicator

DAILY_OUTPUT          (keyword)
10       (int)     number of daily variables to output

620      0 npp
621      1 nep
```

622 2 nee
623 3 gpp
624 4 mr
625 5 gr
626 6 hr
500 7 day_leafc_litfall_incr
638 8 soil C
639 9 total C

ANNUAL_OUTPUT (keyword)
12 (int) number of annual output variables

628 0 annual sum npp
629 1 annual sum nep
620 2 annual sum nee
631 3 annual sum gpp
632 4 annual sum mr
633 5 annual sum gr
634 6 annual sum hr
636 7 vegetation C
638 8 soil C
639 9 total C
307 10 soil mineral N
545 11 annual maximum projected LAI

END_INIT (keyword) indicates the end of the initialization file

APPENDIX A3

Illustration of BIOME-BGC ecophysiological constants file

```
ECOPHYS      DBF  (deciduous broadleaf forest)
1         (flag)   1 = WOODY                 0 = NON-WOODY
0         (flag)   1 = EVERGREEN             0 = DECIDUOUS
1         (flag)   1 = C3 PSN                0 = C4 PSN
0         (flag)   1 = MODEL PHENOLOGY   0 = USER-SPECIFIED PHENOLOGY
100       (yday)    yearday to start new growth  (when phenology flag = 0)
300       (yday)    yearday to end litterfall  (when phenology flag = 0)
0.2       (prop.)   transfer growth period as fraction of growing season
0.2       (prop.)   litterfall as fraction of growing season
1.0       (1/yr)    annual leaf and fine root turnover fraction
0.70      (1/yr)    annual live wood turnover fraction
0.005     (1/yr)    annual whole-plant mortality fraction
0.005     (1/yr)    annual fire mortality fraction
1.0       (ratio)   (ALLOCATION) new fine root C : new leaf C
2.2       (ratio)   (ALLOCATION) new stem C : new leaf C
0.1       (ratio)   (ALLOCATION) new live wood C : new total wood C
0.23      (ratio)   (ALLOCATION) new croot C : new stem C
0.5       (prop.)  (ALLOCATION) current growth proportion
24.0      (kgC/kgN) C:N of leaves
49.0      (kgC/kgN) C:N of leaf litter, after retranslocation
42.0      (kgC/kgN) C:N of fine roots
50.0      (kgC/kgN) C:N of live wood
442.0     (kgC/kgN) C:N of dead wood
0.39      (DIM)     leaf litter labile proportion
0.44      (DIM)     leaf litter cellulose proportion
0.17      (DIM)     leaf litter lignin proportion
0.30      (DIM)     fine root labile proportion
0.45      (DIM)     fine root cellulose proportion
0.25      (DIM)     fine root lignin proportion
0.76      (DIM)     dead wood cellulose proportion
0.24      (DIM)     dead wood lignin proportion
0.041     (1/LAI/d) canopy water interception coefficient
0.5       (DIM)     canopy light extinction coefficient
2.6       (DIM)     all-sided to projected leaf area ratio
30.       (m2/kgC)  canopy average specific leaf area (projected area basis)
2.0       (DIM)     ratio of shaded SLA:sunlit SLA
0.08      (DIM)     fraction of leaf N in Rubisco
0.005     (m/s)     maximum stomatal conductance (projected area basis)
0.00001   (m/s)     cuticular conductance (projected area basis)
0.08      (m/s)     boundary layer conductance (projected area basis)
-0.6      (MPa)     leaf water potential: start of conductance reduction
-2.3      (MPa)     leaf water potential: complete conductance reduction
930.0     (Pa)      vapor pressure deficit: start of conductance reduction
4100.0    (Pa)      vapor pressure deficit: complete conductance reduction
```

APPENDIX A4: Station comparisons

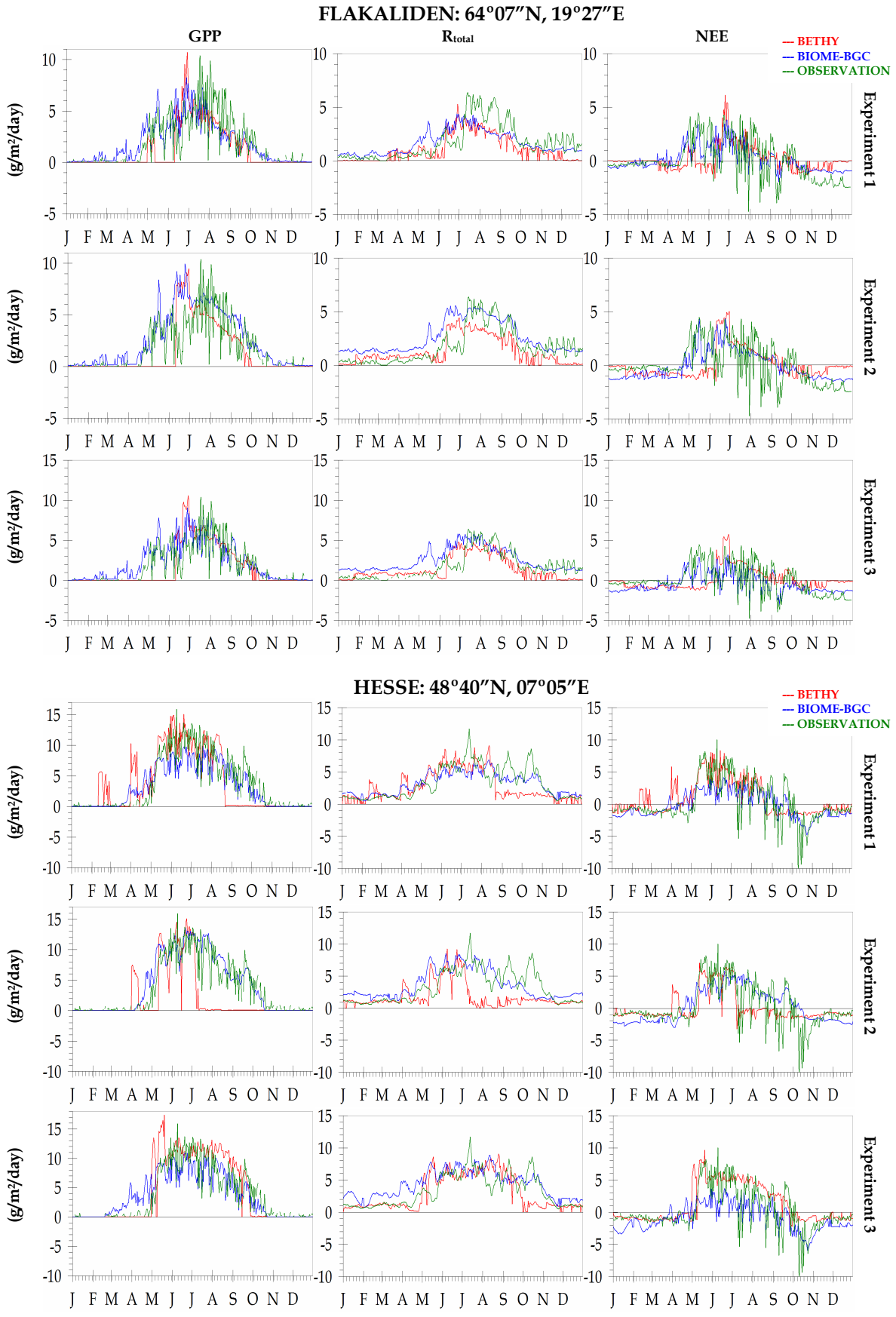

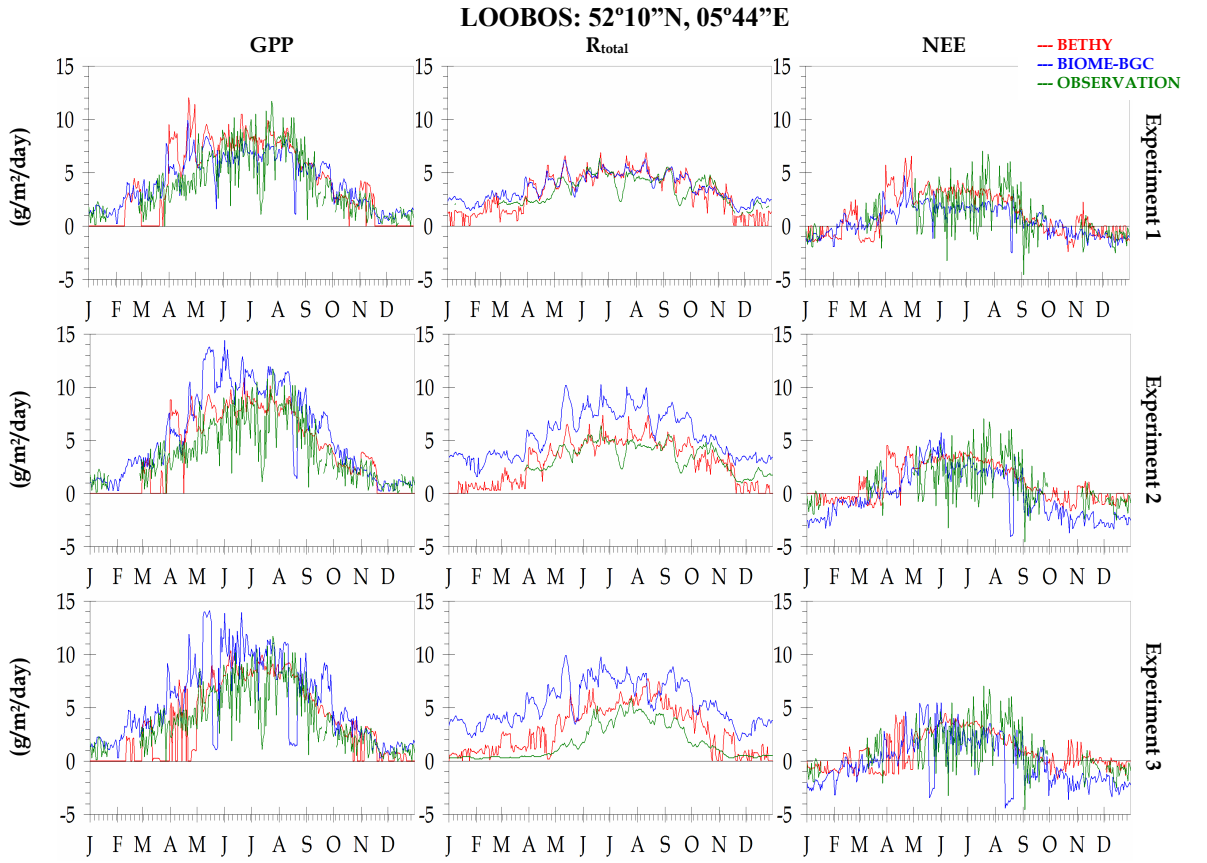
LOOBOS: 52°10”N, 05°44”E
GPP
R_{total}
NEE
--- BETHY
--- BIOME-BGC
--- OBSERVATION
(g/m²/day)
Experiment 1
Experiment 2
Experiment 3
J F M A M J J A S O N D

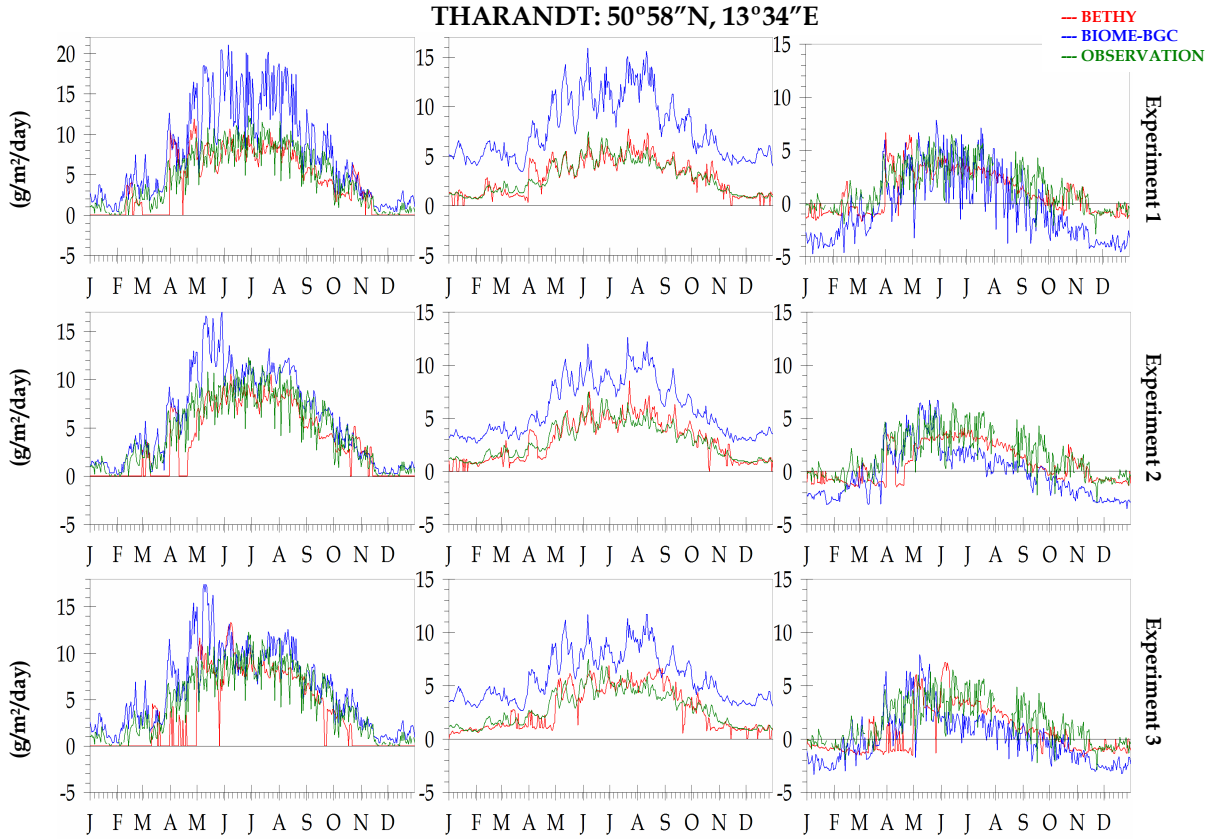
THARANDT: 50°58″N, 13°34″E
--- BETHY
--- BIOME-BGC
--- OBSERVATION
(g/m²/day)
Experiment 1
Experiment 2
Experiment 3
J F M A M J J A S O N D

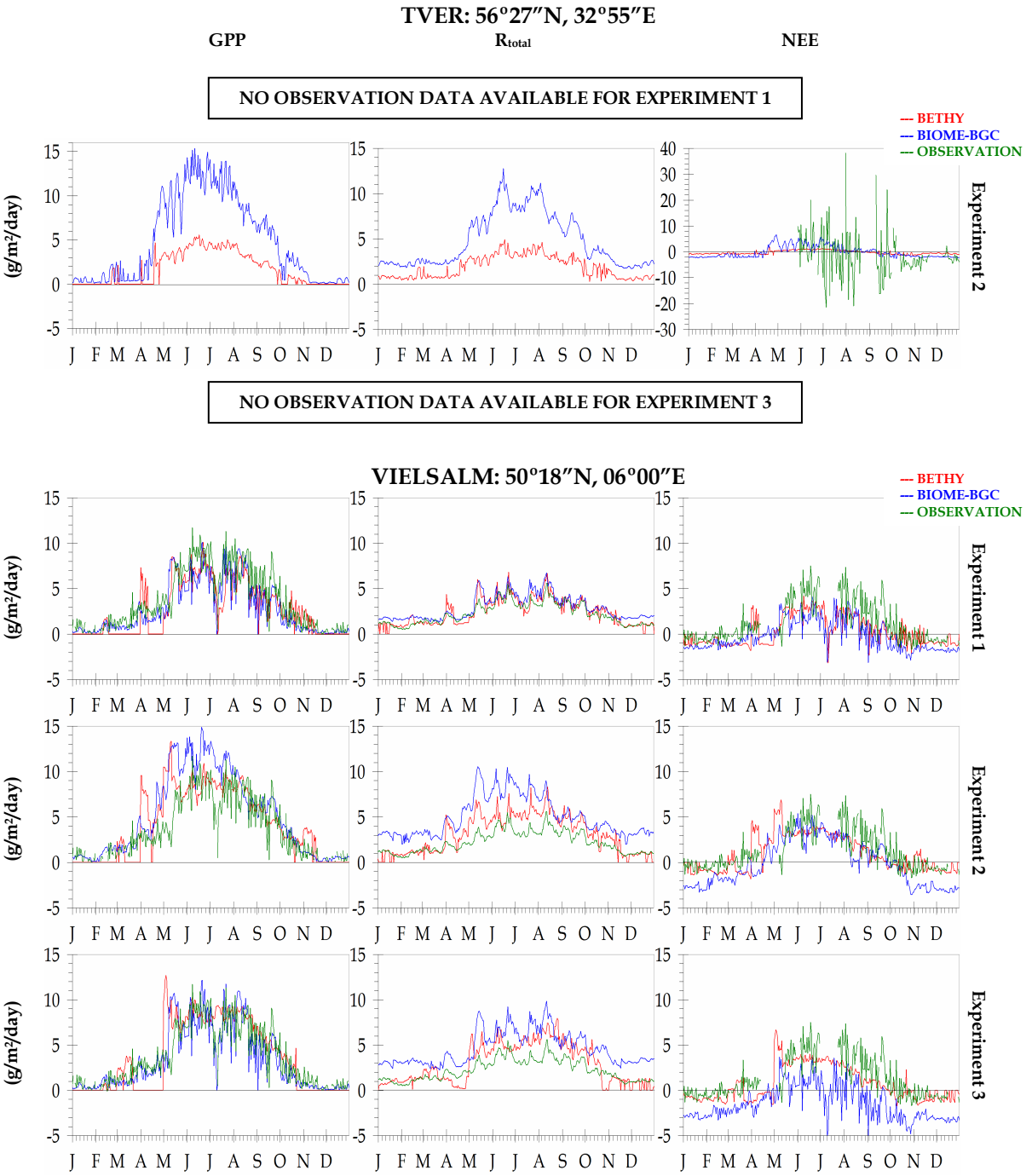
TVER: 56°27″N, 32°55″E
GPP
R_{total}
NEE
NO OBSERVATION DATA AVAILABLE FOR EXPERIMENT 1
--- BETHY
--- BIOME-BGC
--- OBSERVATION
(g/m²/day)
Experiment 2
NO OBSERVATION DATA AVAILABLE FOR EXPERIMENT 3
VIELSALM: 50°18″N, 06°00″E
Experiment 1
Experiment 3
J F M A M J J A S O N D

ZOTINO: 60°45″N, 89°23″E

NO OBSERVATION DATA AVAILABLE FOR EXPERIMENT 1

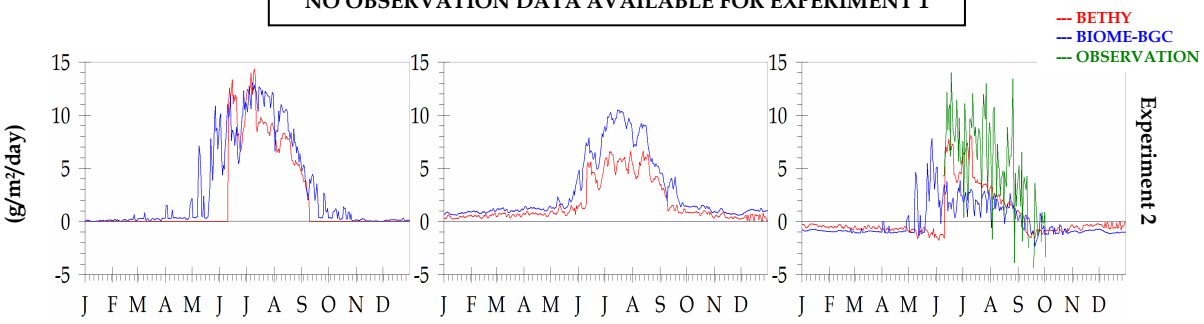

NO OBSERVATION DATA AVAILABLE FOR EXPERIMENT 3

APPENDIX A5

SENSITIVITY TEST I

Simulated CO_2 fluxes from varying root depth inputs to BETHY and BIOME-BGC

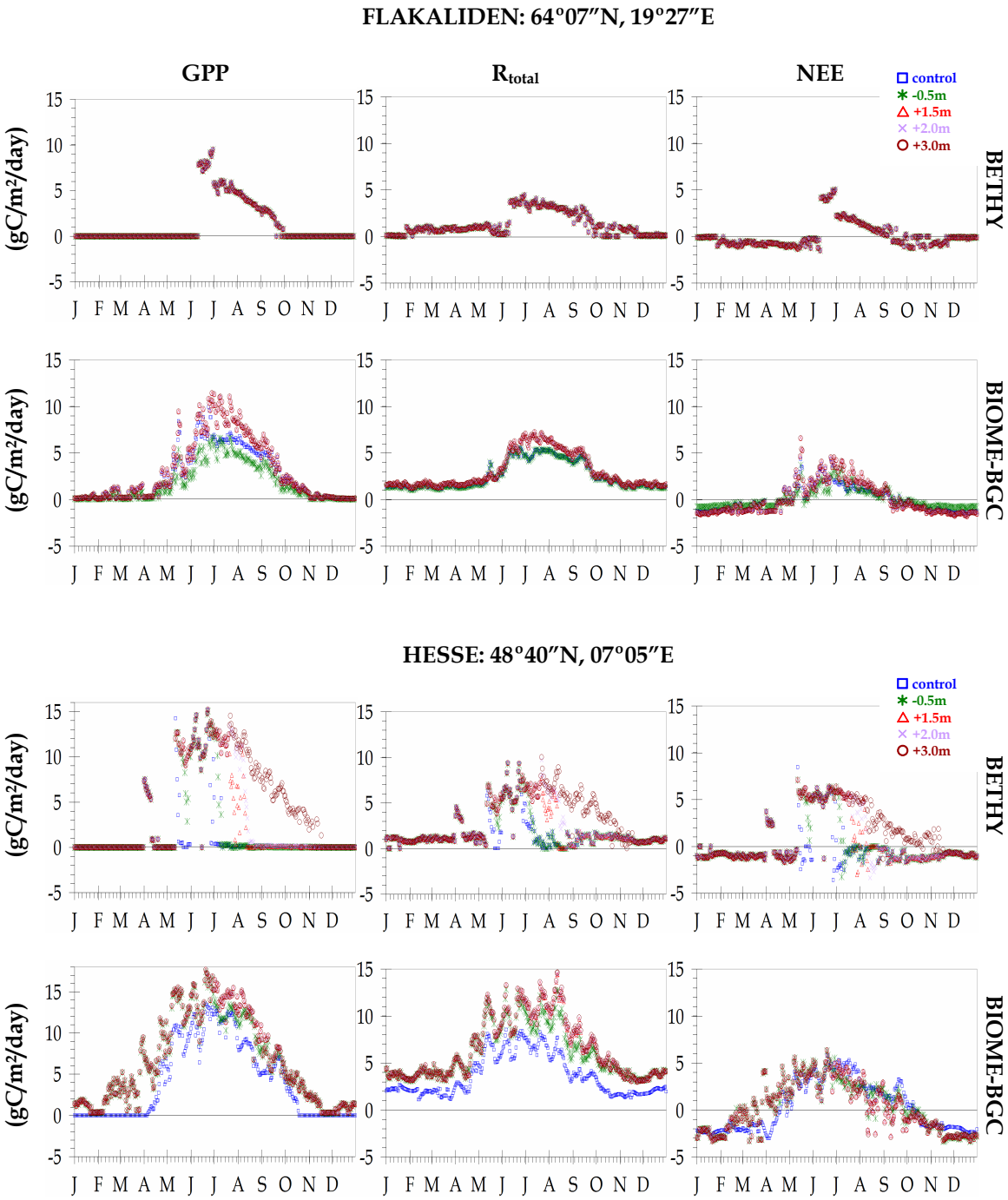

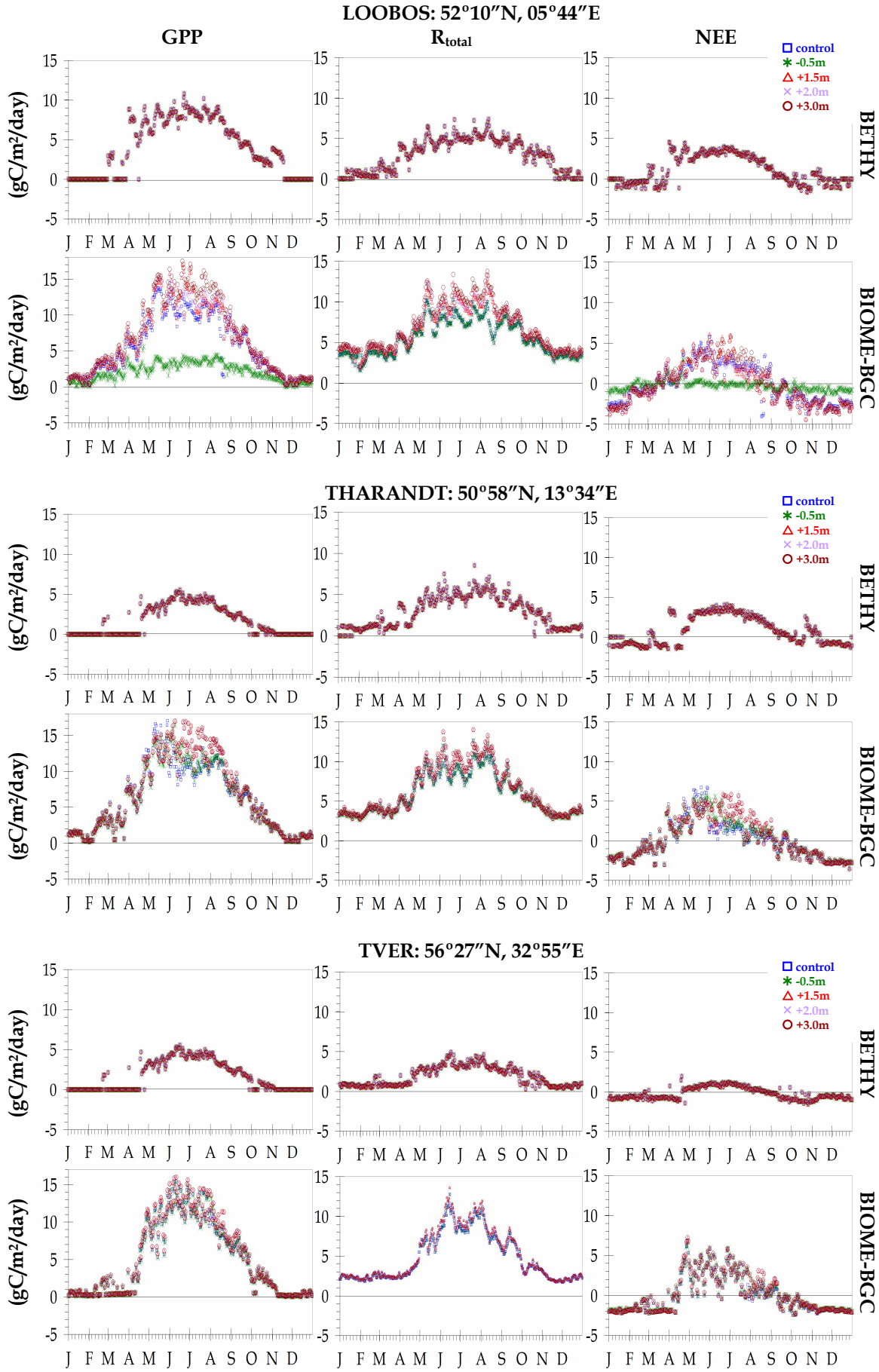
LOOBOS: 52°10″N, 05°44″E
GPP
R_{total}
NEE
control
-0.5m
+1.5m
+2.0m
+3.0m
BETHY
BIOME-BGC
(gC/m²/day)
J F M A M J J A S O N D
THARANDT: 50°58″N, 13°34″E
TVER: 56°27″N, 32°55″E

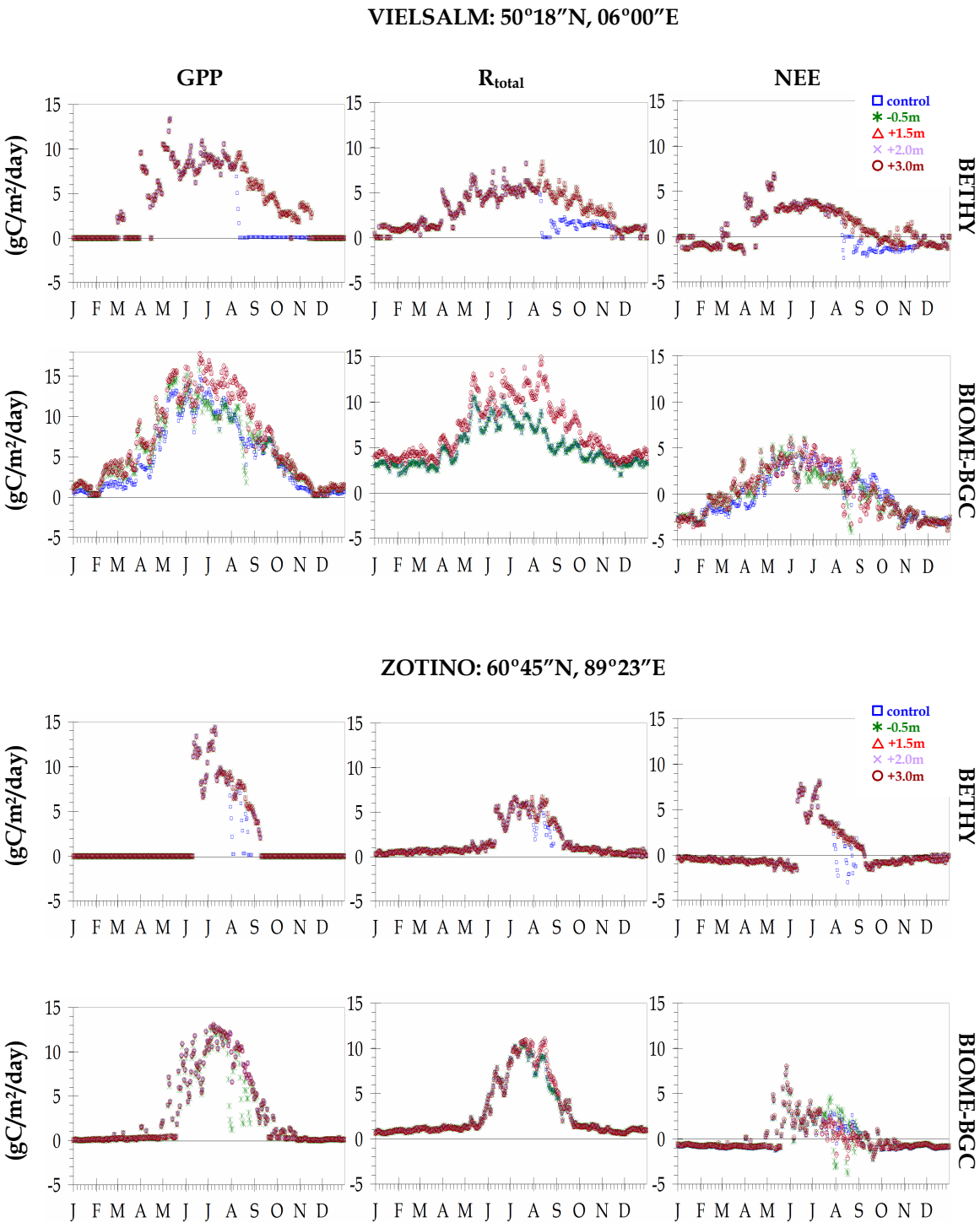
VIELSALM: 50°18″N, 06°00″E
GPP
R_{total}
NEE
control
-0.5m
+1.5m
+2.0m
+3.0m
BETHY
BIOME-BGC
(gC/m²/day)
15
10
5
0
-5
J F M A M J J A S O N D
ZOTINO: 60°45″N, 89°23″E

APPENDIX A6

SENSITIVITY TEST II

Simulated CO_2 fluxes from varying precipitation inputs to BETHY and BIOME-BGC

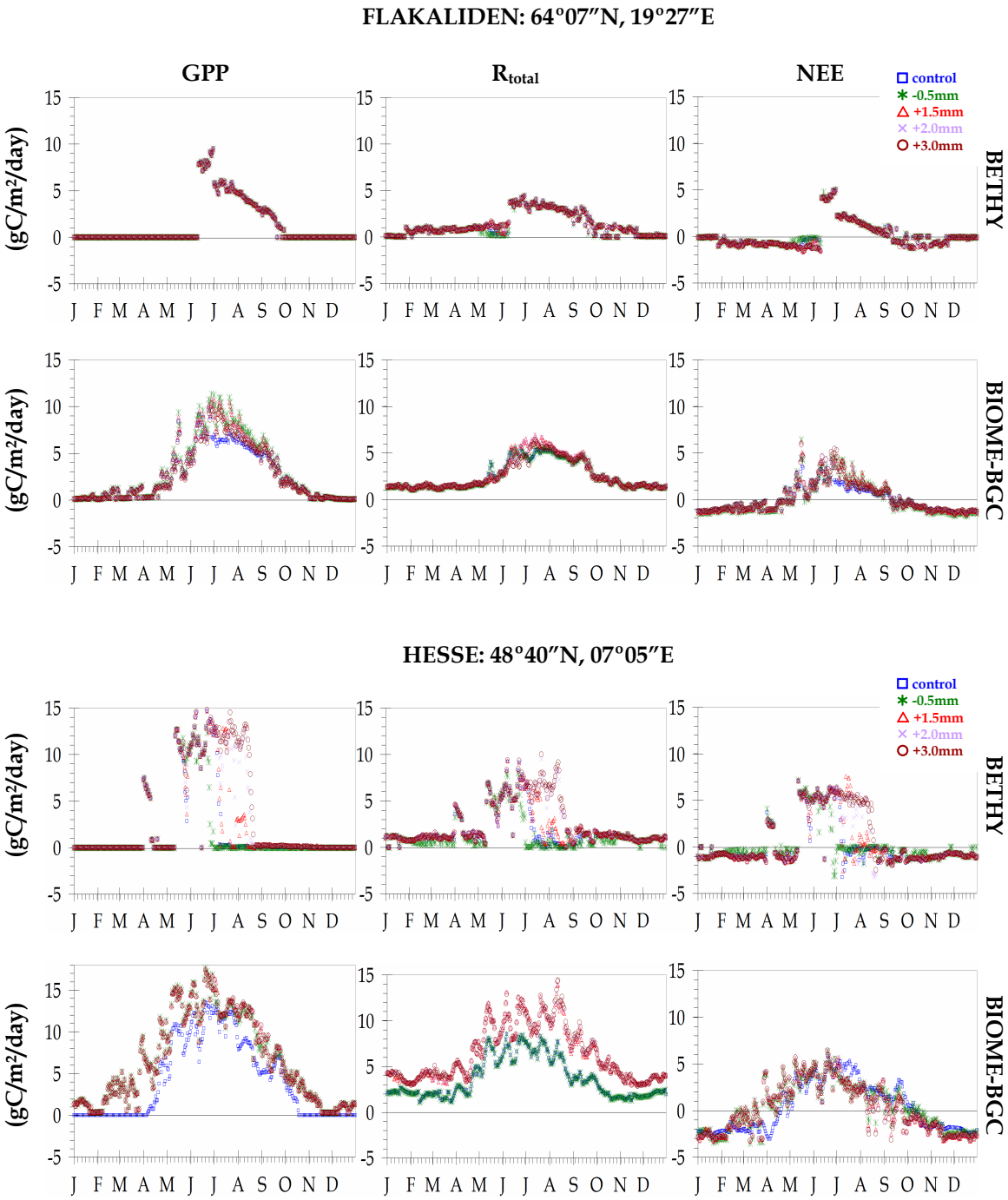

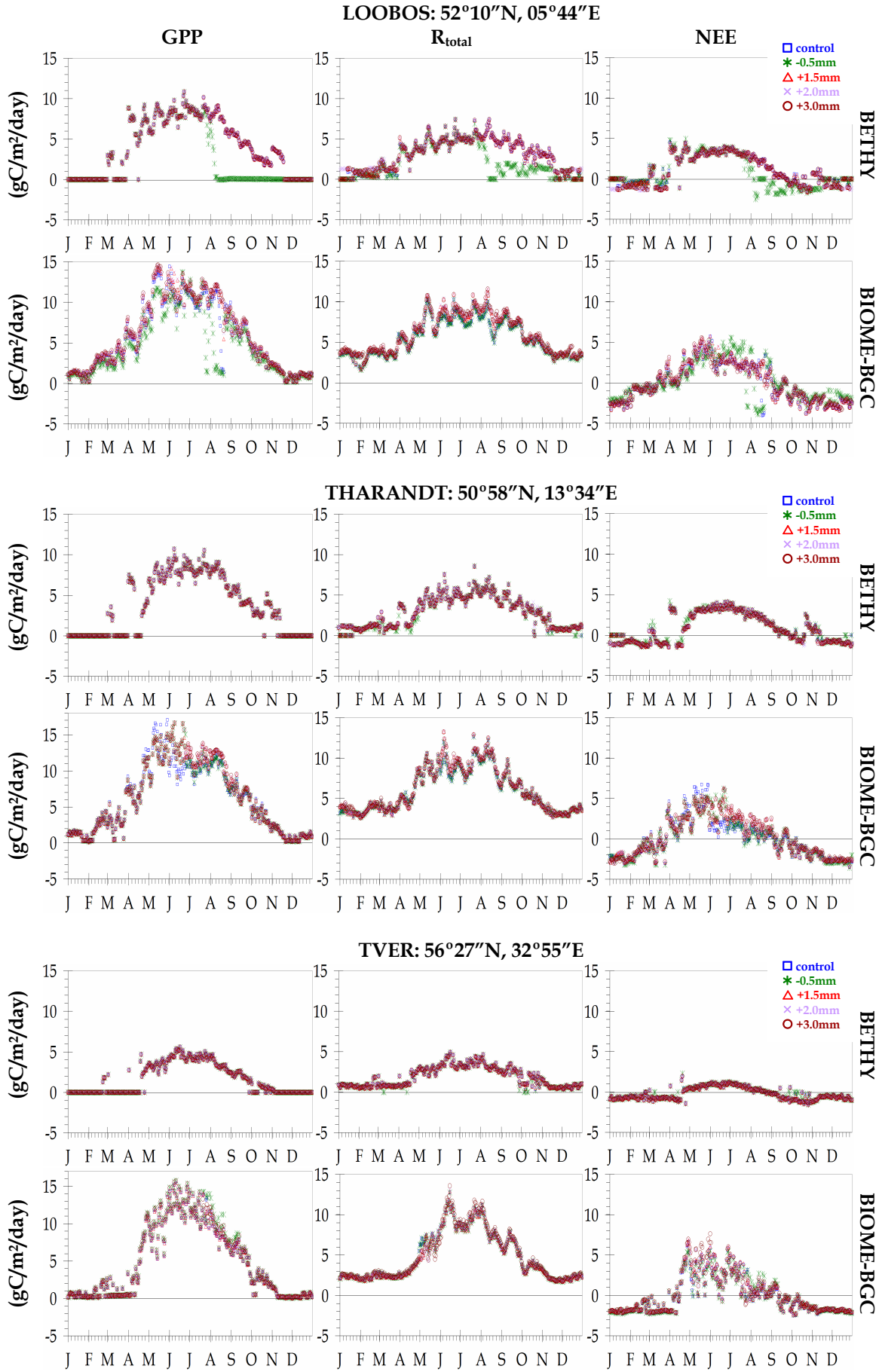
LOOBOS: 52°10″N, 05°44″E
GPP
R_{total}
NEE
control
-0.5mm
+1.5mm
+2.0mm
+3.0mm
BETHY
BIOME-BGC
(gC/m²/day)
J F M A M J J A S O N D
THARANDT: 50°58″N, 13°34″E
TVER: 56°27″N, 32°55″E

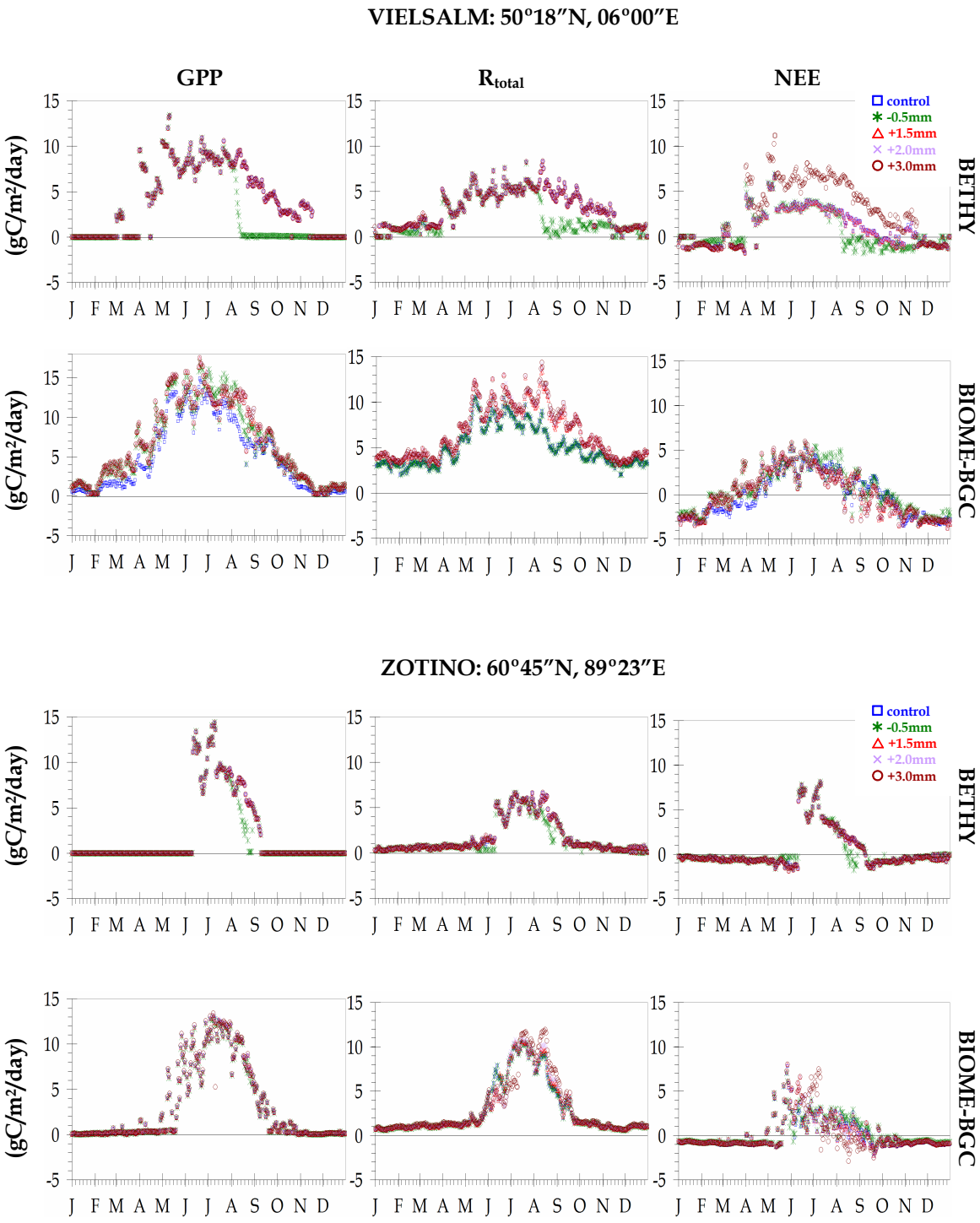
VIELSALM: 50°18″N, 06°00″E
GPP
R_{total}
NEE
control
-0.5mm
+1.5mm
+2.0mm
+3.0mm
BETHY
BIOME-BGC
(gC/m²/day)
15
10
5
0
-5
J F M A M J J A S O N D
ZOTINO: 60°45″N, 89°23″E

APPENDIX A7

SENSITIVITY TEST III

Simulated CO_2 fluxes from varying temperature inputs to BETHY and BIOME-BGC

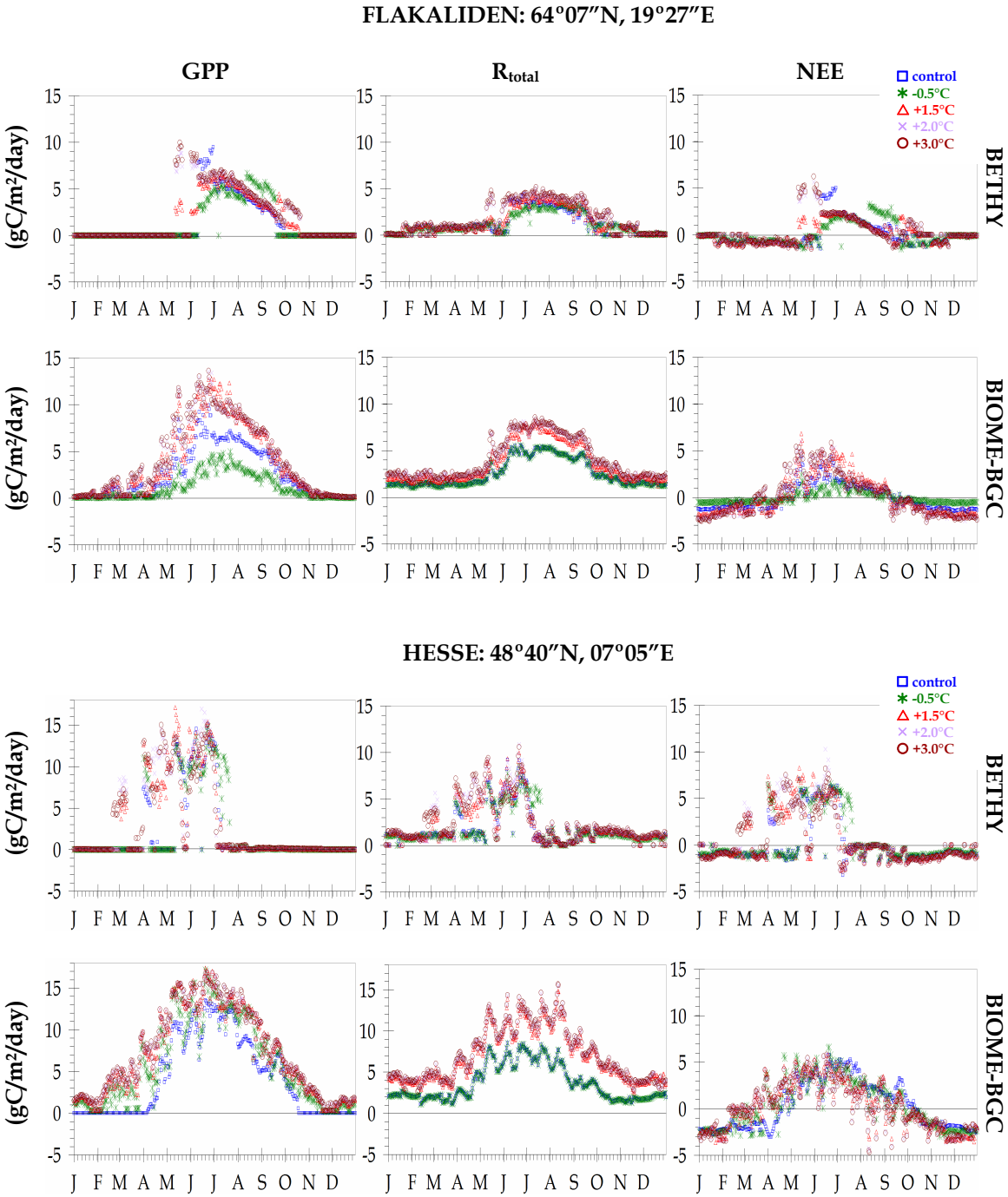

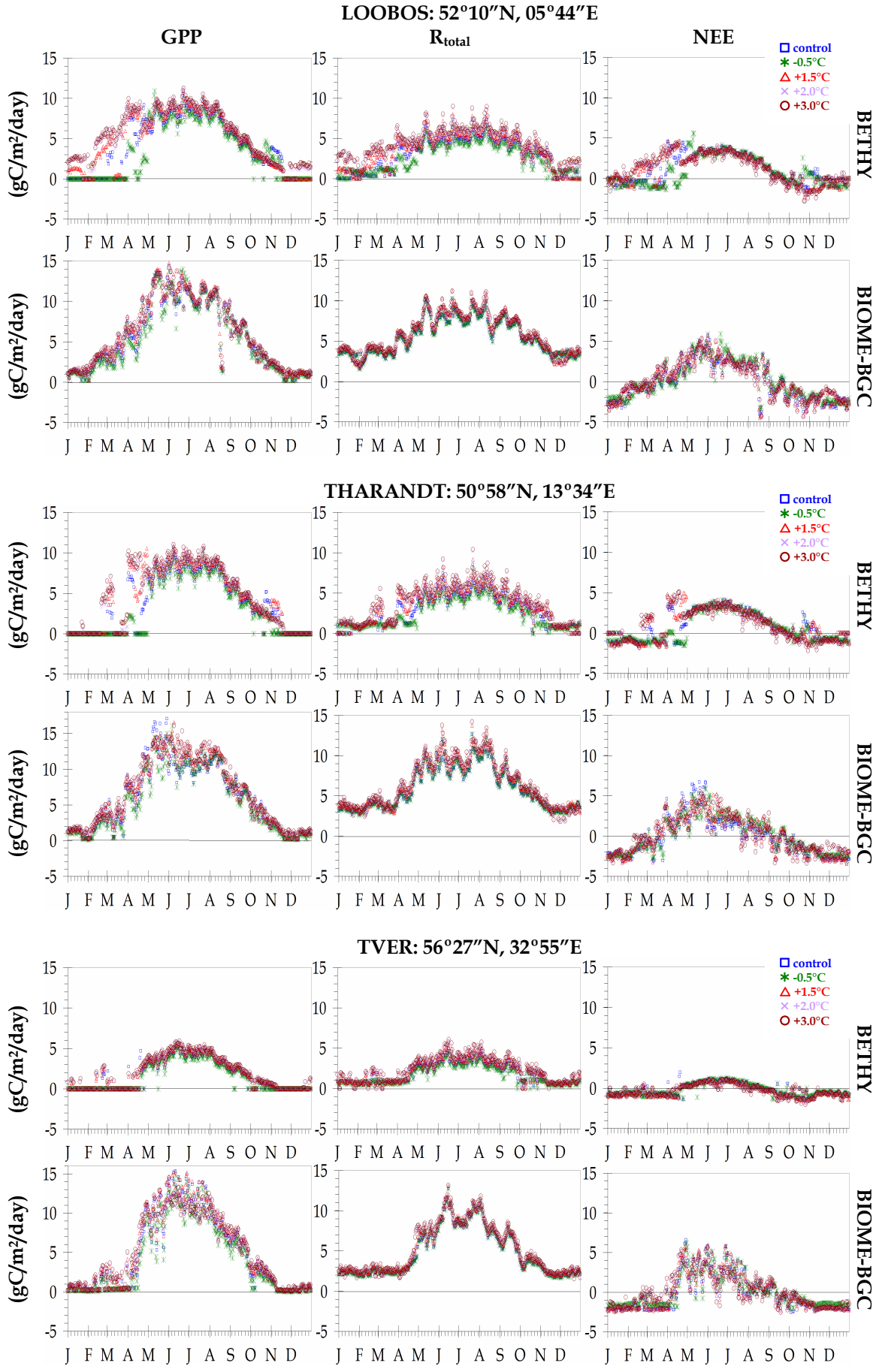
LOOBOS: 52°10″N, 05°44″E
GPP
R_{total}
NEE
control
-0.5°C
+1.5°C
+2.0°C
+3.0°C
BETHY
BIOME-BGC
(gC/m²/day)
15
10
5
0
-5
J F M A M J J A S O N D
THARANDT: 50°58″N, 13°34″E
TVER: 56°27″N, 32°55″E

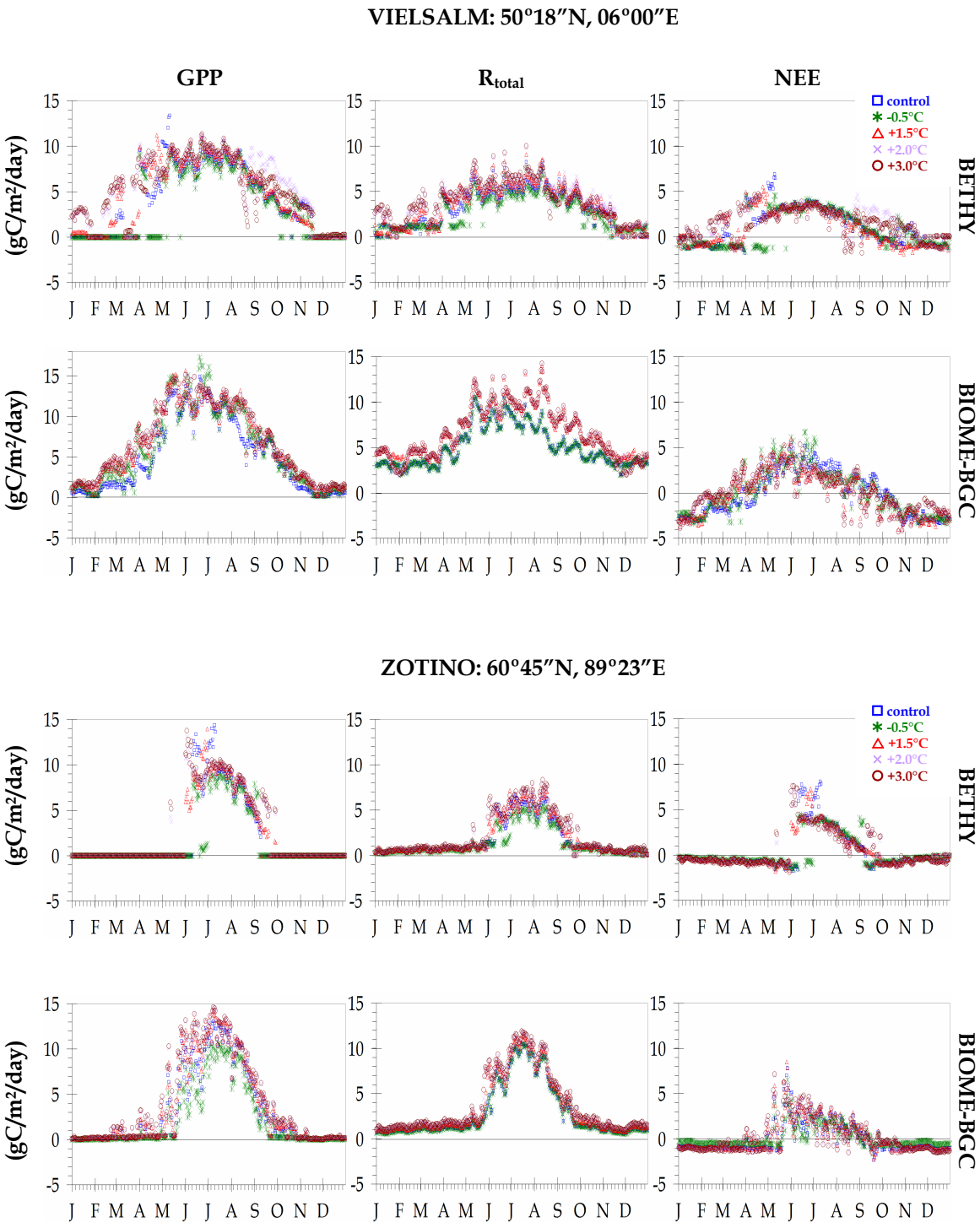
VIELSALM: 50°18″N, 06°00″E
GPP
R_{total}
NEE
control
-0.5°C
+1.5°C
+2.0°C
+3.0°C
(gC/m²/day)
BETHY
BIOME-BGC
J F M A M J J A S O N D
ZOTINO: 60°45″N, 89°23″E

APPENDIX A8

REGIONAL FLUX COMPARISONS AT SELECTED SITES

SIMULATED VERSUS OBSERVED CO_2 FLUXES

SEASONAL CYCLES FOR 1998

(A) Different models, own vegetation maps (Experiments 1, 3, 6):

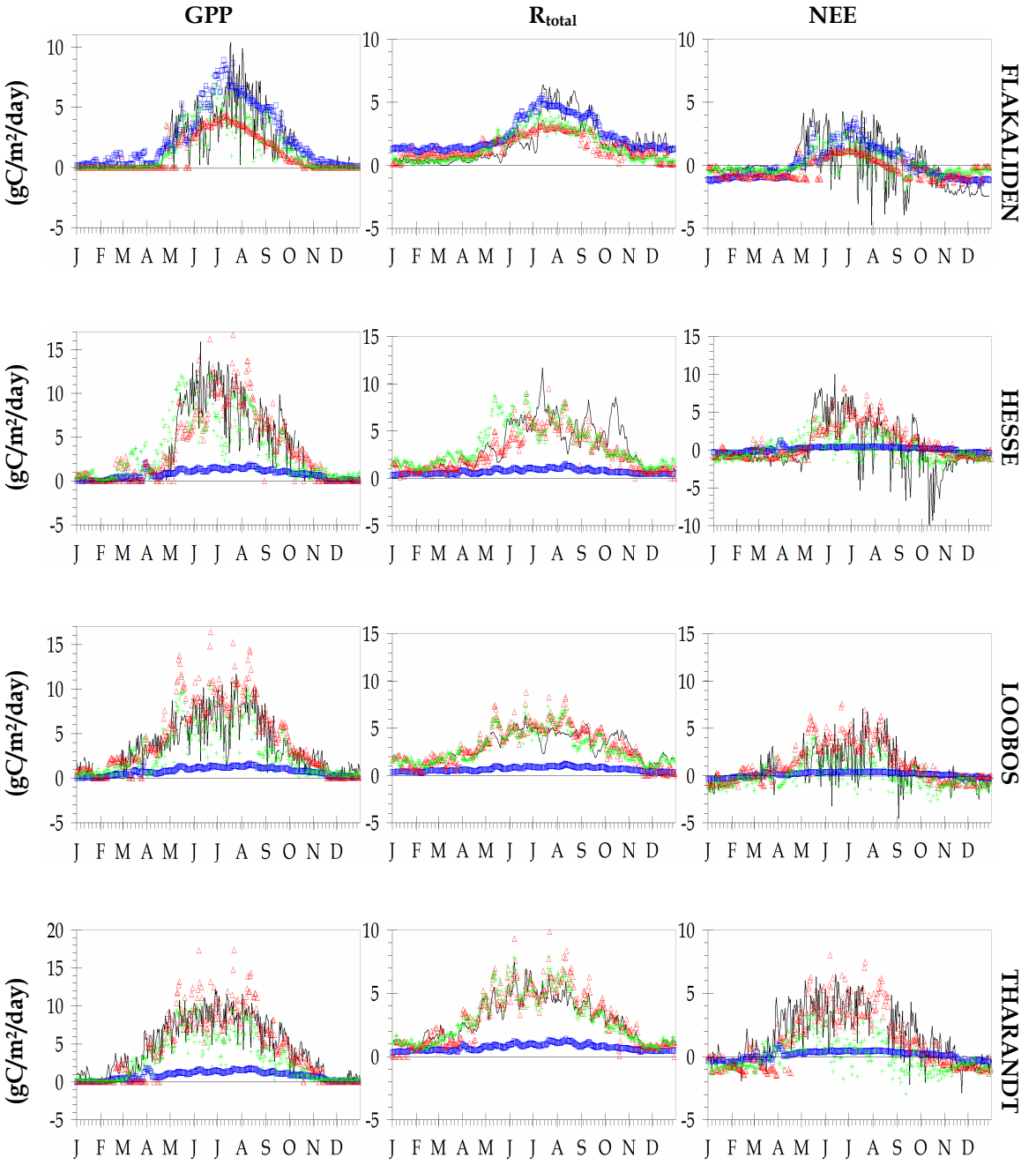

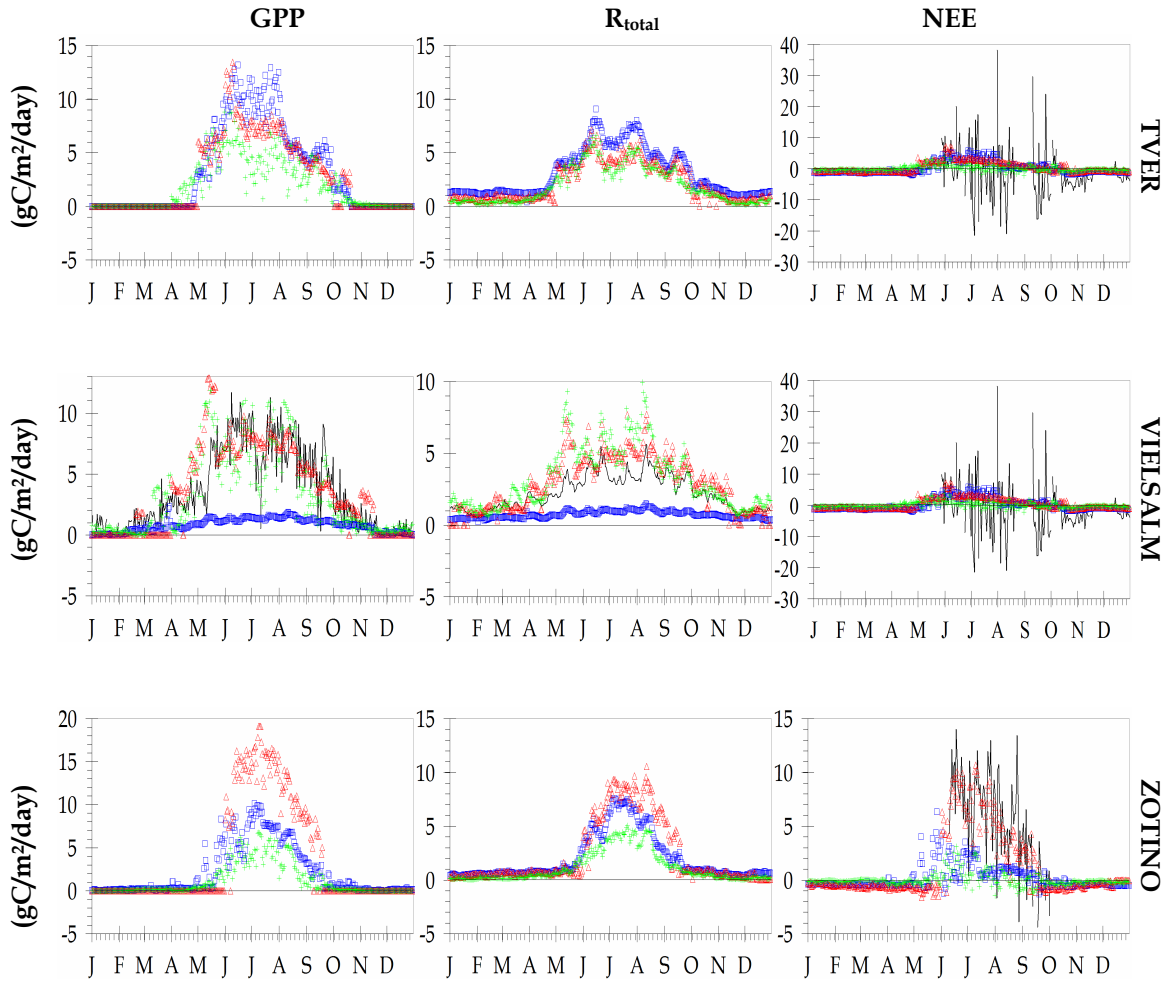
GPP
R_{total}
NEE
(gC/m²/day)
TVER
VIELSALM
ZOTINO
J F M A M J J A S O N D
□ EXPERIMENT 1
Δ EXPERIMENT 3
+ EXPERIMENT 6
– OBSERVATION

(B) Different models, BETHY-derived vegetation map (Experiments 2, 4):

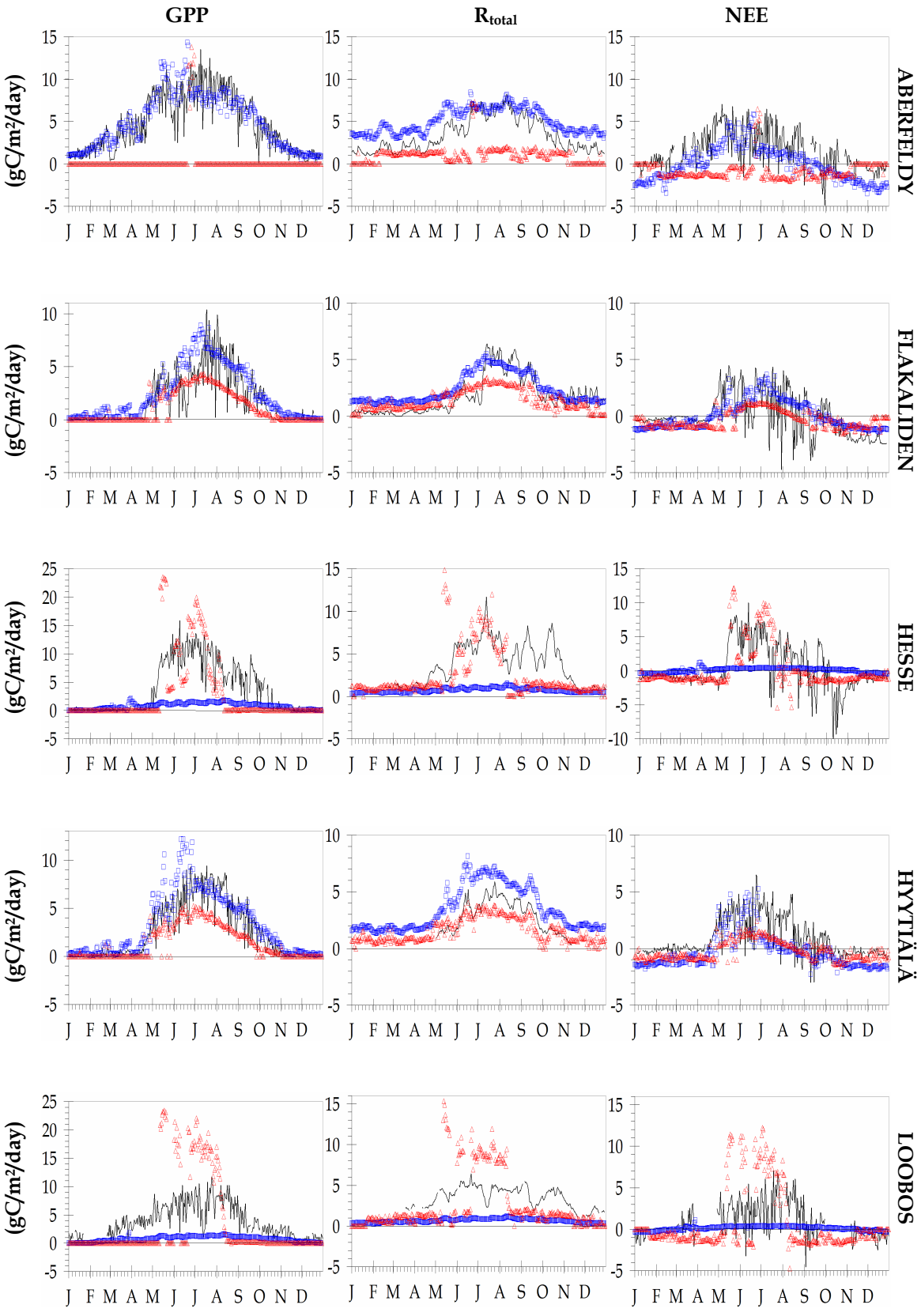

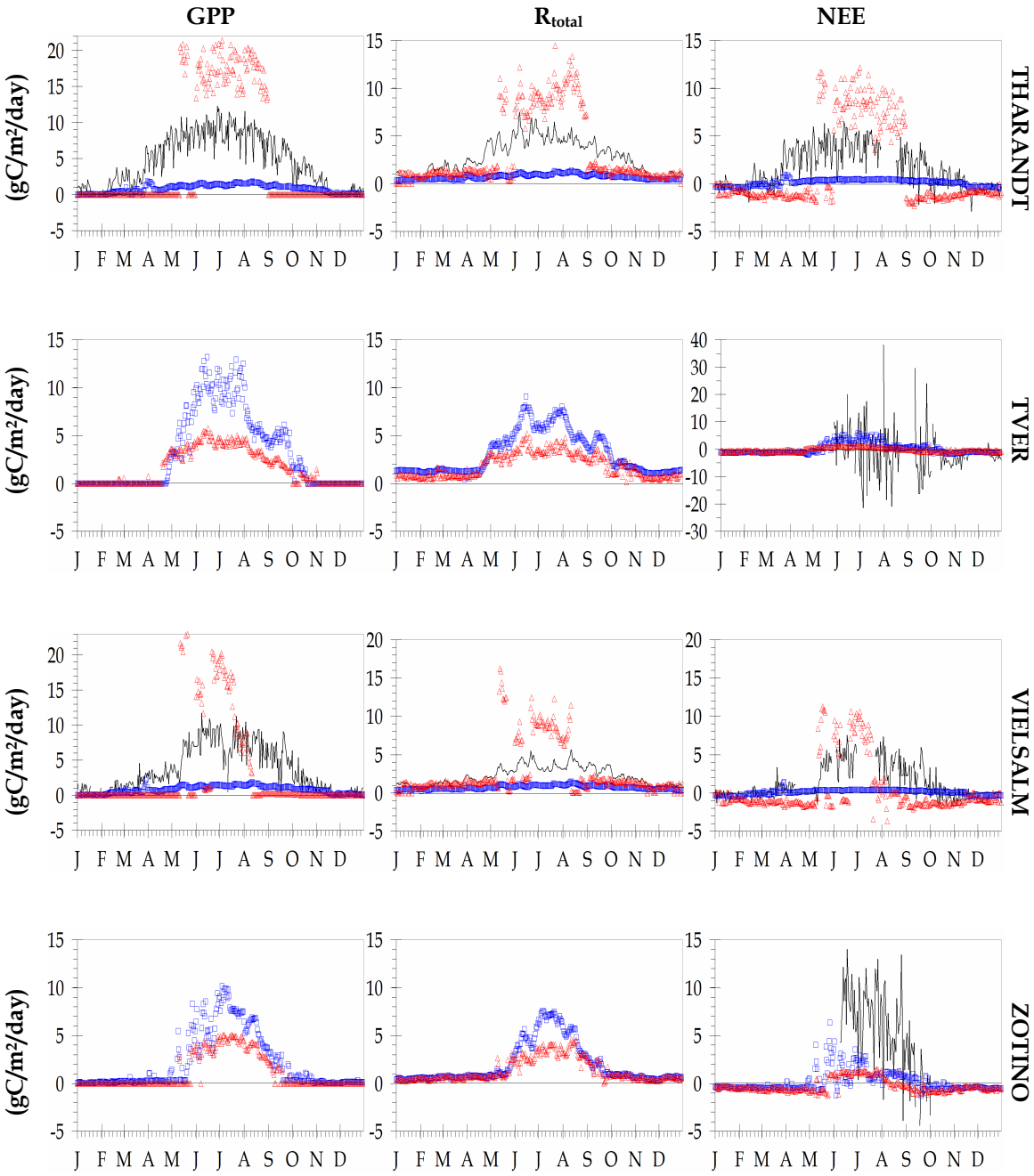
GPP
R_{total}
NEE
(gC/m²/day)
THARANDT
TVER
VIELSALM
ZOTINO
J F M A M J J A S O N D
□ EXPERIMENT 2
Δ EXPERIMENT 4
– OBSERVATION

(C) Different models, BIOME-BGC derived vegetation map (Experiments 1, 5):

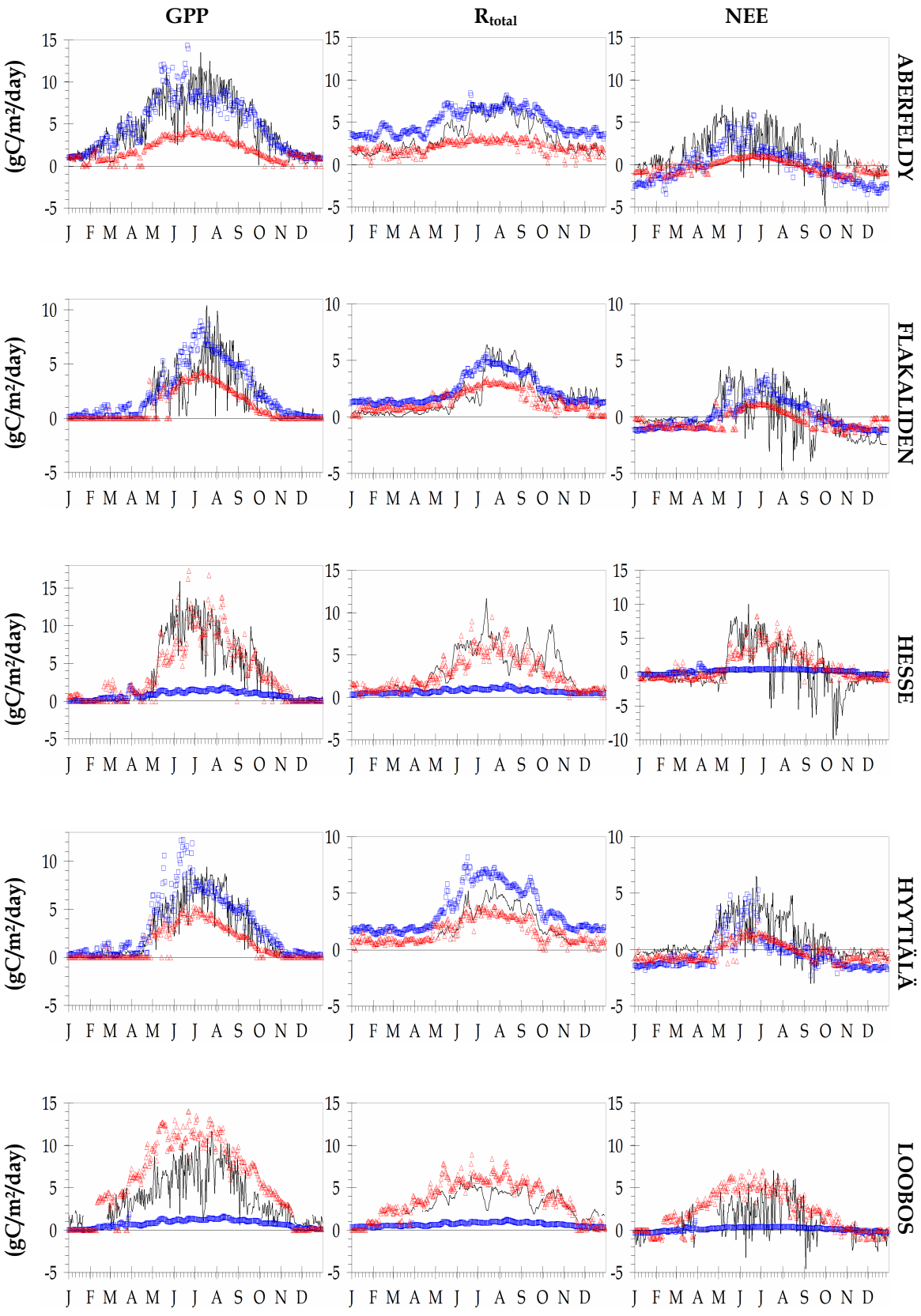

Δ EXPERIMENT 1 □ EXPERIMENT 5 – OBSERVATION

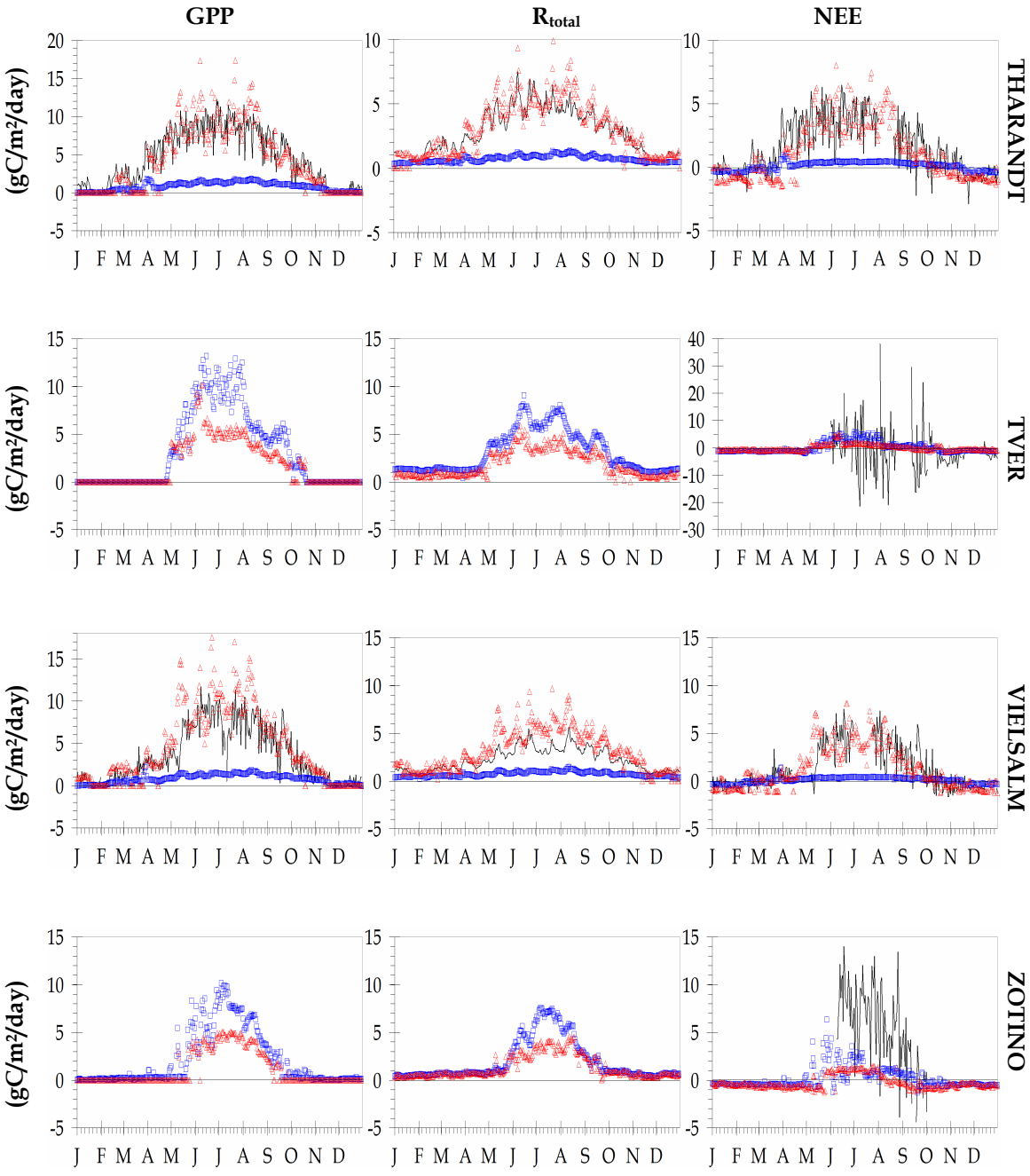
GPP
R_{total}
NEE
(gC/m²/day)
THARANDT
TVER
VIELSALM
ZOTINO
J F M A M J J A S O N D
Δ EXPERIMENT 1
□ EXPERIMENT 5
– OBSERVATION

(D) BETHY simulations with different vegetation maps (Experiments 3, 4, 5):

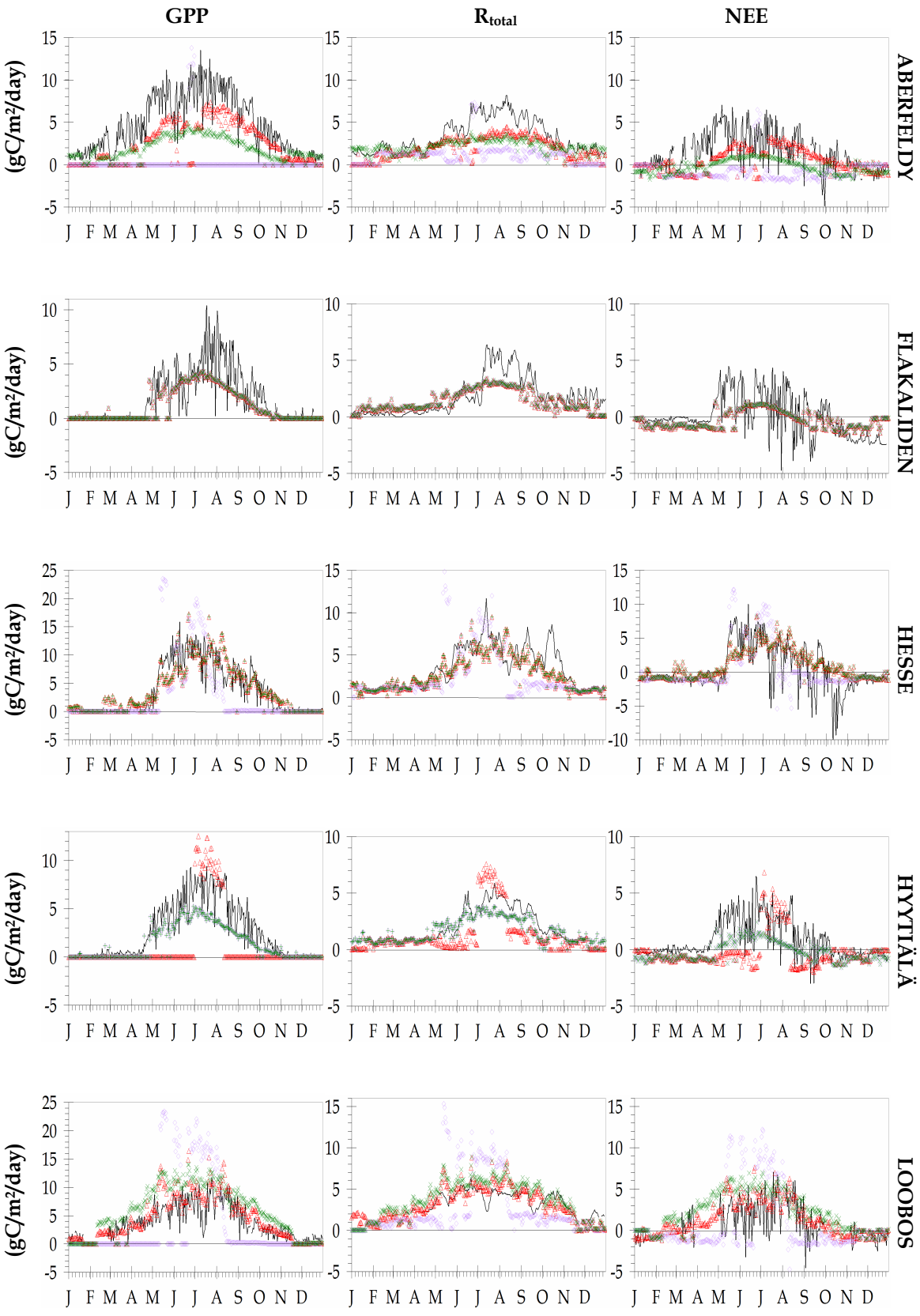

Δ EXPERIMENT 3 ◊ EXPERIMENT 4 × EXPERIMENT 5 – OBSERVATION

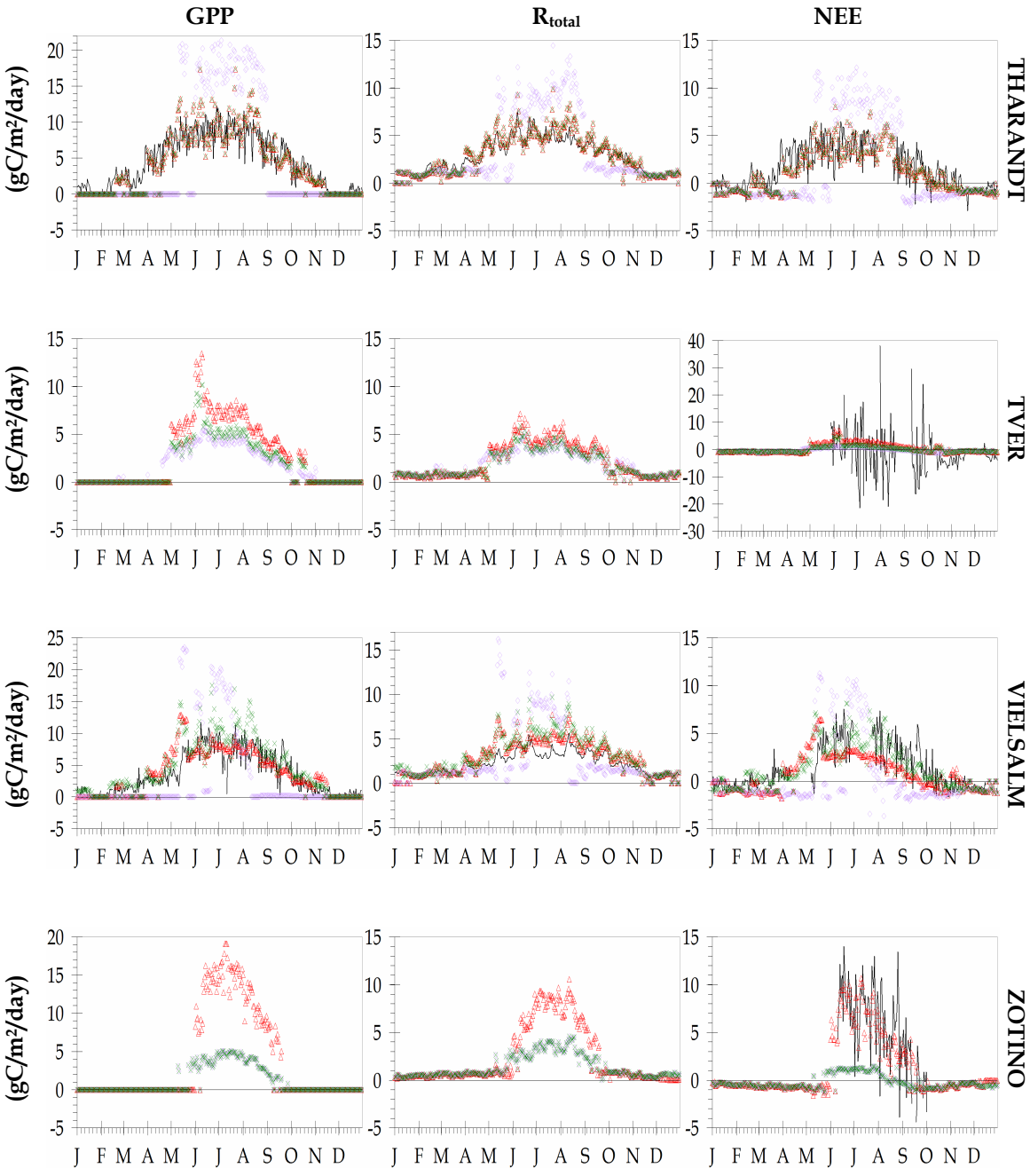
GPP
R_{total}
NEE
(gC/m²/day)
THARANDT
TVER
VIELSALM
ZOTINO
J F M A M J J A S O N D
Δ EXPERIMENT 3
◊ EXPERIMENT 4
× EXPERIMENT 5
– OBSERVATION

(E) BIOME-BGC simulations with different vegetation maps (Experiments 1, 2):

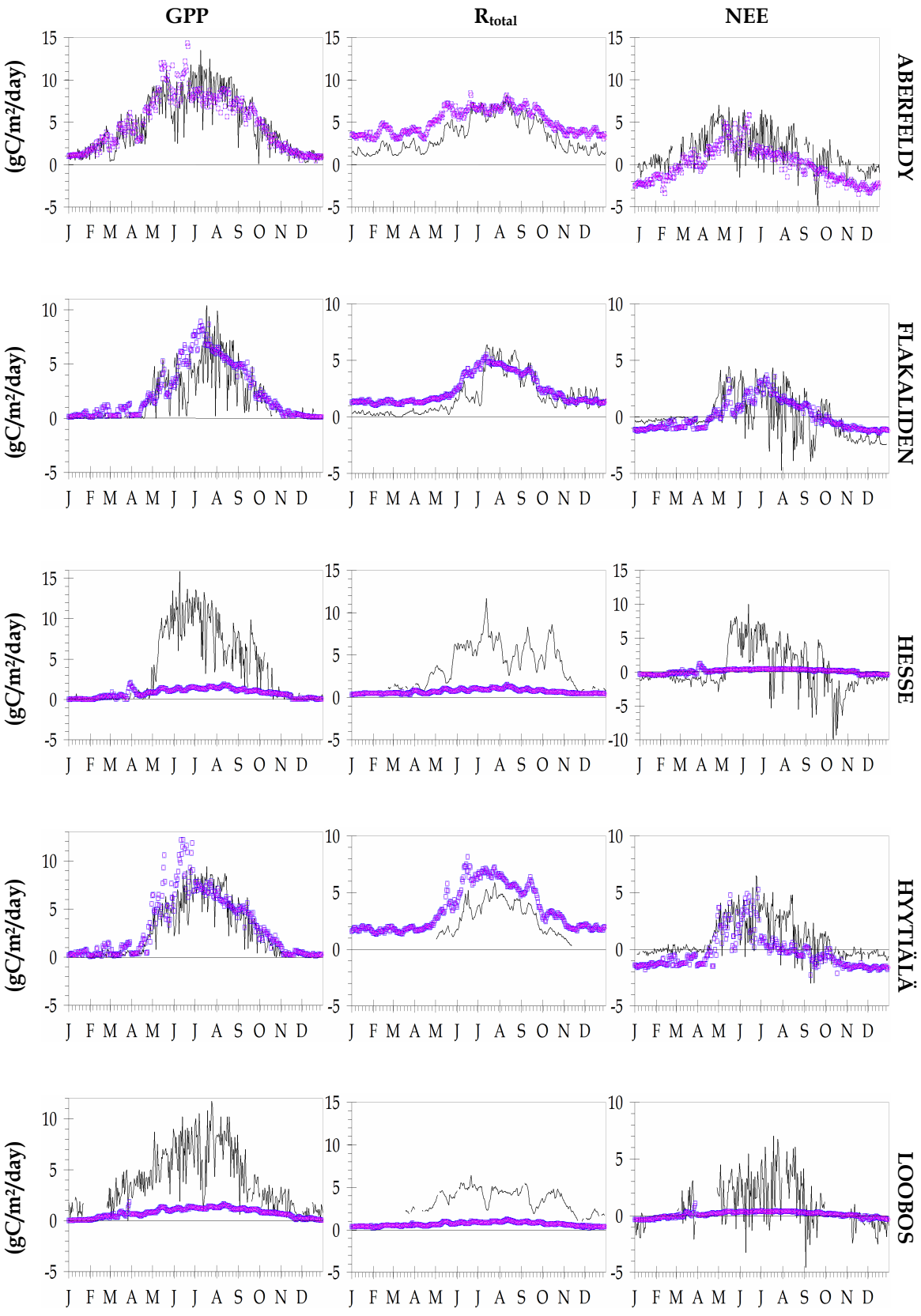

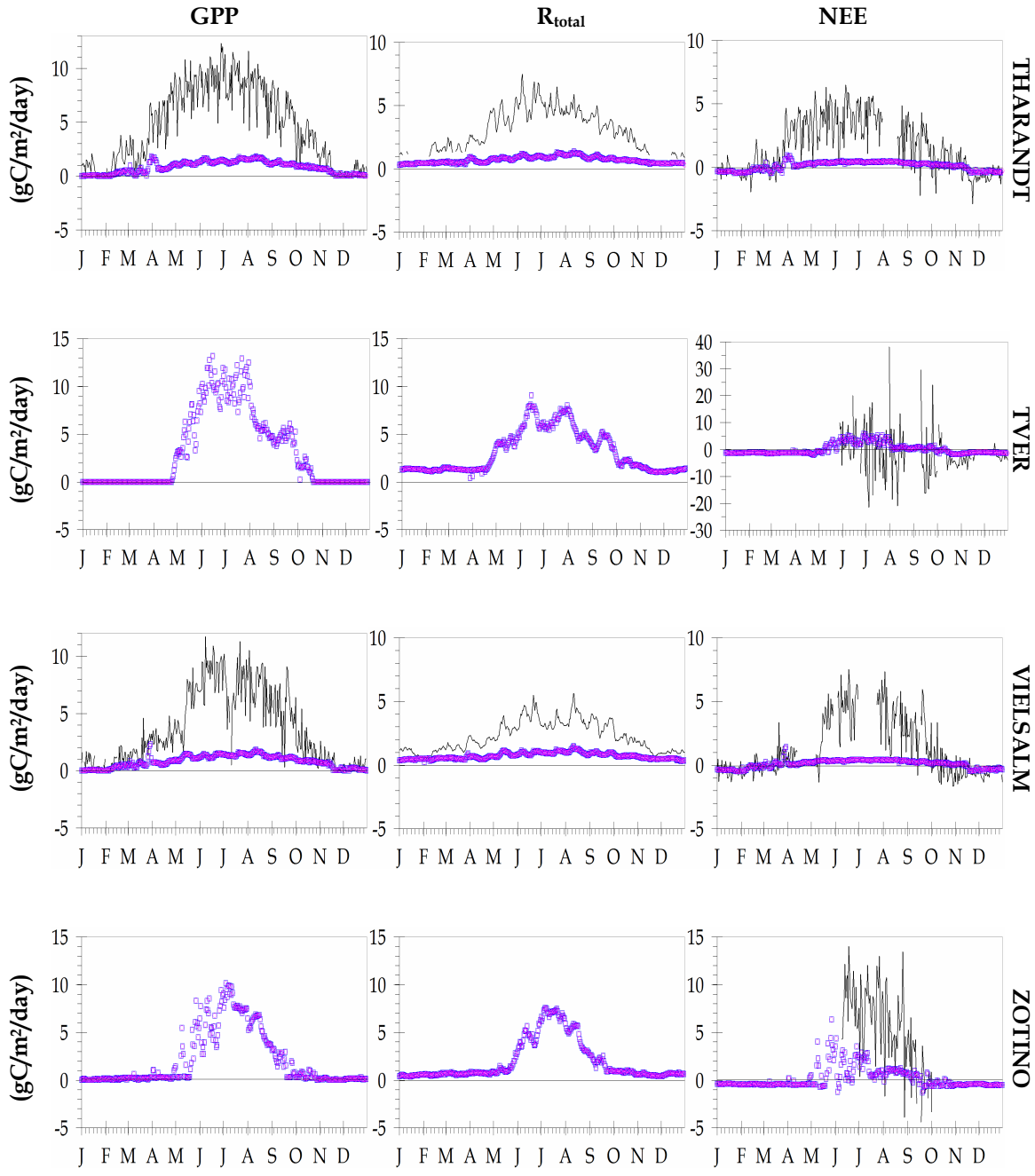
GPP
R_{total}
NEE
(gC/m²/day)
THARANDT
TVER
VIELSALM
ZOTINO
J F M A M J J A S O N D
□ EXPERIMENT 1
o EXPERIMENT 2
– OBSERVATION

APPENDIX A9

REGIONAL ATMOSPHERIC CO_2 COMPARISONS AT SELECTED SITES

SIMULATED VERSUS OBSERVED ATMOSPHERIC CO_2

SEASONAL CYCLES FOR 1998

(A) Biosphere flux inputs from different models using own vegetation maps (Experiments 1, 3, 6):

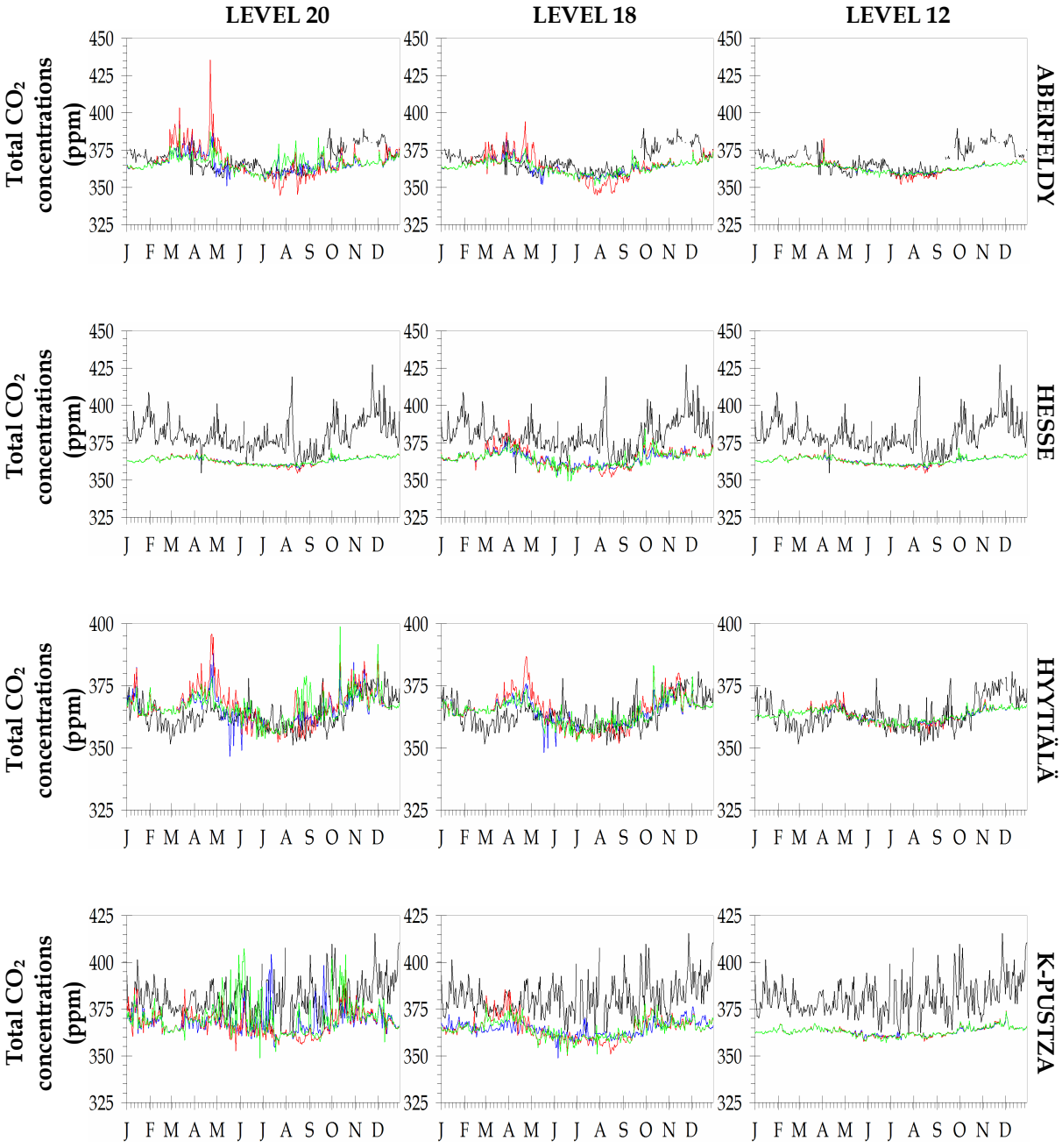

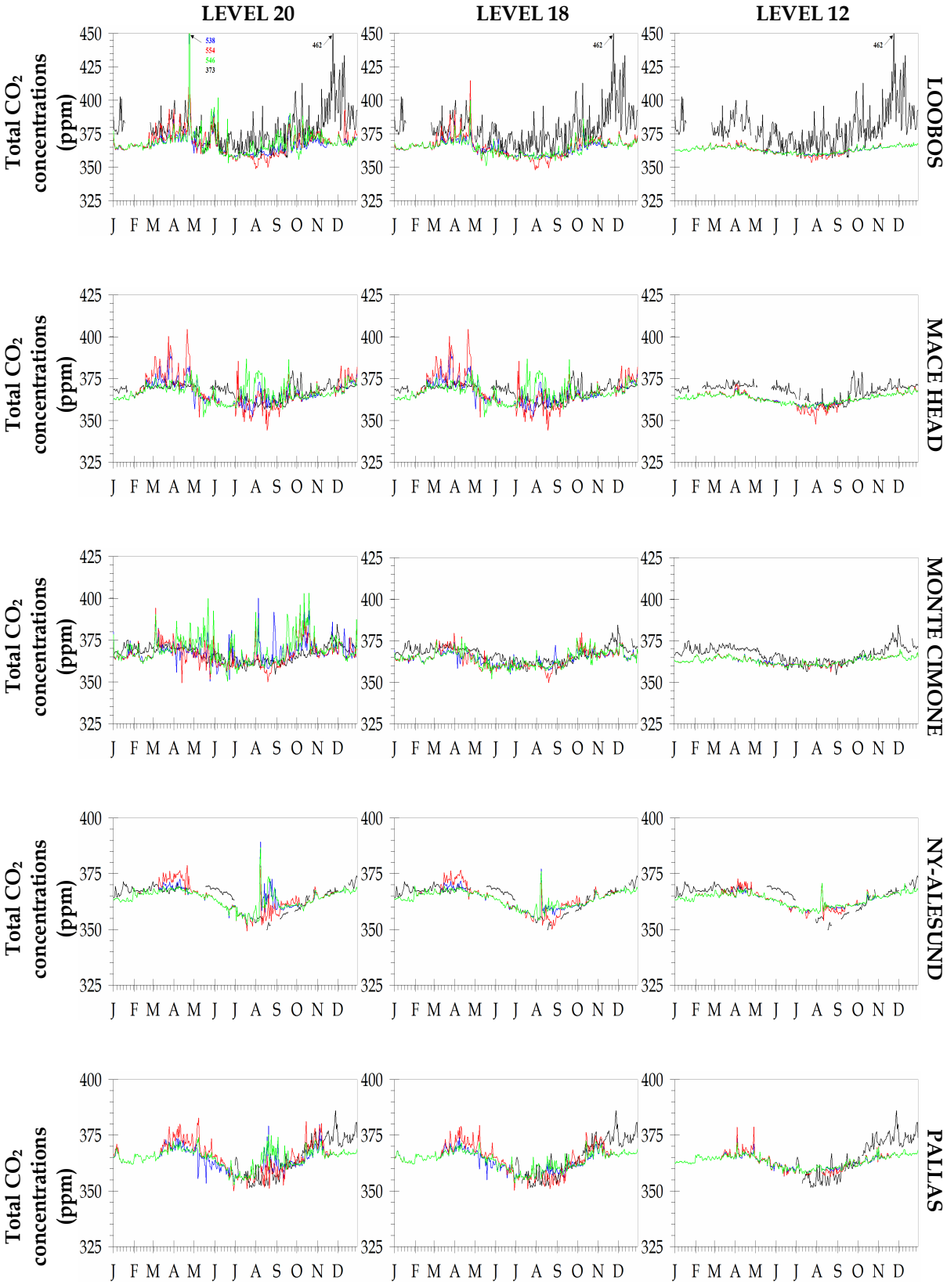

EXPERIMENT 1 EXPERIMENT 3 EXPERIMENT 6 OBSERVATION

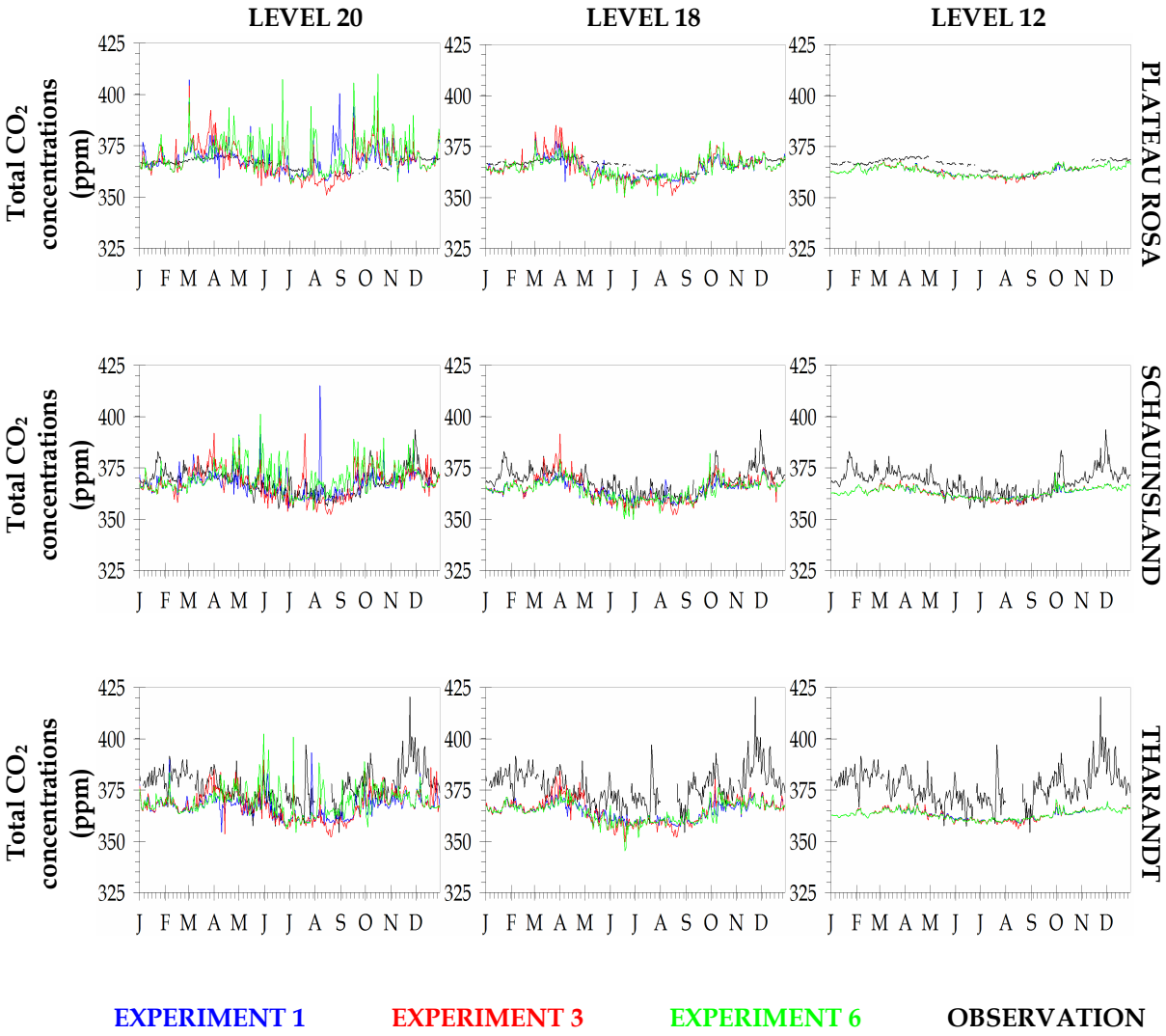
LEVEL 20
LEVEL 18
LEVEL 12
Total CO_2 concentrations (ppm)
425
400
375
350
325
J F M A M J J A S O N D
PLATEAU ROSA
SCHAUINSLAND
THARANDT
EXPERIMENT 1
EXPERIMENT 3
EXPERIMENT 6
OBSERVATION

(B) Biosphere flux inputs from different models using BETHY-derived vegetation map (Experiments 2, 4):

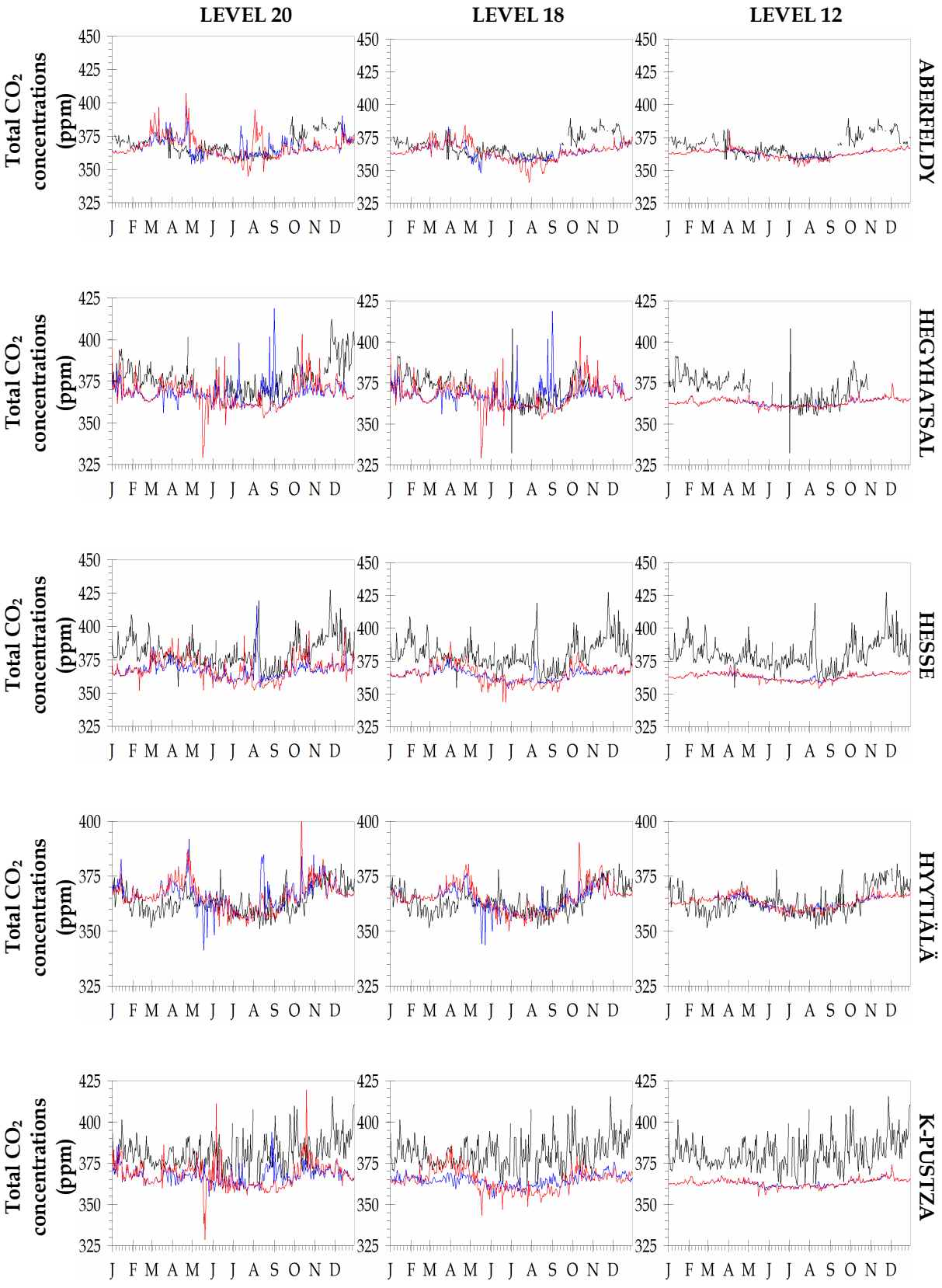

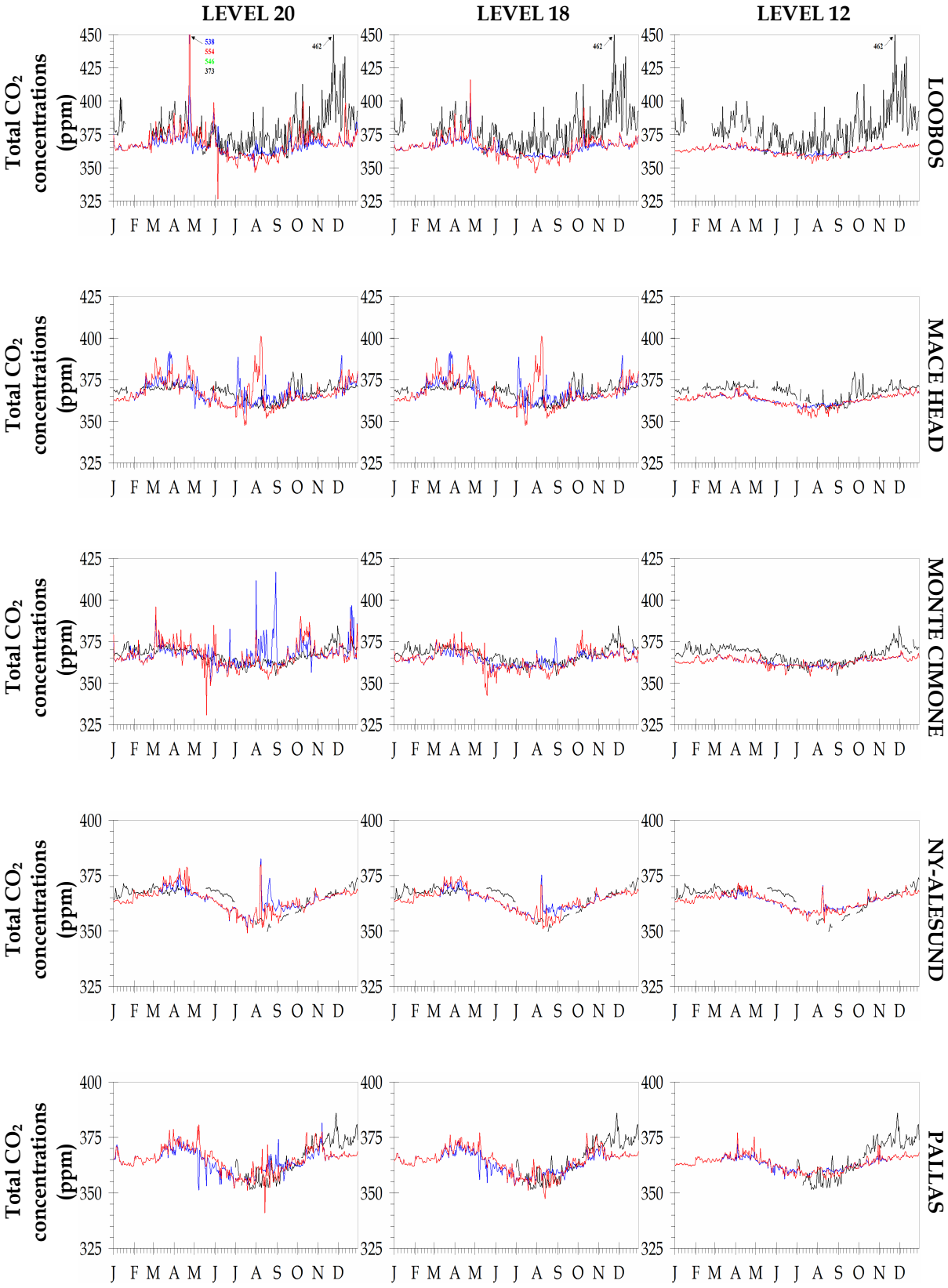

EXPERIMENT 2 EXPERIMENT 4 OBSERVATION

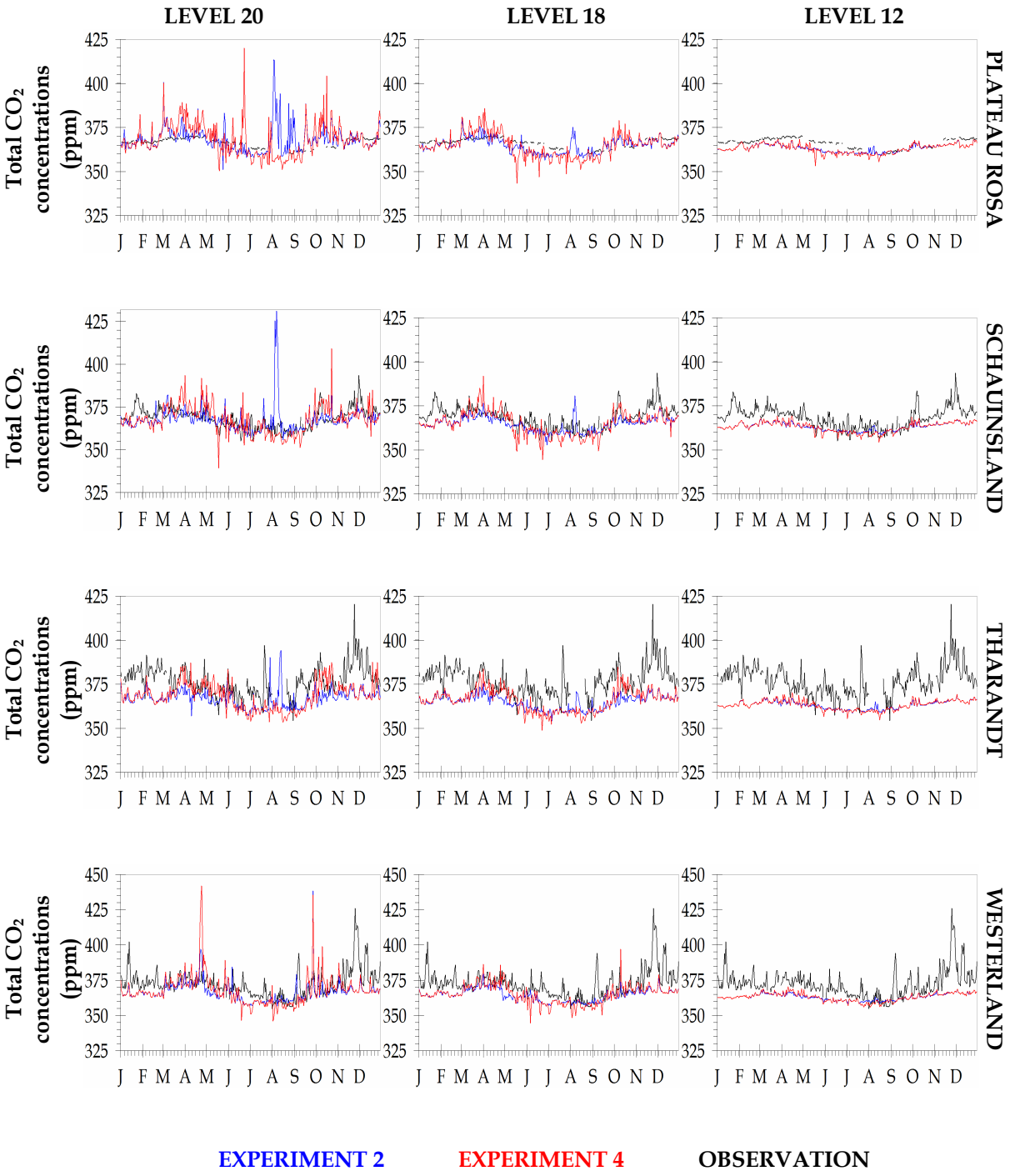
LEVEL 20
LEVEL 18
LEVEL 12
Total CO_2 concentrations (ppm)
PLATEAU ROSA
SCHAUINSLAND
THARANDT
WESTERLAND
425
400
375
350
325
450
J F M A M J J A S O N D
EXPERIMENT 2
EXPERIMENT 4
OBSERVATION

(C) Biosphere flux inputs from different models using BIOME-BGC derived vegetation map (Experiments 1, 5):

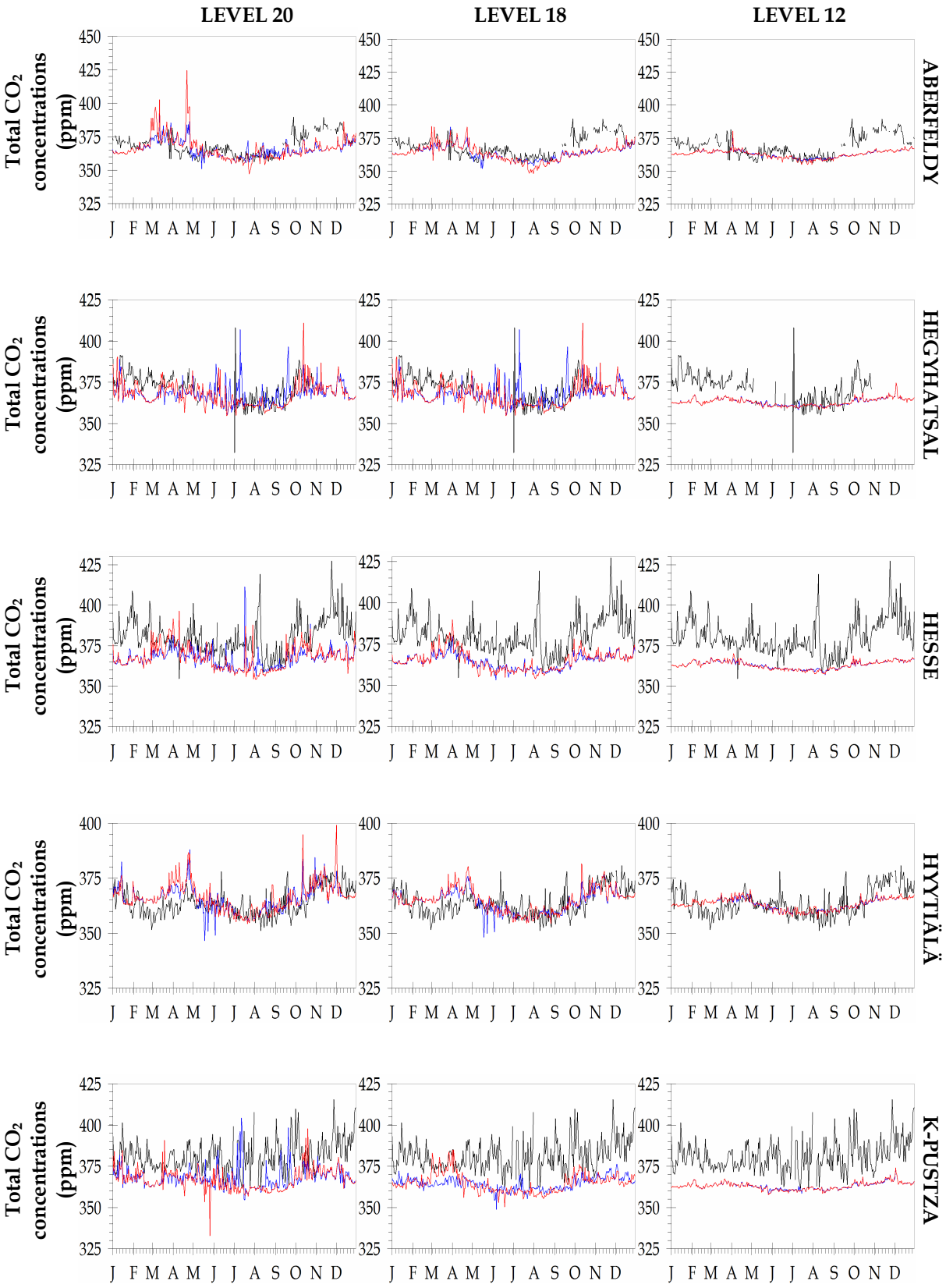

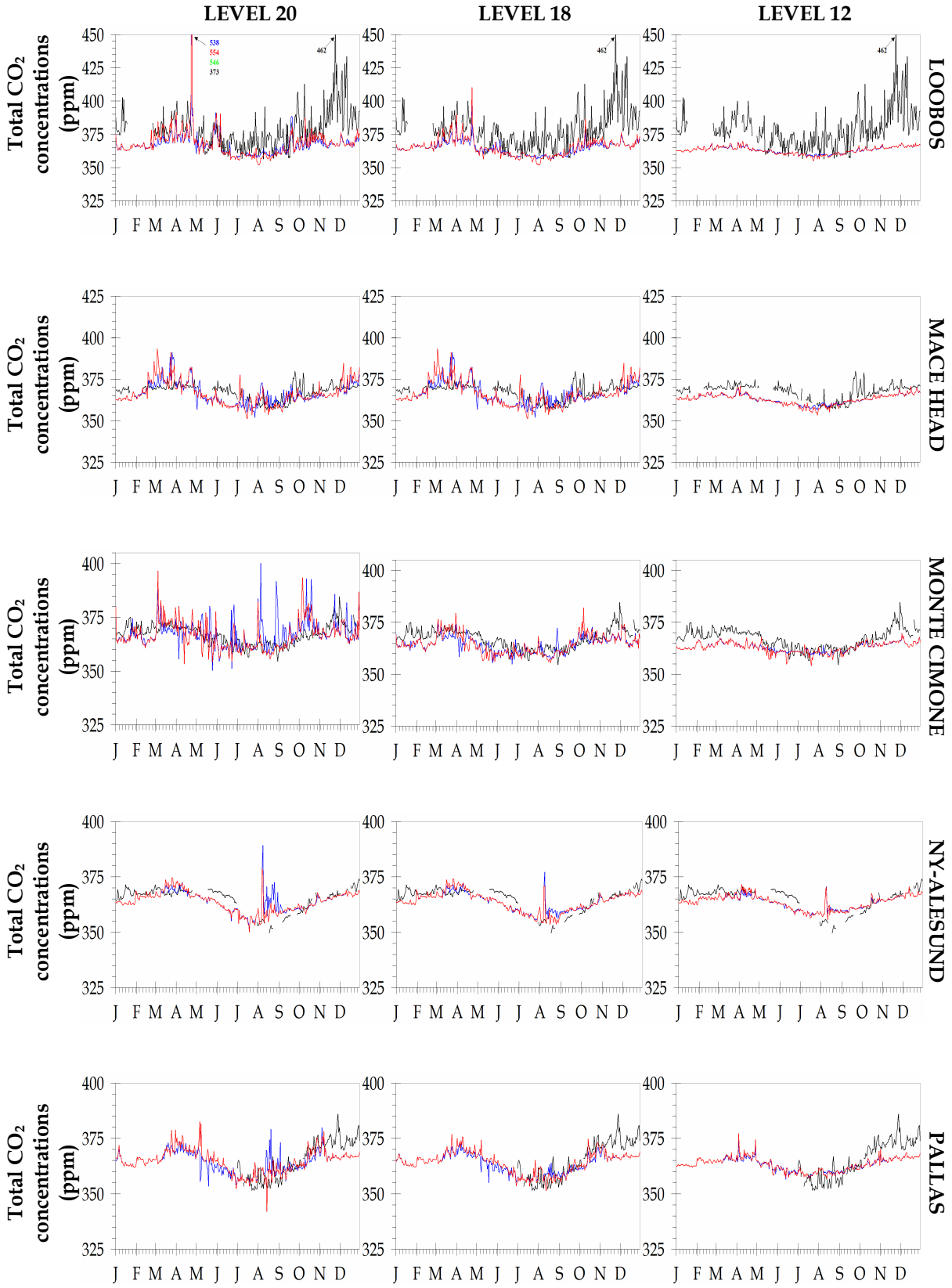
LEVEL 20
LEVEL 18
LEVEL 12
Total CO_2 concentrations (ppm)
LOOBOS
MACE HEAD
MONTE CIMONE
NY-ALESUND
PALLAS
J F M A M J J A S O N D
EXPERIMENT 1
EXPERIMENT 5
OBSERVATION

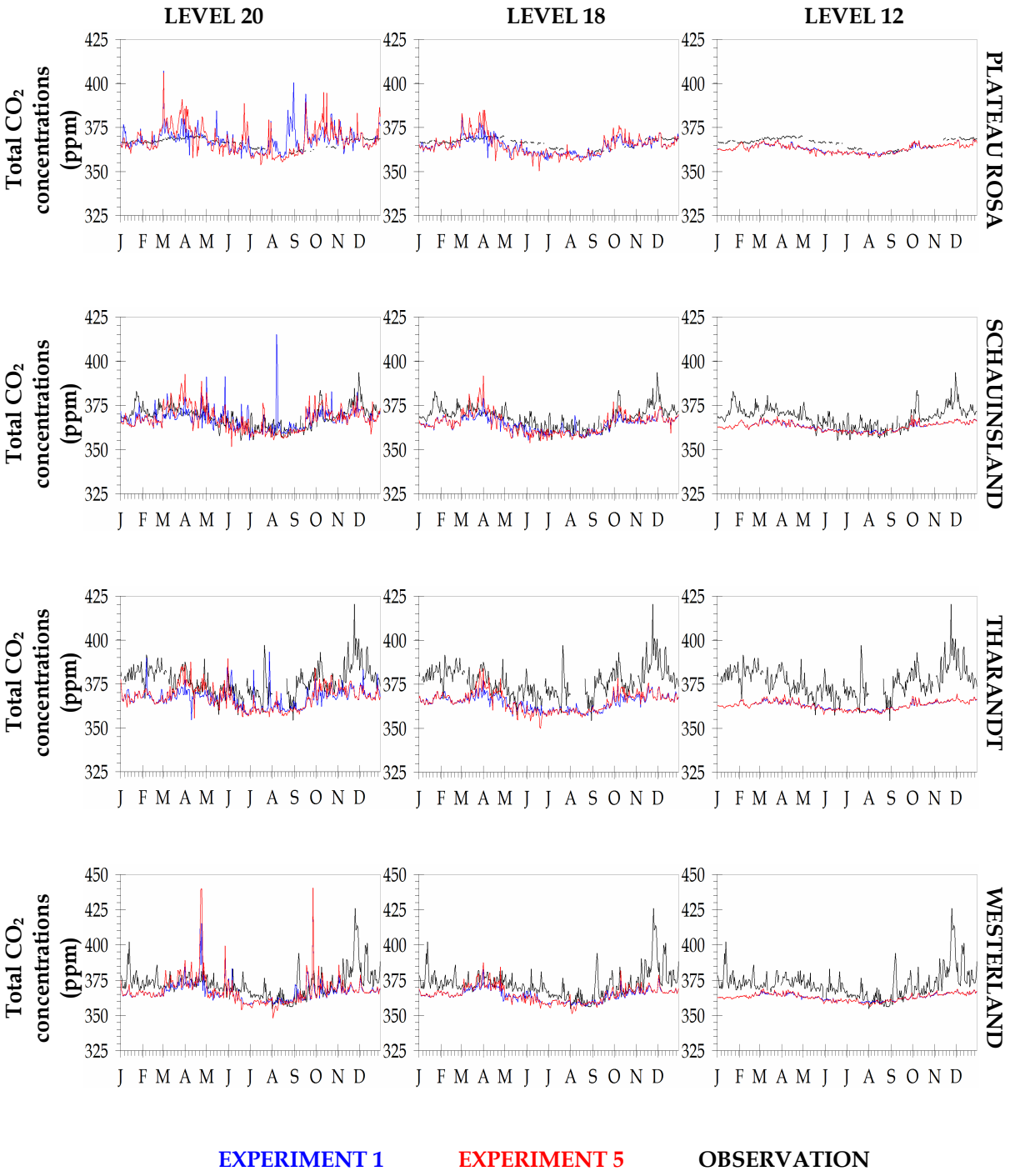
LEVEL 20
LEVEL 18
LEVEL 12
Total CO_2 concentrations (ppm)
PLATEAU ROSA
SCHAUINSLAND
THARANDT
WESTERLAND
425
400
375
350
325
450
J F M A M J J A S O N D
EXPERIMENT 1
EXPERIMENT 5
OBSERVATION

(D) Biosphere flux inputs from BETHY model using different vegetation maps (Experiments 3, 4, 5):

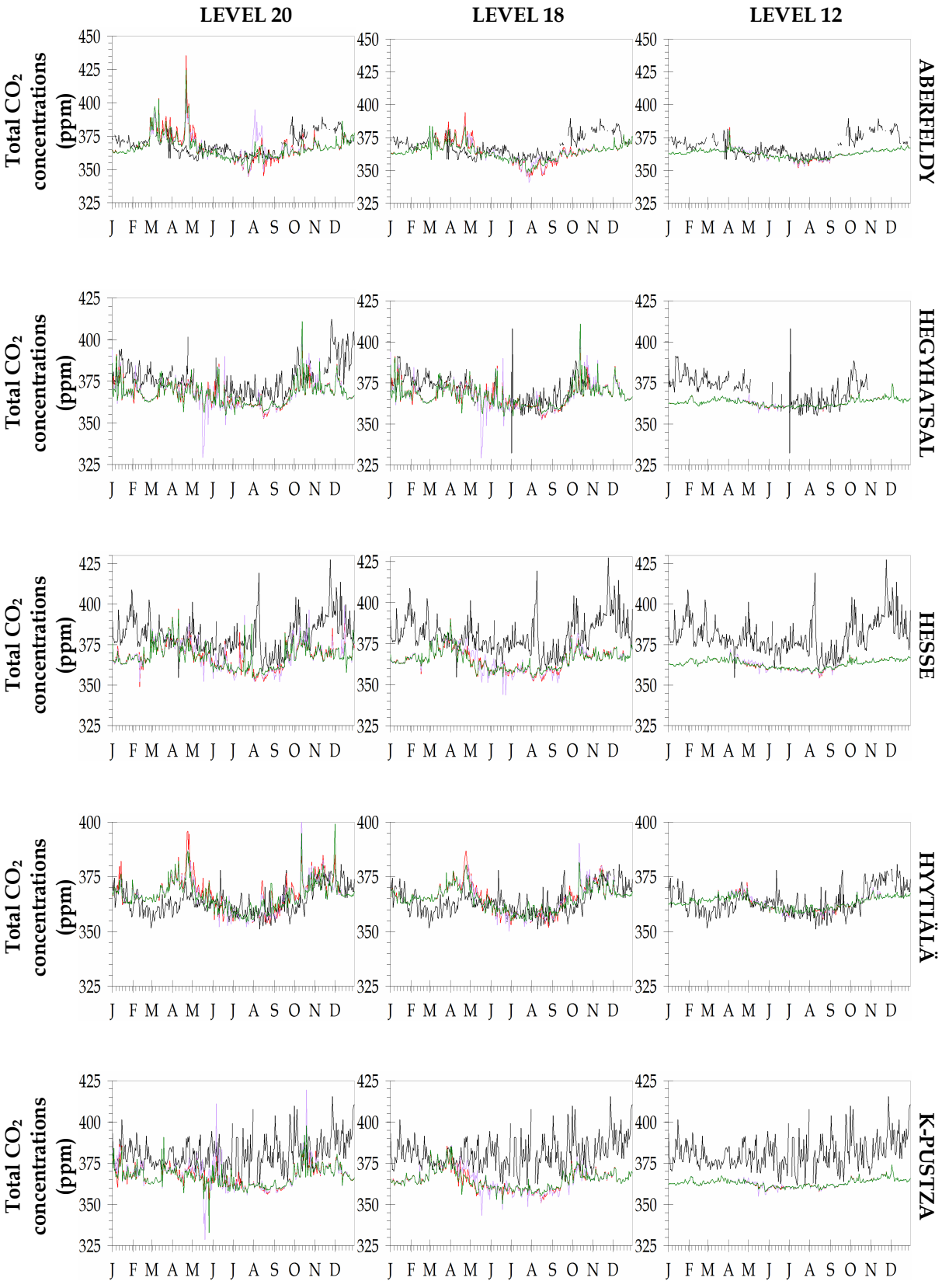

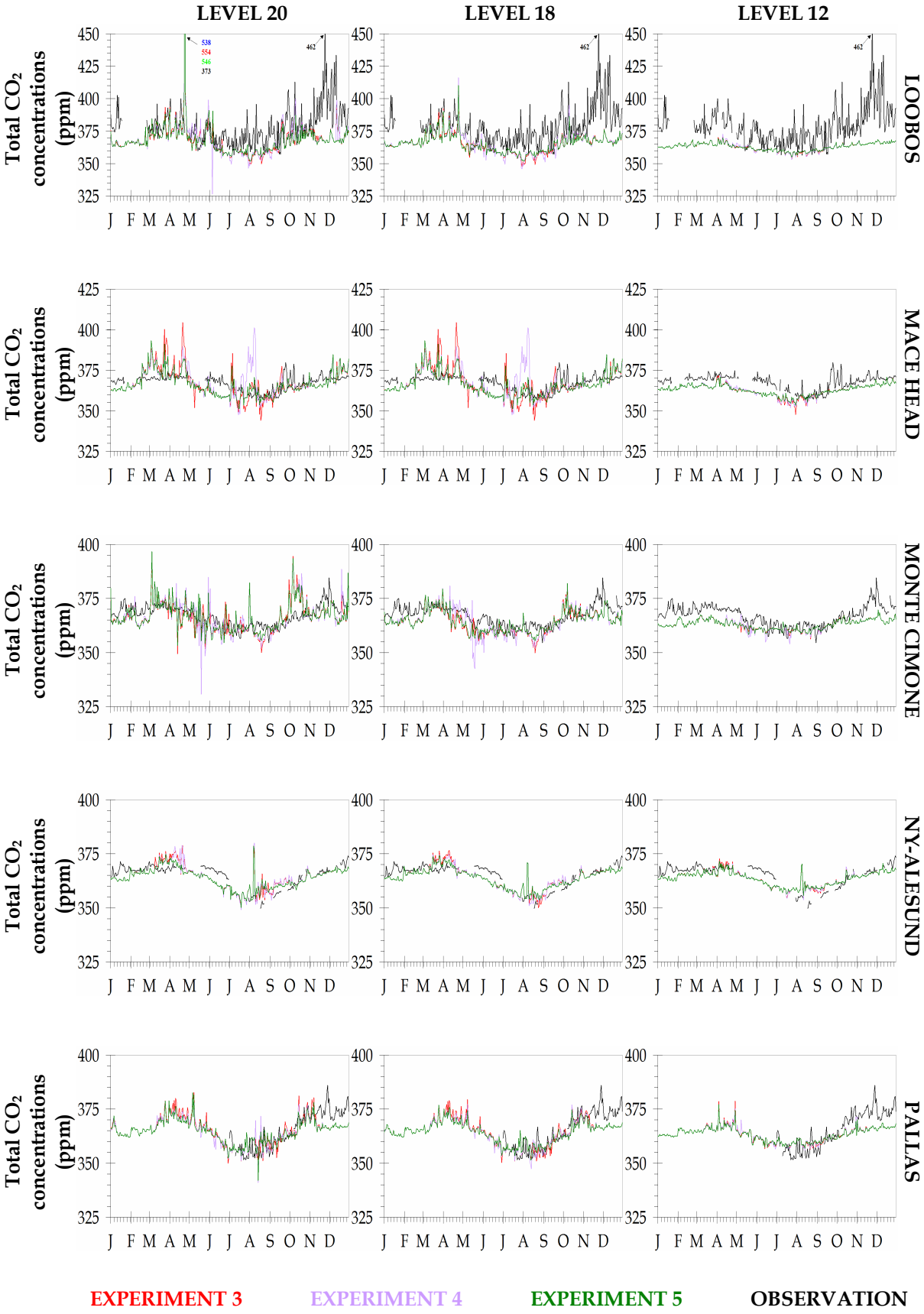
LEVEL 20
LEVEL 18
LEVEL 12
Total CO2 concentrations (ppm)
LOOBOS
MACE HEAD
MONTE CIMONE
NY-ALESUND
PALLAS
J F M A M J J A S O N D
EXPERIMENT 3
EXPERIMENT 4
EXPERIMENT 5
OBSERVATION

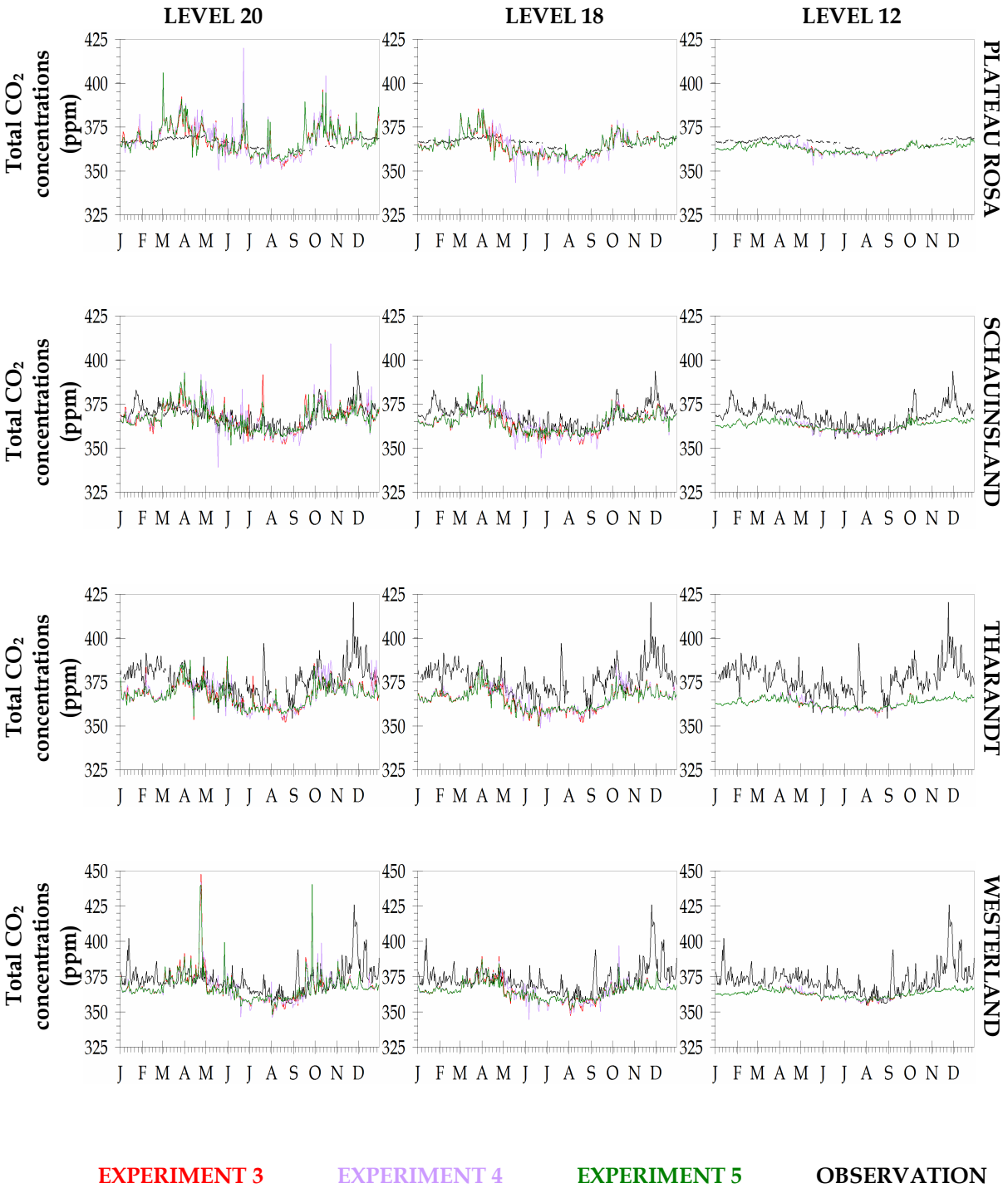
LEVEL 20
LEVEL 18
LEVEL 12
Total CO_2 concentrations (ppm)
PLATEAU ROSA
SCHAUINSLAND
THARANDT
WESTERLAND
425
400
375
350
325
450
J F M A M J J A S O N D
EXPERIMENT 3
EXPERIMENT 4
EXPERIMENT 5
OBSERVATION

(E) Biosphere flux inputs from BIOME-BGC model using different vegetation maps (Experiments 1, 2):

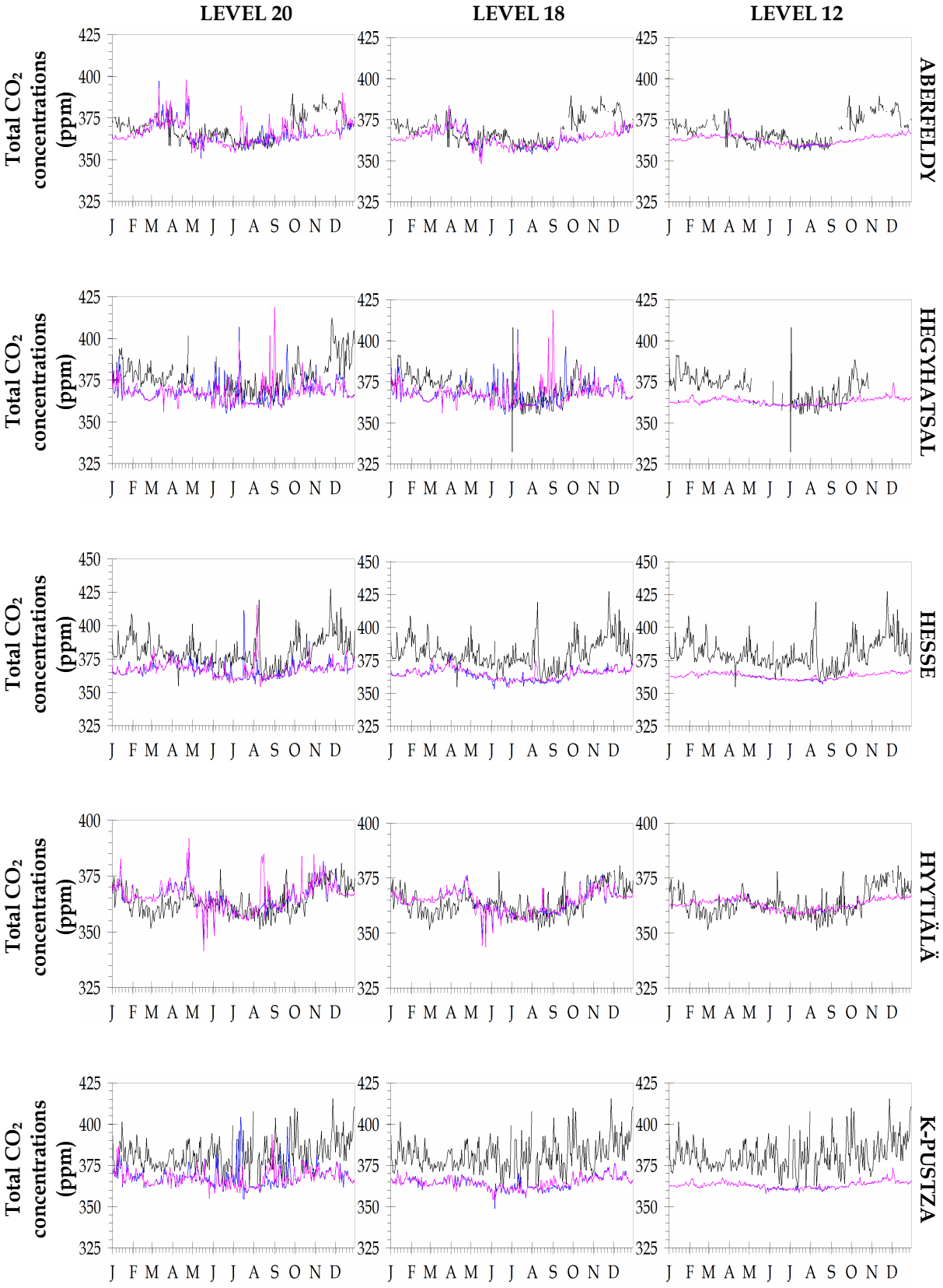

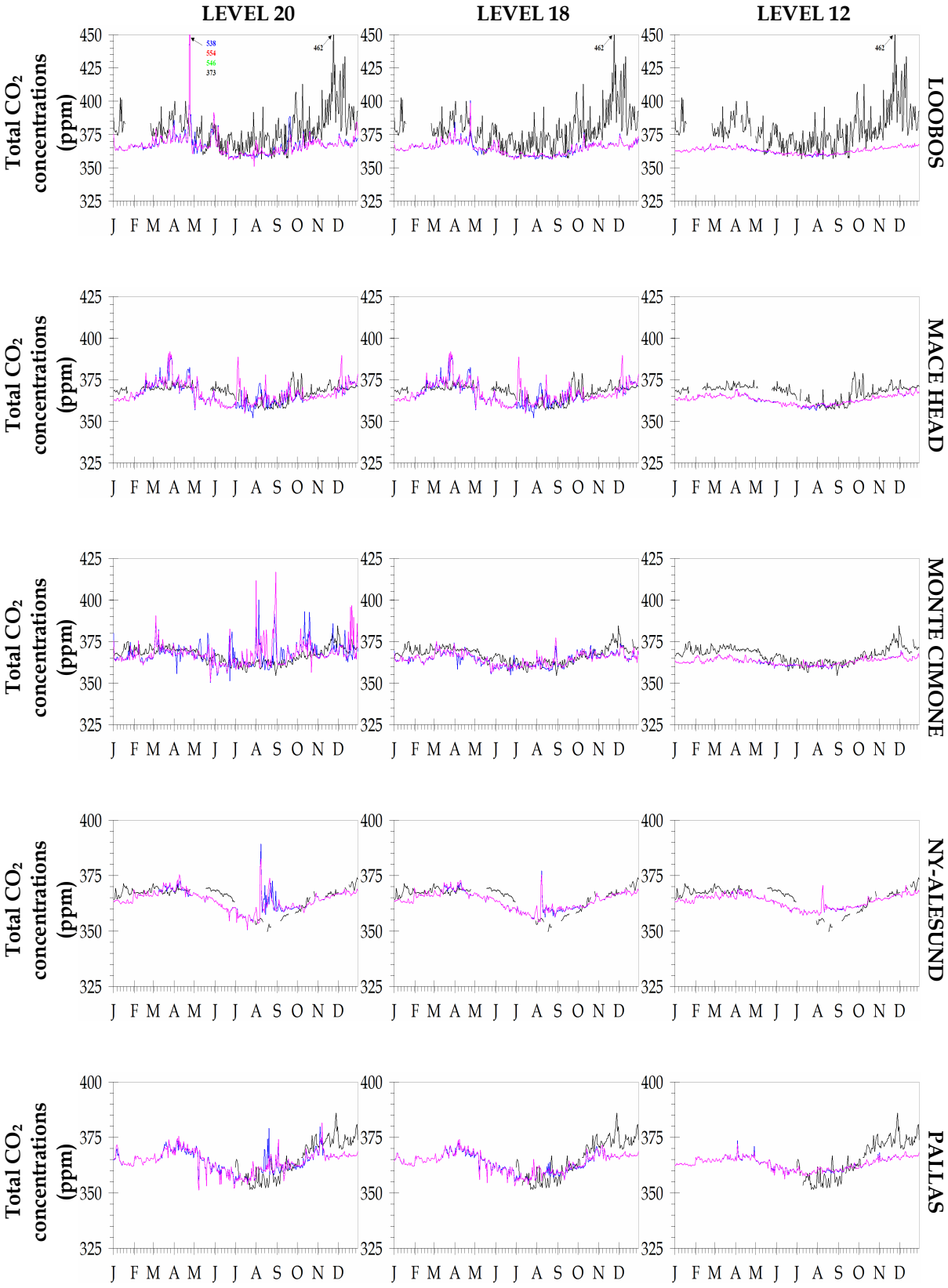

EXPERIMENT 1 **EXPERIMENT 2** **OBSERVATION**

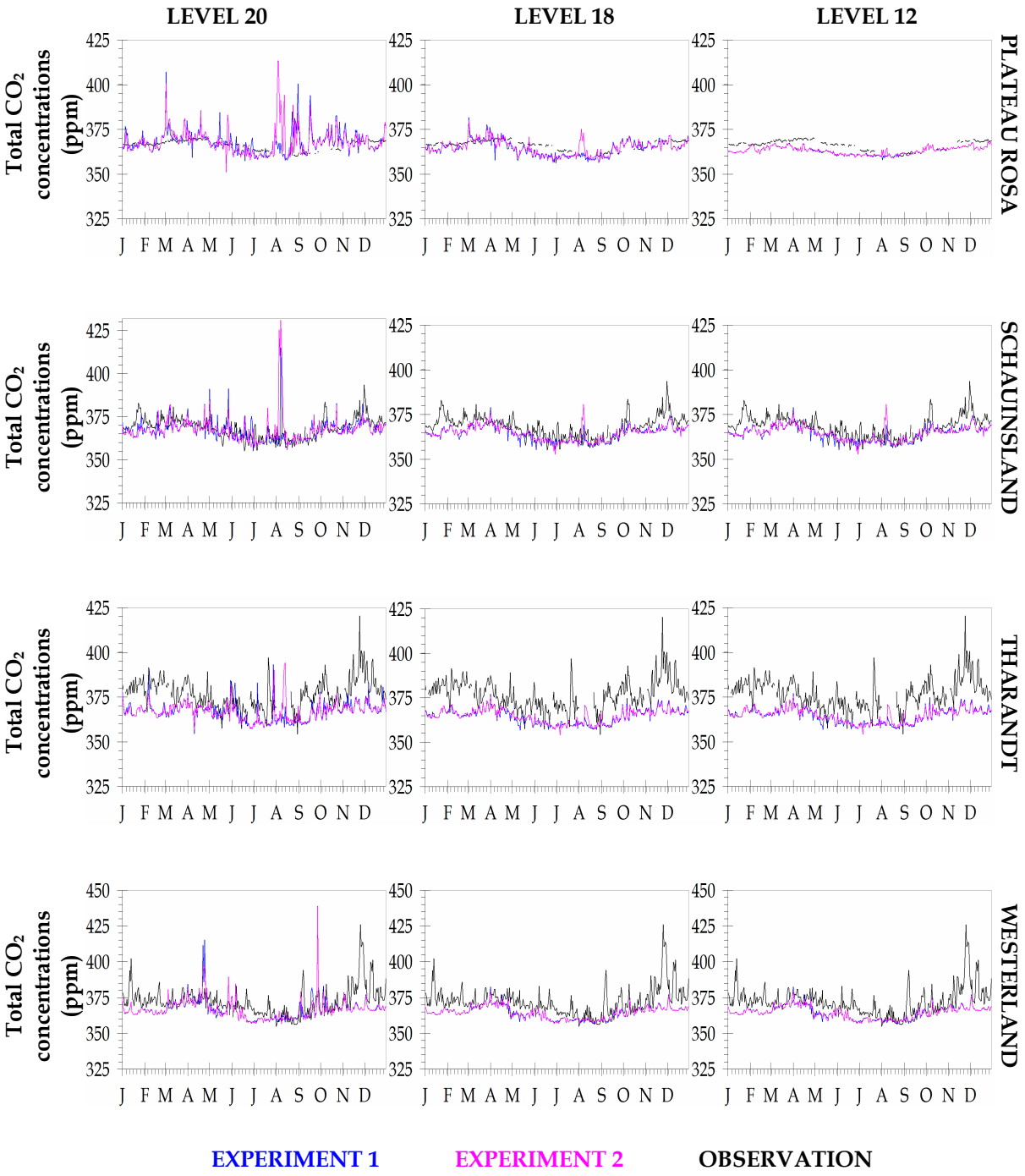
LEVEL 20
LEVEL 18
LEVEL 12
Total CO_2 concentrations (ppm)
PLATEAU ROSA
SCHAUINSLAND
THARANDT
WESTERLAND
425
400
375
350
325
450
J F M A M J J A S O N D
EXPERIMENT 1
EXPERIMENT 2
OBSERVATION

ACKNOWLEDGEMENT

I would like to thank the International Max Planck Research School on Earth System Modelling, and The Max-Planck-Institute for Meteorology for giving me the opportunity to carry out my PhD studies. I thank the ZEIT Stiftung Ebelin und Gerd Bucerius and the Max-Planck-Institute for Meteorology for funding my research work.

My heartfelt gratitude to Professor Martin Heimann from the Max Planck Institute for Biogeochemistry, Jena for the initial ideas and directions for my work. I thank the members of the REMO Group for getting me started at the Institute. A special thanks to the Land Vegetation Group (former group of Dr. Wolfgang Knorr), in particular to Dr. Heiner Widmann for his continued assistance and guidance with the technicalities of biosphere modelling with the BETHY model, and Dr. Thomas Raddatz for statistical and data handling discussions. My very special thanks to Dr. Christian Reick for the continued support, fruitful discussions and useful criticisms in shaping up my work. My gratitude also to Dr. Ute Karstens for her patience and encouragement, especially in dealing with the transport modelling. I greatly acknowledge the help, scientific advices and discussions with Dr. Galina Churkina and for her timely responses to my questions. I sincerely thank my panel members (Dr. Christian Reick, Dr. Galina Churkina and Dr. Ute Karstens) and panel chair, Professor Guy P. Brasseur, for the critical review of my work, both written and

experimental, and for directing me in producing a scientifically viable piece of work. Many thanks to Dr. Galina Churkina, Kristina Trusilova, and Dr. Xu-Ri Xing for their help with the BIOME-BGC model.

Furthermore, I express my gratitude to the CIS Group for the most vital part during my work – keeping my computer alive and in functional order, and when needed, retrieving and saving my work. I thank them for their punctuality and willingness to help. My deep appreciation also to the administration, in particular to Frau Hanna Stadelhofer, for the tremendous help on my arrival in Hamburg. Thanks to Frau Birgit Paulsen and Herrn Reiner Letscher for looking after the financial matters throughout my stay at the Institute. My special thanks to all at the Geschäftszimmer for the friendly services I received.

My special thanks to my family for all the support and encouragement in absentia, from my homeland. I deeply appreciate the moral support I received from the Dankers Family. Thanks also to my friends at the Institute for the enjoyable company, especially to Sven, Tido, Stefan, Diana, Katharina and Ralf Diener. Thanks to Jürgen for always helping me out with the shell scripts and for always being there whenever I was in desperate need. My very special thanks to Yuan for the wonderful company over the years, which I enjoyed very much. I will not forget my deepest gratitude to Manik and Richa for letting me use their flat during the final stage of my work, hence saving me valuable time from travelling. My very special thanks and sincere appreciation for the wonderful and enjoyable company of Gerhard during my stay in Hamburg. Thank you very much indeed. "Vinakavakalevu" to Alex and "Big" Thomas for the much-needed distractions and "relaxing" moments, and for the wee bit of opportunity to reminisce about life in the homeland. I will miss our movie nights and the

spinach pizza. I shall patiently wait for the next Ice Age to come by! I will not forget the pleasant company of "Pilot" Thomas and Frauke during our occasional outings.

This thesis would not have come to be without the special support and encouragement from Rutger. I cannot thank enough for the guidance and tremendous help you have provided. My deepest gratitude to you for your calm and thoughtful nature and for the understanding you showed, for your subtle advices, for putting up with me, and for handling me questioning my own work. Thank you for all that you have been and for all the support, both in your presence and in absence. I dedicate this work to you.

Publikationsreihe des MPI-M
„Berichte zur Erdsystemforschung“ , „*Reports on Earth System Science*“, ISSN 1614-1199
Sie enthält wissenschaftliche und technische Beiträge, inklusive Dissertationen.

Publikationsreihe des MPI-M
„Berichte zur Erdsystemforschung“ , „*Reports on Earth System Science*“, ISSN 1614-1199
Sie enthält wissenschaftliche und technische Beiträge, inklusive Dissertationen.


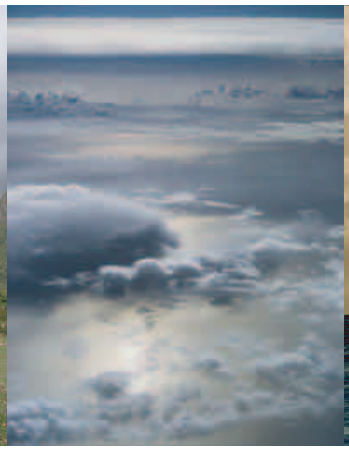


ISSN 1614-1199